5-Substituted Triazolinyls as Novel Counter Radicals in Controlled Radical Polymerization

Thesis for completion of the degree
"Doktor der Naturwissenschaften"
in the Department of Chemistry and
Pharmaceutics of Johannes Gutenberg
University, Mainz

by
Maxim Peretolchin

Mainz 2004

The work completed between October 1999 and November 2002 at the Max-Planck-Institute for Polymer Research, Mainz, Germany under the supervision of

Prof. Dr. K. Müllen.

Content

1. State of the art

1.1. Polymer chemistry

1.1.1. Introduction

Between 1913 and 1915, several reports on the self-condensation of butadiene came from the group of Lebedev.[1,2,3] The products obtained were thought to be cyclic dimers of butadiene, but Lebedev also proposed the possible existence of long chains consisting of butadiene units. In 1920, Staudinger published a paper,[4] in which the polystyrene structure formed by long linear chains of styrene blocks; similarly, the paraformaldehyde structure of repeating oxymethylene units was first proposed. This was one of the first ideas, which laid the ground for the contemporary understanding of polymer structures. Molecules able to add to other molecules of the same kind to form condensation products with relatively high molecular weight and a repeating molecular structure are known as monomers.

The wider scientific community did initially not accept these ideas.[5] Due to incorrect propositions and erroneous experimental data, the essentially correct concept of Staudinger was disregarded. However, Staudinger continued the development of his hypothesis and, in 1929, offered the new idea of the existence of two types of polymer structures: linear polymers and networks.[6] The structure of the polymer strongly influences the properties of the polymer such as solubility, resistance to mechanical shock, and others. After 24 years, the works of Staudinger obtained recognition with the award of Nobel Prize for Chemistry in 1953.[7] Subsequently, work by Carothers, Kuhn, Guth, Mark, and others completely changed generally accepted views in the field of the polymer science.

Since that time, many new ideas have been brought into polymer science, but the initial concept that polymers are long chains consisting of many repeating (monomeric) units remains. New techniques have been developed to enable researchers to visualize and investigate even single molecules. Direct observations of macromolecules such as DNA[8] or even smaller objects by these techniques directly confirm the existence of long polymer chains thus validating the initial concept of Staudinger.

---

[1] S. V. Lebedev; B. K. Merezhkovskii, J. Russ. Phys. Chem. Soc., *45*, 1249, **1913**.
[2] S. V. Lebedev, J. Russ. Phys. Chem. Soc., *45*, 1296, **1913**.
[3] S. V. Lebedev, Chem. Abstracts, *9*, 798, **1915**.
[4] H. Staudinger, Ber., *53*, 1073, **1920**.
[5] P. J. Flory, ***Principles of polymer chemistry***, Cornell University Press: Ithaca and London, *15th ed.*, 22 - 23, **1992**.
[6] H. Staudinger, Angewandte Chemie, *42*, 67, **1929**.
[7] http://www.nobel.se/chemistry/laureates/1953/

Until now, many reactions leading to polymer formation have been discovered. Several of them are used more or less widely in academic laboratories and in the commercial sector. Polymerization processes are divided into two general types. The first is step-growth polymerization and involves stepwise processes in which all intermediate products can be isolated as individual compounds. An example of step-growth polymerization, or polycondensation, is shown in Scheme 1.1. In the first step, as a result of a condensation reaction between diamine (**2**) and terephthalic acid (**1**), a monomeric unit is formed. The monomeric unit in the polymer is the shortest unit, which repeats itself along the polymer chain. The monomer has two functionalities on its ends, allowing it to add either another unit of **2** or **1** to extend the chain. Then, another molecule is added and the process is continued until one of the reacting functional groups is depleted. As result, the polymer (**3**) is formed. A wide variety of monomers can be polymerized using this technique. The main requirement is the presence of two functionalities on the monomer unit able to react with each other.[9,10]

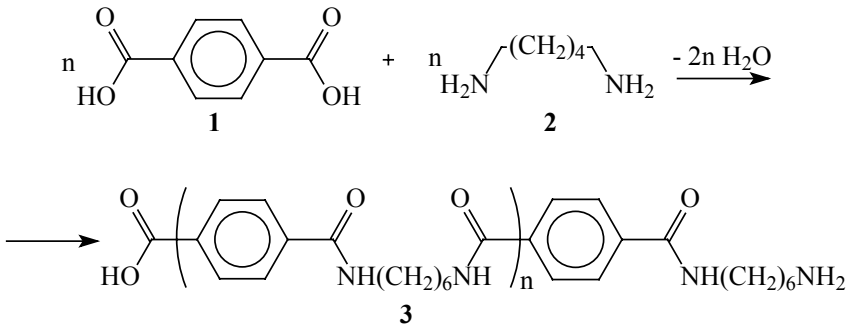

Scheme 1.1. Example of a polycondensation reaction between terephthalic acid (**1**) and 1,6-diaminohexane (**2**).

The other type of polymerization is chain-growth polymerization. In contrast to the step-growth polymerization with its two active sides, this involves a chain having only one active end, to which monomers are continuously added to form the polymer. Chain-growth polymerization can be generally divided into three classes: radical, ionic and coordination polymerizations, depending on the type of active center at the end of the growing chain. Monomers polymerized by chain-growth mechanism generally have an unsaturation of some kind, such as multiple bonds or cycles in their structure. The presence of other functionalities in the monomer structure is not obligatory, though often desirable to simplify polymerization conditions. The following discussion will concern only this type of polymerization. Before discussing the chain-growth

[8] All abbreviations are explained in chapter 7.
[9] D. Braun; H. Cherdron; H. Ritter, ***Praktikum der Makromolekularen Stoffe***, Wiley-VCH: Weinheim, 221 – 289, **1999**.
[10] P. J. Flory, ***Principles of polymer chemistry***, Cornell University Press: Ithaca and London, *15th ed.*, 69 - 105, **1992**.

polymerization types, conditions and properties, a short overview of polymer properties is provided.

1.1.2. Characterization of polymers

Unlike low molecular weight compounds in organic chemistry, synthetic polymers generally do not have a single molecular weight for all molecules present in the sample. Instead they contain a distribution. Indeed, if the reaction shown in Scheme 2.1 is stopped at any time, molecules containing (n-2), (n-1), n, (n+1), (n+2), *etc.* monomer units may be observed. Statistically, molecules with certain molecular weights, depending on the rate of polymerization and other factors, have a higher probability of being formed during the polymerization. Molecules of other molecular weights will also be present, but in lower amounts. The quantitative ratio between all species can be averaged. So average molecular weights are generally employed in polymer chemistry, as well as polydispersity index.

If the average is taken based on the numbers of each kind of polymer molecules, then the weight is called the number average molecular weight, M_n, and is calculated using Equation 1.1.

$M_n = \sum N_i M_i / \sum N_i$, **Equation 1.1**, where *i* is a polymer species present in the polymer sample, M_i is its mass and N_i is the mole fraction of the species.

The number average molecular weight can be directly measured by osmometry, end-group titration, and depression of freezing point or elevation of boiling point of a polymer solution.

Another average molecular weight widely used in polymer chemistry is the weight average molecular weight M_w (Equation 1.2).

$$M_w = \sum N_i M_i M_i / \sum N_i M_i = \sum N_i M_i^2 / \sum N_i M_i = \sum w_i M_i^2 / \sum w_i M_i ,$$

Equation l.2, where w_i is a weight factor.

The weight factor introduced in the Equation 1.2 takes into account that a number of longer polymer molecules weighs more than the same number of shorter molecules, and therefore, they make a greater contribution to the common weight of the whole polymer sample. Many short polymer molecules, having at the same time relatively small common weight greatly influence the number average molecular weight, while a few very long polymer molecules, having relative high weight will influence the weight average molecular weight.

$$D = \frac{M_w}{M_n} , \textbf{ Equation 1.3.}$$

The ratio of M_w to M_n is called the polydispersity index, *D*, (Equation 1.3) and is used as a measure of width of the molecular weight distribution. If the number average and weight

average molecular weights are equal the polymer sample consists of molecules with single chain length. Otherwise, the M_w is always bigger than the M_n.

1.2. Coordination polymerization

In coordination polymerization the growing end of the polymer chain is coordinated with a metal, which is itself the center of a complex. The complexes can be of various kinds. In most cases, at least one of the ligands is carbon centered. Complexes of these kinds are sensitive to handling, moisture, air, and reaction conditions. Probably the most famous coordination polymerization is the polymerization of olefins with Ziegler-Natta catalysts, which are complex mixtures of titanium chlorides and aluminium alkyls. The importance of their research in the field of olefin polymerization was recognized by the scientific community in 1963, when Karl Ziegler and Guilio Natta were awarded a Nobel prize "for their discoveries in the field of the chemistry and technology of high polymers."[11] Later new catalysts (*e.g.* metallocenes[12]) for coordination polymerization were discovered and applied in industry. The world market for polymers such as polyethylene and polypropylene produced *via* coordination polymerization is extremely large and this induces intensive research in the field.

1.3. Ionic polymerization

Ionic polymerization can be divided into two general categories depending on the nature of the active center which adds monomers to the chain. If the center is a carbanion, the polymerization is called anionic polymerization; if it is a carbocation, it is cationic polymerization. The mechanisms of both polymerizations are similar, therefore only anionic polymerization will be addressed here.

Polymerization begins by the addition of an anion (amide anion (**5**) in the case shown in Scheme 1.2) to the monomer (**6**). Strong acids are generally used to initiate cationic polymerization. The counter ion should not form a stable bond with the carbanion produced, otherwise the chain will be deactivated towards subsequent growth. The initiation in the case of ionic polymerization occurs quickly and almost simultaneously for all chains. The initiation generally does not require high temperature and in the case of anionic polymerization, effective cooling often should be provided. The initiators and propagating chains are very sensitive to air,

[11] Nobel e-museum: http://www.nobel.se/chemistry/laureates/1963/index.html
[12] **M*etallocene-Based Polyolefins: Preparation, Properties, and Technology***, ed. J. Scheirs; W. Kaminsky, John Wiley & Sons: New York, **2000**.

moisture, and a variety of polar functional groups, hence there is the necessity for extremely pure and dry conditions during the polymerization.

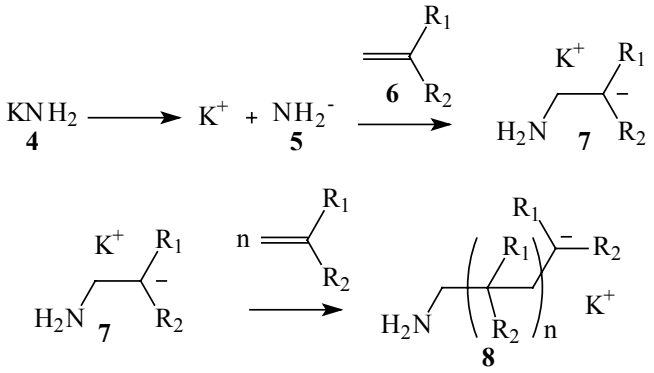

Scheme 1.2. Anionic polymerization of a vinyl monomer initiated by potassium amide.

When the anion (**7**) is formed it adds to another monomer molecule, so one more monomer unit enlarges the chain and the anionic center migrates to its end. Repetition of this step leads to formation of the polymer (**8**). The counter ion follows the end of the growing chain. When all monomer is used up, the reaction ends with polymer chains having active anions on their tails. Since the polymerization of all chains starts almost simultaneously and the propagation rate for all chains is the same, all the chains have very close molecular weights, *i.e.* the polydispersity index is low. From a kinetic point of view important indications of the living ionic polymerization are linear dependences of $\ln([M]/[M]_0)$ ([M] – concentration of monomer) *vs.* time and M_n *vs.* conversion.

In the case of ionic polymerization, electrostatic repulsion between the propagating macroions prevents reactions between themselves. If the polymerization reagents and setup have been cleaned and dried carefully, and no quenching agents are present in the polymerization mixture, the macroions stay active when all monomer is depleted. Such chains, which in the absence of monomer stay active, are termed “living”. They are able to react further, if new monomer is added. In order to stop the polymerization, termination agents must be added in the final stage of the reaction. These can be water, alcohols, or other compounds able to react with the ion to form either an inactive ion or covalent bond and a low molecular weight ion. End-capped or end-functionalized polymers prepared in such way bear certain functionalities on the tails of the chains, arising from the quenching agent, which allow further modification of the polymer. Moreover the living chains can be extended by addition of a second monomer when the first monomer is gone, leading to block copolymers. Schematically, the process of block copolymer synthesis is shown in Scheme 1.3.

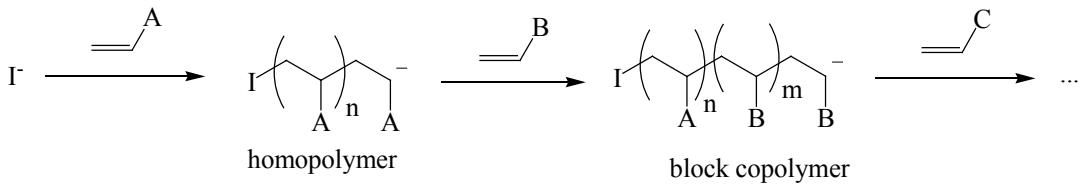

Scheme 1.3. Principle of block copolymer syntheses by anionic polymerization.

It was mentioned above that ionic polymerization is extremely sensitive to a variety of substances including oxygen, carbon dioxide, and water. In order to obtain high molecular weight polymers with narrow polydispersity and to permit synthesis of block copolymers, scrupulous purification of solvents, monomers, and reaction equipment is absolutely necessary. Especially pure argon atmosphere and often low temperatures should be used. If these requirements are not fulfilled, termination reactions of the growing macroions with impurities can occur. These lead to the widening of molecular weight distribution, and potential loss of controlled end-functionalities, which prevents subsequent block copolymer syntheses. Practically, *tri-* and *tetra-* block copolymers are difficult to prepare.[13,14] However, if the polymerization is carried out extremely carefully even five block copolymers can be synthesized.[15]

The limitations of ionic polymerization are caused not only by practical difficulties. Many monomers contain functional groups not tolerant to the active polymerization ions. For example, methacrylates, acrylates, vinyl esters, unsaturated carboxylic acids, and alcohols either cannot be polymerized, or require special reagents, reaction conditions, or protection of the functional groups in order to avoid side reactions with propagating ions.[16,17,18,19] The formation of block copolymers with these monomers experiences the same problems. Scaling from laboratory to industrial level also complicates the goal of obtaining well-defined polymers and copolymers. Although anionic polymerization is performed industrially, it remains a challenging procedure.

[13] G. S. W. Craig; R. E. Cohen; R. R. Schrock; C. Dhenaut; I. LeDoux; J. Zyss, Macromolecules, *27 (7)*, 1875 – 1878, **1994**.
[14] Y. Mogi; H. Kotsuji; Y. Kaneko; K. Mori; Y. Matsushita; I. Noda, Macromolecules, *25 (20)*, 5408 – 5411, **1992**.
[15] H. Funabashi; Y. Miyamoto; Y. Isono; T. Fujimoto; Y. Matsushita; M. Nagasawa, Macromolecules, *16 (1)*, 1 – 5, **1983**.
[16] S. Creutz; P. Teyssie; R. Jerome, Macromolecules, *30 (1)*, 6 – 9, **1997**.
[17] S. Antoun; P. Teyssie; R. Jerome, Macromolecules, *30 (6)*, 1556 – 1561, **1997**.
[18] H. Janeczek; Z. Jedlinski; I. Bosek, Macromolecules, *32 (14)*, 4503 – 4507, **1999**.
[19] A. Hirao; H. Kato; K. Yamaguchi; S. Nakahama, Macromolecules, *19 (5)*, 1294 – 1299, **1986**.

1.4. Free radical polymerization

1.4.1. Principles of radical polymerization

During the initial isolations of vinyl-containing molecules, the formation of a "gelatinous mass" in the case of styrene or a "rubber like substance" in the case of isoprene,[20,21] were observed. However, the mechanism of the polymerization was not elucidated until the 1940's – 1950's.[22,23,24]

The most basic difference with the ionic polymerization discussed in the previous section is that the active center of the growing chain is not ionic but radical in nature. However, this leads to great differences in the mechanism of the reaction and in the properties of the polymer obtained. Unlike the electrostatic repulsion in the case of identically charged ions, radical species react with each other extremely quickly.

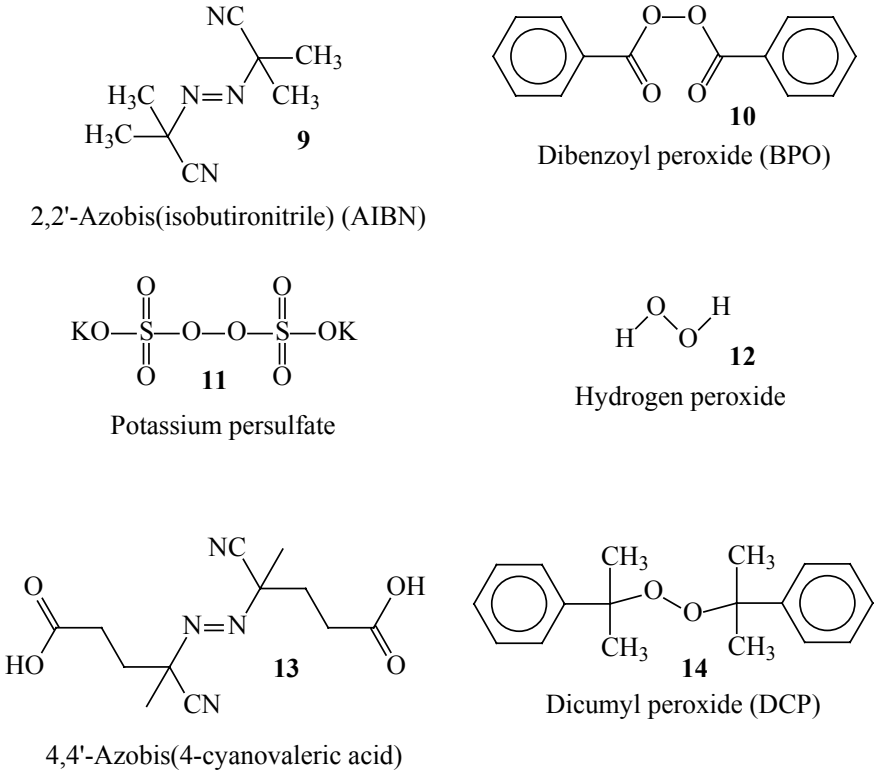

Figure 1.1. Initiators used in radical polymerization.

In order to initiate the polymerization, the formation of a radical, active enough to add to a multiple bond (or open cycle), is necessary. The usual method to obtain such radicals is

[20] E. Simon, Ann., *31*, 265, **1839**.
[21] P. J. Flory, ***Principles of polymer chemistry***, Cornell University Press: Ithaca and London, *15th ed*., 20, **1992**.
[22] A. Rudin; M. D. Samantha; P. M. Reilly, J. Appl. Pol. Sci., *24*, 171, **1979**.
[23] C. Walling, ***Free radical in solutions***, Wiley: New York, 592, **1957**.

decomposition of instable, organic peroxides (**10**, **14**) or diazocompounds (**9**, **13**). The variety of organic radical polymerization initiators is large, however, in most cases, BPO (**10**) and AIBN (**9**) are used as initiators. There are a few examples where inorganic compounds are employed as radical initiators, commonly hydrogen peroxide (**12**) and salts of persulfuric acid (**11**). Examples of commonly used initiators are shown in Figure 1.1. Decomposition of one initiator molecule leads to the formation of two active radicals able to initiate a growing chain. When the decomposition of the initiator has taken place the radical formed adds to the monomer molecule (Scheme 1.4)

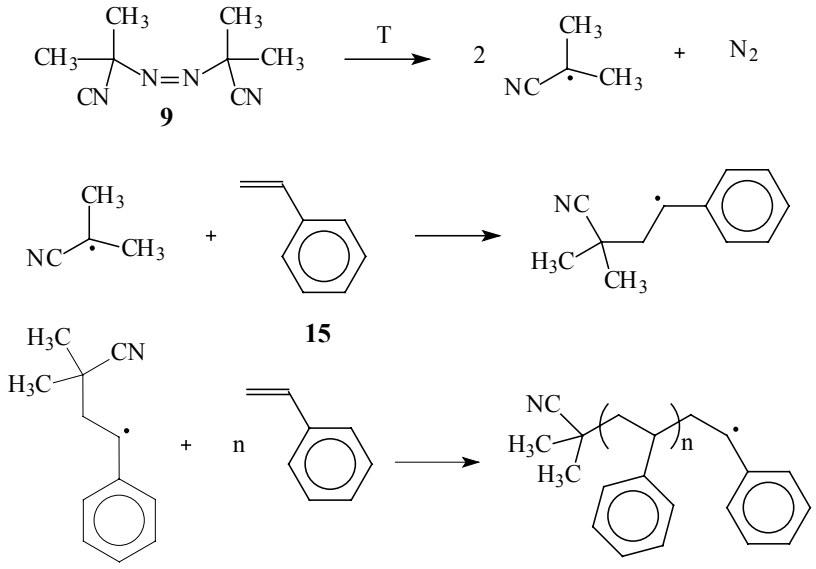

Scheme 1.4. Initiation and propagation in the radical polymerization of styrene (**15**) initiated by AIBN (**9**).

In contrast to ionic polymerization, the initiation takes place slowly, due to the relatively slow decomposition of the initiator molecules. The initiation yield is almost always less than 100 %,[25] because of the high activity of the radicals formed. There are many ways for the radical to be terminated without starting a new polymer chain *e.g.* reactions with solvent, impurities, or even with the walls of the flask. However, the main reasons responsible for the drop in the initiation yield are reaction with oxygen and recombination. Reaction of the radical with an oxygen molecule produces inactive peroxide radical, which is too stable to initiate the polymerization.[26,27] Also, due to the cell effect of the reaction media, two formed radicals can undergo coupling between themselves. The rate of the initiation (rate of decomposition of the initiator) is strongly dependent on the structure of the initiator and temperature. Functional groups able to participate in the delocalization of the electron by conjugation with formed radical

[24] G. Moad; D. H. Solomon, ***The chemistry of free radical polymerization***, Pergamon: Oxford, 1, **1995**.
[25] G. Moad; D. H. Solomon, ***The chemistry of free radical polymerization***, Pergamon: Oxford, 44, **1995**.
[26] C. Decker; A. D. Jenkins, Macromolecules, *18 (6)*, 1241 – 1244, **1985**.
[27] V. A. Bhanu; K. Kishore, Macromolecules, *22 (8)*, 3491 – 3492, **1989**.

center, *e.g.* cyano groups in the case of AIBN, can promote the decomposition of the initiator molecule as the stability of the forming radical is increased.

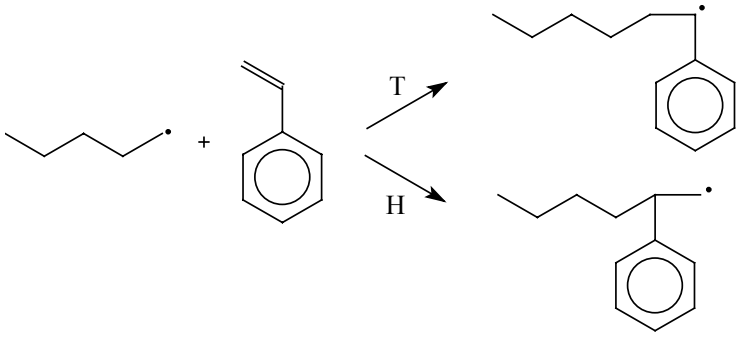

Scheme 1.5. Head (H) and tail (T) addition of styrene molecule.

Once the first monomer has been added to the radical formed in the initiation step, the addition can be further repeated. There are two ways for the monomer to add to the growing chain. The radical can attack the double bond from either more substituted side (head) or less substituted one (tail) (Scheme 1.5). In most cases, addition to the tail is more favored for steric reasons.[28] The possibility of stabilization of the formed radical *via* delocalization over the groups connected to the head also leads to preference for addition to the tail. However, in many cases the head addition is also observed.

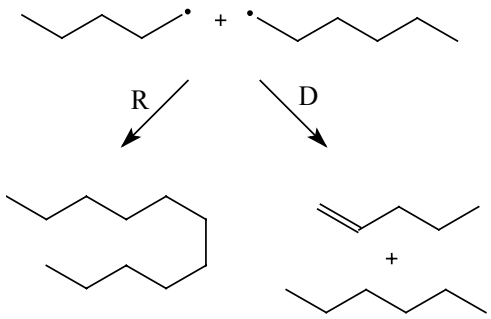

Scheme 1.6. Disproportionation (D) and recombination (R) as the termination reactions in free radical polymerization

Unlike in ionic polymerization, reaction between two growing macroradicals is favored. The activation energy of the reaction between two carbon-centered radicals is very low. The process in some cases is even suspected to be diffusion controlled.[29,30] The products of the reaction can be of two types: first, if two radicals bind to one another to form a single covalent bond the reaction is termed recombination and leads to doubling of the molecular weight (Scheme 1.6). Another possibility is the transfer of the β-hydrogen atom from one of

[28] G. Moad; D. H. Solomon, ***The chemistry of free radical polymerization***, Pergamon: Oxford, 152 - 161, **1995**.
[29] T. E. Paton; K. Matjyaszewski, Adwanced materials, *10*, *12*, 901 - 915, **1998**.
[30] ***Controlled/living radical polymerization***, ed. K. Matjyaszewski, American Chemical Society: Washington, 16, **2000**.

macroradicals to another. This process is known as disproportionation (Scheme 1.6). In this case two polymer molecules are formed, one of which bears an unsaturated bond at its end. Both processes cause termination of the active species and are termed the termination steps for the polymerization. The ratio between the disproportionation and recombination products is strongly dependent on the type of monomer polymerized. For example, investigation of bulky polystyrene radical model compounds has shown their preferable participation in disproportionation, because the recombination must overcome strong steric hindrance.[31,32] On the other hand, less hindered methacrylate model compounds showed a preference to recombine.[33,34] The results obtained not from model compounds, but from polymerization experiments sometimes show the opposite.[35] The investigation of the subject is very complicated, as some discrepant data can be found in the literature.

Few side processes are observed in the radical polymerization. The growing macroradical may react with a compound (solvent, additive, …) forming an adduct and producing a radical species, which may initiate a new chain. This process is called chain transfer (Scheme 1.7). The mechanism of chain transfer was proposed by Flory.[36,37] This process leads to a decrease in the molecular weights of the polymer and is widely used in industry and laboratories to control it. Efficient chain transfer agents are thiols and halides; however, solvents (especially halogen containing), initiators, impurities, monomers, polymers, stirrers, and even the walls of the reaction flask can play the role of chain transfer agents.

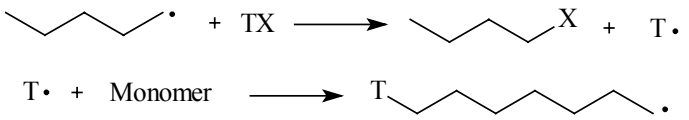

Scheme 1.7. Chain transfer in free radical polymerization.

If a transfer agent is not able to initiate a new chain in the second step in the process shown in Scheme 1.7, it is called an inhibitor. Inhibitors react with the propagating chains and quench the growth of the chain. Inhibitors include a wide variety of reagents: stable radicals, captodative olefins, phenols, and quinones.[38] The most common of them is oxygen, which should therefore, be excluded from the reaction flask in order to allow efficient polymerization. Quinones and hydroquinones are used by chemical companies to preserve monomers from self-

[31] G. Gleixner; O. F. Olaj; J. W. Breitenbach, Makromol. Chem., *180*, 2581, **1979**.
[32] V. A. Schreck; A. K. Serelis; D. H. Solomon, Austr. J. Chem., *42*, 375, **1989**.
[33] S. Bizilj; D. P. Kelly; A. K. Serelis; D. H. Solomon; K. E. White, Austr. J. Chem., *38*, 1657 - 1973, **1985**.
[34] D. J. Trecker; R. S. Foote, JOC, *33*, 3527, **1968**.
[35] G. Moad; D. H. Solomon, ***The chemistry of free radical polymerization***, Pergamon: Oxford, 228 - 233, **1995**.
[36] P. J. Flory, ***Principles of polymer chemistry***, Cornell University Press: Ithaca and London, *15th ed.*, 20, 136, **1992**.
[37] P. J. Flory, JACS, *59*, 241, **1937**.
[38] G. Moad; D. H. Solomon, ***The chemistry of free radical polymerization***, Pergamon: Oxford, 260, **1995**.

polymerization. Commercially available monomers usually contain inhibitors, which must be removed prior to use.

1.4.2. Kinetics of free radical polymerization

All reactions, which take place in the free radical polymerization process, are summarized in Scheme 1.8. Inhibition and chain transfer are not included in this consideration, since they are side processes and in the absence of special agents are insignificant.

The rate of initiation can be calculated according to Equation 1.4.

$v_i = d[M\cdot]/dt = 2fk_{dec}[I]$, **Equation 1.4**, where *f* is the fraction of the radicals formed by decomposition, which initiate a new chain.

Initiation:

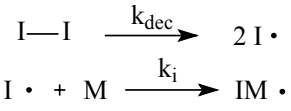

Propagation:

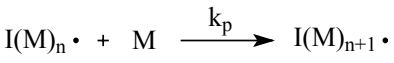

Termination:

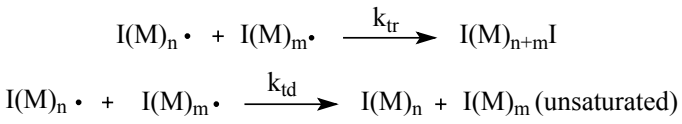

Scheme l.8. Kinetic scheme for free radical polymerization

The rate of the initiation depends directly on the concentration of the initiator, but is independent of the monomer concentration. This is only the case if concentration of the initiator is much less than concentration of the monomer, but is usual. Initiation yield is occasionally dependent on the monomer concentration even when the concentration of the initiator is low; however, usually this is not the case.[39] The quantity of the chains initiated at a given temperature (k_{dec} ~ temperature) is generally dependent only on the initiator concentration. The decrease of initiator concentration during the polymerization process leads to a decrease in the quantity of newly initiated chains.

Termination rate v_t is calculated by Equation 1.5.

$v_t = -d[M\cdot]/dt = 2k_t[M\cdot]^2$, **Equation 1.5**, where 2 comes from the fact that two macroradicals disappear after one termination event.

[39] P. J. Flory, ***Principles of polymer chemistry***, Cornell University Press: Ithaca and London, *15th ed.*, 110-112, **1992**.

Since the method of termination (disproportionation or recombination) is not considered k_t is the average termination constant for the two mechanisms. As mentioned above discrimination between the two types of the main terminations is complicated. In addition the effect of the various types of the terminations influences the molecular weights and the end-functionality but not the kinetics of the polymerization since the result is the same – disappearance of two active species. It is obvious that the termination rate is strongly dependent on the concentration of propagating radicals (squared). The quantity of propagating radicals is dependent only on the concentration of initiator, as shown above.

Under ordinary conditions after a short period of time, the rate of initiation will balance the rate of termination, so in such stationary state $v_i = v_t$ and extracting the concentration of macroradicals from Equations 1.4 and 1.5, the propagation rate is given by Equation 1.6.[40]

$$v_p = k_p[M][M\cdot] = k_p[M]\sqrt{(fk_{dec}[I]/k_t)}$$, **Equation 1.6**.

Due to the fact that much less monomer is used in the initiation step in comparison to the propagation step, the decrease of the monomer concentration with time can be interpreted as rate of polymerization (Equation 1.7).

$$v_p = -d[M]/dt$$, **Equation 1.7.**

The degree of polymerization can be calculated using Equation 1.8. Simple multiplying of the length by the weight of the monomer unit gives the molecular weight of the polymer.

$l = v_p / v_i = v_p / v_t$ **Equation 1.8**, where l is degree of polymerization; $v_i = v_t$ in the stationary state.

Polymers obtained by free radical polymerization generally have broad molecular weight distributions. The factors influencing this are: different types of termination reactions, slow initiation compared to propagation, transfer reactions, and others. The ratio between the rates of propagation and termination reactions is nearly constant during the polymerization. The molecular weights of the polymer obtained almost do not change during the polymerization. It has been shown that polydispersity of the polymer obtained by free radical polymerization is theoretically ≥ 1.5 if chain transfer reactions are absent. However, polydispersities of the polymers obtained are usually around 2 or higher. At higher conversions polydispersity can increase further, though it is seldom above 5. In the cases, where transfer to polymer chain is possible, for instance in the case of auto-acceleration of methylmethacrylate polymerization, polydispersity can reach such extremely high values as ten.[41]

[40] P. J. Flory, ***Principles of polymer chemistry***, Cornell University Press: Ithaca and London, *15th ed.*, 113, **1992**.
[41] F. W. Billmeyer, jr., ***Textbook Of Polymer Science***, John Wiley & Sons: New York, *3rd ed.*, 68 – 71, **1984**.

1.4.3. Comparison of free radical and ionic (living) polymerizations

As has been already mentioned, the differences between free radical and ionic (living) polymerizations at first glance seem relatively small. However, the polymers obtained by these techniques show very different properties. The main differences are summarized in Table 1.1.

In the case of the ionic polymerization, the mechanism is more obvious. All chains are initiated at approximately the same time and grow simultaneously. Since the rate of the propagation of all chains is independent of the chain length, the final molecular weights are very close for all polymer molecules; consequently the polydispersity is low. The chains remain active at the time when all monomer is consumed, so if additional monomer is added, a block copolymer is formed.

Table 1.1. Features of free radical and ionic polymerizations.

Feature	Ionic (living) polymerization	Free radical polymerization
Polydispersity of the polymer obtained	close to 1	>1.5, usually >2
Time of growth of a single chain	all the time of reaction	very short in comparison to the reaction time
Rate of initiation	very fast, all chains are initiated at about the same time	initiation is slow, takes place continuously
Termination	no, in absence of special agents	termination is fast, goes on continuously
Growth of molecular weight	M_n increases linearly with conversion	an average molecular weight quickly reaches a particular value and stays almost constant
Possibility of block copolymer syntheses	yes	no

In the case of free radical polymerization, a kind of equilibrium is present in the system. From one side continuous decomposition of the initiator provides the system with new growing chains. The termination, whose rate is strongly (squared) dependent on the quantity of propagating radicals, destroys active radicals. As a result, soon after the polymerization starts, the equilibrium between the numbers of terminated and initiated chains becomes almost constant. This phenomenon is well known in kinetics as a stationary state.[42] For many polymerization processes the time scale for polymerization of a single chain is about a second.[43] All chains grow for approximately the same time leading to almost constant molecular weights

[42] J. Campbell, ***Sovremennaya Obshaya Khimiya***, Mir: Moscow, *2*, 205 – 207, **1975**.

of the polymer during the whole polymerization process. From the polymerization mechanism it is obvious that obtaining block copolymers is impossible.

From a practical perspective, syntheses of polymers with precisely given properties by living polymerization are very useful. Narrow polydispersity, as well as easy control of the morphology of the polymer, and over molecular weights are very attractive, not only for the laboratory chemists, but even more so for chemical companies. Another useful application of living polymerization is the syntheses of block copolymers and more elaborate molecular structures. However, along with these advantages, ionic polymerization has very serious drawbacks. The conditions required for living ionic polymerization are strenuous; furthermore, the range of monomers polymerizable by anionic polymerization is limited. In areas where ionic polymerization has worst troubles, the radical polymerization has its greatest advantages. The conditions required for radical polymerizations are generally simple. Moreover, they can be changed and tuned over a very wide range depending on the desired goals. Many usual impurities do not influence the polymerization. The main requirement is exclusion of air and other possible inhibitors from the reaction mixture. The presence of small amounts of these agents can be overcome without special purification, *e.g.* by adding an additional amount of initiator. The polymerization can be realized in water, which is a great advantage for industry as it means that emulsion and suspension polymerization can be carried out, instead bulk polymerization, which is not desired in industry due to problems with temperature control in large-scale reactions. The avoidance of large quantities of organic solvents lowers the price of the product and is desirable from an environmental point of view.

As a result of this high tolerance to experimental conditions many different approaches to radical polymerization have been used. Emulsion, suspension, microemulsion, solution and bulk polymerizations and other techniques provide the possibility of preparing polymers with different properties and polymer products in various forms (*e.g.* powders, lattices, bulk material and so on).

The main drawback of free radical polymerization is the loss of control of the polymer structure and the significantly greater challenge of synthesizing complex molecular architectures. The situation was such until the first publications in the field of controlled (living) radical polymerization appeared about ten years ago.

---

[43] ***Controlled/living radical polymerization***, ed. K. Matjyaszewski, American Chemical Society: Washington, 12, **2000**.

1.5. Controlled (living) radical polymerization

1.5.1. Overview

Controlled radical polymerization combines the simplicity of the free radical polymerization technique with the advantages of ionic polymerization. Since the pioneering works of Otsu[44,45] the idea of reversible deactivation of the propagating macroradical for controlling radical polymerization has grown greatly. Currently, the controlled radical polymerization is one of the most intensively investigated subjects in polymer science. Three general ways to obtain control over free radical polymerization processes have been developed. The use of nitroxide stable radicals lies at the foundation of the technique known as nitroxide mediated radical polymerization (NMRP). Nitroxides have been known for a long time to be effective scavengers of active radicals. The possibility of reactivating the captured active radical at elevated temperatures was proposed as the key-feature of the NMRP.[46,47,48] The second method consists of the use of complexes of transition metals, easily able to change their oxidation state by interaction with a halogen end capped polymer molecule to form a macroradical.[49,50,51] The method is known as atom transfer radical polymerization (ATRP) and is the most investigated of all controlled radical polymerization processes. The third approach is the application of a transfer reaction to the polymerization process. The most known chemical transfer reaction applied in controlled radical polymerization is reversible addition fragmentation chain transfer (RAFT). In this case, additives able to transfer a radical center from one polymer chain to another are used to control the polymerization.[52,53,54,55]

---

[44] T. Otsu; A Kuriyama, Polymer Journal, *17 (1)*, 97, **1985**.
[45] T. Otsu; M. Yoshida, Macromol. Chem. Rapid Comm. *3*, 127, **1982**.
[46] D. H. Solomon; E. Rizzardo; P. Cacioli, US patent *4,-581,429* March 27, **1985**.
[47] R. P. N. Veregin; P. M. Kazmaier; G. K. Hamer, Macromolecules, *26*, 2987, **1993**.
[48] C. J. Hawker, JACS, *116*, 11185, **1994**.
[49] J.-S. Wang; K. Matjyaszewski, JACS, *117*, 5614, **1995**.
[50] M. Kato; M. Kamigaito; M. Sawamoto; T. Higashimura, Macromolecules, *28*, 1721, **1995**.
[51] C. Granel; P. Dubois; R. Jerome; P. Teyssie, Macromolecules, *29*, 8576, **1996**.
[52] T. Otsu; A Kuriyama, Polymer Journal, *17 (1)*, 97, **1985**.
[53] J. Chiefari; Y. K. Chong; F. Ercole; J. Krstina; J. Jeffery; T. P. Le; R. T. A. Mayadunna; G. F. Meijs; C. L. Moad; G. Moad; E. Rizzardo; S. H. Thang, Macromolecules, *31*, 5559, **1998**.
[54] T. P. Le; G. Moad; E. Rizzardo; S. H. Thang, PCT int., Appl. *WO 9801478 A1980115*; Chem. Abstr., *128* 115390, **1998**.
[55] Y. K. Chong; T. P. T. Le; G. Moad; E. Rizzardo; S. H. Thang, Macromolecules, *32*, 2071, **1999**.

1.5.2. Atom transfer radical polymerization (ATRP)

As has been mentioned already, the ATRP is the most studied technique among all controlled radical polymerization strategies.[56,57,58]

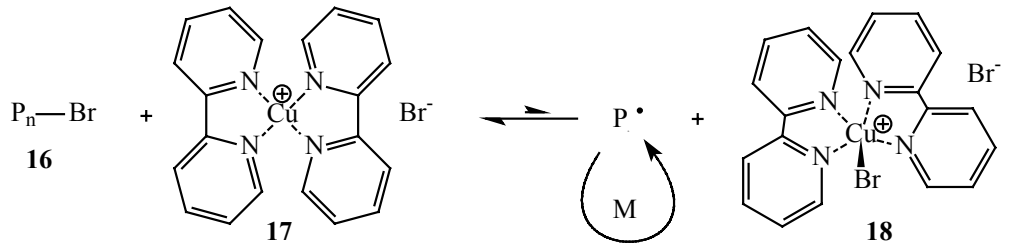

Scheme 1.9. Mechanism of ATRP.

ATRP was first reported by the groups of Matjyaszewski[59,60] and Sawamoto.[61,62] Now ATRP serves as a very useful and easy-to-use tool to modify various molecular structures and obtain different molecular architectures. The key features, which promoted the rapid growth of ATRP, are the simplicity of realization and its flexibility with a wide variety of monomers tolerant to the reaction conditions.

The classical ATRP was realized using an alkyl halide (**16**) as an initiator and a complex of copper (I) with 2,2′-bipyridyl ligands (**17**) (Scheme 1.9). The copper complex **17** homogeneously breaks the bond between the halogen and the rest of the molecule and forms a complex of copper (II) (**18**). At the same time, an active radical is formed from the rest of the halide molecule. It starts to propagate by adding the monomer units. After a period of time, the forming polymer chain reacts with the complex of copper (II) (**18**) to reform **17** and a halogen terminated polymer chain. After each repetition of this cycle the polymer has several monomers more attached. All chains spontaneously and statistically react to form active species, add some monomers and then deactivate again. Due to the statistical character of the activation, all chains grow simultaneously at almost same rate during the polymerization. Therefore, a polymer with low polydispersity and high end-functionalization is formed. However, the termination reactions are not suppressed completely. At high conversions, the process slowly looses control and the

[56] ***Controlled/living radical polymerization***, ed. K. Matjyaszewski, American Chemical Society: Washington, **2000**.
[57] T. E. Paton; K. Matjyaszewski, Advanced Materials, *10*, *12*, 901 - 915, **1998**.
[58] K. A. Davis; H.-J. Paik; K. Matjyaszewski, Macromolecules, *32*, 1767 - 1776, **1999**.
[59] J.-S. Wang; K. Matjyaszewski, Macromolecules, *28*, 7572, **1995**.
[60] J.-S. Wang; K. Matjyaszewski, JACS, *117*, 5614, **1995**.
[61] Y. Kotani; M. Kato; M. Kamigato; M. Sawamoto, Macromolecules, *29*, 6979, **1996**.
[62] M. Kato; M. Kamigato; M. Sawamoto; T. Higashimura, Macromolecules, *28*, 1721, **1995**.

polydispersity of the formed polymer increases. This is a common problem of all controlled radical polymerization approaches.

Later complexes of many transition metals with a variety of ligands were investigated and applied in ATRP. Variations of the ligands often increase the activity of the complex and improve the properties of the polymerization process. Cheng *et al.* reported the use of phenanthroline derivatives in the presence of carbon tetrachloride for the ATRP of methylmethacrylate. The complexes showed higher catalytic activity and better control of the polymerization process.[63,64] A series of copper complexes with N-alkyl-2-pyridinemethamine ligands influenced the polymerization process depending on the length of alkyl side chain.[65] 2,2´-Bipyridyl ligands substituted at 4- and 4`-positions by fluorinated alkyl groups allow ATRP of fluorinated monomers.[66]

The range of complexing metals used in ATRP has also widened. Currently complexes of several transition metals can be utilized to perform ATRP. Sawamoto reported efficient ATRP polymerization of styrene and methylmethacrylate based on ruthenium complexes.[67,68] Interestingly, even metallocene complexes have been utilized as ATRP agents; complexes of this kind are known to be very effective catalysts of olefin polymerization[69] (see Section 1.2). The oxidation-reduction pair Ru (II) – Ru (III) was used in this case. Another example is the use of complexes of lithium molybdate (V) complexes in the ATRP of styrene.[70]

Attempts to achieve ATRP of various monomers in aqueous medium have been successful.[71,72,73] Also, emulsion polymerization of *n*-butylmethacrylate has been realized.[74] A presence of a small amount of oxygen in the polymerization mixture can be overcome by addition of excess of the metal complex.[75]

Use of supercritical carbon dioxide as solvent is a very convenient choice for industrial applications. ATRP of fluorinated methacrylates in CO_2 under high pressure has been carried out.[76] All this shows that ATRP is tolerant to a wide range of solvents and impurities. It opens

---

[63] G. L. Cheng; C. P. Hu; S. K. Ying, Polymer, *40*, 2167 - 2169, **1999**.
[64] G. L. Cheng; C. P. Hu; S. K. Ying, Journal of Molecular Catalysis A: Chemical, *144*, 357 - 362, **1999**.
[65] A. J. Amass; C. A. Wyres; E. Colclough; I. Marcia Horn, Polymer, *41*, 1697 - 1702, **2000**.
[66] J. Xia; T. Johnson; S. C. Gaynor; K. Matjyaszewski; J. DeSimone, Macromolecules, *32*, 4802 - 4805, **1999**.
[67] H. Takanashi; T. Ando; M. Kamigaito; M. Sawamoto, Macromolecules, *32*, 3820 - 3823, **1999**.
[68] T. Ando; M. Kamigato; M. Sawamoto, Tetrahedron, *53*, *45*, 15445 – 15457, **1997**.
[69] ***Metallocene Catalyzed Polymers: Materials, Properties, Processing & Markets***, ed. George M. Benedikt; ed. Brian L. Goodall, Plastics Design Library: New York, **1998**.
[70] J. A. M. Brandts; P. van de Geijn; E. E. van Faassen; J. Boersma; G. van Koten, Journal of Organometallic Chemistry, *584*, 264 - 253, **1999**.
[71] J.-S. Wang; K. Matjyaszewski, JACS, *117*, 5614, **1995**.
[72] T. Nishikawa; T. Ando; M. Kamigaito; M. Sawamoto, Macromolecules, *30*, 2244, **1997**.
[73] S. Coca; C. Jasieczek; K. L. Beers; K. Matjyaszewski, Journal of Polymer Science: Part A: Polymer Chemistry, *36*, 1417, **1998**.
[74] J. Qiu; S. G. Gaynor; K. Matjyaszewski, Macromolecules, *32*, 2872 - 2875, **1999**.
[75] K. Matjyaszewski; S. Coca; S. G. Gaynor; M. Wei; B. E. Woodworth, Macromolecules, *31*, 5967 - 5969, **1998**.
[76] J. Xia; T. Johnson; S. C. Gaynor; K. Matjyaszewski; J. DeSimone, Macromolecules, *32*, 4802 - 4805, **1999**.

the possibility of performing living polymerizations in relatively simple conditions and using a wide variety of monomers.

A variety of advanced molecular architectures have been prepared *via* ATRP. Block copolymers can be synthesized by polymerization of different monomers by the ATRP technique.[77,78] Also block copolymers can be synthesized using ATRP for one block formation, with the second block being synthesized by a different method, *e.g. via* ionic polymerization.[79,80] The possibility of initiating several chains from one molecule allows the syntheses of graft, star, and other architectures of polymers and copolymers.[81,82] Surface modification *via* ATRP has been used to produce functional nanoparticles.[83]

In general the method of ATRP is very powerful. However, it still has drawbacks. The polymers obtained by ATRP usually have relatively low molecular weight: in the range of 10000 – 15000. The use of metal complexes requires for many applications its subsequent removal from the polymer sample. While relatively unimportant on the laboratory scale, this problem stands in the way of wide use of ATRP in industrial applications. Many monomers having functional groups (like vinyl pyridines) able to complex with the metal used as additive cause complications in the polymerization by the ATRP technique. ATRP of vinyl acetate and similar monomers have not been successful to date.

1.5.3. Reversible addition fragmentation chain transfer (RAFT)

The second approach to control the radical polymerization is application of transfer reactions to the radical polymerization. The method utilizes additives able to transfer a radical center from one polymer chain to another. The intermediates (**19**) formed during the transfer of the radical are not reactive with monomers. Due to the presence of the additives in higher concentration in comparison to the propagation species, a decrease in the active radical concentration is achieved. As the result, the termination reactions are significantly reduced.[84] The principal mechanism of RAFT is shown in Scheme 1.10. Usually RAFT agents are thiocarbonylthiocompounds,[85,86] disulfides,[87] or other substances (*e.g.* iodides) able to produce

[77] Z.-B. Zhang; S.-K. Ying; Z.-Q. Shi, Polymer, *40*, 5439 - 5444, **1999**.
[78] T. E. Paton; K. Matjyaszewski, Advanced Materials, *10*, *12*, 901 - 915, **1998**.
[79] B. S. Shemper; A. E. Acar; L. J. Mathias, Journal of Polymer Science: Part A: Polymer Chemistry, *40*, 334 – 343, **2002**.
[80] K. Jankova; J. H. Truelson; X. Chen; J. Kops; W. Batsberg, Polymer Bulletin, *42*, 153 – 158, **1999**.
[81] X.-S. Wang; N. Luo; S.-K. Ying; Polymer, *40*, 4515 - 4520, **1999**.
[82] T. E. Paton; K. Matjyaszewski, Advanced Materials, *10*, *12*, 901 - 915, **1998**.
[83] T. von Werne; T. E. Patten, JACS, *121*, 7409 - 7410, **1999**.
[84] A. Goto; K. Sato; Y. Tsujii; T. Fukuda, ICR Annual Report, *7*, 30 - 31, **2000**.
[85] D. G. Hawthorne; G. Moad; E. Rizzardo; S. H. Thang, Macromolecules, *32*, 5457 - 5459, **1999**.
[86] C. P. Rechunadhan Nair; G. Clouet, JMS-Ev. Macromol. Chem. Phys., *c31 (2 & 3)*, 311 – 340, **1991**.

relatively inert radicals. The general mechanism of chain transfer for different additives can vary from the RAFT process shown in Scheme 1.10; however, the key feature of the transport of the reactive center from one chain to another stays the same.

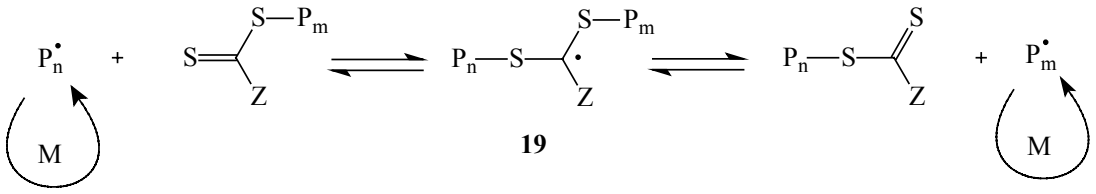

19

Scheme 1.10. The mechanism of the RAFT.

As in the case of ATRP, block copolymers of various monomers have been prepared by RAFT technique.[88,89] RAFT polymerization under very high pressure has been reported.[90] The major advantage of the RAFT process is the possibility to polymerize wider range of vinyl monomers in comparison to other controlled radical polymerization techniques. The nature of the solvent has little influence on the polymerization, which permits emulsion, suspension, and other kinds of heterogeneous RAFT polymerizations in aqueous media.[91,92] In comparison to ATRP, higher molecular weights are easily achieved. However, the unpleasant odor of the sulfur-containing compounds, usually used as additives is a big disadvantage of the RAFT technique.

1.6. Stable free radical polymerization (SFRP)

Like the metal complex in the case of ATRP, the agent reversibly deactivating the growing macroradical can be a stable radical. In this case, the stable radical reacting with the propagating radical forms a covalent bond that can be broken again at higher temperature required for this reaction. The cleavage of the stable radical produces a macroradical, which can propagate until it reacts with another stable radical.

Many radicals have been observed to inhibit the radical polymerization of vinyl monomers.[93,94] Later, it was observed that at higher temperatures the covalent bond formed by their addition was reversibly broken. This reversible process lies at the base of stable free radical polymerization, which will be the subject of the following discussion.

---

[87] K. Endo; T. Shiroi; K. Murata, Journal of Polymer Science: Part A: Polymer Chemistry, *39*, 145 - 151, **2001**.
[88] T. Otsu; A. Kuriyama, Polymer Journal, *17*, *1*, 97 - 105, **1985**.
[89] C. P. Rechunadhan Nair; G. Clouet, JMS-Ev. Macromol. Chem. Phys., *c31 (2 & 3)*, 311 – 340, **1991**.
[90] J. Rzayev; J. Panelle, Macromolecules, *35*, 1489 - 1490, **2002**.
[91] M. S. Donovan; T.A. Sanford; A. B. Lowe; B. S. Sumerlin; Y. Mitsukami; C. L. McCormick, Macromolecules, *35 (12)*, 4570 - 4572, **2002**.
[92] S. W. Prescott; M. J. Ballard; E. Rizzardo; R. G. Gilbert, Macromolecules, *35*, 5417, **2002**.
[93] E. G. Rozantsev; M. D. Gol'dfein; A. V. Trubnikov, Uspekhi Khimii, *55*, 1881 – 1897, **1986**.
[94] E.G.Rozantsev, M.D.Gol'dfein, A.V.Trubnikov, Russian Chemical Reviews, *55 (11)*, 1070 – 1080, **1986**.

1.6.1. Nitroxide mediated radical polymerization (NMRP)

Nitroxide radicals have been known to capture carbon-centered radicals quantitatively.[95,96,97] Moad *et al.* showed various ways that carbon centered radicals are captured by the nitroxide radicals in their study of the self-initiation of styrene.[98] Later it was discovered that at elevated temperatures an adduct formed from the combination of a nitroxide radical and a macroradical can dissociate back to reform the initial radicals.[99,100] The coupling and the breaking of the bond, then, are reversible processes at elevated temperatures. Since the equilibrium exists, it can be utilized in controlled radical polymerization. The mechanism of the NMRP is shown in Scheme 1.11 for the example of the best-known stable radical - commercially available 2,2,6,6-tetramethylpiperidine-N-oxyl (TEMPO) (**20**). The TEMPO radical is a very stable compound, which can be stored for years without decomposition. The cleavage of the oxygen-carbon bond requires relatively high temperatures (120 – 130°C), therefore, initially NMRP was applied only to styrenic monomers[101] and vinyl pyridine.[102] Polymerization of 1,3-butadiene has been reported recently.[103] Attempts to polymerize other monomers (acrylates, methacrylates) using TEMPO as an additive have failed. The polymerization in these cases stopped at early stages and only oligomers could be isolated.[104] The slowing down and stopping of the polymerization are caused by termination reactions, which lead to a decrease in the concentration of the active macroradical, with simultaneous increase in the nitroxide concentration.

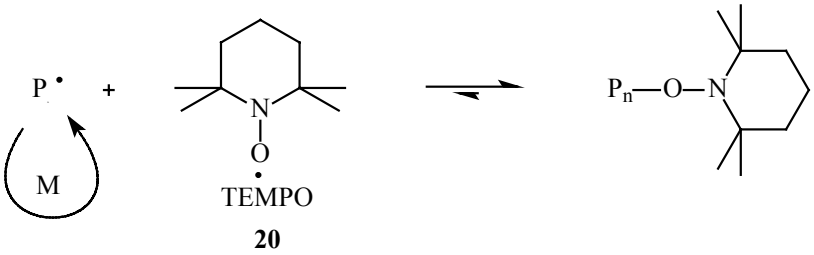

20

Scheme 1.11. Mechanism of TEMPO mediated controlled radical polymerization.

[95] D. Braun; W. K. Czerwinski, Makromol. Chem., *188*, 2371, **1987**.
[96] G. Moad; D. H. Solomon, ***The chemistry of free radical polymerization***, Pergamon: Oxford, 120 - 122, **1995**.
[97] T. Fukuda; Y.-D. Ma; H. Inagaki, Macromolecules, *18*, 17, **1985**.
[98] G. Moad; E. Rizzardo; D. H. Solomon, Polymer Bulletin, *6*, 589 - 593, **1982**.
[99] G. Moad; E. Rizzardo, Macromolecules, *28*, 8722 - 8728, **1995**.
[100] D. H. Solomon; E. Rizzardo; P. Cacioli, US patent *4,-581,429* March 27, **1985**; Chem. Abstracts, *102*, 221335q, **1985**.
[101] D. Greszta; K. Matjyaszewski, Macromolecules, *29*, 7661 - 7670, **1996**.
[102] X. Z. Ding; A. Fischer; A. Brembilla; P. Lochon, Journal of Polymer Science: Part A: Polymer Chemistry, *38*, 3067 - 3073, **2000**.
[103] J. L. Pradel; B. Boutevin; B. Ameduri, Journal of Polymer Science: Part A: Polymer Chemistry, *38*, 3293 - 3302, **2000**.

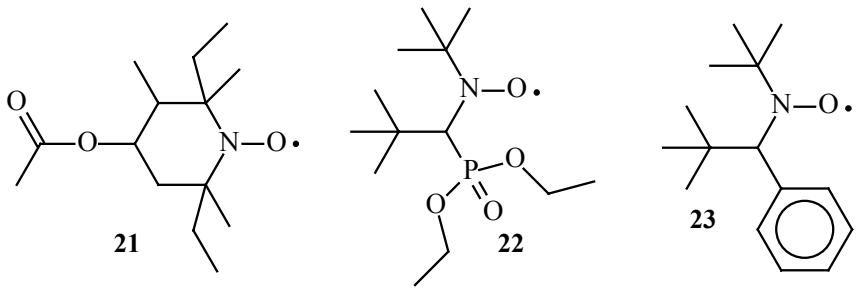

Figure 1.2. Nitroxide radicals allowing controlled radical polymerization of acrylates.

Recently, the use of new advanced nitroxide derivatives (**21** – **23**), shown in Figure 1.2, allowed NMRP to be applied to acrylates but not methacrylates.[105,106] The reason reported is a higher equilibrium constant between the dormant and the active species. Another problem in the case of methacrylates is *β*-hydrogen transfer leading to the formation of hydroxylamine (**24**) and an unsaturated C-C bond at the end of the chain. The process is shown in Scheme 1.12. Despite these recent developments, NMRP permits polymerization of relatively few monomers. Further investigations are required to widen the monomer range which are being carried out currently in many research groups.

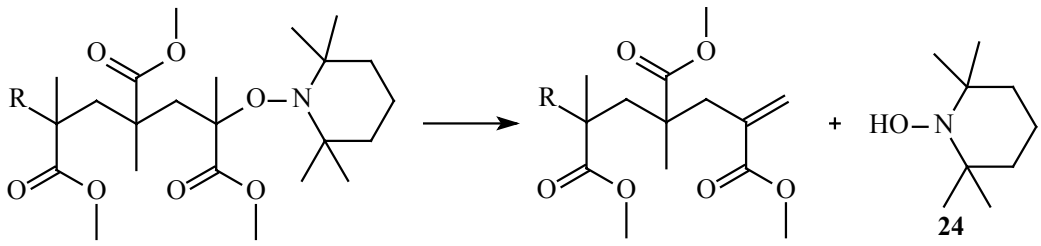

Scheme 1.12. *β*-Elimination in NMRP of methylmethacrylate.

As in the case of the RAFT technique, the molecular weights of the polymers obtained by NMRP can reach as high as several hundred thousand, depending on the polymerization conditions. Since the TEMPO adduct requires relatively high temperatures for the reaction, the TEMPO mediated polymerization is difficult to apply to aqueous systems. However, recently several approaches to carry out NMRP using emulsion conditions were successful.[107,108,109] Another promising possibility for performing the nitroxide mediated controlled radical

---

[104] ***Controlled/living radical polymerization***, ed. K. Matjyaszewski, American Chemical Society: Washington, 20, **2000**.
[105] H. Fischer, Chem. Reviews, *101*, 3581 - 3610, **2001**.
[106] P. Lacroix-Desmazes; J.-F. Lutz; F. Chauvin; R. Severac; B. Boutevin, Macromolecules, *34 (26)*, 8866 - 8871 **2001**.
[107] C. Marestin; C. Noel; A. Guyot; J. Claverie, Macromolecules, *31*, 4041 – 4044, **1998**.
[108] S. A. F. Bon; M. Bosveld; B. Klumperman; A. L. German, Macromolecules, *30*, 324 - 327, **1997**.
[109] A. Guyot, Colloids and Surfaces: A: Physiochemical and Engineering Aspects, *153*, 11 - 21, **1999**.

polymerization in aqueous medium is microemulsion polymerization, which has also been achieved.[110,111,112] Although these processes are more complicated due to the distribution of the counter radical between the aqueous and organic phases (which changes during the polymerization) and the necessity to use temperatures lower than 100°C, both methods worked. This opens the possibilities to realize NMRP on an industrial scale, where for different reasons, bulk (overheating and high viscosity) and solution (solvent pollutions and high energy consumption) polymerizations are not desirable.

Syntheses of new radicals for use as counter radicals are constantly being reported. Puts and Sogah reported the synthesis of a chiral nitroxide **25** (Figure 1.3) and the controlled polymerization of styrene in its presence.[113] Oxazolidinyl-N-oxyls stable radicals (**26**, **27**) have been used to control polymerization of styrene by Yamada *et al.*[114] *β*-Sulfinyl nitroxide **28** is reported to be unstable, but still allows controlled radical polymerization of styrene.[115]

Many groups from all over the world have used NMRP to synthesize new materials ever since its discovery. A review by Hawker[116] shows the range of application of NMRP to the synthesis of a great variety of molecular architectures: block copolymers, star polymers, brushes, dendritic structures and others.

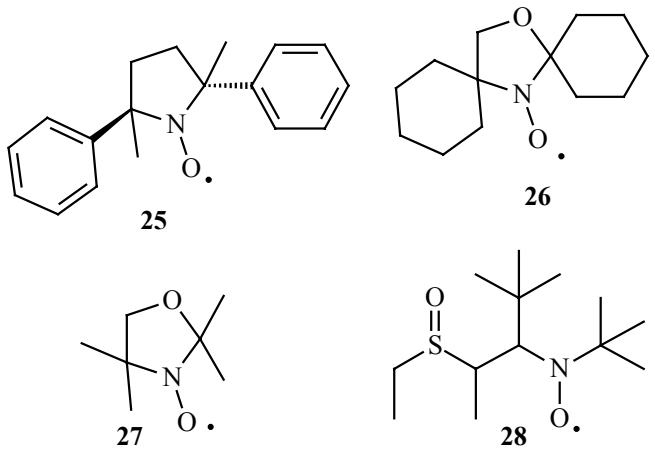

Figure 1.3. Recently synthesized nitroxide radicals used to control the radical polymerization.

Several papers have been published which report the combination of nitroxide radicals with dendrimer-functionalized chemistry. An attempt to control the diffusion of the monomer to the radical center by using a dendrimer-capped nitroxide was unsuccessful. The control observed

[110] C. Farcet; M. Lansalot; B. Charleux; R. Pirri; J. P. Vairon, Macromoleculs, *33*, 8559 – 8570, **2000**.
[111] P. J. MacLeod; R Barber; P. G. Odell; B. Keoshkerian; M. K. Georges, Macro. Symp., *155*, 31 - 38, **2000**.
[112] C. Farcet; B. Charleux; R. Pirri, Macromolecules, *34*, 3823 - 3826, **2001**.
[113] R. D. Puts; D. Y. Sogah, Macromolecules, *29*, 3323 - 3325, **1996**.
[114] Y. Muira; S. Mibae; H. Oto; N. Makamura; B. Yamada, Polymer Bulletin, *42*, 17 - 24, **1999**.
[115] E. Drockenmuller; J.-M. Catala, Macromolecules, *35 (7)*, 2461 – 2466, **2002**.
[116] C. J. Hawker, Accounts of Chemical Research, *30*, *9*,373 - 382, **1997**.

was worse than for TEMPO.[117] The authors concluded that the dendritic shell hindered the diffusion of the growing polymeric chain to the nitroxide radical, which led to an increase in the amount of termination reactions. Another approach used a dendrimer containing initiator in the NMRP, allowing synthesis of a polymer chain bearing a dendrimer on its end.[118,119]

A great variety of block copolymers have been synthesized by the NMRP technique.[120] A polystyrene-*b*-poly-*n*-butylmethacrylate copolymer was synthesized by the group of Vairon[121] using TEMPO as additive. A block copolymer of styrene and *tert*-butylstyrene was prepared by the group of Catala.[122] Lochon *et al.* reported the synthesis of block copolymers of 4-vinylpyridine and N,N-dimethylacrylamide.[123] Even tri-block copolymers can be prepared, as shown by Mariani at al.,[124] who made a polystyrene-*b*-polyphtalimide methylstyrene-*b*-polystyrene copolymer.

As in the case of ATRP the blocks of copolymer can be obtained not only by controlled radical polymerization but also by other techniques. If the polymer obtained by a different strategy is functionalized with a nitroxide moiety on its end, it can be reinitiated in the presence of another monomer to form block copolymers. In such a way block copolymers from monomers unable to be polymerized by radical polymerization can be obtained. For example, block copolymers of polytetrahydrofuran and polystyrene have been synthesized using this technique.[125,126] A combination of conventional radical polymerization and NMRP can be used for block copolymer preparation. In the first step an initiator end-capped with a nitroxide moiety is used in a normal radical polymerization. Then the temperature is elevated and controlled radical polymerization is carried out with the other monomer.[127] Poly(ε-caprolactone)-*b*-polystyrene has been obtained in this way by Yoshida and Osagawa.[128]

Random copolymers composed of chloromethylstyrene and trimethylsilylvinylbenzoate monomers synthesized by the NMRP technique have been applied in the electronics research as photoresists.[129] End-functionalized random copolymers of styrene and methylmethacrylate show affinity for the silicon surface. The affinity changes with a change of the ratio of the monomers,

---

[117] K. Matjyaszewski; T. Shiegemoto; J. M. J. Frechet; M. Leduc, Macromolecules, *29*, *12*, 4167 - 4171, **1996**.
[118] M. R. Leduc; C. J. Hawker; J. Dao; J. M. J. Frechet, JACS, *118*, 11111 - 11118, **1996**.
[119] K. Matjyaszewski; T. Shiegemoto; J. M. J. Frechet; M. Leduc, Macromolecules, *29*, *12*, 4167 - 4171, **1996**.
[120] M. Steenbock; M. Klapper; K. Müllen; N. Pinhal; M. Hubrich, Acta Polymer., *47*, 276 – 279, **1996**.
[121] C. Burguiere; M.-A. Dourges; B. Charleux; J.-P. Vairon, Macromolecules, *32*, 3883 - 3890, **1999**.
[122] S. Jousset; S. Oulad Hammouch; J.-M. Catala, Macromolecules, *30*, 6685 - 6687, **1997**.
[123] A. Fischer; A. Brembilla; P. Lochon, European Polymer Journal, *37*, 33 - 37, **2001**.
[124] M. Mariani; M. Lelli; K. Sparnacci; M. Laus, Journal of Polymer Science: Part A: Polymer Chemistry, *37*, 1237 –1244, **1999**.
[125] E. Yoshida; A. Sugita, Macromolecules, *29*, 6422 - 6426, **1996**.
[126] Y. Yagci; A. Baskan Duz; A. Onen, Polymer, *38*, *11*, 2861 - 2863, **1997**.
[127] I. Q. Li; B. A. Howell; M. T. Dineen; P. E. Kastl; J. W. Lyons; D. M. Meunier; P. B. Smith; D. B. Priddy, Macromolecules, *30*, *18*, 5195 – 5199, **1997**.
[128] E. Yoshida; Y. Osagawa, Macromolecules, *31*, 1446 - 1453, **1998**.
[129] M. Chiara Bignozzi; C. K. Ober; A. J. Novembre; C. Knurek, Polymer Bulletin, *43*, 93 - 100, **1999**.

which opens the possibility to manipulate polymer-surface interactions.[130] A variety of graft copolymers have also been synthesized by NMRP.[131,132,133]

The examples mentioned above show that the NMRP is a very powerful tool in polymer chemistry allowing a wide range of polymer syntheses. However, some limitations of the nitroxides have not yet been overcome, the most crucial of which, is the range of suitable monomers. Styrene and its derivatives are used in most cases; new radicals in some cases allow polymerization of acrylates, but many important monomers, like methacrylates cannot be polymerized *via* the NMRP. On the other hand, the molecular weights of the polymers obtained can be as much as 10 or even 20 times higher than from ATRP, and polydispersities are usually low.

1.6.2. Controlled radical polymerization mediated by stable radicals other than nitroxides

Although nitroxides are the most commonly used radicals in controlled radical polymerization, many other additives have been found to be applicable as counter radicals. There are generally two other types of the radicals, used as additives in CRP: nitrogen-centered radicals and carbon-centered radicals. Several compounds, which have been used in SFRP as additives are summarized in Figure 1.4.

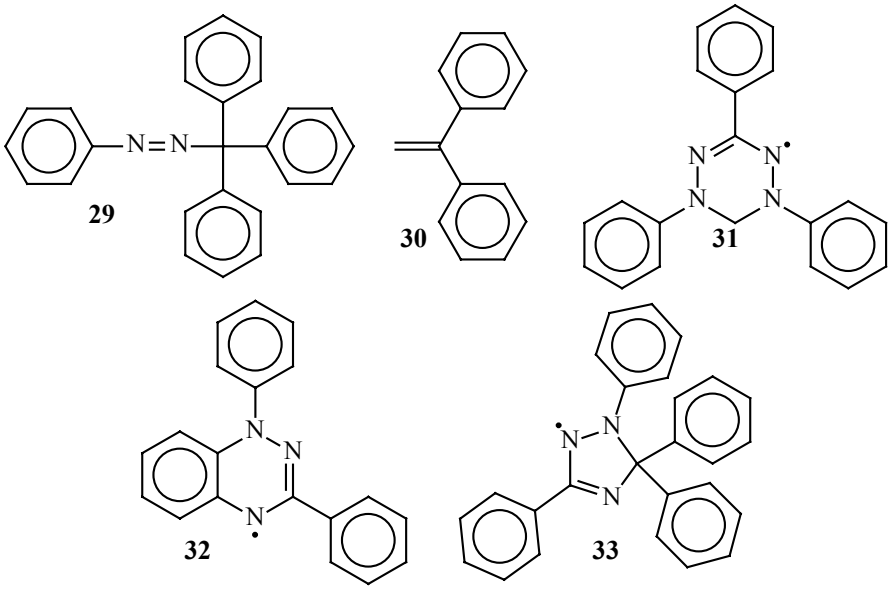

Figure 1.4. Organic additives in SFRP.

[130] P. Mansky; Y. Liu; E. Huang; T. P. Russel; C. Hawker, Science, *275*, 1458 - 1460, **1997**.
[131] I. E. Serhatli; A. Baskan Duz; Y. Yagci, Polymer Bulletin, *44*, 261 - 268, **2000**.
[132] M. Baumert; J. Heinemann; R. Thomann; R. Muelhaupt, Macromolecular Rapid Communications, *21*, 271 - 276, **2000**.

1.6.3. Carbon-centered radicals

The carbon-centered radials include different types of highly substituted ethane derivatives, which decompose forming stable radicals at elevated temperatures. These radicals are able to serve as counter radicals in SFRP. The relatively high stability of the triphenylmethyl radicals (**35**) has been long known.[134] This stability is due to the delocalization of the unpaired electron and also steric hindrance at the radical center. The radicals are stable at higher temperature but recombine upon cooling to form compound **34** (Scheme 1.13). The mechanism of the reversible deactivation of the growing species is similar to that described above for nitroxides.

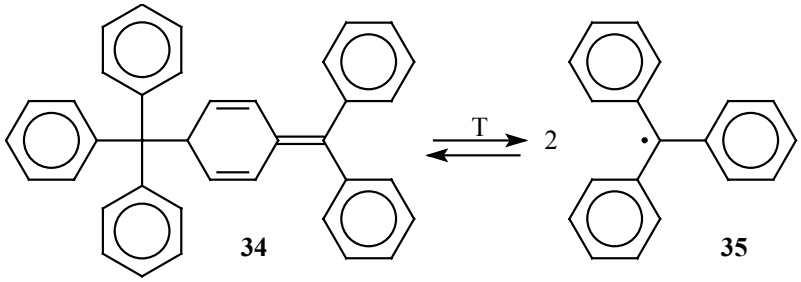

Scheme 1.13. Formation of triphenylmethyl radical (**35**) at elevated temperature

Radical polymerization of styrene initiated by the diazocompound **29**, showed some features of a controlled process, but the polymers obtained had broad polydispersity.[135,136,137] The radicals serving as counter radicals in this case were found to be triphenylmethyl radicals (**35**). Controlled radical polymerization of styrene using 1,1-diphenylethene (**30**) has been reported. The mechanism involves the reversible addition of **30** to the end of the growing polymer chain.[138]

Polystyrene-*b*-polymethylmethacrylate,[139] polystyrene-*g*-polymethylmethacrylate,[140] and polystyrene-*g*-polybutylacrylate[141] have been prepared using hindered carbon centered radicals as counter species.

---

[133] Y. Sun; D. Wan; J. Huang, Journal of Polymer Science: Part A: Polymer Chemistry, *39*, 604 - 612, **2001**.
[134] ***Organikum***; H. G. O. Becker et al., *20 Auflage*, Johann Ambrosius Barth Verlag: Heidelberg, 183, **1996**.
[135] E. V. Chernikova; E. S. Garina; M. Y. Zaremskii; A. V. Olenin; M. B. Lachinov; V. B. Golubev, Vysokomolekulyarnye Soedineniya, Ser. A, *37*, *10*, 1638 - 1643, **1995**.
[136] E. V. Chernikova; E. S. Garina; M. Y. Zaremskii; A. V. Olenin; M. B. Lachinov; V. B. Golubev, Polymer Science, Ser. A, *37*, *10*, 988 - 993, **1995**.
[137] J. R. Ebdon; T. N. Huckerby; B. J. Hunt; S. Rimmer; M. J. Shepherd; M. Teodorescu, Polymer, *39* (*20)*, 4943 - 4948, **1998**.
[138] P. C. Wieland; B. Raether; O. Nuyken, Macromol. Rapid Communications, *22*, 700 - 703, **2001**.
[139] B. Yamada; H. Tanaka; K. Konishi; T. Otsu, J.M.S. – Pure Appl. Chem., *a31 (3)*, 351 - 366, **1994**.
[140] G. Morales; R. Guerrero, Journal of Applied Polymer Science, *83*, 12 - 18, **2002**.

1.6.4. Nitrogen-centered radicals

The nitrogen-centered radicals used in controlled radical polymerization include DPBT (**32**) 1,3,5-triphenylverdazyl (**31**), and triazolinyl (**33**) stable radicals. Few results with controlled radical polymerization using these radicals as additives have been reported. The verdazyl radicals are known to reversibly bind to active carbon centered radicals. Polymerization of styrene performed in the presence of **31** shows features of a controlled process.[142] Investigations of controlled radical polymerization in the presence of the DPBT stable radical (**32**) have been performed.[143] Polymerization of styrene in the presence of DPBT was found to be controlled. Another type of nitrogen-centered radical used in controlled radical polymerization is a triazolinyl radical which will be discussed in the next section.

1.7. Triazolinyl radicals

1.7.1. Syntheses and properties

All the radicals mentioned above except for a few nitroxides are stable within the polymerization timescale and to the polymerization conditions. The differences in the polymerization behavior when they are used as additives can be explained by differences in the bond dissociation energy of the bond between the radical center and the macroradical, and in the equilibrium between the active and dormant species. Triazolinyl radical **33** has been found to be unstable in the polymerization conditions. However, radical polymerization in its presence is controlled. Moreover, it has several advantages in comparison to the previously used counter radicals.

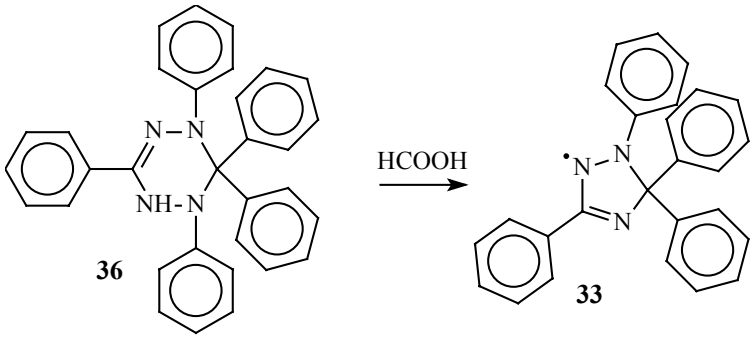

Scheme 1.14. The first approach to the synthesis of triazolinyl radical **33**.

[141] G. Morales; R. Guerrero, Journal of Applied Polymer Science, *83*, 19 - 26, **2002**.
[142] E. G. Rozantsev; M. D. Gol'dfein; A. V. Trubnikov, Russian Chemical Reviews, *55 (11)*, 1070 - 1080, **1986**.

Triazolinyl radicals were first synthesized by Neugebauer *et al.*[144] by oxidative ring contraction of tetrazole derivative **36** using formic acid (Scheme 1.14). The reaction proceed with very low yield, however it allows 1,3,5,5-tetraphenyl-Δ^3-1,2,4-triazolin-2-yl (**33**) to be obtained. The structure of **33** was confirmed by ESR spectroscopy and X-ray scattering. In order to obtain other derivatives of triazolinyl, a new synthetic strategy was developed.[145] The key reaction in the novel synthetic route (Scheme 1.15) is cyclization between commercially available benzhydrylamine (**38**) and N-phenylbenzenecarbohydrazonoyl chloride (**37**), which needs to be prepared from phenylhydrazone and benzoyl chloride in two-step reaction.[146] Following oxidation proceeds with very high yields, and isolation of the product does not cause any problems. This approach gave higher yields; however, the cyclization step (2 in Scheme 1.15) is still arduous and often proceeds with relatively low yields. Using this strategy the group of Neugebauer succeeded to synthesize a series of triazolinyl radicals, which are summarized in Table 1.2. Further, this library of compounds was used in NMR experiments in order to determine the degree of delocalization of the unpaired radical. The stability of the radical was not investigated by Neugebauer, however from the difficulties experienced by his group during NMR and ESR studies, it can be concluded that radicals having protons and non-aromatic substituents at position 1, 3, and 5 were less stable than the phenyl substituted ones. For some derivatives, the ESR measurements have not been reported.

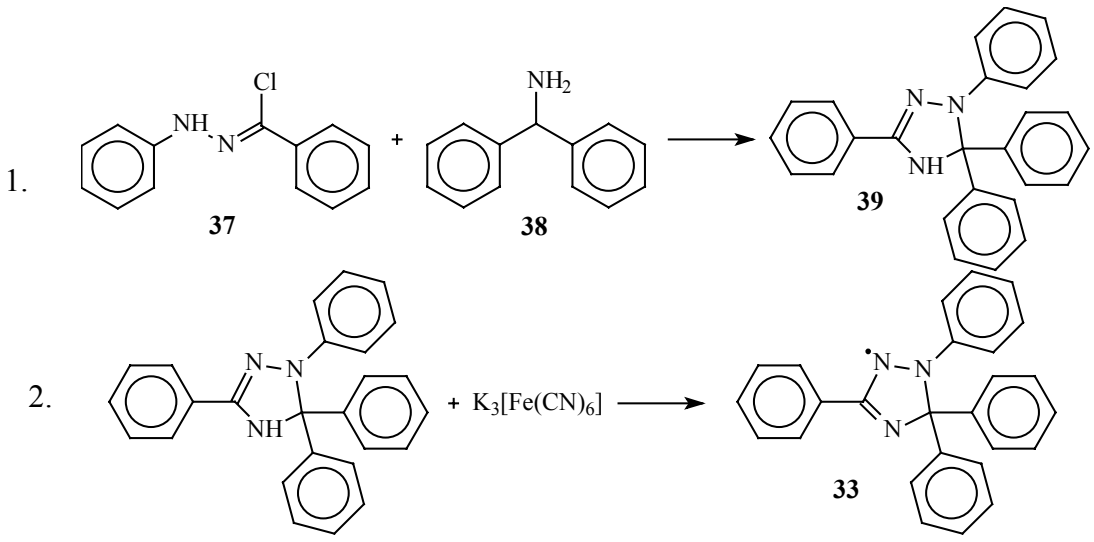

Scheme 1.15. The synthetic route for the triazolinyl radical syntheses.

[143] Unpublished results, Emma Caputo in the group of Prof. Müllen at the MPI-P
[144] F. A. Neugebauer; H. Fischer; C. Krieger, Angew. Chemie, *101*, *4*, 486 – 488, **1989**.
[145] F. A. Neugebauer; H. Fischer, Tetrahedron, *51*, *47*, 12883 – 12898, **1995**.
[146] R. Huisgen; M. Seidel; G. Wallbillich; H. Knupfer, Tetrahedron, *17*, 3, **1962**.

Table 1.2. Triazolinyl radicals synthesized by Neugebauer and coworkers, R_n are substituents at n-position of the triazolinyl ring (Figure 1.5).

R_1	R_2	R_5, R_5	N^{15}
H	H	H, H	
Ph	H	Me, Me	
Me	Ph	Me, Me	
Ph	Ph	Me, Me	
Ph	Ph	$[D_3]$Me, $[D_3]$Me	
Ph	Ph	Me, Me	4-^{15}N
Ph	Ph	Me, Me	2,4-$^{15}N_2$
Ph	Me	Ph, Ph	
Ph	Ph	Ph, Ph	
$[D_5]$Ph	$[D_5]$Ph	Ph, Ph	
Ph	Ph	[3,5-D_2]Ph, [3,5-D_2]Ph	
Ph	Ph	biphenyl-2,2´-diyl	
Ph	Ph	$[D_8]$biphenyl-2,2´-diyl	
Ph	Ph	6,6´-dimethylbiphenyl-2,2´-diyl	
Ph	Ph	5,5´-dimethylbiphenyl-2,2´-diyl	

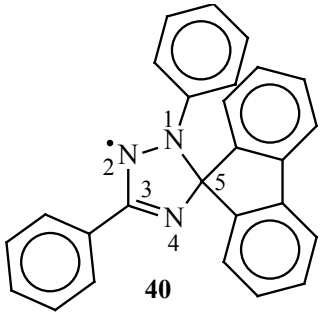

40

Figure 1.5. Stable 1´,3´-diphenylspiro[9H-fluorene-9,5´-[Δ^3-1,2,4-triazolin]-2-yl] (**40**) radical.

Later, decomposition of **33** was observed. The mechanism of the decomposition was proposed and confirmed by Steenbock and coworkers.[147] When heated, the triazolinyl **33** cleaves the substituent at the 5-position to form a phenyl radical (**42**) and a stable triazole aromatic compound (**41**) (Scheme 1.16). Also it was found that 1´,3´-diphenylspiro[9H-fluorene-9,5´-[Δ^3-1,2,4-triazolin]-2-yl] (**40**) (Figure 1.5) is stable at elevated temperatures. The stability of **40** is explained by the obvious impossibility of the fuul cleavage of the substituent at the 5-position. Interestingly, the conjugation of the unpaired electron does not spread over the carbon atom at the 5-position. However, in order to cleave the phenyl radical at the 5-position, the unpaired radical should be delivered from the 2-position of the triazolinyl ring. Therefore, there must be a conjugation between either the π-orbital of the C(carbon-3)-N(nitrogen-4) bond or *n*-orbital of

[147] M. Steenbock; M. Klapper; K. Müllen; C. Bauer; M. Hubrich, Macromolecules, *31*, 5223 - 5228, **1998**.

the nitrogen-1 and σ-bond between the carbon-5 atom and its substituent, at least in an intermediate of the decomposition process. Confirming this hypothesis Neugebauer has noticed extremely high hyperconjugation observed by NMR at the carbon-5 in the triazolinyl radical having protons as substituents at 5-position. When the protons were substituted by methyl groups at this position the interaction between the unpaired electron delocalization area and the protons of the methyl groups decreased, as indicated by the values of the coupling constant values in the NMR spectra.[148]

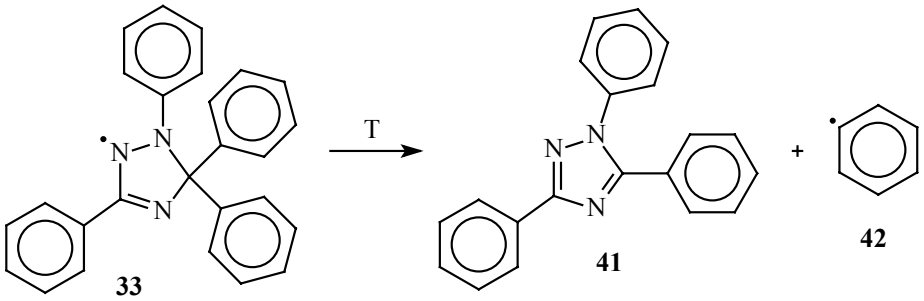

Scheme 1.16. Decomposition of the triazolinyl radical at elevated temperature.

Of course, the stability of the radicals is also influenced by the substituents at the 1- and 3-positions, due to the change of the area, over which the unpaired electron is delocalized. This is not unexpected since it is well known that extended delocalization of the unpaired electron improves stability of a radical. Conjugation of the unpaired spin with the phenyl ring at 1-position was found to be much larger than with the substituent at 3-position.

Formation of a formally similar lophyl radical **43** has been observed at low temperature under UV-irradiation (Figure 1.6). However, when the temperature was raised the radical forms a dimer.[149] Another known triazolinyl-like stable radical is the tetrazolyl radical **44**[150] (Figure 1.6).

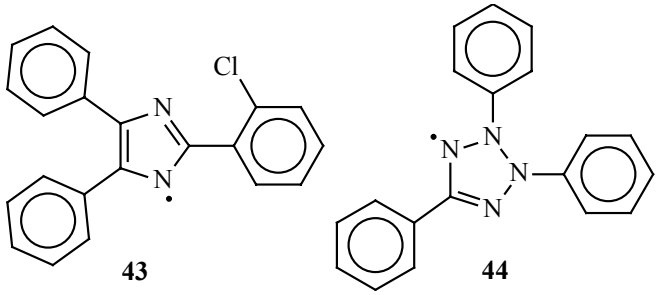

Figure l.6. Lophyl radical (**43**) obtained at low temperature by UV-irradiation and stable tetrazolyl (**44**) radical.

[148] F. A. Neugebauer; H. Fischer, Tetrahedron, *51*, *47*, 12883 – 12898, **1995**.
[149] J. Abe; T. Sano; M. Kawano; Y. Ohashi; M. M. Matsushita; T. Iyoda, Angew. Chemie, *113*, *3*, 600 - 602, **2001**.

1.7.2 Triazolinyl mediated controlled radical polymerization

Triazolinyl radicals can be used as counter radicals in SFRP, as has been shown by Colombani and coworkers.[151] Moreover, use of the triazolinyls allows regulation of the polymerization by the decomposition of the triazolinyl during the polymerization. This key-feature of the triazolinyl radical is very important in cases where an excess of counter radical is formed during the polymerization. This often happens at higher polymerization degrees due to incompletely suppressed termination reactions. Increasing the concentration of the counter radical leads to slowing down and finally stopping of the polymerization process. As a result, low molecular weight polymers and/or oligomers are formed and the conversion of the monomer is low. In the case of the triazolinyl, decomposition keeps the concentration of the counter radical at the level allowing continuation of the polymerization process. The effect is known as the self-regulation concept and will be discussed in the following sections (see Section 1.9.1).

Use of triazolinyls as additives permits the controlled radical polymerization of methylmethacrylate, *n*-butylmethacrylate, styrene and other monomers.[152] In comparison to TEMPO mediated polymerizations, controlled polymerization of methacrylates is easily achieved. Obviously it is explained by the decomposition of the excess of triazolinyl during the reaction. Under the same conditions, the increase in concentration of the TEMPO radicals stops the polymerization at early stages. Recently, controlled radical polymerization of 2-(trimethylsiloxy)ethylmethacrylate (TMSEMA) has been carried out by Brand *et al.*[153] End-functionalization of the polymer with triazolinyl moieties allowed its use in block copolymer syntheses. End-functionalized poly-TMSEMA was reinitiated by heating in the presence of styrene and poly-TMSEMA-*b*-polystyrene has been obtained. A variety of monomers should in principle be polymerizable in a controlled manner when the triazolinyls are used as additives.[154,155] The reason for this is the possibility of tuning the radical properties for specific monomer and polymerization conditions simply by change of the substituents at the 1-, 3-, and 5-position. Recent results of controlled radical polymerization of other monomers using triazolinyls as counter radicals have been obtained and will be published shortly.

---

[150] E.G.Rozantsev, M.D.Gol'dfein, A.V.Trubnikov, Russian Chemical Reviews, *55 (11)*, **1986**.
[151] D. Colombani; M. Steenbock; M. Klapper; K. Müllen, Macromol. Rapid. Comm., *18*, 243 - 251, **1997**.
[152] D. Colombani; M. Steenbock; M. Klapper; K. Müllen, Macrmol. Chem. Phys., *199*, 763 - 769, **1998**.
[153] A. Dasgupta; T. Brand; M. Klapper; K. Müllen, Polymer Bulletin, *46*, 131 - 138, **2001**.
[154] D. Colombani; M. Steenbock; M. Klapper; K. Müllen, Macrmol. Chem. Phys., *199*, 763 - 769, **1998**.
[155] M. Steenbock; M. Klapper; K. Müllen, Acta Polym., *49*, 376 –378, **1998**.

1.8. Comparison of ATRP, SFRP and RAFT

Obviously each of the controlled radical polymerization approaches has its advantages and drawbacks. The properties of ATRP, SFRP and RAFT are summarized in Table 1.3.

Table 1.3. Features of ATRP, SFRP and RAFT.[156]

Feature	System		
	SFRP	ATRP	RAFT
Monomers	styrene (TEMPO); acrylates and acrylamides (new nitroxides); methacrylates (triazolinyls)	almost all common monomers, except vinyl acetate, difficulties with nitrogen containing monomers	almost all common monomers
Conditions	sensitive to oxygen, elevated temperatures, water does not cause problems	large temperature range, tolerance to water and small amount of oxygen and inhibitor at special conditions	elevated temperatures for certain monomers, tolerance to water, sensitive to oxygen
End groups	covalently bound radical species, thermally unstable	halides, thermally stable	dithioesters, iodides and methacrylates, colored, odor, thermally and photo less stable
Additives	radical initiator, stable radical	transition metal complex, must be removed	radical initiator, transfer agent

1.9. Kinetics of SFRP

The main difference between living ionic polymerization and free radical polymerization (since fast initiation of the radical process can be achieved by *e.g.* photoinitiation) is the presence of termination reactions in the case of radical polymerization. It was shown above that the propagation rate v_p of the free radical polymerization depends linearly on the concentration of the propagating species. At the same time the rate of termination reactions is dependent quadratically on the concentration of active chains. This difference opens the possibility to decrease the termination rate more than the chains-growth rate if the concentration of the active species is lowered. In all cases of the controlled radical polymerizations, the effect of "control" is achieved by a dramatic decrease in the concentration of the propagating chains. This allows one to decrease the amount of terminated chains, which keeps the polymerization "living". A general kinetic scheme of the stable free radical polymerization is shown in Scheme 1.17. For the best

[156] ***Controlled/living radical polymerization***, ed. K. Matjyaszewski, American Chemical Society: Washington, 23, **2000**.

results, at any given time, as few as possible radicals should be active in the system. This allows one to exclude almost all termination reactions. However, in the case of only a few propagating radicals at a given time, the polymerization time becomes enormous. In order to have an acceptable polymerization time and still good control over the polymerization, a compromise between the rate of the reaction and perfection of the CRP has to be made. As a result, termination reactions occur, but are much more seldom than in conventional radical polymerization. Therefore, the process is better described by the term "controlled", rather than "living" radical polymerization. The control is understood as the possibility to regulate the amount of termination reactions; and therefore, the properties of the polymer obtained by the proper choice of the equilibrium constant K (Equation 1.9) between the active and the dormant species.

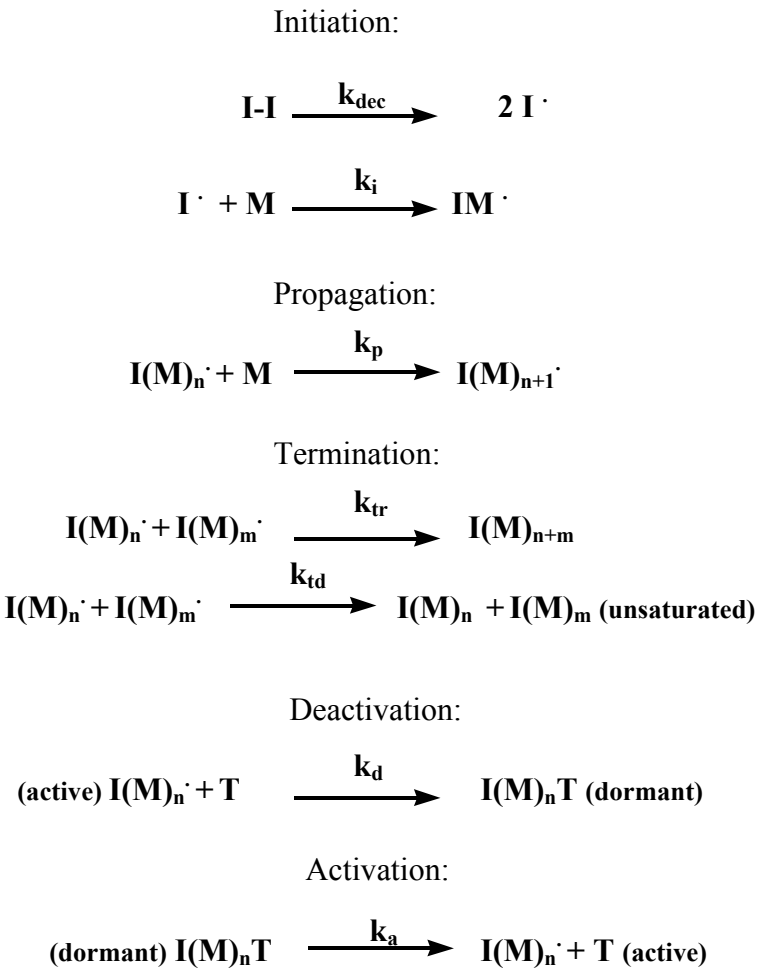

Scheme 1.17. Basic kinetic scheme of stable free radical polymerization.

The constants k_a and k_d are the rate constants of the activation and deactivation processes. Due to the requirement of low concentration of active species, k_d must be much bigger than k_a.

Or in other words, K should always be low enough to permit a low concentration of the propagating species. Rapidly after the start of polymerization, an equilibrium state is attained and the equilibrium can be described by equilibrium constant K (Equation 1.9).

$$K = \frac{k_a}{k_d}$$ **Equation 1.9**, where K is the equilibrium constant.

The values of the equilibrium constant and rate constants of the activation and deactivation vary for different monomer and counter radical pairs. For the model system of styrene polymerization in the presence of the TEMPO, a value of $K = 10^{-11}$ has been estimated.[157,158]

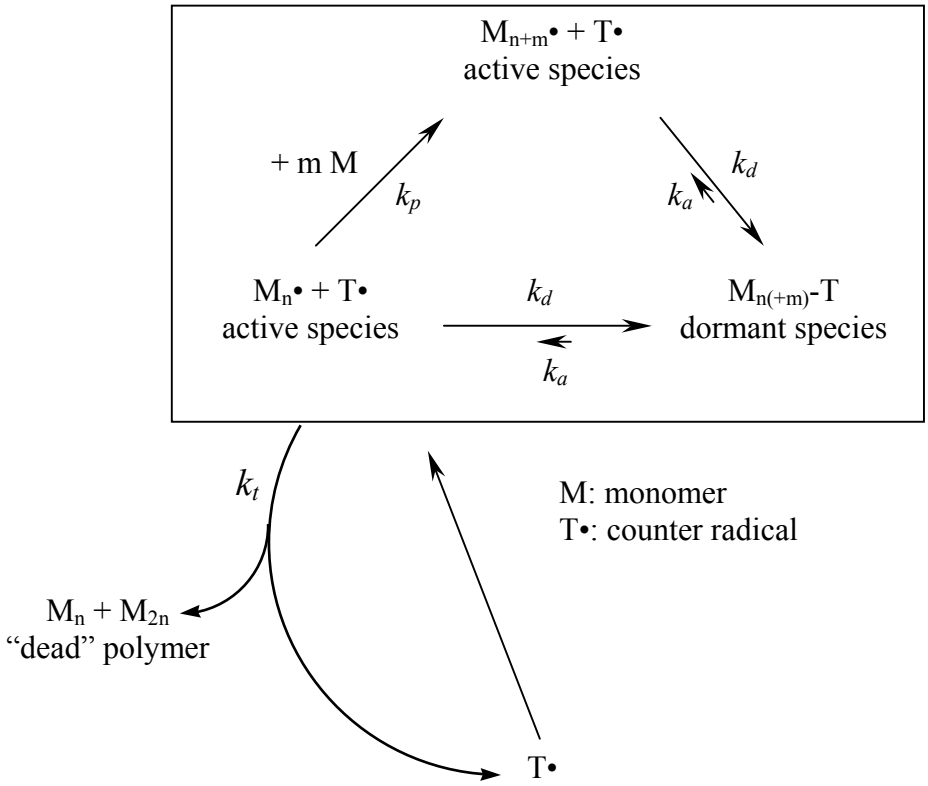

Scheme 1.18. Controlled radical polymerization in the presence of stable counter radical.

The kinetic law of stable free radical polymerization and equations for polymerization degree and polydispersity of the polymer obtained can be calculated by Equations 1.10 – 1.12.[159]

$$v_p = k_p K [I]_0 / [T\cdot]$$ **Equation 1.10**, where v_p is propagation rate, $[T\cdot]$ – concentration of the counter radical, and $[I]_0$ is concentration of the initiator at the time = 0;

$$P_n = \Delta[M]/[I]_0$$ **Equation 1.11**, where P_n is degree of polymerization, and $[M]$ – concentration of monomer;

[157] A. Goto; T. Terausghi; T. Fukuda; T. Miyamoto, Macromol. Rapid Comm., *18*, 673, **1997**.
[158] H. Fischer; J. Polym. Sci.: Part A: Polymer Chemistry, *37*, 1885 - 1901, **1999**.
[159] ***Controlled/living radical polymerization***, ed. K. Matjyaszewski, American Chemical Society: Washington, 6, **2000**.

$D = 1 + (2/p - 1)(k_p[I]_0)/(k_{dec}[T\cdot])$ **Equation 1.12**, where D is polydispersity, p is conversion.

From these equations an important feature of the controlled process can be extracted. The number average molecular weight grows linearly with conversion (Δ*[M]* is a change of the monomer concentration, and can be interpreted as conversion: $p = (1 - [M]) \cdot 100\%$, where *[M]* is a concentration at a given time) polymerization is a linear dependence of ln([M]/[M]$_0$) *versus* time. These two criteria are used to estimate the "controlness" of the polymerization. In fact these criteria are the same as were already mentioned for the living ionic polymerization (see Section 1.3). However, as it was mentioned above, one of the major problems in the SFRP is the fact that termination reactions are not suppressed completely. They cause a loss of active species and an increase in the concentration of the counter radicals. As a result of both factors the equilibrium shifts to the dormant side during the polymerization and at a certain stage the polymerization stops. The process is shown in Scheme 1.18. The "dead" polymer so formed broadens the polydispersity of the final product. Moreover, from the kinetic point of view the linearity of the plot ln([M]$_0$/[M]) *vs.* time exhibits downward curvature at the higher degrees of polymerization. In order to count the effect of the increase of the counter radical (persistent radical) concentration due to the termination reactions Fischer introduces new kinetic law leading to the new criteria of control radical polymerization, where persistent radical effect operates (Equation 1.13).[160,161] This phenomenon, called persistent radical effect, can be investigated in experiment. In this case instead of usual linearity of the plot ln([M]$_0$/[M]) *vs.* time, ln([M]$_0$/[M]) *vs.* $t^{2/3}$ is linear. Boutevin and coworkers reported polymerization of styrene in the presence of phosphorylated nitroxide derivatives where the effect is concluded to be very important.[162]

$\ln([M]_0/[M]) = (3k_p/2)(K[I]_0/3k_t)^{1/3} t^{2/3}$ **Equation 1.13**, where $[I]_0$ is concentration of the initiator at the time = 0, K – equilibrium constant (Equation 1.9), $[M]$ is concentration of the monomer, and k_p and k_t are rate constants for propagation and termination respectively.

For all monomers except styrene and its derivatives, only oligomers can be obtained from polymerizations using stable radicals (*e.g.* TEMPO) as additives. The reason for success in this case is that self-initiation of the styrene continuously provides the polymerization with new initiating species. The mechanism of self-initiation as proposed by Mayo[163,164] is given in Scheme 1.19. The new active radicals shift the equilibrium back to the active side and allow

---

[160] H. Fischer, Chem. Rev., *101*, 3581 – 3610, **2001**.
[161] H. Fischer, Journal of Polymer Science: Part A: Chemistry, *Vol. 37*, 1885 – 1901, **1999**.
[162] J.-F. Lutz, P. Lacroix-Desmazes, B. Boutevin, Macomol. Rapid Commun., 22, 189 – 193, **2001**.
[163] F. R. Mayo, Polym. Prepr. (Am. Chem. Soc., Div. Polym. Chem.), *2*, 55, **1961**.
[164] G. Moad; D. H. Solomon, ***The chemistry of free radical polymerization***, Pergamon: Oxford, 93, **1995**.

polymerization. In the case of other monomers, the equilibrium may move to the desired side only by adding new initiating species in the system. Such initiating species can be provided by continuous addition of small amounts of initiator by the use of two initiators: one of which decomposes quickly and the second one slowly within the timescale of the polymerization or by using unstable radicals. The approach where the instability of the counter radical during the polymerization provides the system with new initiating species, formed by its decomposition is known as self-regulation and is discussed in the next section.

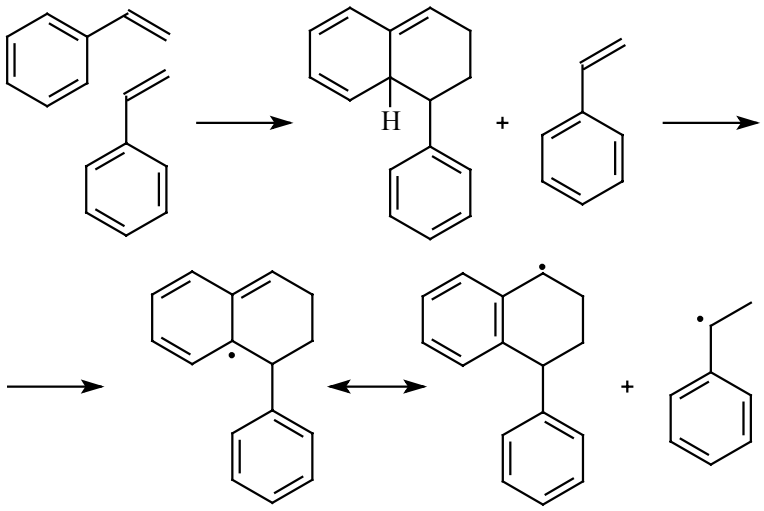

Scheme 1.19. Mayo mechanism of styrene self-initiation.

1.9.1. Self-regulation concept

A new solution of the problem caused by the shift of the equilibrium between active and dormant species has been found recently. The tendency of the triazolinyl radicals to decompose forming phenyl radicals (see Section 1.7.1) was used to provide the system with new initiating species. The phenyl radicals, produced during triazolinyl decomposition are active enough to initiate a new chain. It is because, it has been shown that phenyl radicals are actual initiating species in the case when BPO (common radical polymerization initiator) is used as the initiator.[165] The self-regulation concept is schematically shown in Scheme 1.20.

Use of the triazolinyl radical **33** as an additive in controlled radical polymerization of styrene led to poorer control in comparison to that observed when TEMPO was used.[166] The polydispersity increased to almost 1.5 and deviations from linearity in the characteristic plots ($\ln([M]/[M]_0)$ *versus* time and M_n *versus* conversion) were observed, especially at higher

[165] G. Moad; D. H. Solomon, ***The chemistry of free radical polymerization***, Pergamon: Oxford, 69, **1995**.

conversions. This result can be explained by two factors. First is the equilibrium between the dormant and the active species, which is probably more on the active side, due to the reduced strength of the bond between the macroradical and the counter radical. The reason for that is the weakening of the C-N bond (in the case of the triazolinyl counter radical) as compared with the C-O bond (in the case of the TEMPO counter radical) formed by addition of the chains to the counter radicals respectively. Another factor is the formation of new initiating species, which in the case of styrene adds to self-initiation. Both processes lead to the formation of more active radicals than is necessary. These factors cause some loss of control of the polymerization. However, when the spiro-triazolinyl **40**, which is stable at the polymerization conditions, was used as an additive, the polymerization was well controlled. Here due to the stability of the additive the additional initiation during the polymerization does not occur. Therefore, the control over the polymerization is restored. In the case of other monomers unable to self-initiate, the decomposing triazolinyl radical is only an "equilibrium shifter". Therefore, the controlled radical polymerization with triazolinyls can be realized for those monomers, which are not polymerizable with conventional stable radicals *i.e.* methacrylates. This has been proven by their successful use in polymerizing methylmethacrylate and *n*-butylmethacrylate, with which polymerization using the TEMPO failed. Attempts to polymerize methylmethacrylate using the stable spiro-triazolinyl **40** as additive similarly to the TEMPO resulted in oligomer formation.

An important point is that only those triazolinyl radicals, which are free (not bound to a macroradical) are able to undergo decomposition. In the beginning of the polymerization, when no dead polymer has yet formed, the equilibrium is effective. It allows the polymerization of the monomer and additional initiation is not required. Most of the triazolinyl radicals are bound to the macroradical; therefore, their decomposition is diminished. As the polymerization proceeds, dead chains appear and triazolinyl radicals become free simultaneously. These free radicals are not connected to a macroradical and start to decompose. The phenyl radicals so formed again participate in the SFRP equilibrium as initiator. They capture any excess of the triazolinyls and the equilibrium allows further continuation of the polymerization. Hence the radicals by themselves determine the rate of the reinitiation process. The rate of reinitiaton depends on the nature of the radical, and what is important, on the rate of termination reactions. This is a big advantage in comparison to self-initiation, where the rate of appearance of new initiating species is not dependent on the rate of termination reactions.

[166] M. Steenbock; M. Klapper; K. Müllen; C. Bauer; M. Hubrich, Macromolecules, *31*, 5223 - 5228, **1998**.

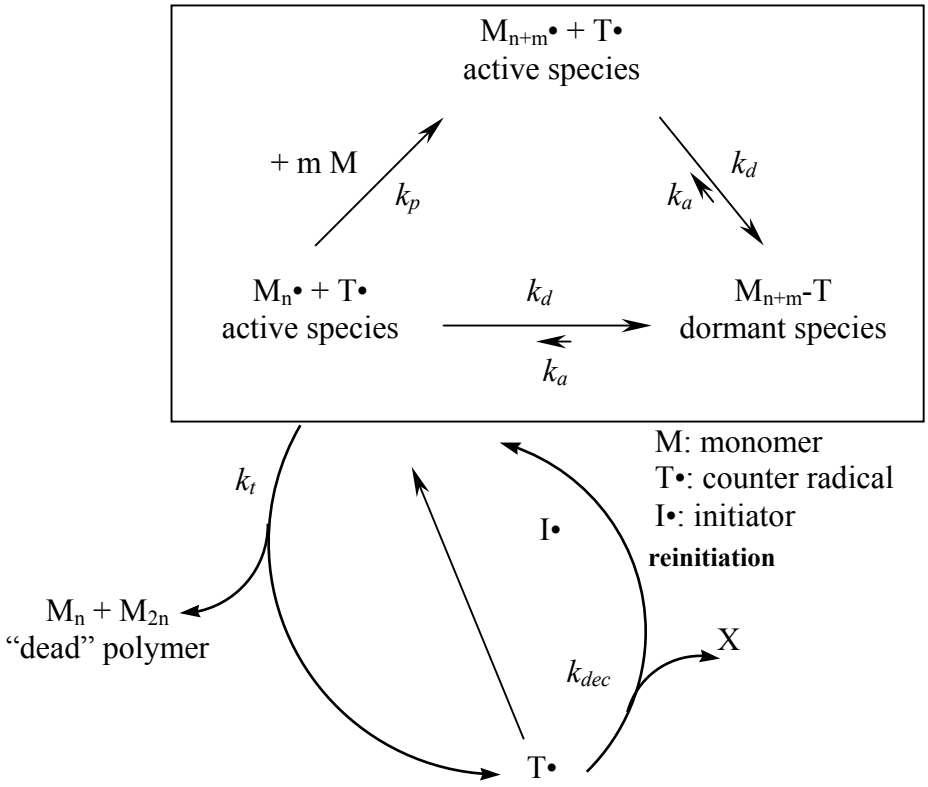

Scheme 1.21. Illustration of the mechanism of self-regulation concept in stable free radical polymerization.

Tuning the radical's properties is possible. It opens possibilities for varying the rate of the decomposition of the radical and so influences the self-regulation. The nature of the triazolinyl can be tuned also to allow variation of the affinity of the radical to the growing macroradical. By changing this affinity between the triazolinyl and macroradical it is possible to influence the equilibrium. As a result, all the properties of the triazolinyl mediated SFRP can be tuned separately, which gives fuller control over the polymerization and should allow polymerization of any monomer by using various triazolinyl derivatives and reaction conditions.

1.10. Materials, academic and industrial prospects

Polymers having narrow molecular weight distribution are not trivially prepared on a large scale, since until recently these polymers could be prepared only by anionic polymerization. Such polymers have special properties, which are often different from the properties of similar materials with broad molecular weight distributions. Using controlled radical polymerization, polymers from a wide range of monomers with low polydispersity can be synthesized without the rigorous conditions required for the anionic polymerization.

Block copolymer syntheses are one of the most important goals in polymer science at the moment. Most polymers are not miscible with each other and sometimes even samples of the

same polymer with different molecular weights cannot be mixed. In the same time the properties of materials consisting of a mixture of a monomeric units in different combinations are very attractive. One way to overcome the problems with miscibility of the polymers is preparation of the block copolymers. Block copolymers have very attractive properties for surface modification and compatibilization of materials. Again, as in the case of polymers with narrow molecular weight distribution, until recently, the only way to synthesize block copolymers was ionic polymerization. Controlled radical polymerization now allows block copolymer syntheses under milder conditions. Many other kinds of macromolecular architectures, for example, star, gradient, graft, branched, and hyper-branched polymers and copolymers now have been prepared by controlled radical polymerization.

The simplicity of controlled radical polymerization is its greatest advantage and an important point for the possible industrial development of the technique. However, drawbacks which have been mentioned above, do not currently permit wide-spreading of controlled radical polymerization in industrial applications. It should be possible to overcome some of them by improving the properties of the processes used. The industrial potential mentioned above underlines the importance of further investigations into the field of controlled radical polymerization.

2. Goals of the current work

The importance of the SFRP and its good prospects for future industrial use and practical applications have been discussed above. Investigations into the controlled radical polymerization with triazolinyl radicals as additives have been ongoing in the group of Professor Müllen at the Max-Planck-Institute for Polymer Research for several years. The work was focused on the development of new additives for controlled radical polymerization based on the triazolinyl radical **33**, which might allow widening the range of monomers suitable for the CRP and block copolymer syntheses. The results achieved have demonstrated good progress, which however, needs to be further developed. The self-regulation concept established by the group gave the prospect for future use of the triazolinyls as smart agents in the CRP, providing the regulation of the process by them. In October of 1999 the current project was started. At that time, the self-regulation concept was only recently established and required verification and further development. A promising way to clarify the role of decomposition of the radical on its behavior as a counter radical, was by changing the stability of the utilized triazolinyl. This can possibly be done by systematic variation of the substituents on the triazolinyl ring. The subject of this work, which is not only a separate project, but also a part of wider research into this field, is the syntheses of 5-substituted triazolinyl radicals and investigation of the influence of the substituent on the self-regulation of the stable free radical polymerization.

The specific goals set for this work were:

1. *Syntheses of triazolinyl derivatives with various substituents at the 5-position.* As has been shown (see Section 1.7.1), the substituents at the 5-position of the triazolinyl ring participate in the decomposition process. Therefore, it must be possible to change the rate of the decomposition by modifying the cleaved radical. The first examples of such kind have been already mentioned: the spiro-triazolinyl **40** is very stable, in the same time triazolinyls having aliphatic substituents at this position show lower stability as compared to **33** (Figure 2.1).

   For instance introducing electron donating (amino, ether groups) or withdrawing substituents (halogens, acyl groups) may influence the stability of the radical *via* a change of electron density in the phenyl ring of new-formed radical (Scheme 2.1). It is of interest to investigate how the properties of the radical will be changed if the phenyls are substituted with heteroaromatic substituents with different electron density on the ring, such as, for example, pyridine (electron-poor) or thiophene (electron-rich). Another approach is the substitution by the radicals bringing to the molecule special physical properties, in particular, solubility. So oligoethyleneglycole chains can be used to provide

water solubility. Siloxane or perfluorinated substituents often help to solubilize molecules in supercritical carbon dioxide, which becomes more and more important solvent in the industry (Figure 2.2).

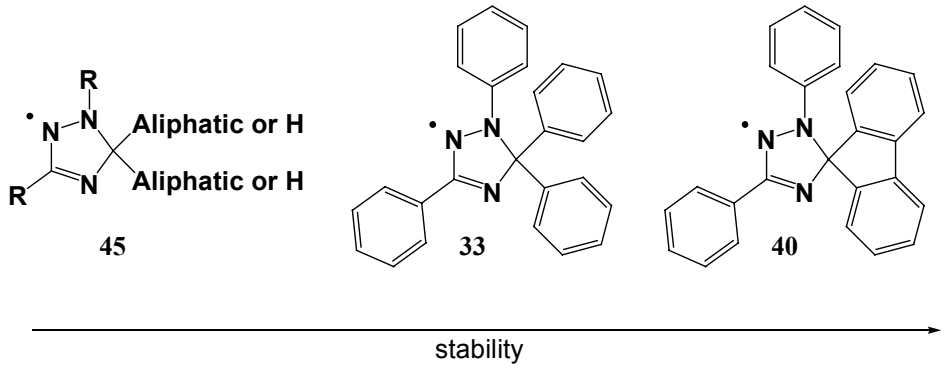

Figure 2.1. Stability of known triazolinyls depending on the substituent at the 5-position.

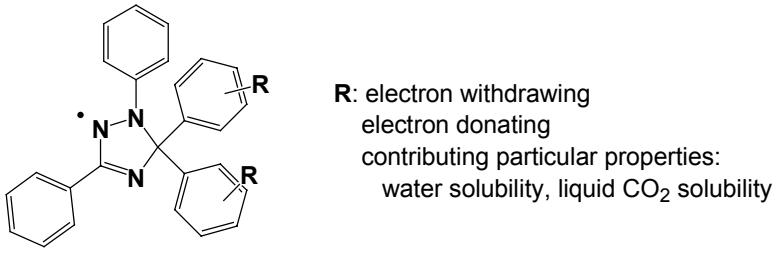

Figure 2.2. Target substituents for syntheses of new triazolinyl derivatives.

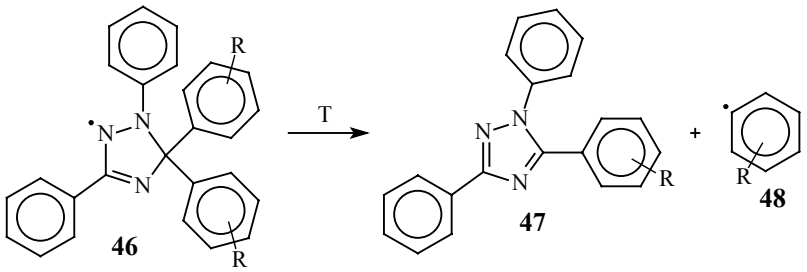

Scheme 2.1. Decomposition of triazolinyl radicals at elevated temperature.

2. *Determination of the influence of the substituents at the 5-position on the stability of the radical.* The substituent at the 5-position influences stability of triazolinyl as it was already mentioned (see Section 1.7.1). Therefore, it is of interest to find out, which change in the stability will be observed when the phenyls (in the case of **33**) are substituted with other groups. For that, the stability of the radicals at elevated temperatures will be determined. Electron spin resonance is very useful method in this case, since it allows following the change of the concentration of the radical with time. Such experiments will permit determination of the rate constants and half-life times for

the decomposition process at different temperatures. Having determined theses values at more than two different temperatures within narrow temperature range (< 50° C) the Arrhenius equation will allow calculating the activation constants of the decomposition within this temperature range. Since controlled radical polymerization experiments in the presence of triazolinyl are carried out in the temperature range 70° C - 100° C, it will give the possibility to calculate the rate constants of the decomposition at any temperature in this range without performing additional experiments.

3. *Kinetic investigations of the polymerizations of different monomers depending on the stability of the triazolinyl used as additive.* In order to better understand the influence of the stability of the radicals on the polymerization behavior, kinetic investigations will be performed. The development of conversion, molecular weights, and polydispersity with time will be followed during the reaction. Conversion will be determined by either gravimetrical analyses or gas chromatography. Molecular weights and polydispersity index will be measured using gel permeation chromatography. Obtained data will permit construction of the graphs $\ln([M]/[M]_0)$ *versus* time and M_n *versus* conversion, which are the criteria used to assess controlled radical polymerization. Initially, the experiments will be focused on the polymerizations of styrene and methylmethacrylate mediated by differently stable triazolinyls, in order to reveal the differences in the process of polymerization. The polymerization conditions, if possible, will be kept constant for one monomer in order to perform direct comparison of kinetic graphs. Further, in the case that these experiments are successful, the range of the monomers will be widened. Preference will be given to methacrylates, since they are difficult to be polymerized by other stable free radical polymerization approaches.
4. *Verification of the self-regulation concept, on the basis of the results of kinetic investigations.* Self-regulation concept predicts that the polymerization of monomers such as methylmethacrylate, unable to self-initiate the polymerization, will be possible with unstable radicals such as triazolinyl. In the same time, the polymerization of styrene does not need the additional initiation provided by the decomposition of triazolinyl (see Sections 1.9 and 1.9.1). Therefore, the higher the stability of the triazolinyl radical is, the higher is the expected control over the polymerization of styrene. Furthermore, the control over polymerization of MMA should be observed when triazolinyl with a certain rate of decomposition is used. Determination of the radical with the most applicable for the polymerization of MMA decomposition rate will provide the most suitable additive for achieving efficient control over the polymerization of this monomer. Both more and less stable radicals in this case should give worse results; in the case of more stable

radicals polymerization should stop at earlier or later stage, in the case of less stable radicals, control over the polymerization should decrease. If this behavior is observed, this will give additional proof of the importance of the additional initiation provided by triazolinyls, and will confirm the validity of the self-regulation concept.

5. *Syntheses of block copolymers.* One of the major advantages of the controlled radical polymerization is the possibility to synthesize block copolymers with even more advanced macromolecular structures. Therefore, polymers prepared by triazolinyl mediated controlled radical polymerization will be tested for possible chain elongation with different monomers: styrene, methacrylates, acrylates, *etc*. This will be done with polymer precursors taken at different degrees of polymerization and from polymerizations in the presence of various triazolinyls for the estimation of the influence of the conversion on the efficiency of the block copolymer preparation. The formation of block copolymers will be monitored by change in the molecular weights before and after block copolymer preparation by GPC.
6. *Application of the synthesized radicals to controlled polymerization in various conditions.* The synthesis of triazolinyl radicals with substituents providing solubility of the radicals in water or supercritical CO_2, if successful, will open a door to triazolinyl-mediated polymerization in these solvents. Therefore, controlled radical polymerization of suitable monomers in these media will be attempted.

3. Results and discussion

3.1. Planning of syntheses of new triazolinyl derivatives

The importance of the substituents at the 5-position of the triazolinyl ring for its stability has been previously established; therefore, syntheses of new derivatives were planned.

Initially, due to the very limited literature data about the functional substitution of the triazolinyls, several criteria were set to choose the functionalities to be introduced in the triazolinyl structure. The most promising way to change the stability of the radical was variation of electron density in the aromatic rings at the 5-position. Therefore, both electron-withdrawing groups such as F, Cl, Br, $COCH_3$, NO_2, CF_3, and electron donating groups (amino groups, OCH_3) were planned to be introduced. Another important goal was solubilization of the radical in water and supercritical carbon dioxide. For this, phenyl rings bearing oligosiloxane derivatives or perfluorinated alkyl chains for CO_2 solubilization and oligoethyleneglycole chains for water solubilization had to be introduced. An interesting approach is the possible synthesis of heteroaromatic analogues of the triazolinyl **33**. The substituents of interest planned to be introduced at the 5-position of triazolinyl are summarized in Figure 3.1.

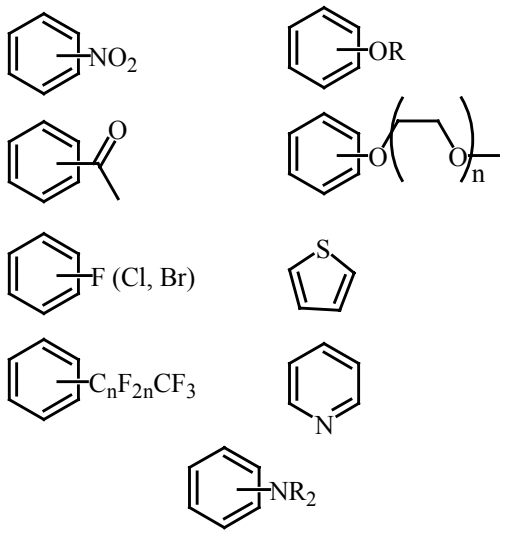

Figure 3.1. Planned substituents to be introduced at the 5 position of triazolinyl **33**.

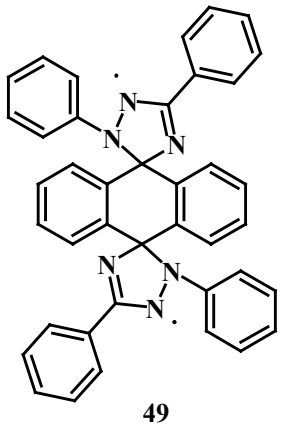

49

Figure 3.2. Triazolinyl biradical.

A biradical compound (**49**) structurally driven from anthraquinone is another triazolinyl derivative of interest (Figure 3.2). In the case of successful synthesis of this derivative it might be possible to make the mechanism of decomposition of the radical clearer by investigating the possible interactions between two radical centers by ESR.

The choice of the substituents was also based on the commercial availability or relative simplicity of the syntheses of the initial compounds. The synthetic scheme of Neugebauer has been proven to be the most effective way to triazolinyls to date (see Section 1.7.). It involves a condensation of N-phenylbenzenecarbohydrazonoyl chloride (**37**) with benzhydrylamine derivatives (**50**) (Scheme 3.1). Since the benzhydrylamine derivatives used in this approach, except benzhydrylamine itself are not commercially available, they had to be synthesized.

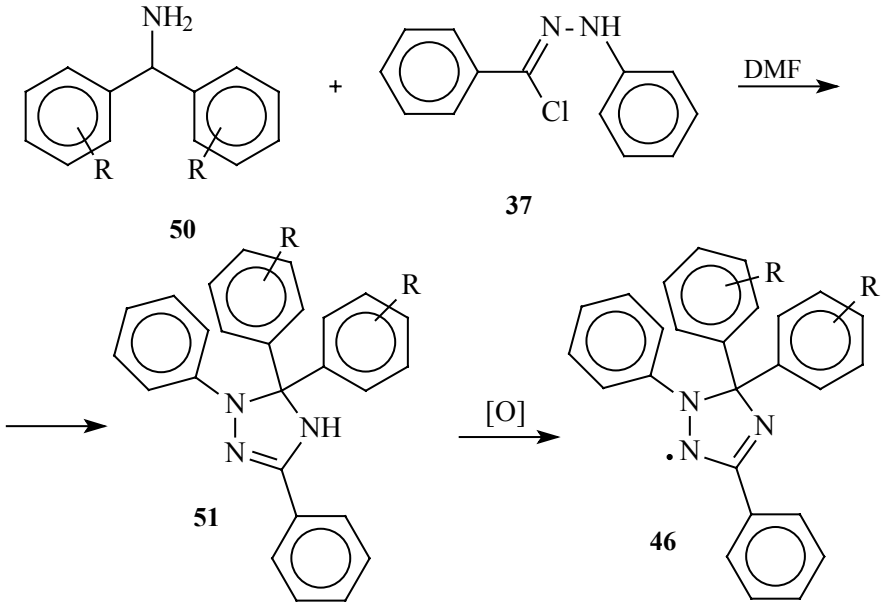

Scheme 3.1. Synthetic route to the triazolinyl radical offered by Neugebauer.

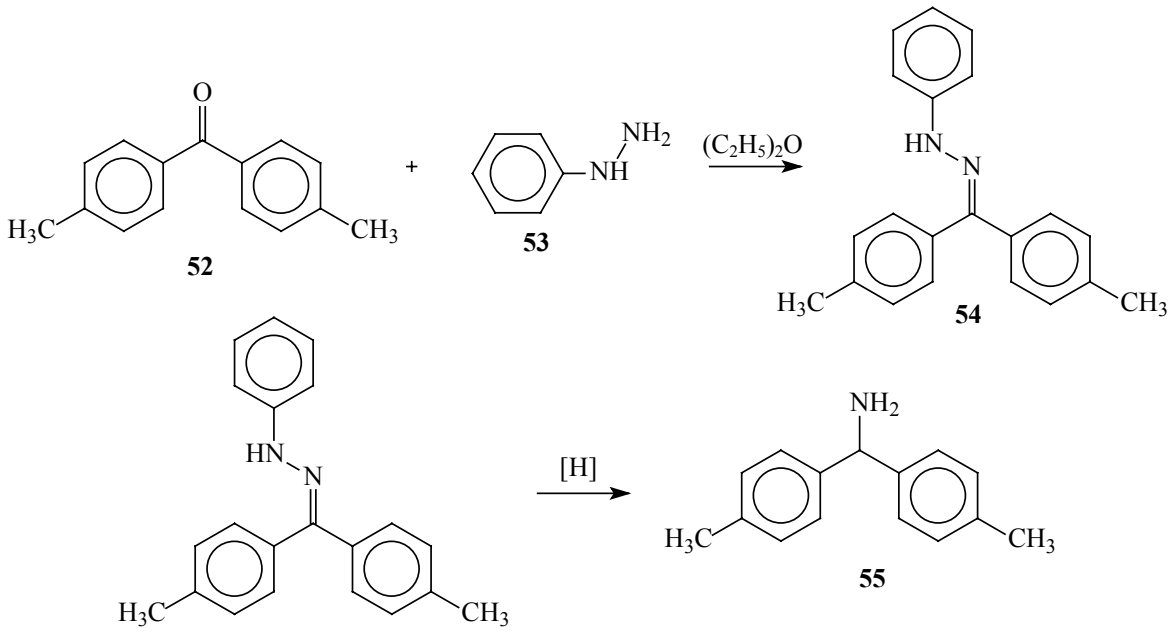

Scheme 3.2. Synthesis of 4,4`-methylbenzhydrylamine (**55**) *via* hydrazone carried out previously.

For the syntheses of various benzhydrylamine derivatives, a synthetic route allowing preparation of substances with different functional groups had to be developed. It must be

tolerant to a wide range of functional groups and allow multigram syntheses of benzhydrylamine derivatives. The last criterion is necessary due to low yields achieved in the step for the preparation of triazolin cycles **51**. Previously Langela[167] has achieved synthesis of such amines by two different methods. He successfully synthesized 4,4´-methylbenzhydrylamine (**55**) *via* formation of hydrazone **54** (Scheme 3.2). The formation of hydrazone proceeds with high yields in boiling toluene with addition of catalytic amounts of toluenesulfonic acid. The second step requires more drastic conditions. For instance, the reduction of hydrazone **54** to amine **55** is realized by sodium in boiling ethanol. For synthesis of 4,4`-fluorobenzhydrylamine (**58**), Langela used another strategy. Namely, it was Gabriel synthesis (Scheme 3.3). However, this approach is complicated due to facile hydrolysis of bromide **57** to the benzhydrol derivative; the sensitivity of diphenylmethylhalides to moisture is well known[168] (Scheme 3.4). As the result, the purification is complicated and involves fractional distillation, which is impossible for bromides with higher boiling points.

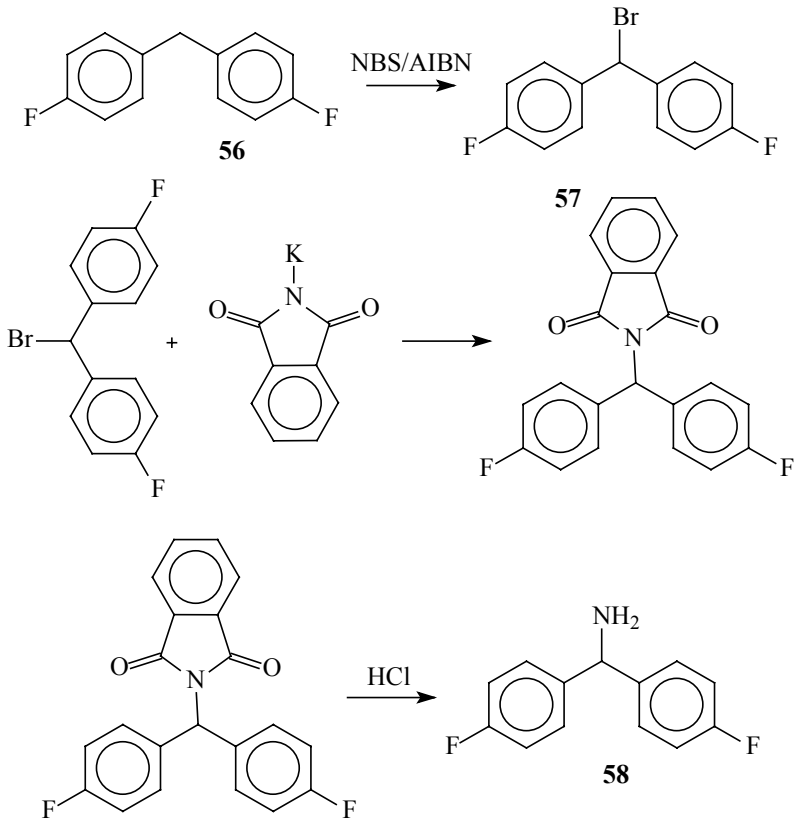

Scheme 3.3. Synthesis of 4,4`-fluorobenzhydrylamine (**58**) by Gabriel synthesis.

[167] M. Langela, ***Diploma Thesis***, Johannes-Gutenberg-University/Max-Planck-Institute for Polymer Research: Mainz, **1999**.

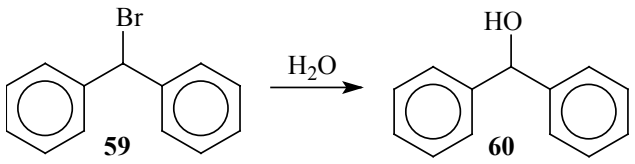

Scheme 3.4. Hydrolysis of diphenylmethylbromide **59** to benzhydrol **60**.

3.2. Development of synthetic route to benzhydrylamine derivatives

3.2.1. Previously used methods

Initially the synthetic route *via* the hydrazone formation offered by Langela was attempted to be applied to other benzophenone derivatives. In spite of the drastic conditions, this method looked more promising in comparison to the Gabriel syntheses, which needs very dry conditions and involvement of bromination realized by radical mechanism. Another argument to choose the hydrazone route is the large range of commercially available benzophenone derivatives, which can be used as starting compounds for the syntheses. The method was applied to the syntheses of 4,4`-methoxybenzhydrylamine (**62**) and 4,4`-chlorobenzhydrylamine (**64**) (Scheme 3.5). However, in both cases the reduction step failed. The use of Na/alcohol, initially suggested by Langela returned only initial hydrazone in the case of methoxy derivative, and in the case of chloro derivative significant cleavage of chlorine was observed. Use of hydrogenation over palladium on carbon 10% in sulfuric acid or mixture of acetic acid and methanol was also not effective.

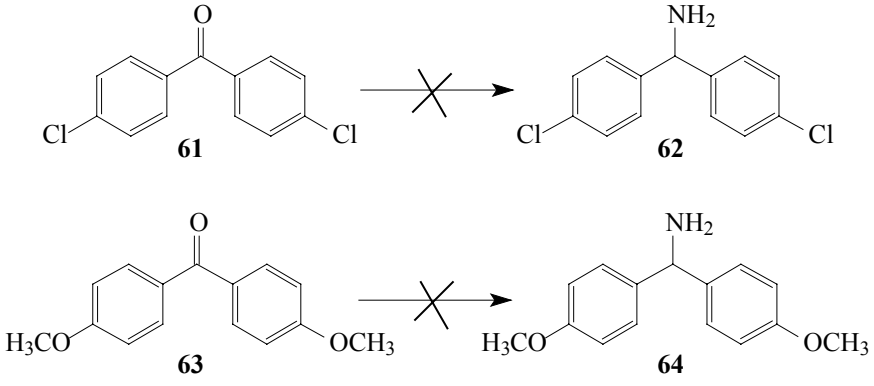

Scheme 3.5. Attempts to syntheses of 4,4`-methoxybenzhydrylamine (**64**) and 4,4`-chlorobenzhydrylamine (**62**) via hydrazones.

[168] J. D. Roberts; M. C. Caserio, ***Osnovy Organicheskoi Khimii***, Mir: Moscow, *2*, 344, **1978**.

As the result, even more drastic conditions for the reduction step must be used. Use of nickel aluminium alloy together with hydrogen at high pressure has been reported to reduce many kinds of hydrazones to amines. However, the simultaneous cleavage of functional groups such as halogens has been observed under these conditions.[169] As the result, the synthetic route *via* the hydrazones was considered to be unacceptable as a general method for preparing a variety of benzhydrylamines. Since the previously used synthetic routes have been found unsatisfactory for large scale synthesis of benzhydrylamine derivatives, a new route had to be developed.

3.2.2. Synthetic route *via* oximes

Due to easy accessibility of the benzophenone derivatives, attempts to find other applicable synthetic methods to convert the ketone functionality to the amine were made. Direct synthesis of amines from benzophenone derivatives *via* reductive amination with cyanohydridoborate anion was unsuccessful (Scheme 3.6). This could be due to a relative steric hindrance of the benzophenone derivative. Borsch and coworkers reported a drop in the yields of this reaction in the order aldehydes > alkyl, alkyl ketones > alkyl aryl ketones.[170,171]

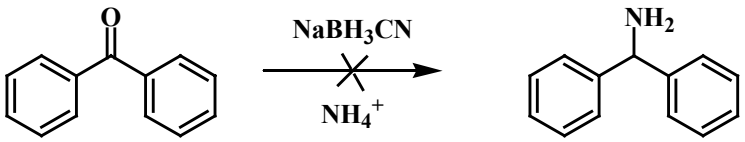

Scheme 3.6. Reductive amination of benzophenone.

A second approach was to use hydroxylamine in order to convert the ketone to the oxime with following reduction step, leading to the target amine (Scheme 3.7). This method proved to be very efficient and was used for the syntheses of most benzhydrylamine derivatives prepared during this work. The major draw back of this synthetic route is intolerance to functional groups sensitive to the reduction step; including the nitro and acyl groups planned to be involved in the syntheses. Therefore, for these derivatives another synthetic route had to be found. This will be discussed in Section 9.9.

[169] L. K. Keefer; G. Lunn, Chemical Reviews, *89*, *3*, 459, **1989**.
[170] R. F. Borch; H. D. Durst, JACS, *91*, *14*, 3996 - 3997, **1969**.
[171] R. F. Borch; M. D. Bernstein; H. D. Durst, JACS, *93*, *12*, 2897 - 2904, **1971**.

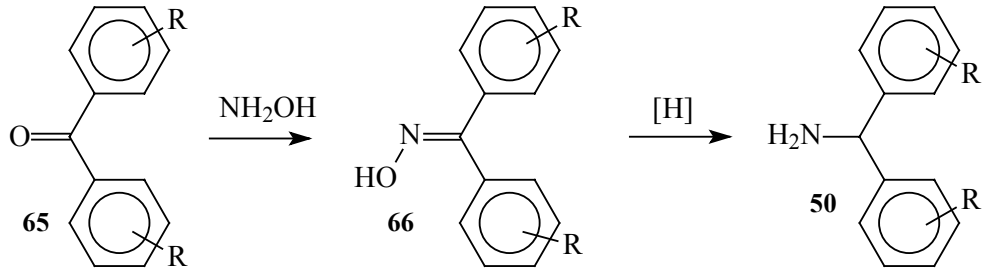

Scheme 3.7. Synthetic route to benzhydrilamine derivatives *via* oximes.

3.3. Syntheses of benzhydrylamine derivatives

3.3.1. Synthesis of 4,4`-(perfluoro-*n*-hexyl)benzophenone (73) and 4,4´-{2-[2-(2-methoxy-ethoxy)-ethoxy]-ethoxy}benzophenone (70)

4,4`-(Perfluoro-*n*-hexyl)benzophenone (**73**) and 4,4´-{2-[2-(2-methoxy-ethoxy)-ethoxy]-ethoxy}benzophenone (**70**) are the only commercially unavailable derivatives within the range of all used for syntheses of benzhydrylamines benzophenones. Therefore, they had to be synthesized. For the synthesis of **70** commercially available triethyleneglycole monomethyl ether was initially converted to methyl tosyl ether with a yield of 71 %, in order to introduce a better leaving group. It was followed by nucleophilic substitution by phenolates of 4,4'-dihydroxybenzophenone **69** to give the target compound (Scheme 3.8). Both reactions proceed with moderate yields and easily allow purification by column chromatography.

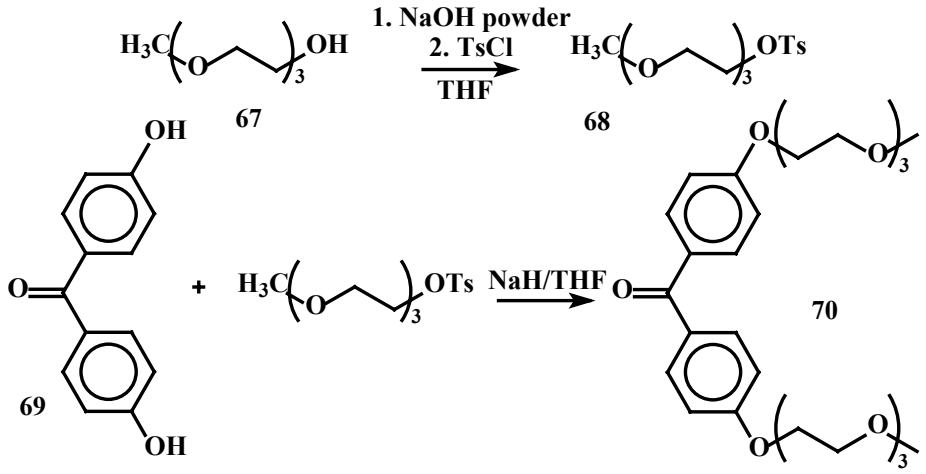

Scheme 3.8. Synthesis of 4,4´-{2-[2-(2-methoxy-ethoxy)-ethoxy]-ethoxy}benzophenone (**89**).

Preparation of **73** was a straightforward one-step synthesis (Scheme 3.9). The procedure was similar to the coupling reaction described in the literature[172,173] which uses Cu powder and a catalytic amount of 2,2`-bipyridyl in DMSO. The yield of the reaction was 65 %, however, due to poor solubility of the product, it is easily purified by recrystallization.

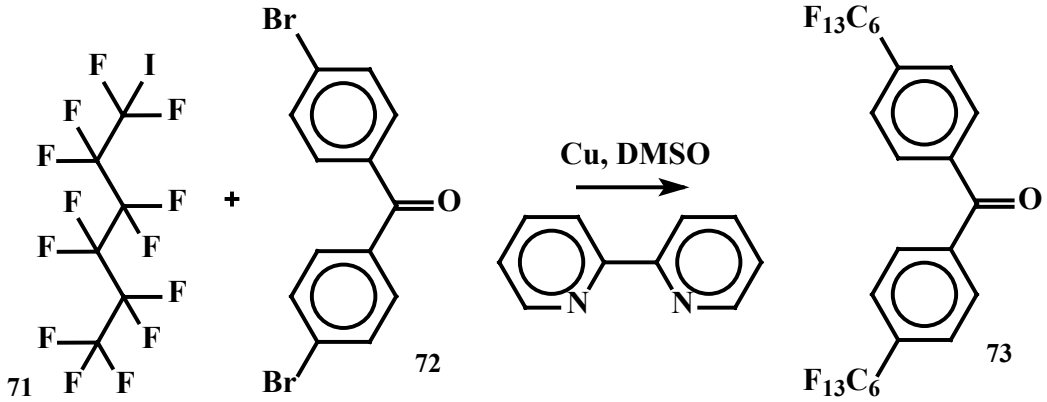

Scheme 3.9. Synthesis of 4,4`-diperfluoro-*n*-hexylbenzophenone (**73**).

Although these two benzophenone derivatives are not commercially available, they both can be easily prepared on a multi-gram scale from inexpensive precursors. Therefore, the following preparation of the corresponding benzhydrylamines is possible.

3.3.2 Syntheses of benzophenone oxime derivatives

In the first step of the developed synthetic route, the ketones (**65**) are transformed to the oximes (**66**) (Scheme 3.10). Two various methods were used to accomplish this step. The first method used a boiling water/ethanol mixture as reaction media. The mixture of solvents chosen allowed partial solubilization of both the ketone and the oxime, which generally have very different solubility properties. The oximes are more polar and require more polar solvents in order to be dissolved. Sodium hydroxide was used as a base in order to prepare the free form of hydroxylamine from its hydrochloric salt. This reaction usually proceeded in high or even quantitative yield. The procedure is similar to that described by Lee and Newmann.[174] The only exception was in the case of 4,4`-diphenylbenzophenone oxime (**72**), which reacted in moderate yields (60 %), probably due to the poor solubility of both the ketone and the oxime in the reaction media. In some cases, for example for the syntheses of 9,10-anthraquinone dioxime (see Section 9.1.2), di(2-thiophenyl)ketone oxime (see Section 5.12), and 4,4`-(perfluoro-*n*-

[172] V. C. R. McLoughlin; J. Thrower, Tetrahedron, *25*, 5921 - 5940, **1969**.
[173] W. Chen; J. Xiao, Tetrahedron Letters, *41*, 3697 - 3700, **2000**.

hexyl)benzophenone oxime (**91**), another approach had to be applied. It was previously used for preparation of 9,10-anthraquinone dioxime.[175,176] This procedure utilizes pyridine as both the reaction media and the base, abstracting HCl from the hydroxylamine salt. The yields from the second method were similar, or even higher, than those from the first one, as the solubility of the products and reagents in pyridine is better than in water/ethanol mixture. Use of the strong base (NaOH) and water is not necessary in this case. In contrast to the first method, this procedure allowed preparation of 9,10-anthraquinone dioxime, which could not be prepared in water/ethanol reaction medium. However, the difficulty of removing the pyridine from the product and its unpleasant odor are major drawbacks of the second procedure. Fortunately, pyridine does not influence the following reduction step, so traces of pyridine can be left in the product and removed after the reduction step. The yields and conditions of the oxime preparation step are summarized in Table 3.1.

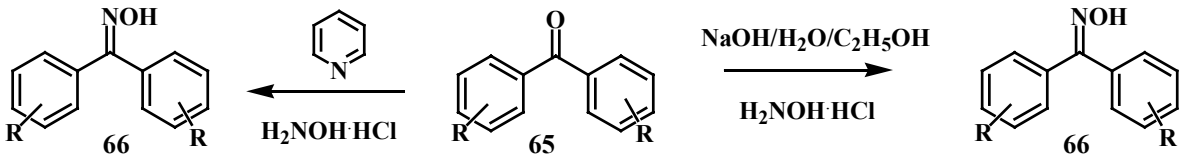

Scheme 3.10. Synthetic approaches to benzophenone oxime derivatives.

Table 3.1. Oxime synthesis step datasheet.

Oxime	Method	The yield, %
4,4`-dichlorobenzophenone oxime (**104**)	C_2H_5OH/H_2O/NaOH	93
4,4`-dibromobenzophenone oxime (**116**)	C_2H_5OH/H_2O/NaOH	98
4,4`-difluorobenzophenone oxime (**114**)	C_2H_5OH/H_2O/NaOH	90
4,4`-dimethoxybenzophenone oxime (**102**)	C_2H_5OH/H_2O/NaOH	100
4,4`-bis(dimethylamino)benzophenone oxime (**107**)	C_2H_5OH/H_2O/NaOH	95
4,4`-diphenylbenzophenone oxime (**111**)	C_2H_5OH/H_2O/NaOH(repeated twice)	60
bis(2-thiophenyl)ketone oxime (**130**)	pyridine	100
3,3`-bis(trifluoromethyl)benzophenone oxime (**123**)	C_2H_5OH/H_2O/NaOH	100
4,4`-di(perfluoro-*n*-hexyl)benzophenone oxime (**126**)	pyridine	83
bis(2-pyridyl)ketone oxime (**134**)	C_2H_5OH/H_2O/NaOH	91
9,10-anthraquinone dioxime (**142**)	pyridine	100
4,4´-{2-[2-(2-methoxy-ethoxy)-ethoxy]-ethoxy}benzophenone oxime (**138**)	pyridine	68

[174] V. Lee; M. S. Newmann, JOC, *40*, *3*, 381 - 382, **1975**.
[175] J. Meisenheimer; E. Mahler, Ann., *185*, 508, **1934**.
[176] R. M. Elofson; J. G. Atkinson, Canadian Journal of Chemistry, *34*, 4 - 13, **1956**.

3.3.3. Syntheses of benzhydrylamine derivatives from oximes

The reduction of oximes to amines can be performed using a large variety of reagents. However, in order to diminish formation of side products and improve the yields of the reaction, various reaction conditions and reducing reagents were utilized. Reduction by sodium in alcohol (ethanol or *iso*-propanol) used by Langela[177] to reduce the hydrazones to amines was utilized. This method successfully converted methoxy (**102**) and bis(dimethylamino) (**107**) benzophenone oxime derivatives to the corresponding amines. The reaction is straightforward, proceeds with moderate to high yields (see Table 3.2), and the products are easily purified. The change from ethanol as initially used by Langela to *iso*-propanol improved the yields, as it was reported to increase the reducing strength of the reagent.[178] However, similarly to the observed cleavage of chlorine in the case the hydrazone synthetic route (see section 3.2.1) during the reduction of oxime **104**, a significant amount of chlorine was cleaved under these conditions. This induced a search for milder reducing agents, able to perform the required conversion of the benzophenone oximes to the corresponding amines.

Reduction of the oxime **104** with hydrogen at atmospheric pressure in the presence of palladium on carbon led to the formation of not only the primary amines but also secondary derivatives. This phenomenon is known and appears to be due to nucleophilic attack of the amine formed on the unreacted oxime.[179] In order to prevent the formation of the secondary amine, the reduction was conducted at low pH. Amino groups formed during the reaction at these conditions are converted to the ammonium salt form, which does not react with the oxime. The ratio between the secondary and the primary amines in the product obtained dropped, but formation of the secondary amine was not completely suppressed. Separation of the primary and secondary amines was complicated. Therefore, the catalytic reduction was found to be inefficient for the preparation of the benzhydrylamine derivatives.

Use of lithiumaluminiumhydride was another approach for the milder reduction of benzophenone oxime derivatives to the amines. Using this method it was possible to obtain a range of amines with moderate to good yields (see Table 3.2). Initially, diethyl ether, THF and dioxane were tested as reaction media. Reduction of **104** in dioxane gave a mixture of products, while the use of diethyl ether gave a low yield of the product. The highest yields and lowest amount of side products were obtained using refluxing THF as a solvent; therefore, it was chosen for all following cases. Lithiumaluminiumhydride was always used in large excess. The yields of

[177] M. Langela, ***Diploma Thesis***, Johannes-Gutenberg-University/Max-Planck-Institute for Polymer Research: Mainz, **1999**.
[178] ***Organikum***; H. G. O. Becker et al., *20 Auflage*, Johann Ambrosius Barth Verlag: Heidelberg, 475 - 476, **1996**.
[179] ***Organikum***; H. G. O. Becker et al., *20 Auflage*, Johann Ambrosius Barth Verlag: Heidelberg, 470, **1996**.

the amine obtained by reduction with $LiAlH_4$ were somewhat lower than in the case of Na/alcohol. In addition, several side products were formed in the reaction, which meant extensive purification of the products by column chromatography was required. However, this procedure permitted prevention of the cleavage of the chlorine, which was observed using Na/*iso*-propanol system. Unfortunately, when the method was used to reduce 4,4`-dibromobenzophenone oxime (**116**) cleavage of the bromine was observed. So in the range of F-Cl-Br 4,4'-substituted benzophenone oximes each following derivative required milder conditions for the reduction step in order to avoid simultaneous cleavage of the halogen. The ease of the cleavage directly corresponds to the energy of the carbon-halogen bond. The relatively low yields (in comparison to the Na/*iso*-propanol system) suggested to look for more optimized conditions to perform the reduction. In order to further soften the reduction conditions sodium borohydride in methanol was employed as reducing agent, however, only starting material was recovered in this case. Most probably reducing strength of this reagent is too weak to perform the required reduction.

The third method used was reduction with zinc dust in water/ethanol mixture with addition of ammonia and ammonium acetate, as reported in a literature procedure.[180] This method was the most efficient for the reduction of the benzophenone oximes. In comparison to the previously used approaches it required less time and gave high yields with a minimum of side products which can be removed by column chromatography. Using this method it was possible to convert most of the benzophenone oximes to the corresponding amines, even 9,10-dihydroantracene-9,10-diamine (**143**), which previously could be obtained electrochemically.[181] Use of other reducing agents was not efficient leading to formation of anthraquinone.

However, even using Zn/NH_4OH reduction of 4,4`-dibromobenzophenone oxime (**79**) was not achieved without simultaneous cleavage of the bromine. Bromine cleavage was also observed during purification, drying and storing of the product of the reaction, even if any reducing agents were absent. The process was monitored by mass spectrometry. The intensity of the peak corresponding to the bi-substituted derivative decreased during processing and the peaks related to non-substituted and mono-substituted benzhydrylamines increased.

The yield of the di(4-biphenyl)methylamine (**73**) was lower than other derivatives, probably due to the poor solubility of both the oxime and the amine in the reaction media. The conditions and yields of the oxime-to-amine reduction step are summarized in Table 3.2.

[180] M. Renz; C. Hemmert; B. Meunier, Eur. J. Org. Chem., 1271 - 1273, **1998**.
[181] R. M. Elofson; J. G. Atkins, Canadian Journal of Chemistry, *34*, 4 – 13, **1956**.

Table 3.2. The yields and conditions for the benzophenone oximes to benzhydrylamines reduction step.

Amine	Method	The yield, %
4,4´-dichlorobenzhydrylamine (**62**)	$LiAlH_4$/THF	70
4,4´-dichlorobenzhydrylamine (**62**)	H_2/Pd(C)/CH_3COOH/H_2SO_4	40
4,4´-dichlorobenzhydrylamine (**62**)	Na/i-C_3H_7OH	cleaves chlorine
4,4´-dibromobenzhydrylamine (**117**)	$LiAlH_4$/THF, Zn/NH_4OH	cleaves bromine
4,4´-difluorobenzhydrylamine (**58**)	$LiAlH_4$	86
4,4´-dimethoxybenzhydrylamine (**64**)	Na/i-C_3H_7OH	65
4,4´-bis(dimethylamino)benzhydrylamine (**108**)	Na/i-C_3H_7OH	83
di(4-biphenyl)methylamine (**112**)	$LiAlH_4$/THF	45
di(2-thiophenyl)methylamine (**131**)	Zn/NH_4OH	79
3,3´-di(trifluoromethyl)benzhydrylamine (**124**)	Zn/NH_4OH	73
4,4´-di(perfluoro-*n*-hexyl)benzhydrylamine (**127**)	Zn/NH_4OH	67
di(2-pyridyl)methylamine (**135**)	Zn/NH_4OH	67
9,10-dihydroantracene-9,10-diamine (**143**)	Zn/NH_4OH	72
4,4´-di{2-[2-(2-methoxy-ethoxy)-ethoxy]-ethoxy}benzhydrylamine (**139**)	Zn/NH_4OH	61

An interesting property of the trifluoromethyl (**124**) and perfluoro-*n*-hexyl (**127**) benzhydrylamine derivatives was observed. In the mass spectra (field desorption) no peaks at all could be seen, whereas the initial oximes and the triazolins synthesized at the next step give normal spectra with only one peak corresponding to the molecular ion. Other benzhydrylamine derivatives also always gave usual mass spectra with the molecular ion peak only. This strange behavior thus is observed only in the cases when fluoroalkyl substituents are present in the molecule together with primary amine functionality.

3.3.4. Syntheses of benzhydrylamine derivatives functionalized by groups sensitive to reduction

Several amines had to be obtained by different approaches due to the limitations of the method. Particularly, due to the sensitivity of the functional groups such as nitro and acyl and the reaction conditions of the developed synthetic route (reduction step), they had to be synthesized by a different method. In both cases, direct aromatic electrophilic substitution was performed. For the synthesis of 4,4`-diacylbenzhydrylamine (**75**) the amine function was protected with an acyl group to avoid complexation of the amino group with the aluminium chloride, used as Lewis acid (Scheme 3.11). Acylation was carried out in carbon disulfide using acetyl chloride and aluminium chloride in a procedure similar to that described in the literature for acylation of

p-acetanilide.[182] Fortunately, the active acylation agent is a bulky complex of acetyl chloride and aluminium chloride, which leads to only substitution at the *para*-position of the phenyl rings, as confirmed by ^{1}H-NMR spectra where two doublets near 7 ppm were observed. The obtained acetyl protected 4,4'-diacetylbenzhydrylamine (**74**) was not isolated, instead the crude product of the acylation was treated with refluxing 6N HCl, directly yielding the unprotected 4,4`-diacylbenzhydrylamine (**75**) (Scheme 34).

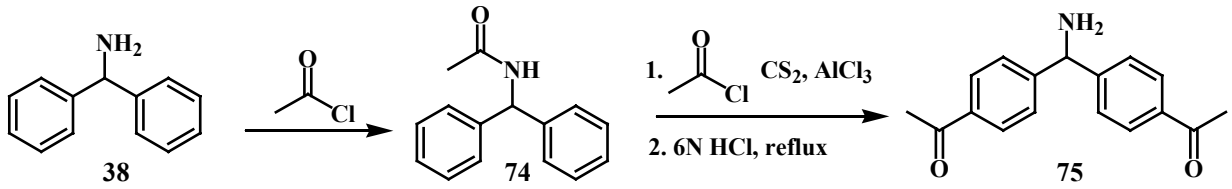

Scheme 3.11. Synthesis of 4,4`-diacylbenzhydrylamine (**75**).

Similarly, nitro substituted benzhydrylamine derivative **76** was prepared by direct nitration of benzhydrylamine with a mixture of concentrated H_2SO_4 and 68% HNO_3 (Scheme 3.12). Unfortunately, unlike the acylation, nitration gave a mixture of isomers as confirmed by HPLC analysis and NMR experiments. This is not surprising, since the actual active nitration agent, the NO_2^+ ion is not space demanding. Therefore, relatively sterically hindered 2 and 6 positions of the phenyl rings can undergo substitution. Attempts to separate the isomers failed, and the mixture of isomers was used in the next step. As the result the nitro-substituted triazolinyl was obtained only as a mixture of the isomers.

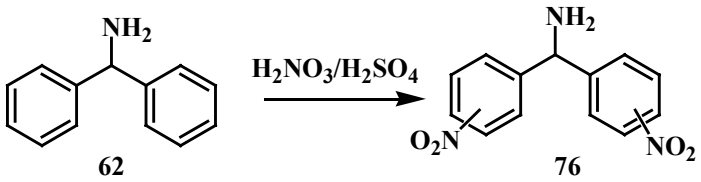

Scheme 3.12. Synthesis of dinitrobenzhydrylamine (mixture of isomers) (**76**).

3.3.5. Syntheses of triazolins (cyclization step)

Cyclization step was always performed using the procedure described by Neugebauer.[183] In his procedure the excess of benzhydrylamine is used both as one of the reagents and the base, which captures HCl formed during the reaction. This is convenient, because due to absence of additional bases in the system the amount of possible side reactions is lowered. However, unlike

[182] E. Ferber; H. Bruekner, Ber. d. D. Chem. Geselschaft, *5*, 995 - 1002, **1939**.
[183] F. A. Neugebauer; H. Fischer, Tetrahedron, *51*, *47*, 12883 – 12898, **1995**.

the commercially available benzhydrylamine used in the synthesis of 1,3,5,5-tetraphenyl-Δ^2-1,2,4-triazolin (**33**), benzhydrylamine derivatives for syntheses of other triazolinyls have to be synthesized, therefore an additional base was used in order to capture HCl. Usually triethylamine or pyridine is used for such purposes, however, the high temperature (~ 180° C) required for this reaction is higher than their boiling points, so tri-*n*-butylamine was chosen as the base in all cases. In several cases (syntheses of **128**, **125**: see Section 5), the temperature of the reaction had to be decreased due to a lowering of the yield and side reactions occurring at 180°C, as observed *via* monitoring of the reaction by TLC. The time of the reaction was increased from 40 - 60 minutes to several hours in these cases, in order to achieve more complete conversion of the reactants to the products. The yields of the cyclization step were often low. For instance, in the cases of C_6F_{13} (**128**) and $COCH_3$ (**137**) derivatives it did not exceed or were close to 10 % after purification.

Table 3.3. The yields of the triazolin derivatives synthesis.

Triazolin	The yield
1,3–diphenyl-5,5-di(4-chlorophenyl)-Δ^2-1,2,4-triazolin (**105**)	38
1,3–diphenyl-5,5-di(4-bromophenyl)-Δ^2-1,2,4-triazolin (**119**) & 1,3,5–triphenyl-5-(4-bromophenyl)-Δ^2-1,2,4-triazolin (**120**)	15 (calculated from oxime)
1,3–diphenyl-5,5-di(4-fluorophenyl)-Δ^2-1,2,4-triazolin (**115**)	24
1,3–diphenyl-5,5-di(4-methoxyphenyl)-Δ^2-1,2,4-triazolin (**103**)	35
1,3–diphenyl-5,5-bis(4-dimethylaminophenyl)-Δ^2-1,2,4-triazolin (**109**)	26
1,3–diphenyl-5,5-di(4-biphenyl)-Δ^2-1,2,4-triazolin	not isolated
1,3–diphenyl-5,5-di(2-thiophenyl)-Δ^2-1,2,4-triazolin (**132**)	12
1,3–diphenyl-5,5-di(3-trifluoromethylphenyl)-Δ^2-1,2,4-triazolin (**125**)	13
1,3–diphenyl-5,5-di(4-(perfluoro-*n*-hexyl)phenyl) -Δ^2-1,2,4-triazolin (**128**)	11
1,3–diphenyl-5,5-di(2-pyridyl)-Δ^2-1,2,4-triazolin (**136**)	15
1′,3′,1′′,3′′-tetraphenyl-dispiro(9,10-dihydroantracene-[9.5′,10.5′′]-di-(Δ^2-1,2,4-triazolin) (**144**)	not isolated
1,3–diphenyl-5,5-di-(4{2-[2-(2-methoxy-ethoxy)-ethoxy]-ethoxy}phenyl)-Δ^2-1,2,4-triazolin (**140**)	not isolated
1,3–diphenyl-5,5-di(4-acylphenyl)-Δ^2-1,2,4-triazolin (**137**)	7
1,3–diphenyl-5,5-di(nitrophenyl)-Δ^2-1,2,4-triazolin (**121**)	36
1,3,5,5-tetraphenyl-Δ^2-1,2,4-triazolin (**39**)	56

The 1,3-diphenyl-5,5-di(4-biphenyl)-Δ^2-1,2,4-triazolin was not obtained as a pure compound. During its processing the substance continuously decomposed, and hence, the crude material was used in the next oxidation step only after partial purification (extraction and column chromatography). Due to the formation of many side products and difficulties during column

chromatography, caused by decomposition of the target molecules isolations of 1´,3´,1´´,3´´-tetraphenyl-dispiro(9,10-dihydroantracene-[9.5´,10.5´´]di(Δ^2-1,2,4-triazolin) and 1,3–diphenyl-5,5-di-(4{2-[2-(2-methoxy-ethoxy)-ethoxy]-ethoxy}phenyl)-Δ^2-1,2,4-triazolin were not achieved (see Sections 9.1.1 and 9.1.2). The yields of the triazolins obtained *via* cyclization of benzhydrylamine derivatives and **37** are summarized in Table 3.3.

3.3.6. Syntheses of triazolinyls (oxidation step)

Oxidation of the triazolins to the corresponding triazolinyls was performed using potassium hexacyanoferrate (III) as oxidant. This is a relatively mild reagent allowing realization of the reaction without formation of side products when performed carefully and at low (<-10°C) temperatures. Langela performed this oxidation step at room temperature.[184] However, under these conditions, formation of side products in the cases of methoxy and fluorine derivatives was observed. Therefore, the temperature was always lowered to avoid these side reactions. If side products still formed, the triazolinyls can be purified by column chromatography. This is however, not desired due to decomposition of the radical during the chromatography, which is probably caused by silica gel, leading to lowering of the yields of the product. The purification of the products at this stage is relatively easy, because of the very dark and specific color of the triazolinyl radicals. Use of other oxidants such as PbO_2 in dichloromethane and KIO_4 (in water solution, the triazolin in an organic solvent) also lead to formation of the triazolinyl radicals. However, potassium hexacyanoferrate (III) was chosen, due to its lower electrochemical potential and the absence of side reactions. PbO_2 in dichloromethane was used to oxidize pyridyl triazolin in non-aqueous media for ESR measurement purposes. The advantage of this oxidant is the possibility to avoid use of water in the reaction which causes problems during the performance of the ESR measurements. In Figure 3.3, the obtained triazolinyl stable radicals are summarized. Formation of radicals **88** and **89** during the oxidation was observed as indicated by appearance of the dark red color of the reaction mixture, caused by formed triazolinyl. However, when the temperature increased to 20° C, the color disappeared indicating decomposition of the radicals. Additional confirmation of the formation of **88** was done by ESR measurement performed at low temperature. Because of the poor stability of these two radicals they were not isolated.

[184] M. Langela, ***Diploma Thesis***, Johannes-Gutenberg-University/Max-Planck-Institute for Polymer Research: Mainz, **1999**.

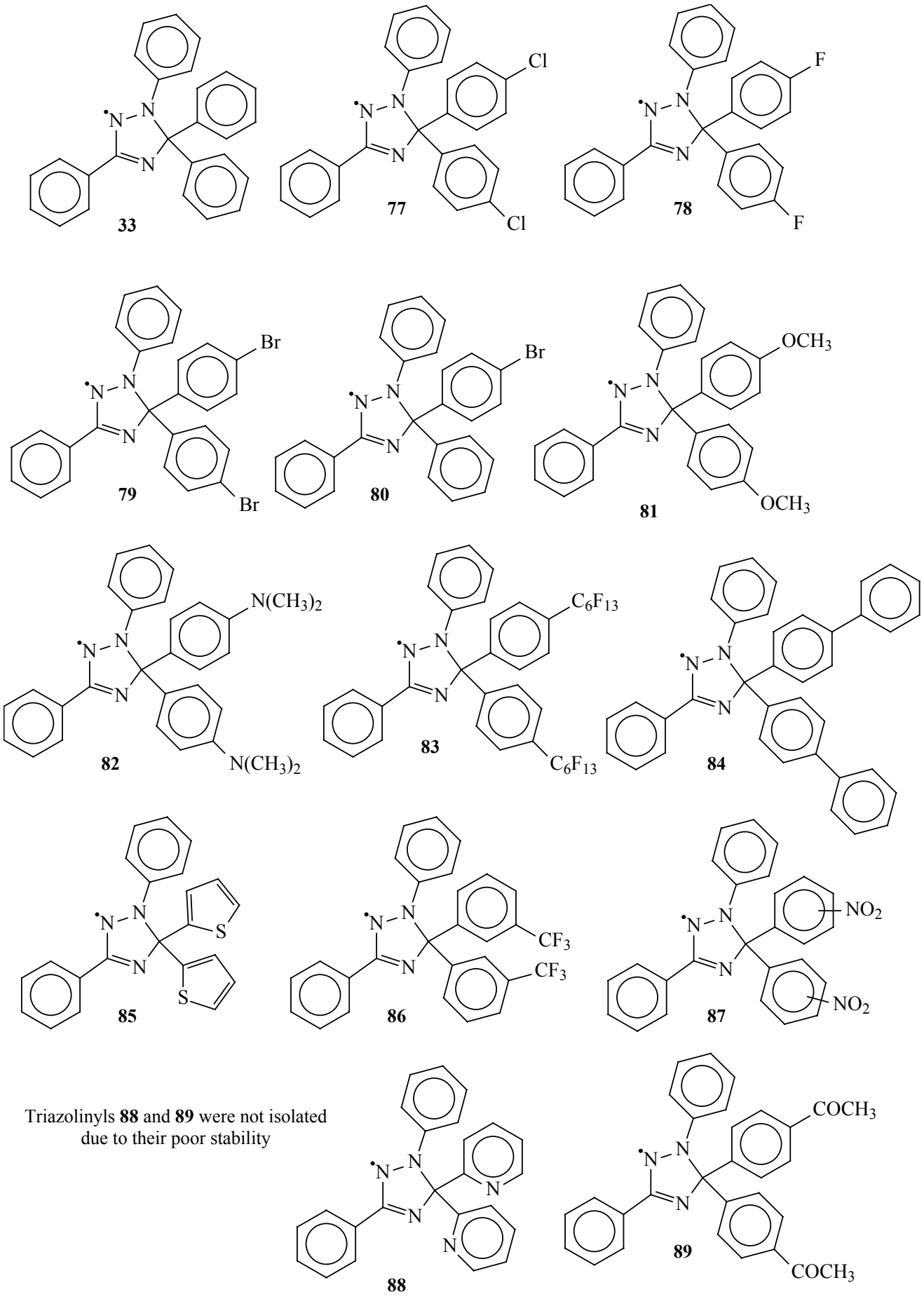

Figure 3.3. Synthesized triazolinyl radical derivatives.

3.4. Properties of the synthesized triazolinyl radicals

3.4.1. Optical spectroscopy

If a triazolinyl was prepared carefully and as a consequence, did not require chromatographic purification it was obtained as a very fine powder. The color of all pure initial triazolin cycles (non radicals) is yellow or orange. During processing due to the exposure to air, traces of corresponding triazolinyl radicals can be formed by oxidation with oxygen. This might be the reason for the appearance of the darker orange tint of the triazolins. During oxidation to the corresponding triazolinyl radicals the color dramatically changes to dark red-red. The color of the powder ranged from brown to black. Highly diluted solutions are a dirty yellow in color. UV-Vis spectra were recorded in dichloromethane for all synthesized triazolinyls. The recorded spectra are given in Section 5 in chapters devoted to the syntheses of the compounds, and a typical spectrum is given in Figure 3.4.

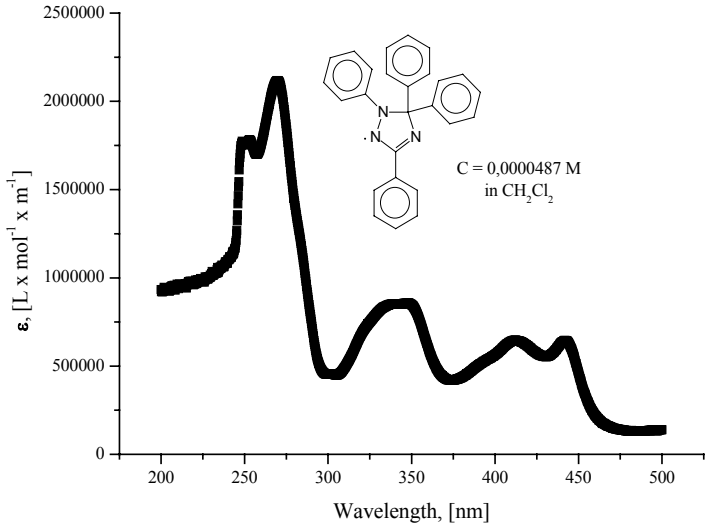

Figure 3.4. UV-Vis spectra of 1,3,5,5-tetraphenyl-Δ^3-1,2,4-triazolin-2-yl (**33**) in CH_2Cl_2.

The spectra show two areas of absorption. The first is between 320 and 500 nm and consists of several absorption bands. Since the initial triazolins do not show significant absorbance in this region as indicated by their light yellow color, the absorption bands in the area 320 - 500 nm, which are responsible for the dark color of the radical, are caused by absorption by the unpaired spin. The conjugation of the unpaired electron is spread over nitrogen atoms 1, 2, 4 and carbon 3 atom. The substituents at 1- and 3-positions also participate in delocalization of the unpaired spin. A 3D structure of the molecule calculated from X-ray diffraction analyses obtained by Neugebauer showed that the phenyl rings at the positions 1 and 3 lie almost in the same plane with the triazolinyl ring. This allows very effective conjugation of the π-systems of

these phenyl substituents and the π-system of the triazolinyl ring.[185] At the same time the planes of aromatic substituents at the 5-position lie almost perpendicular to the plane of the triazolinyl ring. Therefore, they cannot participate in the delocalization of the unpaired electron. As a result the absorption bands of the substituents at the 5-position appear in their usual range of wavelength 210 – 300 nm: this is the second region of absorption in the UV-Vis spectra of triazolinyls. Variation of the substituent at the 5-position does not lead to any considerable change in the absorption spectra in the range of 320 - 500 nm. However, the shape and the maxima of the spectra in the range 210 – 300 nm are greatly influenced by this variation. Such independent change of the spectra confirms the existence of two almost independent chromophores in the triazolinyl molecule. This is due to the absence of conjugation between π-system, where radical is delocalized: π-system of the triazolinyl ring and phenyl substituents at the positions 1 and 3; and the substituents at the 5-carbon atom. The change in the UV-Vis absorption spectra can be used as characteristic features of the radical and applied to its concentration measurements and characterization. One of the possible ways of determination of the stability of the radical is following the change in absorption of the triazolinyl in the region 320 - 500 nm at high temperature. Identification by color was widely used during purification and isolation. The TLC plates used to control the column chromatography separation and following the reactions in the presence of triazolins were developed using potassium hexacyanoferrate solution in water/acetone mixture allowing easy identification of the presence of the triazolins as is described in Section 6.9. Change of the color of the triazolinyl during the polymerization experiments is a good indication of the capturing of the free triazolinyl radicals by macroradicals. Initially deep red-red solution of free triazolinyl radical, initiator and monomer changes color to pale yellow upon heating (see Section 6.10).

[185] F. A. Neugebauer; H. Fischer; C. Krieger, Angew. Chem., *101*, *4*, 486 - 488, **1989**.

3.4.2. ESR & stability

All ESR spectra of triazolinyls were taken in toluene solutions. The resolution of the fine structure of the spectra was not persued since the spectra were used to investigate only the

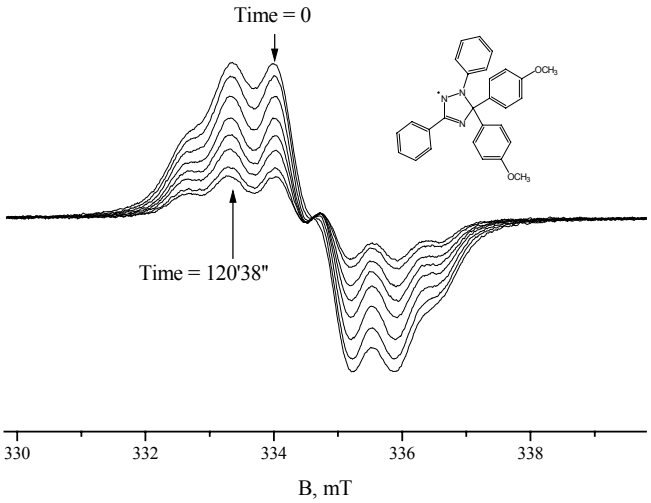

Figure 3.5. Decrease of the ESR signal intensity with time of toluene solution of **81** at 95°C.

thermal stability of the radicals, but not the interaction of the unpaired electron with neighboring atoms. The usual spectrum is shown in Figure 3.5. The spectra of triazolinyls are similar and consist of six lines. This is due to the presence of two nitrogen atoms (1-position and 2-position) with spins = 1. Coupling of the unpaired spin with each of the nitrogen atoms provide splitting of the signal to triplet, finally giving the observed 6-lines spectrum. For determination of the kinetic parameters of the decomposition toluene solutions of the triazolinyls were heated up to desired temperature in the range of 70 - 100°C and the ESR spectra were taken at intervals of several minutes. A thermostate attached to the ESR machine permitted adjustment of the temperature of the sample within an error range ± 1°C, leading to good accuracy of the final results. Integration of the obtained spectra at different time points gave the possibility to follow the change in the concentration of the radical. The absolute concentration of the radicals in the solution was not calculated, because it would require additional calibration measurements. Instead the values obtained by integration of the signal at different time points were related to the intensity of the signal at time = 0, in such way giving the relative concentration of the radical to its initial concentration. This provided all the necessary data for the calculation of the rate constants. The logarithm of the reversed ratio I_0/I gave the value, required for the kinetic analyses. Three such measurements were performed for each triazolinyl radical at different temperatures in the range of 70 – 100°C. As expected, the intensities of the spectra in all cases decreased during the measurements, indicating decomposition of the triazolinyls at elevated temperature (Figure 3.5

and series of Figures 3.6 – 3.17). For all investigated triazolinyl radicals the dependencies of $\ln(I_0/I)$ *vs.* time were linear, indicating that the decomposition of the triazolinyl is a first order reaction. The kinetic law for the first order reactions is given in Equations 3.1 – 3.2.[186] As the decomposition of the triazolinyl is confirmed to be 1st order reaction it proves that the process proceeds due to thermal instability of the compound, but not *via* possible reactions with other molecules (impurities, dissolved gases, *etc.*), which may be present in the ESR tubes do not participate in the decomposition process. Other factors such as for instance reactions of the formed phenyl radicals with triazolinyl molecules are negligible. Otherwise the deviations from the linearity in the plots $\ln(I_0/I)$ *vs.* time must arise. However, this is correct only for relatively dilute solutions as were used in these studies (concentrations of order 10^{-3} - 10^{-4} M). This concentration range was chosen because it is close to that used further in the polymerization experiment. As the result, the obtained kinetic parameters of the decomposition process are more reliable when considering the polymerization experiments. If the concentration of the radical is higher, new pathways for the decomposition might appear. For instance, at relatively high concentrations, the phenyl radicals, formed by the decomposition of triazolinyls, might react with other triazolinyls forming adducts (Figure 3.13). The slope of these graphs directly gave the values of the rate constant of the decomposition at different temperatures.

$$-\frac{d[A]}{dt} = k[A];\ \ln\frac{[A]_0}{[A]_t} = kt$$, **Equations 3.1 – 3.2**, where k is rate constant, $[A]$ – concentration of the reagent, t – time.

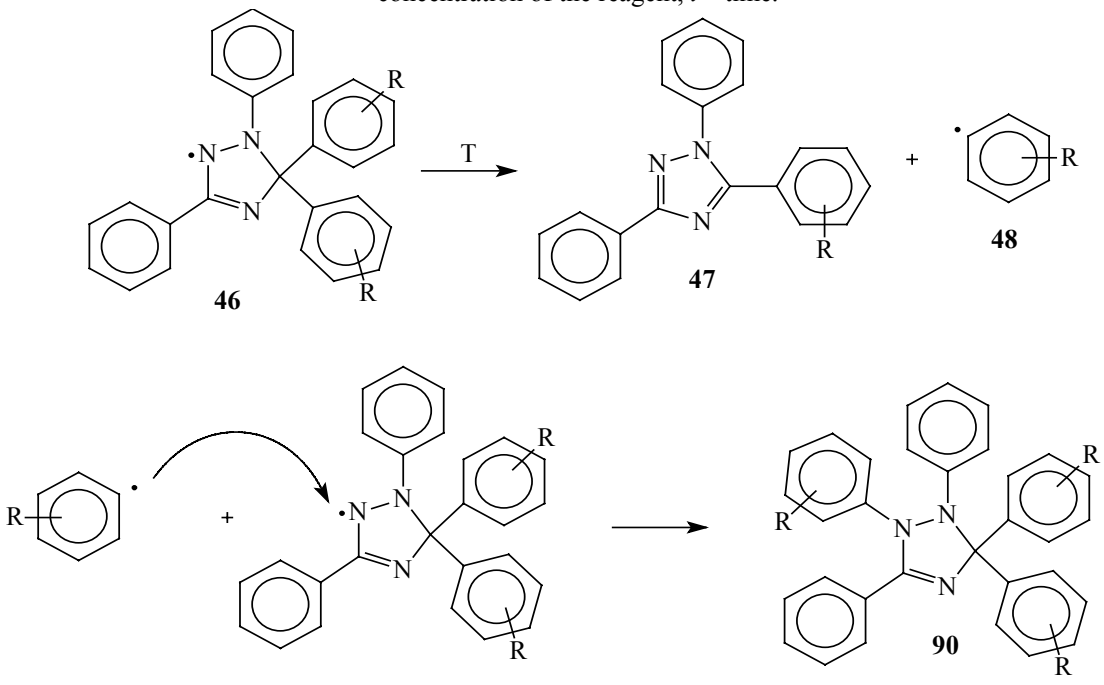

Scheme 3.13. Possible reaction of the phenyl radical formed via decomposition of triazolinyl with another triazolinyl molecule, as one of possible ways of disappearance of triazolinyls at higher concentration upon heating.

[186] J. Campbell, ***Sovremennaya Obshaya Khimia***, Mir: Moscow, *2*, 207 – 209, **1975**.

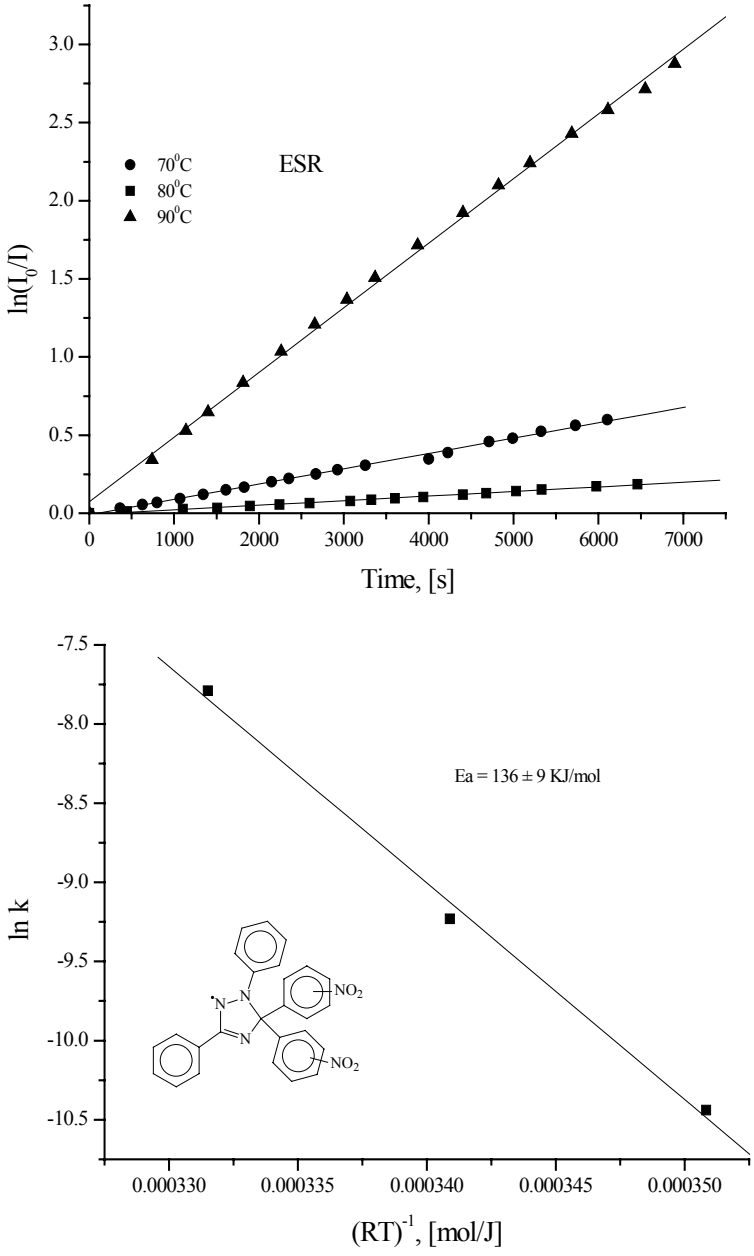

Figure 3.6. $\ln(I_0/I)$ (ESR) *vs.* time plot used for determination of rate constants and Arrhenius plot used for determination of activation energy of decomposition of **87** at elevated temperature.

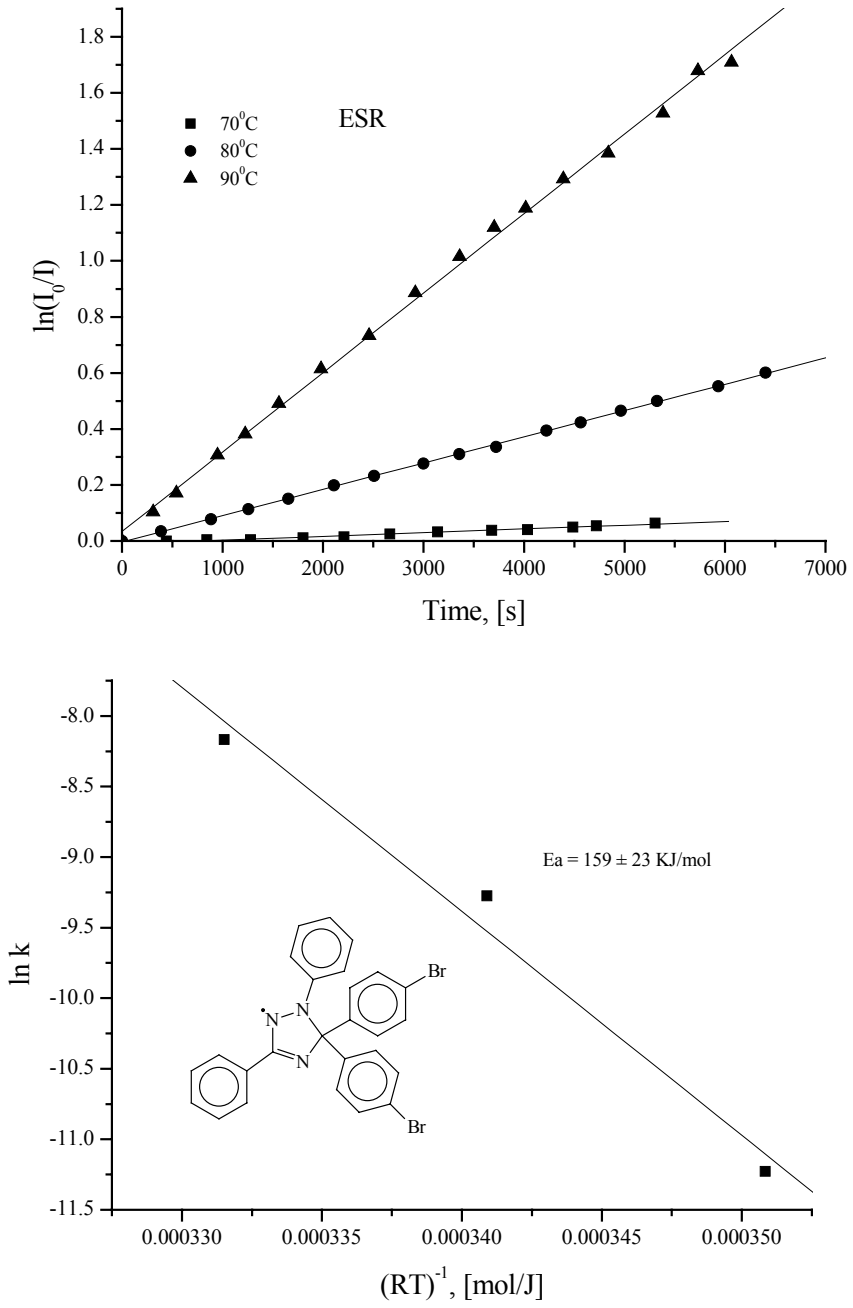

Figure 3.7. $\ln(I_0/I)$ (ESR) *vs*. time plot used for determination of rate constants and Arrhenius plot used for determination of activation energy of decomposition of **79** at elevated temperature.

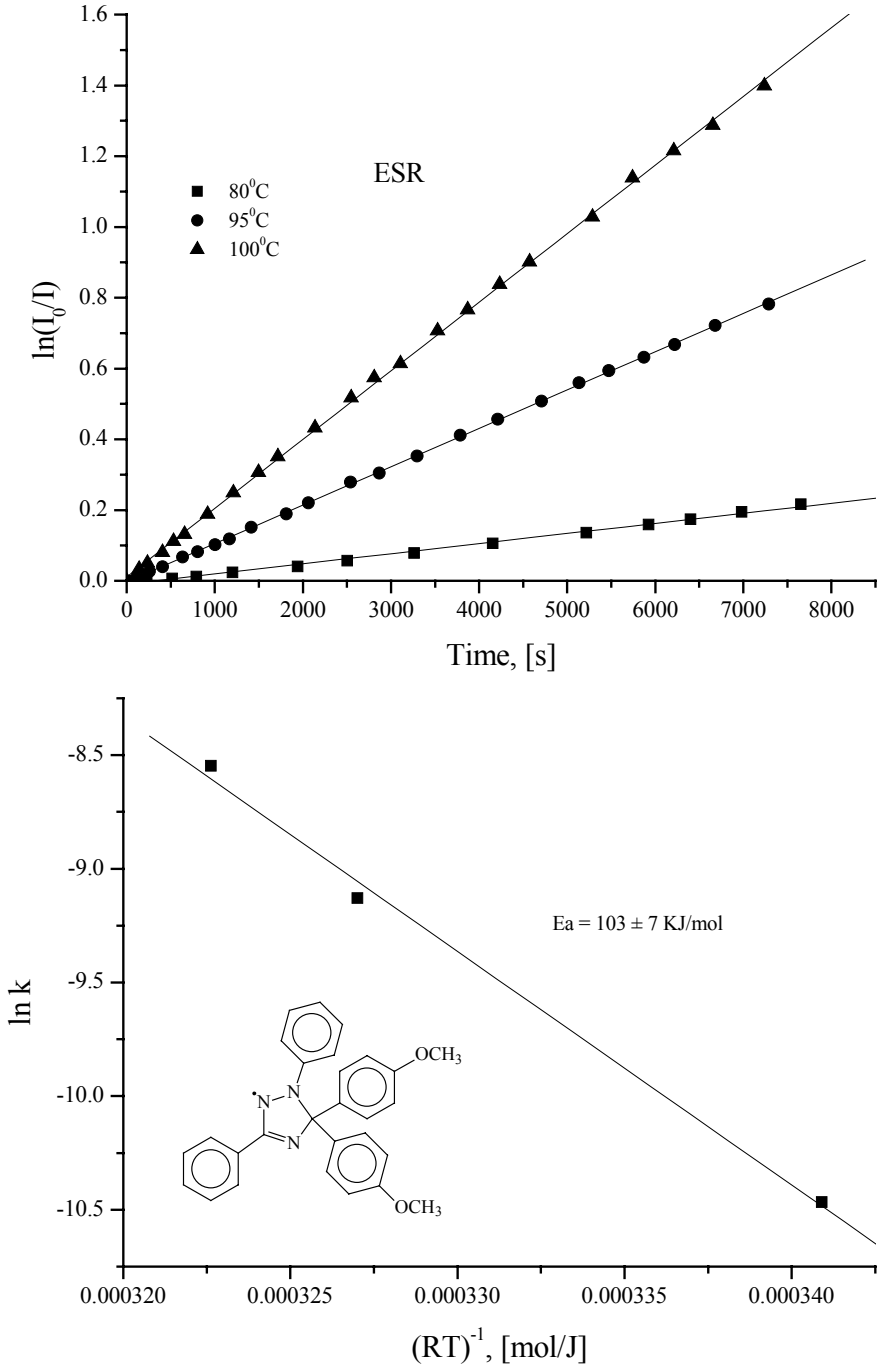

Figure 3.8. $\ln(I_0/I)$ (ESR) *vs*. time plot used for determination of rate constants and Arrhenius plot used for determination of activation energy of decomposition of **81** at elevated temperature.

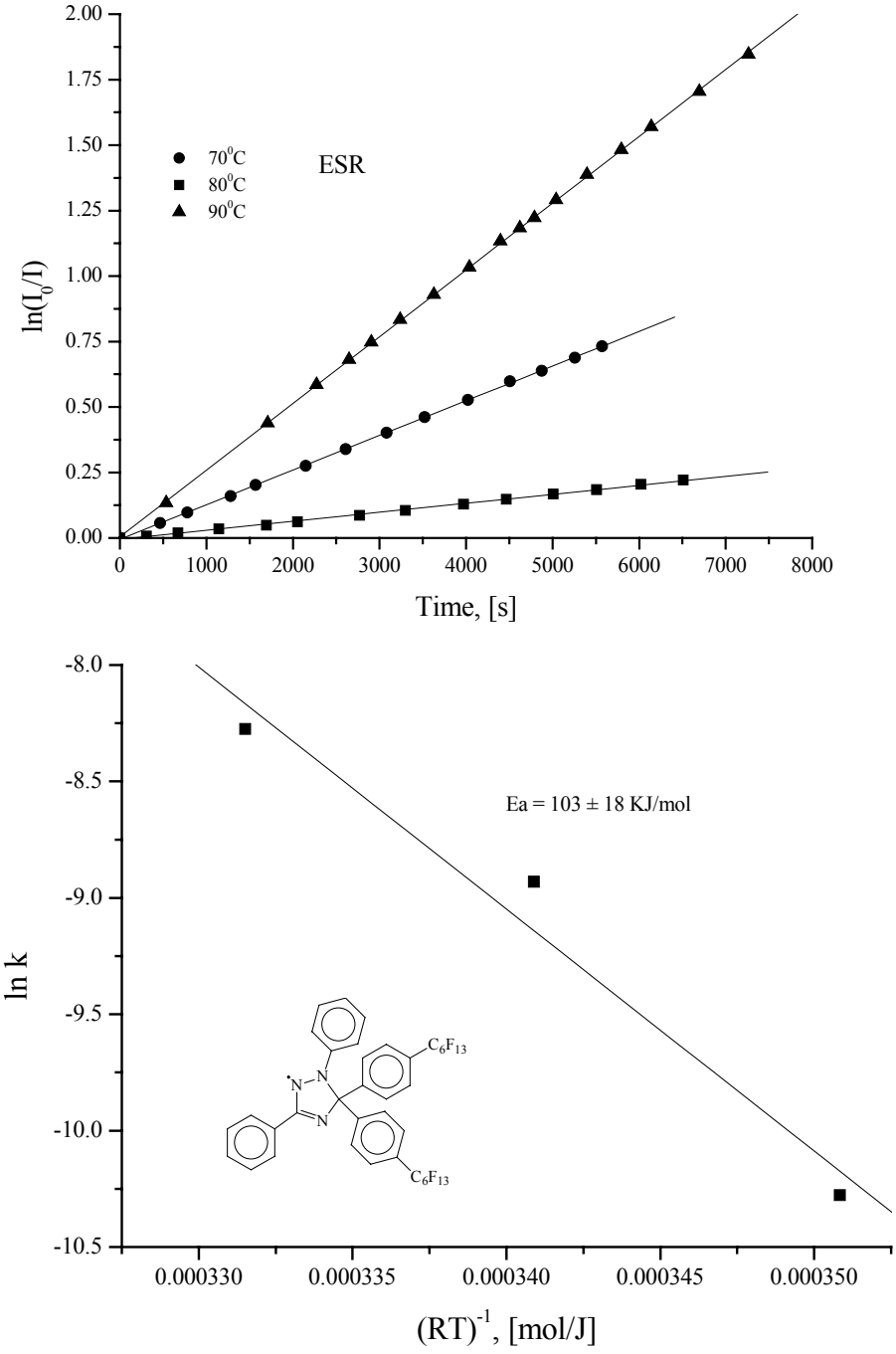

Figure 3.9. $\ln(I_0/I)$ (ESR) *vs*. time plot used for determination of rate constants and Arrhenius plot used for determination of activation energy of decomposition of **83** at elevated temperature.

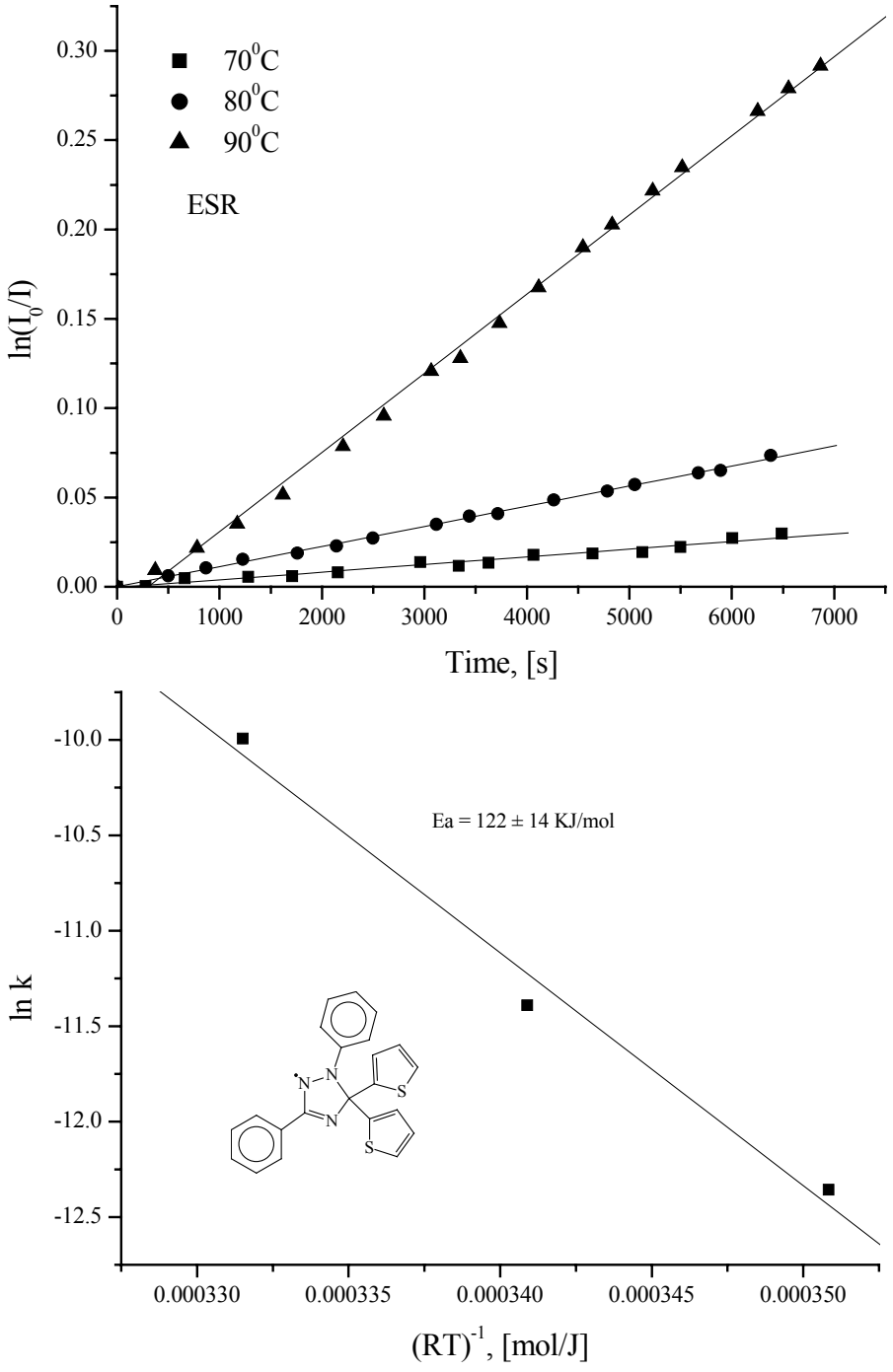

Figure 3.10. ln(I_0/I) (ESR) *vs*. time plot used for determination of rate constants and Arrhenius plot used for determination of activation energy of decomposition of **85** at elevated temperature.

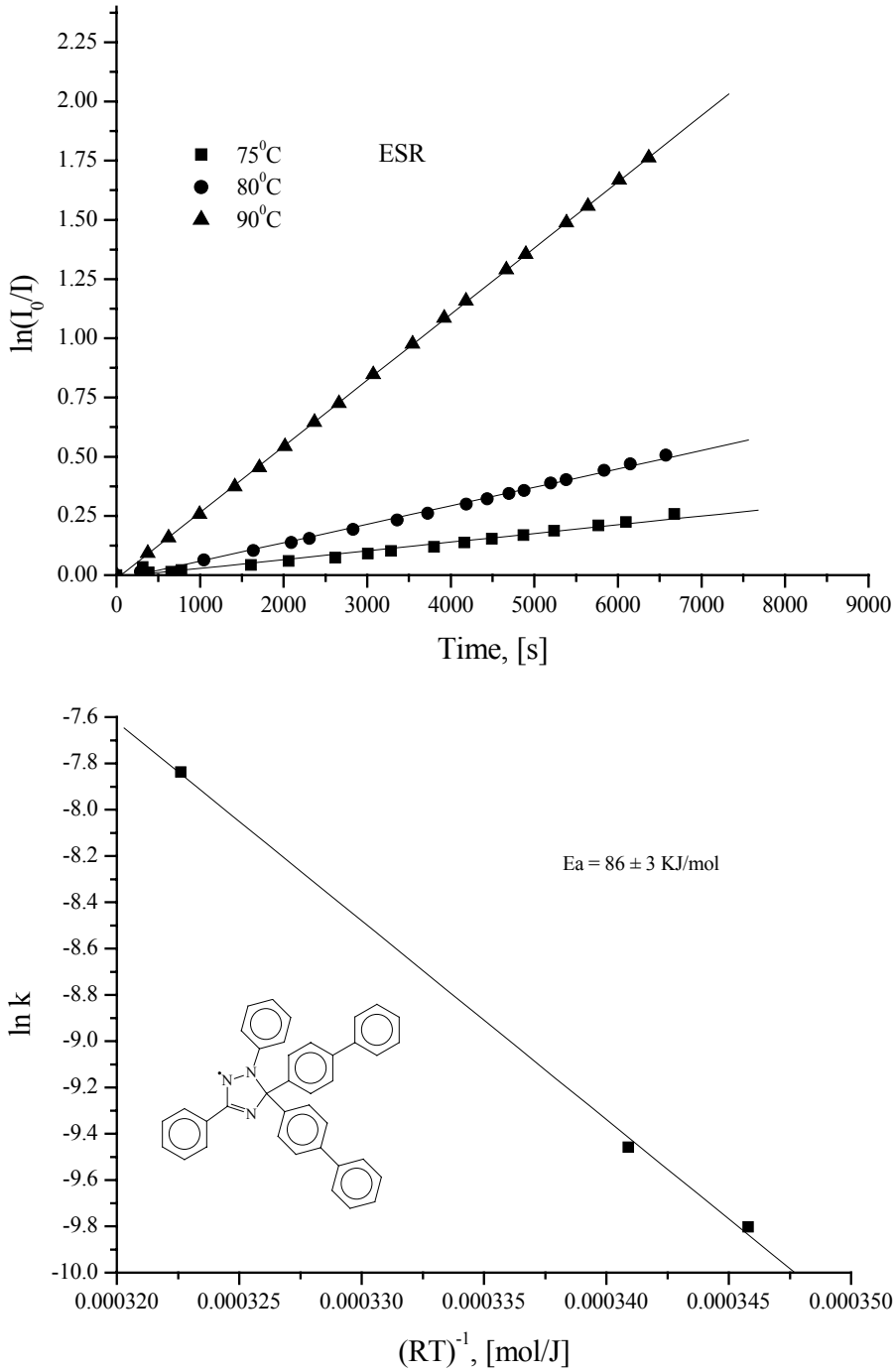

Figure 3.11. $\ln(I_0/I)$ (ESR) *vs*. time plot used for determination of rate constants and Arrhenius plot used for determination of activation energy of decomposition of **84** at elevated temperature.

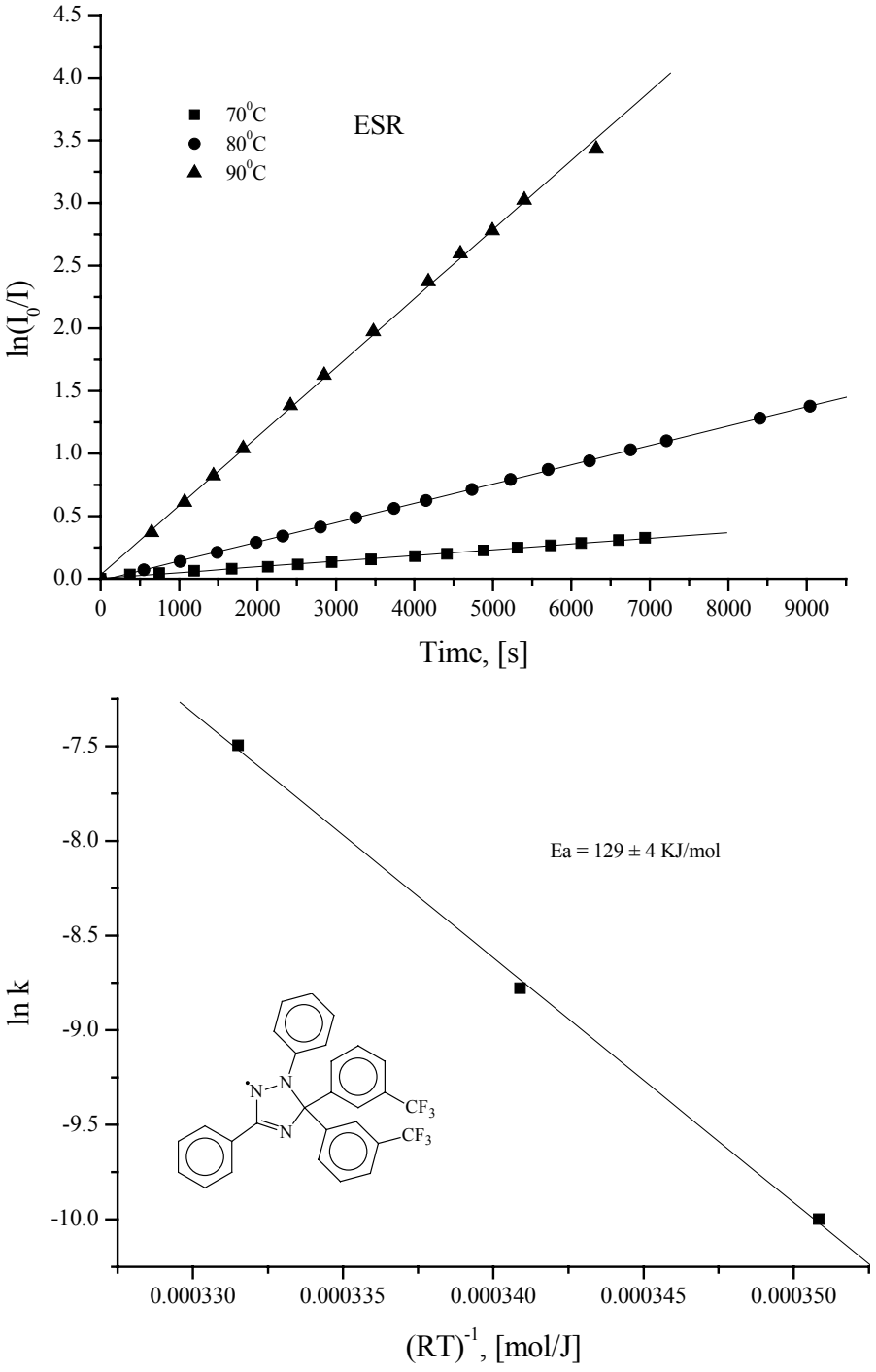

Figure 3.12. $\ln(I_0/I)$ (ESR) *vs*. time plot used for determination of rate constants and Arrhenius plot used for determination of activation energy of decomposition of **86** at elevated temperature.

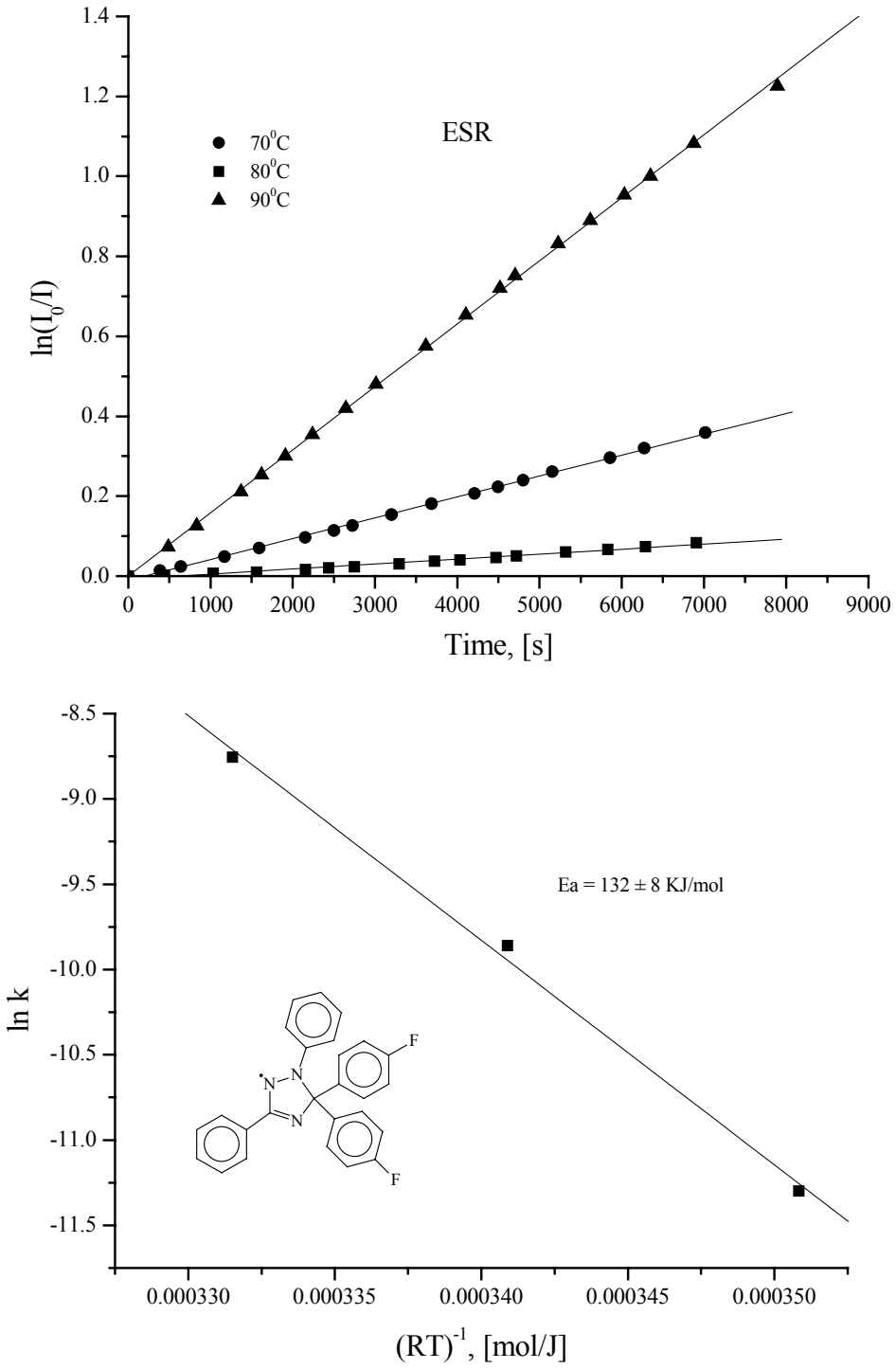

Figure 3.13. ln(I_0/I) (ESR) *vs.* time plot used for determination of rate constants and Arrhenius plot used for determination of activation energy of decomposition of **78** at elevated temperature.

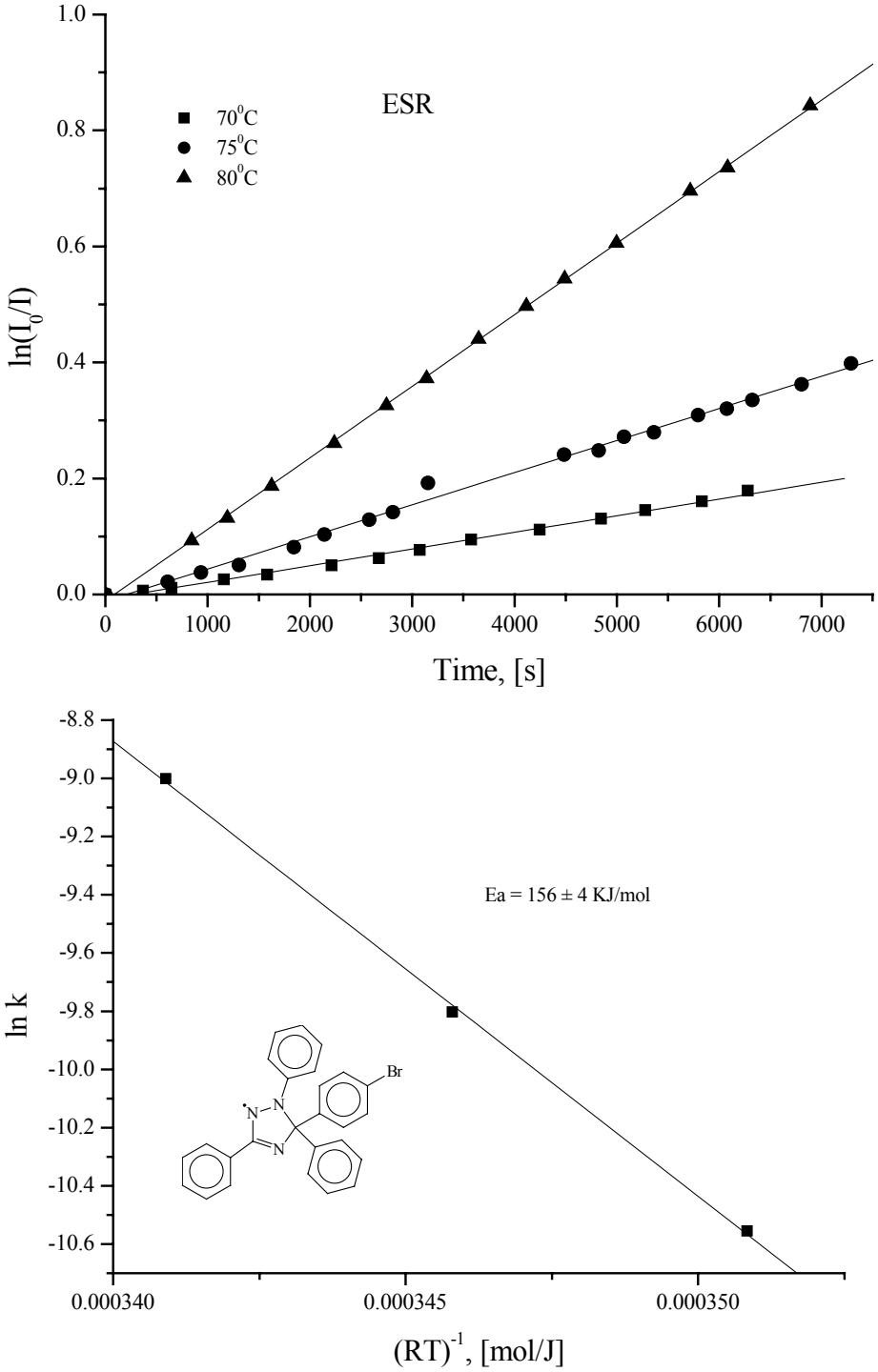

Figure 3.14. $\ln(I_0/I)$ (ESR) *vs*. time plot used for determination of rate constants and Arrhenius plot used for determination of activation energy of decomposition of **80** at elevated temperature.

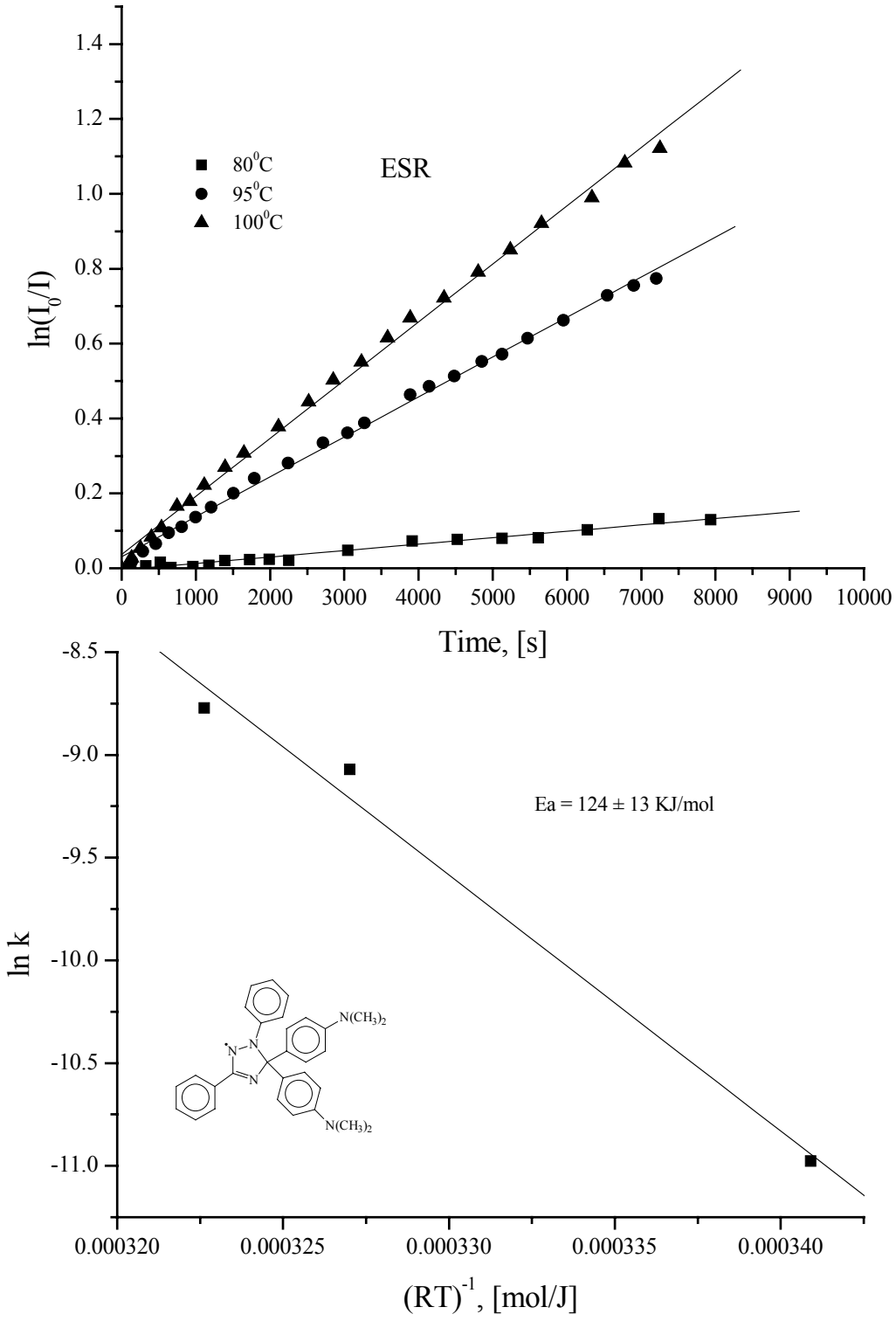

Figure 3.15. $\ln(I_0/I)$ (ESR) *vs*. time plot used for determination of rate constants and Arrhenius plot used for determination of activation energy of decomposition of **82** at elevated temperature.

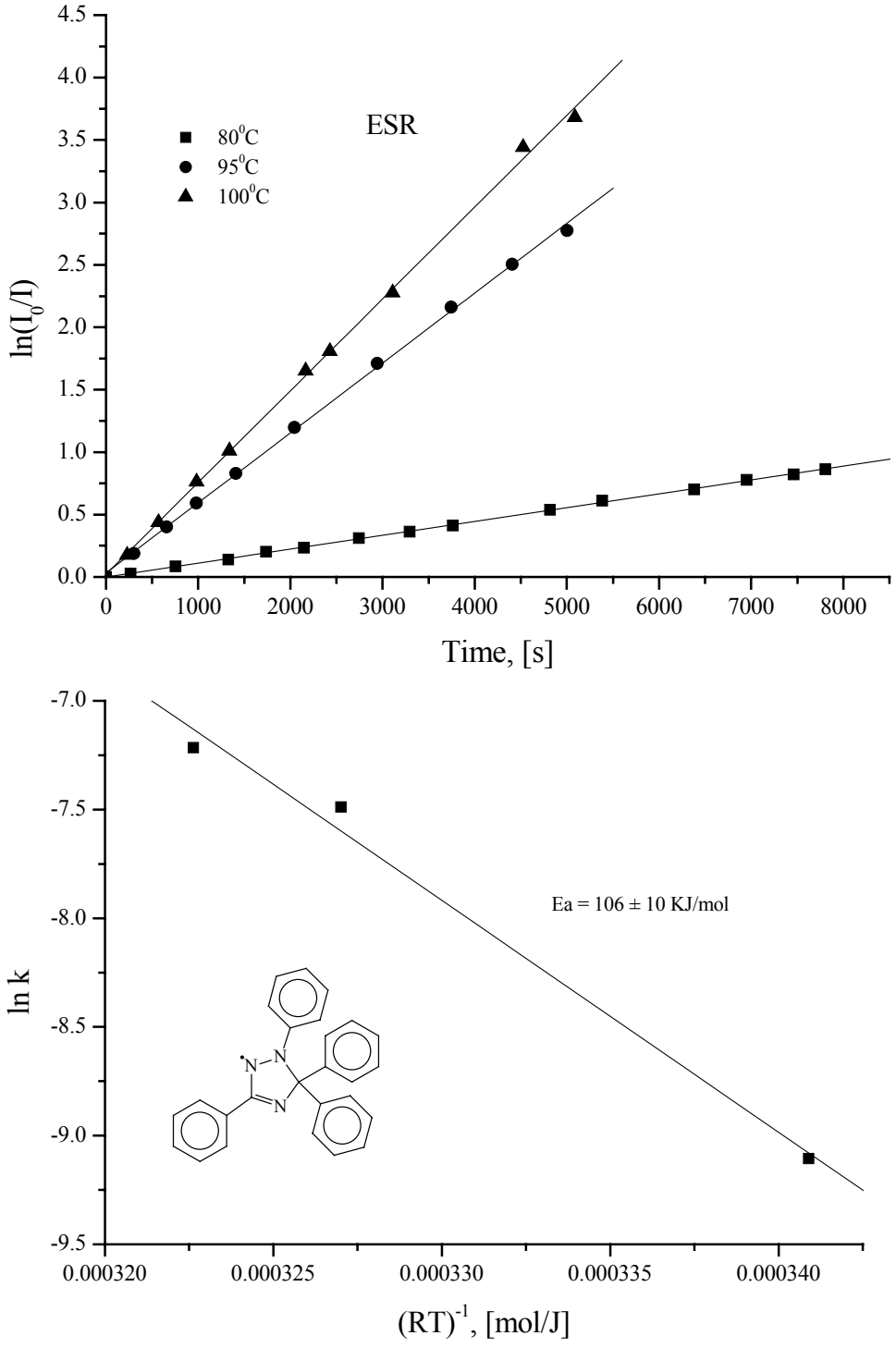

Figure 3.16. $\ln(I_0/I)$ (ESR) *vs*. time plot used for determination of rate constants and Arrhenius plot used for determination of activation energy of decomposition of **33** at elevated temperature.

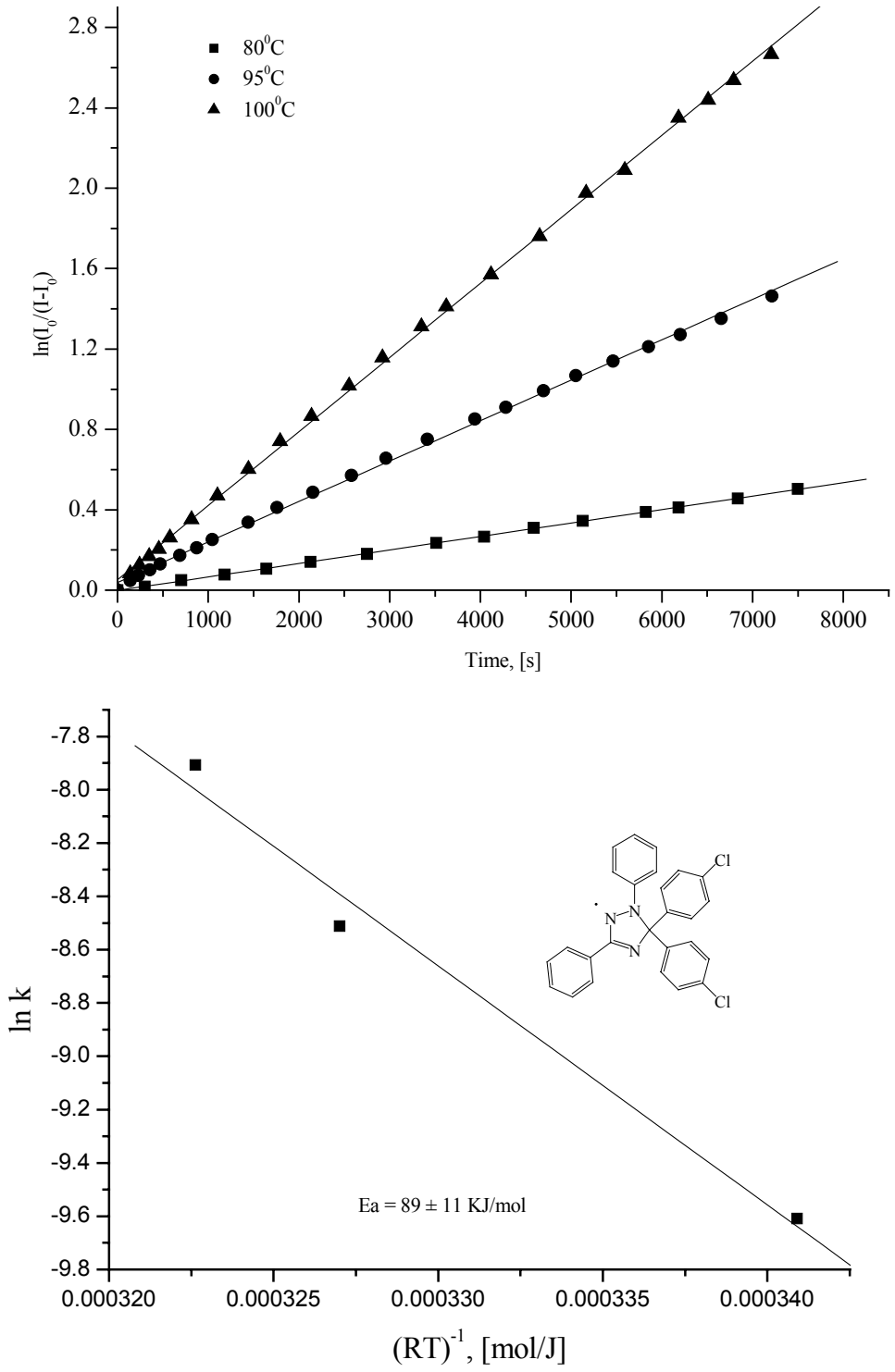

Figure 3.17. $\ln(I_0/I)$ (ESR) *vs*. time plot used for determination of rate constants and Arrhenius plot used for determination of activation energy of decomposition of **77** at elevated temperature.

Half-life times as a more visual parameter characterizing the stability of the radicals were calculated using Equation 3.3.

$t_{1/2} = \frac{0.693}{k}$, **Equation 3.3**, where $t_{1/2}$ is half-life time (for 1st order reactions).

The measurement of the decomposition rate constants at different temperatures allowed a rough determination of the activation energies of the decomposition process using the Arrhenius equation (Equation 3.4). For the evaluation of the activation energy data, the a graph ln*k vs.* $(RT)^{-1}$ was plotted for each triazolinyl derivative. The linearity of the plots allowed calculation of the rate constant in the temperature range 70 - 100° C (Figures 3.6 - 3.17).

$\ln \frac{k_{T_1}}{k_{T_2}} = \frac{E_a}{R(T_2 - T_1)}$, **Equation 3.4**, R = 8.31 J/(mol·K), E_a – activation energy, T_1 and T_2 – temperatures, k_{T1} and k_{T2} - rate constants at the temperatures T_1 and T_2.

The half-life times and activation energies of triazolinyl decomposition are summarized in Table 3.4. Rate constants are given in Table 3.5.

Table 3.4. Half-life times and activation energies of thermal decomposition of triazolinyl derivatives.

Radical	$t_{1/2}$, 70°C, [s]	$t_{1/2}$, 75°C, [s]	$t_{1/2}$, 80°C, [s]	$t_{1/2}$, 90°C, [s]	$t_{1/2}$, 95°C, [s]	$t_{1/2}$, 100°C, [s]	E_a, [KJ/mol]
33	-	-	6240	-	1240	940	106 ± 10
81	-	-	24300	-	6390	3570	103 ± 7
82	-	-	40500	-	6030	4470	124 ± 13
77	-	-	10300	-	3450	1880	89 ± 11
78	55900	-	13300	4400	-	-	132 ± 8
84	-	18700	8890	2480	-	-	86 ± 3
79	52100	-	7390	2440	-	-	159 ± 23
80	26600	-	5620	4400	-	-	156 ± 4
83	20200	-	5240	2720	-	-	103 ± 18
87	23700	-	7070	1670	-	-	136 ± 9
86	15200	-	4480	1250	-	-	129 ± 4
85	161200	-	61300	15200	-	-	122 ± 14

Table 3.5. Rate constants of decomposition of triazolinyl derivatives.

Radical	k, 70°C, [s^{-1}]	k, 75°C, [s^{-1}]	k, 80°C, [s^{-1}]	k, 90°C, [s^{-1}]	k, 95°C, [s^{-1}]	k, 100°C, [s^{-1}]
33	-	-	$1.110 \pm 0.007 \cdot 10^{-4}$	-	$5.599 \pm 0.06 \cdot 10^{-4}$	$7.35 \pm 0.09 \cdot 10^{-4}$
81	-	-	$2.85 \pm 0.06 \cdot 10^{-5}$	-	$1.084 \pm 0.003 \cdot 10^{-4}$	$1.94 \pm 0.01 \cdot 10^{-4}$
82	-	-	$1.71 \pm 0.07 \cdot 10^{-5}$	-	$1.15 \pm 0.02 \cdot 10^{-4}$	$1.55 \pm 0.07 \cdot 10^{-4}$
77	-	-	$6.71 \pm 0.03 \cdot 10^{-5}$	-	$2.01 \pm 0.02 \cdot 10^{-4}$	$3.68 \pm 0.02 \cdot 10^{-4}$
78	$1.24 \pm 0.04 \cdot 10^{-5}$	-	$5.22 \pm 0.05 \cdot 10^{-5}$	$1.576 \pm 0.007 \cdot 10^{-4}$	-	-
84	-	$3.7 \pm 0.1 \cdot 10^{-5}$	$7.8 \pm 0.1 \cdot 10^{-5}$	$2.792 \pm 0.006 \cdot 10^{-4}$	-	-
79	$1.33 \pm 0.05 \cdot 10^{-5}$	-	$9.38 \pm 0.05 \cdot 10^{-5}$	$2.84 \pm 0.03 \cdot 10^{-4}$	-	-
80	$2.605 \pm 0.01 \cdot 10^{-5}$	$5.53 \pm 0.08 \cdot 10^{-5}$	$1.233 \pm 0.006 \cdot 10^{-4}$	-	-	-
83	$3.44 \pm 0.04 \cdot 10^{-5}$	-	$1.323 \pm 0.005 \cdot 10^{-4}$	$2.550 \pm 0.006 \cdot 10^{-4}$	-	-
87	$2.93 \pm 0.05 \cdot 10^{-5}$	-	$9.8 \pm 0.1 \cdot 10^{-5}$	$4.14 \pm 0.05 \cdot 10^{-4}$	-	-
86	$4.55 \pm 0.06 \cdot 10^{-5}$	-	$1.541 \pm 0.004 \cdot 10^{-4}$	$5.56 \pm 0.05 \cdot 10^{-4}$	-	-
85	$4.3 \pm 0.3 \cdot 10^{-6}$	-	$1.13 \pm 0.02 \cdot 10^{-5}$	$4.57 \pm 0.04 \cdot 10^{-5}$	-	-

A great influence of the substituent at the 5-position of the triazolinyl ring on the decomposition rate found by experiment is not obvious from mechnistic point of view. Earlier it was mentioned that bridging of these two substituents leads to formation of thermally stable radical **40** (see Section 1.7.1). Although it is clear that the decomposition of the triazolinyls proceeds *via* cleavage of one of the substituent at the 5-position, as confirmed by mass spectroscopy of the decomposition products,[187] the mechanism of the decomposition is not clear. As was mentioned above, delocalization of the unpaired spin does not spread over the substituents at carbon-5 atom of the triazolinyl ring. Transfer of the unpaired electron from either nitrogen-1 or nitrogen-4 atoms to the phenyl ring with simultaneous formation of double bond probably includes overlapping of the nitrogen π-orbital with the σ-bond between carbon-5 and substituent at 5-position. Moreover, the transfer from the nitrogen atom 4 seems to be more reasonable, due to the observed migration of the double bond at this atom (Scheme 4.4). In this case the influence of the substituents on the phenyl ring at the 5-position, which was observed, can be explained by the change in the stability of the formed radicals (formally substituents at the 5-position). If the formed radical is more stable, it should lead to easier decomposition and *vice versa*, if the formed radical is less stable it should lead to more stable triazolinyl. Unfortunately, due to the absence of the data on the relative stability of the differently substituted phenyl radicals, this hypothesis cannot be confirmed or disregarded so far. However,

[187] M. Steenbock; M. Klapper; K. Müllen; C. Bauer; M. Hubrich, Macromolecules, *31*, 5223 - 5228, **1998**.

if this proposition is correct, the electronic factors (mainly inductive effect) must play the major role in the stability variations.

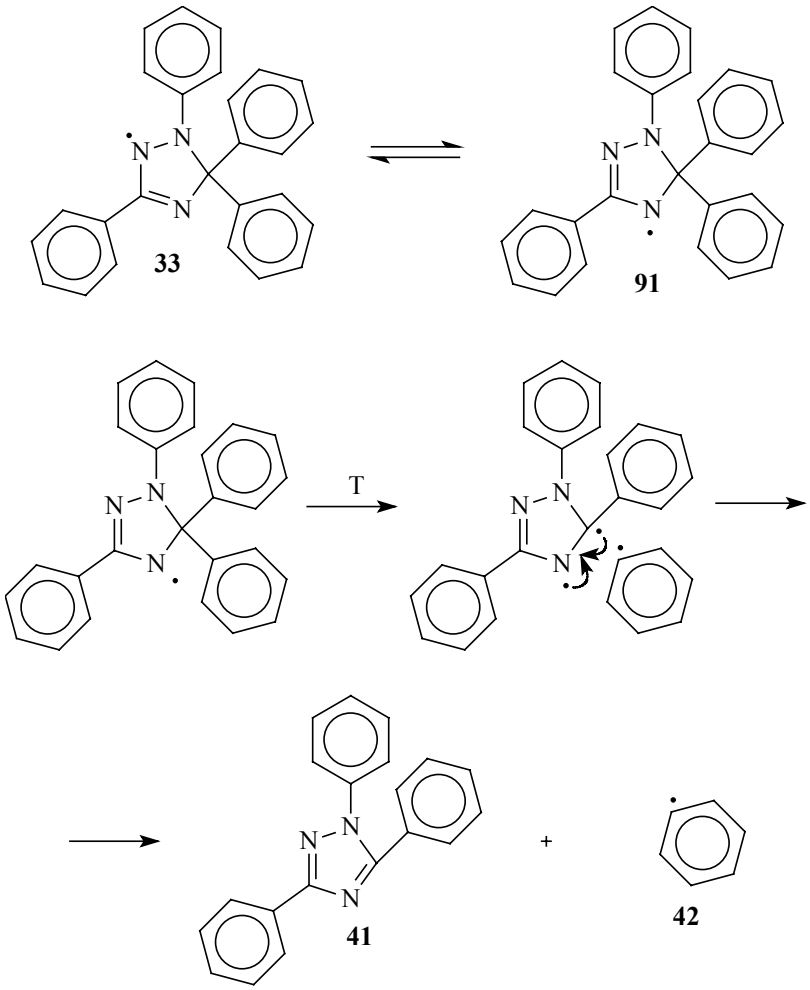

Scheme 3.5. Possible mechanism of triazolinyl decomposition.

Table 3.6. Hammett constants of the triazolinyl radical substituents at 5-position.

Radical	Hammett constant
82 (*p*-$N(CH_3)_2$)	-0.83
81 (*p*-OCH_3)	-0.268
84 (*p*-C_6H_5)	-0.01
33 (H)	0
78 (*p*-F)	0.062
77 (*p*-Cl)	0.227
79 (*p*-Br)	0.232
86 (*m*-CF_3)	0.43
83 (considered as *p*-CF_3)	0.54
87 (considered as *p*-NO_2)	0.75

The Hammett correlations are the most well known parameters enabling quantitative estimation of the influence of substituents on phenyl rings on their chemical activity in a variety of reactions. For instance the pKa of differently substituted benzoic acids showed very good correspondence to the Hammett constants of the substituents on the ring.[188] This influence is mainly due to electron density factors, which gives a good chance to correlate the stability of the radicals to the Hammett constants values. Therefore, the Hammett constants have been correlated to the observed half-life times of the triazolinyl derivatives having substituted phenyl rings at 5-position. The Hammett constants[189] of the substituents are given in Table 3.6. The plot of the half-life time *vs.* the Hammett constant at 80°C for toluene solutions is given in Figure 3.18.

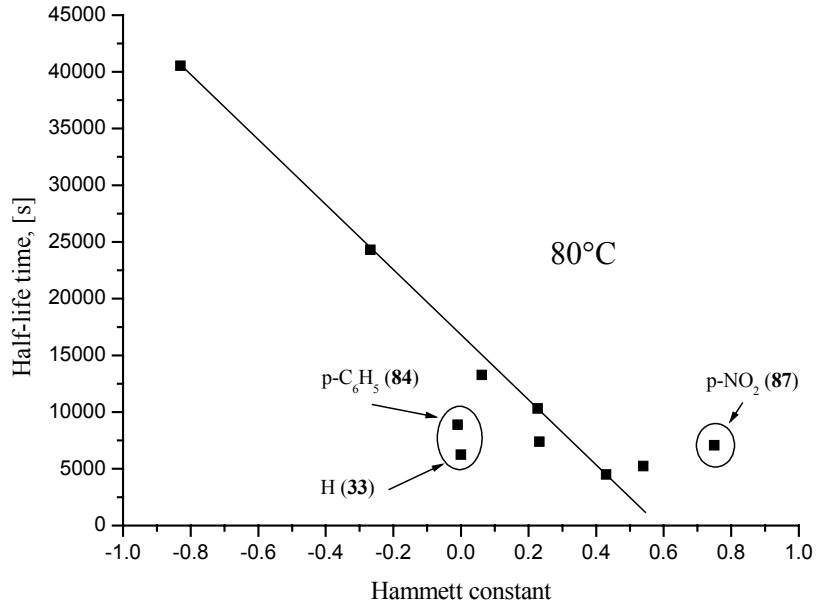

Figure 3.18. Correlation of the half-life times of the decomposition of 5-substituted triazolinyl derivatives at 80°C in toluene solution monitored by ESR to Hammett constants.

A linear dependence of the half-life times upon the Hammett constants is observed for most of the triazolinyl derivatives, which confirms the proposition about the major importance of the electronic effects of the substituents for the stability of the radical. The radicals having as substituents at 5-position unsubstituted phenyl rings (**33**), 4-biphenyls (**84**) and nitrophenyls (mixture of izomers) (**87**) show significant deviations from this linear dependence. In the case of **87** the deviation can possibly be explained by the fact, that instead of one isomer the isomer mixture is used in the experiment. The Hammett constant is however, taken for the *para* substituent. The presence of the *ortho*-substituted groups at the 5-position might lead to less efficient overlap of the π-orbital of nitrogen with the σ-bond between carbon-5 and the

[188] Ssylka na Roberts caserio
[189] A. J. Gordon; R. A. Ford, ***The Chemist's Companion***, John Wiley & Sons: New York, 145 - 146, 1972.

substituent leading to difficulties in the decomposition process and subsequently to higher stability of the triazolinyl radical. The mismatch of the stability of the *para*-biphenyl triazolinyl derivative **84** with the general linear dependence might be caused by the other routes of decomposition of this radical. As mentioned in Section 3.3.5 yet its precursor 1,3-diphenyl-5,5-di(4-biphenyl)-Δ^2-1,2,4-triazolin was not isolated due to continuous decomposition. Here again this radical shows significantly lower stability as it could be expected from the graph in Figure 3.18. Linear dependence indicates that increasing the electron-withdrawing ability of the substituent at 5-position, or in other words, decreasing electron density in the aromatic ring destabilizes the triazolinyls. This is also supported by the fact that the triazolinyls with low electron density on the C-5 aromatic substituents such as 1,3–diphenyl-5,5-di(4-acylphenyl)-Δ^3-1,2,4-triazolin-2-yl (**88**) and 1,3–diphenyl-5,5-di(2-pyridyl)-Δ^3-1,2,4-triazolin-2-yl (**89**) could not be isolated due to their rapid decomposition during preparation and isolation. In the same time, aromatic substituents at the 5-position bearing electron donating groups or in other words electron-rich aryl substituents stabilize the radical. Another proof of this general tendency is the high stability of 1,3–diphenyl-5,5-di(2-thiophenyl)-Δ^3-1,2,4-triazolin-2-yl (**85**) radical having electron-rich thiophenyl substituents at the 5-position.

3.4.3. Other properties

All radicals synthesized are solid at room temperature. Most of the radicals could be kept in a freezer (- 18°C) without decomposition over one year. This has been confirmed by mass spectrometry several times during the period mentioned, which did not show any peaks corresponding to possible products of decomposition. As mentioned above, the acetylphenyl derivative **89** and pyridyl derivative **88** were not isolated, but formation of the radicals was confirmed during the oxidation step by ESR in the case of **88** and visually (by their specific red-red color) in both cases. The radicals **78**, and **86** bearing fluorinated substituents showed solubility in freon and supercritical carbon dioxide, which permitted attempts to realize the polymerization in supercritical CO_2. All synthesized radicals are very readily soluble in most organic solvents and monomers. Radicals having no solubilizing groups are completely insoluble in water. **82** can be dissolved in diluted acids.

3.5. Polymerization experiments in the presence of triazolinyl radicals

The triazolinyls synthesized were used as additives in radical polymerization experiments. Polymerizations of styrene, 4-vinylpyridine, methylmethacrylate, *n*-

butylmethacrylate, ethyl methacrylate and 2,2,2-trifluoroethylmethacrylate (Figure 3.19) in the presence of various triazolinyl radicals were attempted. In order to investigate the influence of the stability of the radical on the behavior of the polymerization process, polymerizations of methylmethacrylate and styrene were performed with various triazolinyls and the results were compared and analyzed.

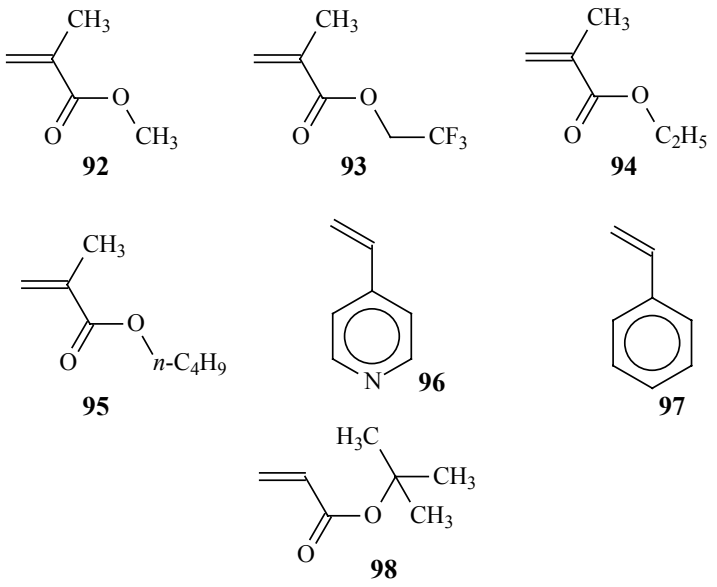

Figure 3.19. Monomers used in the polymerization and copolymerization experiments.

Since, as was discussed above, the substituents at the 5-position of the triazolinyl ring do not participate in the conjugation with the radical center, the influence of these substituents on the equilibrium between the dormant and active species is negligible. Hence, the differences in the polymerization behavior are only due to the different stability of the radicals used as additives leading to the change of the reinitiation process in the self-regulation concept.
During the polymerizations the degree of monomer conversion was monitored and the molecular weights of the polymers obtained at different stages of the polymerization were measured. This allowed investigation of the kinetics of the polymerizations. All polymerization experiments were performed in a similar way, according to the method given in Section 6.10.

3.5.1 Polymerizations of styrene in the presence of triazolinyl radicals

Polymerization of styrene in the presence of 1,3,5,5-tetraphenyl-Δ^3-1,2,4-triazolin-2-yl (**33**) has already been reported in the literature.[190,191,192] However, the polymerization was

[190] M. Steenbock; M. Klapper; K. Müllen, Macromol. Chem. Phys., *199*, 763 – 769, **1998**.
[191] D. Colombani; M. Steenbock; M. Klapper; K. Müllen, Macromol. Rapid Commun. *18*, 243 – 251, **1997**.

repeated in order to confirm the reproducibility of the technique used and to obtain data for comparison with further polymerization results. In order to be consistent with the previous experiments performed in the group BPO was used as initiator in all cases. The mixture of the required amounts of the initiator, monomer, and triazolinyl radical was degassed and distributed into several reaction vessels. Later at different polymerization stages the reaction vessels were taken one by one out of the thermostat, and the polymerization was quenched by putting the vessels into liquid N_2. The method is described more in-depth in Section 6.10. This procedure allowed better reproducibility and easier completion of the kinetic measurement in comparison to other methods, such as for instance taking samples out of the reactor with the use of a syringe. The amount of the obtained polymer with regard to the loaded monomer permitted calculation of the conversion of the monomer. The obtained polymer samples were analyzed by GPC to give M_n, M_w and D values. The polymerization was controlled as indicated by the linear plots of $\ln([M]_0/[M])$ *vs.* time and M_n *vs.* conversion (Figures 3.20, 3.21).[193] Analyses showed that in the presence of **33** there was a very rapid growth of molecular weights of formed PS at the beginning of the polymerization. The polydispersity of the polymer slowly decreased from 2 at the beginning to 1.6 at the moment of quenching of the polymerization (250 minutes, 50 % conversion) (Figure 3.22). At this conversion the polymerization mixture became very viscous, which complicated further polymerization. The polymer was isolated as described in Section 6.7. The data obtained showed good correspondence to the results published earlier. Therefore, the method was presumed to give reproducible results, and therefore the results could be directly compared one with another.

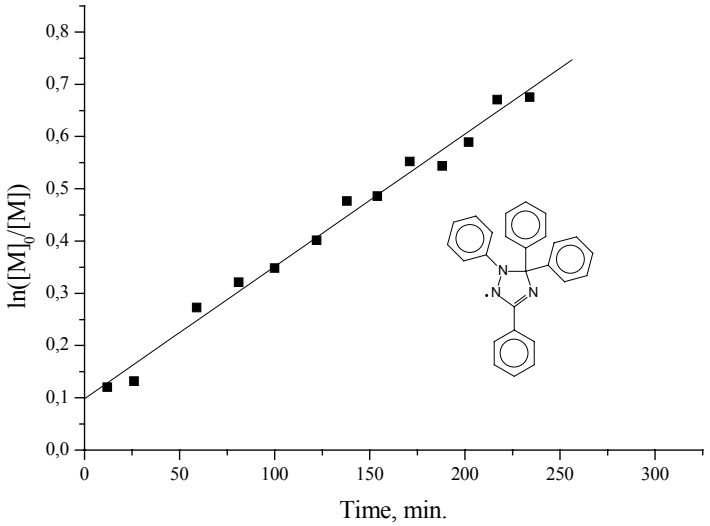

Figure 3.20. $\ln([M]_0/[M])$ *vs.* time plot for the polymerization of styrene in the presence of **33**, styrene/BPO (mol.): 1000, triazolinyl/BPO (mol.): 1.5, 120ºC.

[192] M. Steenbock; M. Klapper; K. Müllen; C. Bauer; M. Hubrich, Macromolecules, *31*, 5223 – 5228, **1998**.

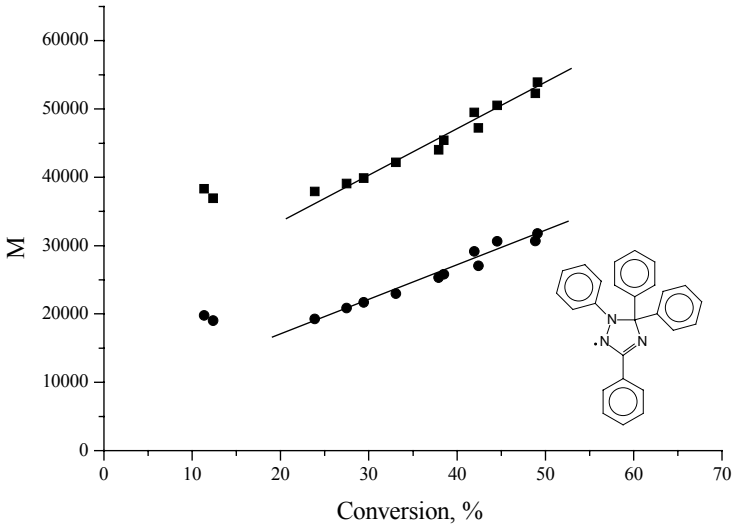

Figure 3.21. Molecular weights (M_w: ■; M_n: ●) *vs.* conversion plot for the polymerization of styrene in the presence of **33**, styrene/BPO (mol.): 1000, triazolinyl/BPO (mol.): 1.5, 120ºC.

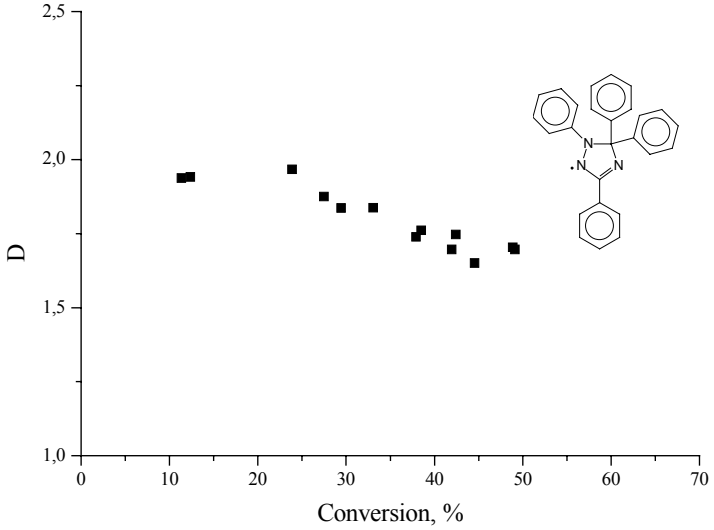

Figure 3.22. Polydispersity (D) *vs.* conversion plot for the polymerization of styrene in the presence of **33**, styrene/BPO (mol.): 1000, triazolinyl/BPO (mol.): 1.5, 120ºC.

As shown by the ESR experiments 1,3–diphenyl-5,5-di(4-methoxyphenyl)-Δ^3-1,2,4-triazolin-2-yl (**81**) was more stable than **33**. However, the change in the stability had almost no influence on the polymerization behavior. This was actually not expected because more stable radicals were suspected to provide better control (more pronounced increase in M_n with conversion, lower polydispersity indexes). Possible the differene in the stability between **33** and **81** was not significant enough to induce a remarkable change in the polymerization behavior, which could clearly be measured by the used method. If it so the further increase in stability shoud have provided more clear influence of the triazolinyl stability on the polymerization

[193] More detailed kinetic datasheets for all performed polymerization experiments are given in tables in the supplement section.

behavior. Still, the characteristic plots were linear, indicating controlled character of the polymerization (Figures 3.23 – 3.25).

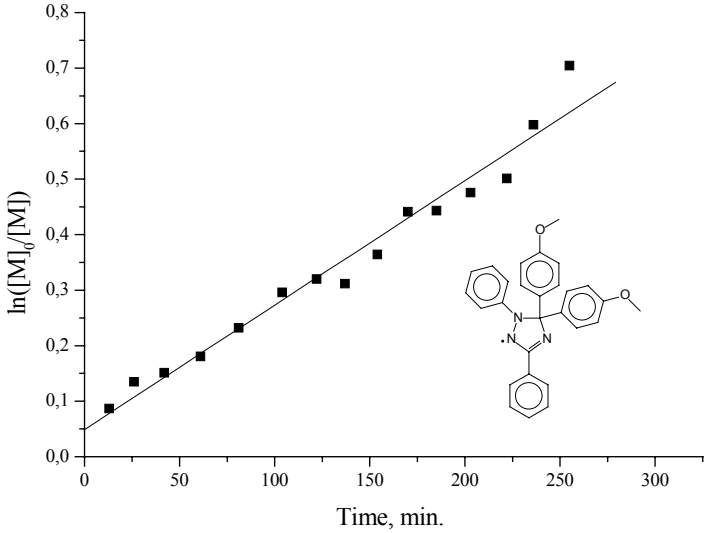

Figure 3.23. $\ln([M]_0/[M])$ *vs.* time plot for the polymerization of styrene in the presence of **81**, styrene/BPO (mol.): 1000, triazolinyl/BPO (mol.): 1.5, 120ºC.

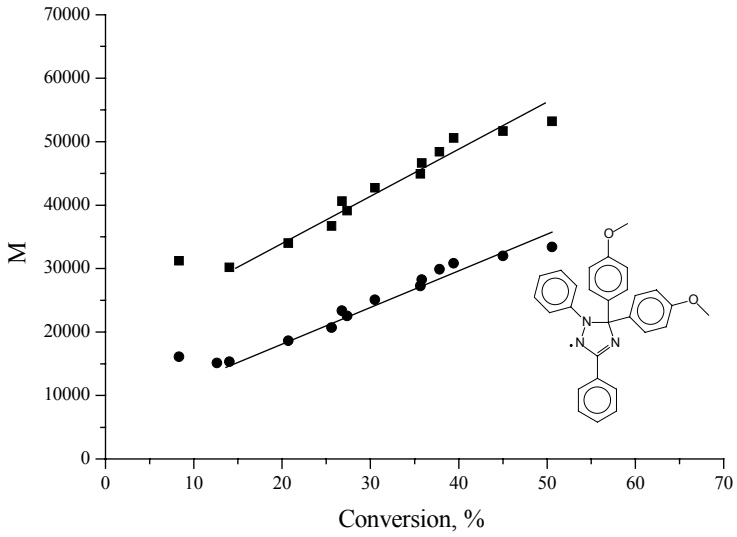

Figure 3.24. Molecular weights (M_w: ■; M_n: ●) *vs.* conversion plot for the polymerization of styrene in the presence of **81**, styrene/BPO (mol.): 1000, triazolinyl/BPO (mol.): 1.5, 120ºC.

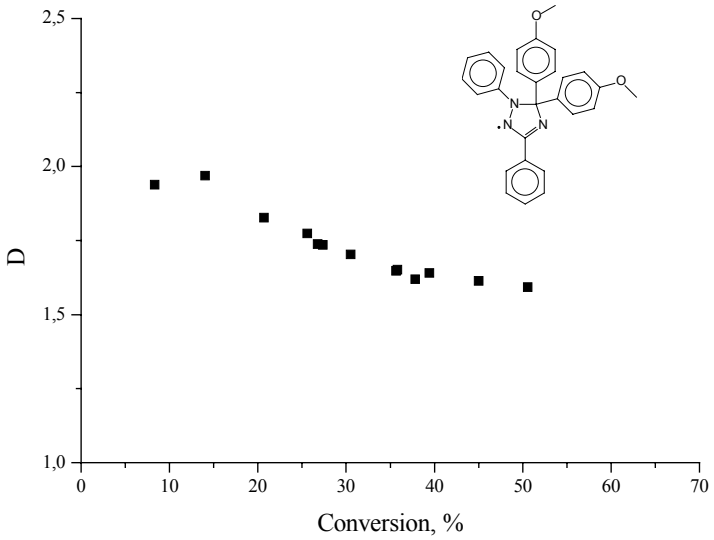

Figure 3.25. Polydispersity (D) *vs.* conversion plot for the polymerization of styrene in the presence of **81**, styrene/BPO (mol.): 1000, triazolinyl/BPO (mol.): 1.5, 120ºC.

Comparing the plots obtained in the presence of the methoxy triazolinyl **81** with previously obtained results in the presence of the **33** almost no changes are observed. Similarly in the very beginning of the polymerization the conversion and the molecular weights showed rapid growth. In both cases the conversion plot is a straight line indicating that the controlled character of the polymerization does not go through zero point as it must be in the case if the efficient equilibrium is achieved directly at the start of the polymerization (Figure 3.23). The behavior of the molecular weights in the beginning of the polymerization is also very similar: the M_n and M_w increase very quickly, after which they grow linearly with conversion indicating a controlled process. Both factors indicate the absence of an efficient equilibrium between the dormant and active species in the beginning of the polymerization. As the phenomenon was observed in two different systems; in the presence of triazolinyls with various stability, there should be a common reason for this. There are several possibilities for such behavior. One might be the slow capturing of the formed macroradical, caused by low affinity of the macroradicals to triazolinyl radicals. But it is quite improbable, because of the requirement of the low *K* value for the realization of the controlled radical polymerization. As soon as at following stages of the polymerization control over the whole reaction is achieved the value of *K* must be low enough for efficient capturing of the macroradicals. Otherwise, the control over the polymerization must be low over whole polymerization time and this is not the case as seen from the characteristic kinetic plots. More reasonable seems to be the possibility that in the beginning of the polymerization due to relatively slow initiation, high concentration of free (not bound to the macroradical) triazolinyl radicals is in the system. These radicals might also contribute to the initiation through decomposition during the time in the beginning of the process when they are

not yet bound to the formed macroradicals. This will lead to the appearance of too many initiating species, which must be responsible for the rapid growth of the conversion and molecular weights in the beginning of the polymerization. Later the equilibrium between the dormant and the active species is reached, which leads to the appearance of the linear region in the characteristic plots. This explanation seems to be more reasonable for the observed behavior. Also similar to the polymerization in the presence of **33** polydispersity decreased from 2 in the beginning to 1.55 at 50 % conversion (270 minutes of polymerization) (Figure 3.25). In both cases the polydispersity is quite high in comparison to the TEMPO mediated polymerizations were polydispersity indexes ~ 1.1 are easily achieved. Similar results were also observed in the previous investigations[194] (see Section 1.9.1) and are explained by somewhat "less controlled" character of polymerization in the case of triazolinyl radicals.

Another triazolinyl used as counter radical was the biphenyl derivative **84**. According to the ESR measurements its stability was slightly higher than the stability of the non-substituted radical **33**. As the stability of **84** was close to **33** and **81**, and the control over the polymerization in the two latter cases did not show remarkable changes, use of this derivative also should have not lead to huge differences in the polymerization behavior. The confirmation of this expectation would be another proof that in the series of 5-substituted triazolinyls, the stability of the radical and not the nature of the substituent plays a major role in the control over the process if change of the other substituents was not done. This was indeed the case. The results of the polymerization of styrene in the presence of **84** showed that the radical behaved similarly to the triazolinyls **33** and **81** described above. The characteristic plots are shown in Figures 3.26 – 3.28. As was seen in the kinetic plots in the presence of methoxy triazolinyl **81** and non-substituted derivative **33** the initial increase in the molecular weight and conversion is also observed. The rates of the polymerization in all three cases are very similar.

[194] M. Steenbock; M. Klapper; K. Müllen; C. Bauer; M. Hubrich, Macromolecules, *31*, 5223 - 5228, **1998**.

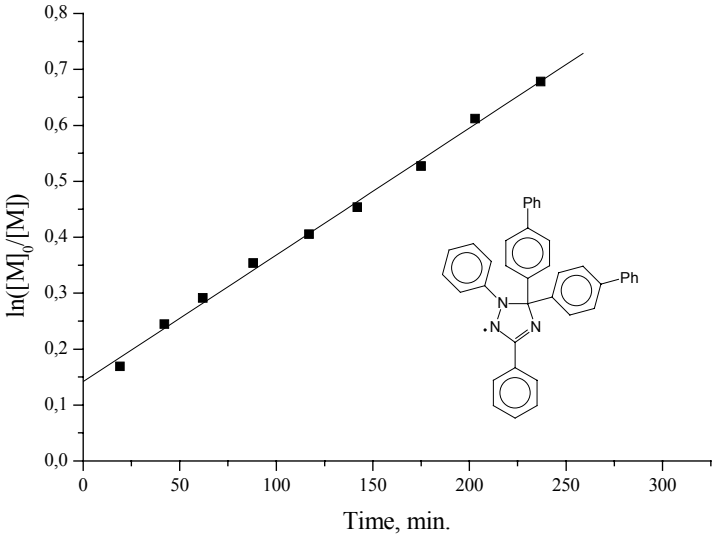

Figure 3.26. ln([M]$_0$/[M]) *vs.* time plot for the polymerization of styrene in the presence of **84**, styrene/BPO (mol.): 1000, triazolinyl/BPO (mol.): 1.5, 120ºC.

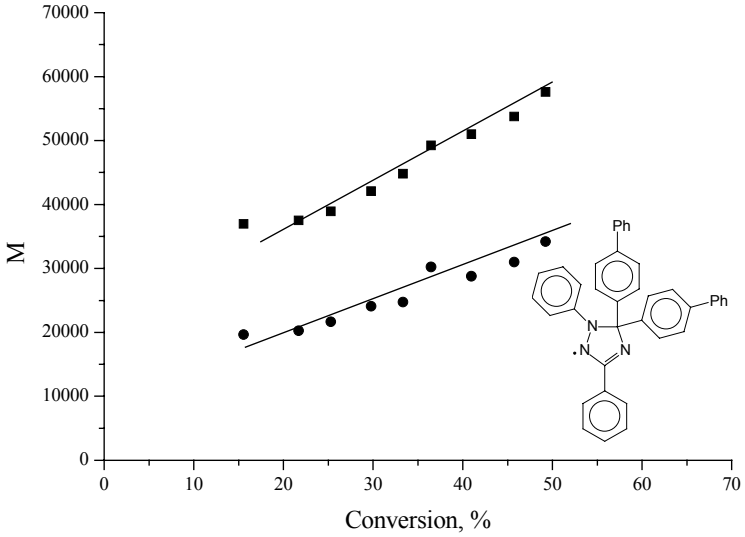

Figure 3.27. Molecular weights (M_w:■; M_n:●) *vs.* conversion plot for the polymerization of styrene in the presence of **84**, styrene/BPO (mol.): 1000, triazolinyl/BPO (mol.): 1.5, 120ºC.

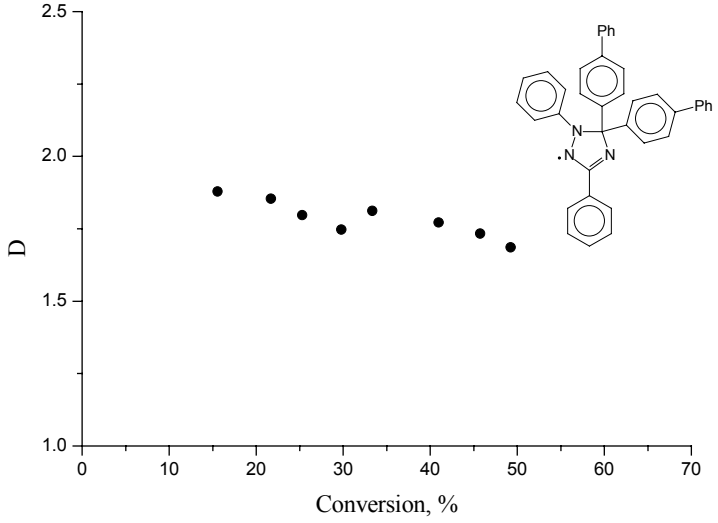

Figure 3.28. Polydispersity (D) *vs.* conversion plots for the polymerization of styrene in the presence of **84**, styrene/BPO (mol.): 1000, triazolinyl/BPO (mol.): 1.5, 120ºC.

The polymerization was certainly controlled as shown by characteristic linear plots (Figures 3.26 and 2.27). Within 250 minutes, molecular weights reached 60000 and 35000 for M_w and M_n respectively. At the end of the polymerization polydispersity index reached 1.66, which was slightly higher than in the previous cases (Figure 3.28). The conversion reached 50 % within 250 minutes. These development is again similar to previous cases.

1,3–Diphenyl-5,5-di(4-chlorophenyl)-Δ^3-1,2,4-triazolin-2-yl (**77**) was one of the less stable triazolinyls synthesized here and used for polymerizations experiments. Less stable radicals provide the system with more initiating species due to the faster decomposition of the radical during the polymerization. As a result, more active radicals, which might cause deviation from controlled character of the polymerization in the case of styrene, are formed. However, since the slight increase in the stability provided by the use of triazolinyls **81** and **84** did not lead to significant changes in the polymerization behavior, the possible influence of slightly less stable radical was not easily predictable. The further increase in the amount of newly formed initiating species provided by triazolinyl decomposition might have not been very important for the attainment of the controlled polymerization. In this case the results must be similar to the previously described polymerizations of styrene in the presence of **33**, **81**, and **84**. Then the stability of the radical must be change more drastically or the whole self-regulation concept might be misleading. However, if the increase in the amount of the initiating species formed by decomposition of less stable radicals will lead to worse controlled polymerization, it would confirm the initial proposition.

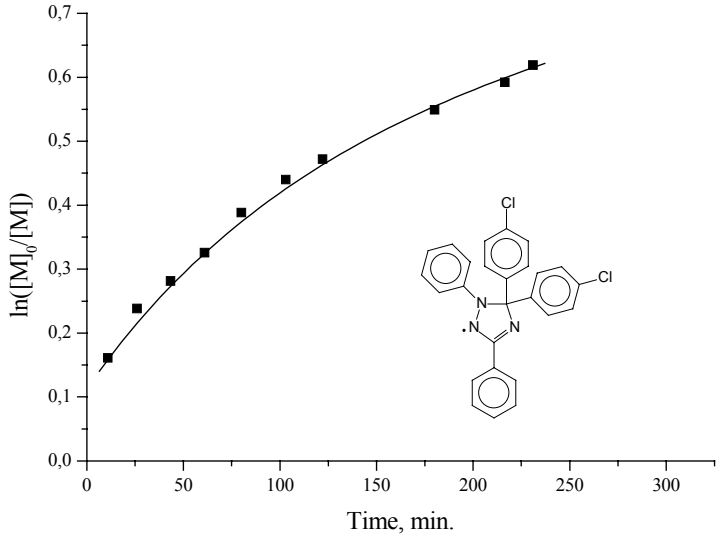

Figure 3.29. Molecular weights (M_w:■; M_n:●) *vs.* conversion plot for the polymerization of styrene in the presence of **77**, styrene/BPO (mol.): 1000, triazolinyl/BPO (mol.): 1.5, 120°C.

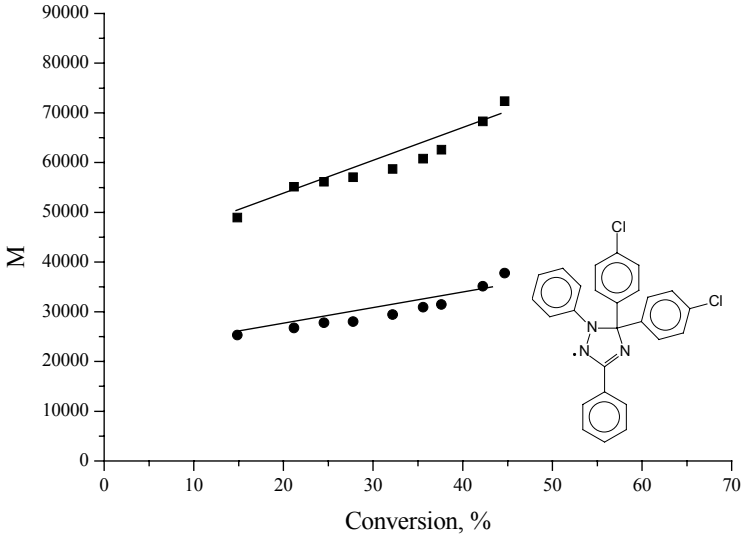

Figure 3.30. Molecular weights (M_w:■; M_n:●) *vs.* conversion plot for the polymerization of styrene in the presence of **77**, styrene/BPO (mol.): 1000, triazolinyl/BPO (mol.): 1.5, 120°C.

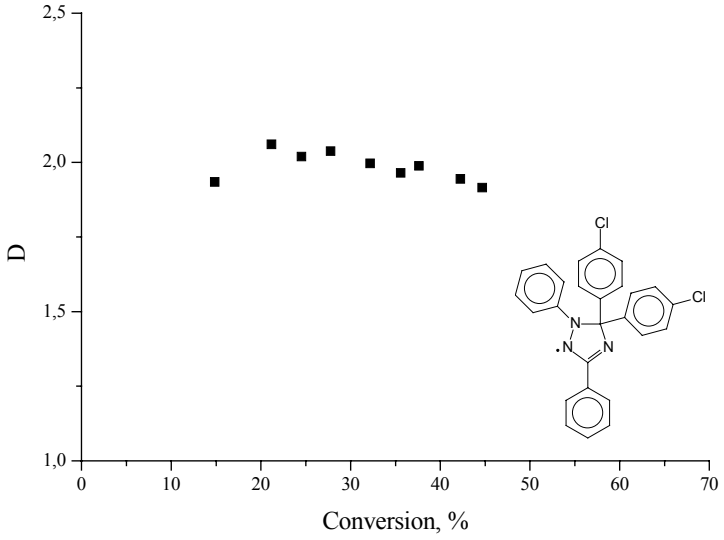

Figure 3.31. Polydispersity (D) vs. conversion plot for the polymerization of styrene in the presence of **77**, styrene/BPO (mol.): 1000, triazolinyl/BPO (mol.): 1.5, 120°C.

The experiment with **77** as additive showed less controlled character of polymerization in comparison with the experiments described above. Therefore, the second possibility was more correct and the self-regulation concept is still working. When the usual polymerization recipe was used, a remarkable loss of control was observed. In comparison to the previously described polymerizations in presence of **33**, **81** and **84**, where the plot $\ln([M]_0/[M])$ *vs.* time was linear, the corresponding plot in this case, given in Figure 3.29 shows considerable deviations from linearity. The increase in number average molecular weights with time was considerably lower in comparison to previous experiments (M_n from ~ 25000 to 35000) and was not linear but more flat with a slight increase when 40 % conversion was achieved (Figure 3.30). The polydispersity

was nearly 2 during the whole polymerization (Figure 3.31). This is again different from the previously observed decrease in the polydispersity during the polymerization, when more stable radicals were used for the polymerization as additives. The polydispersity values were also higher than in the previous cases. Within 250 minutes 50 % conversion was reached.

Attempts to change either the radical concentration or reaction temperature were made in order to reveal possible changes in the polymerization behavior, which might improve the control over the polymerization process. First, the amount of the triazolinyl was increased from 1.5 equivalents in respect to the BPO to 2 equivalents. This caused slight changes in polymerization behavior (Figures 3.32 – 3.34). The deviations from linearity of the plot $\ln([M]_0/[M])$ *vs.* time became negligible (Figure 3.32).

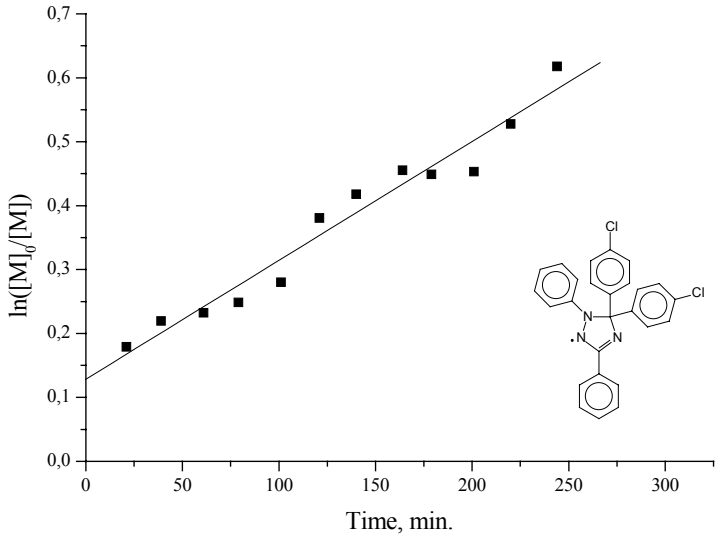

Figure 3.32. $\ln([M]_0/[M])$ *vs.* time plot for the polymerization of styrene in the presence of **77**, styrene/BPO (mol.): 1000, triazolinyl/BPO (mol.): 2, 120°C

However, the M_n *vs.* conversion plot (Figure 3.33) gave no increase in the molecular weights during the polymerization. Instead it shows a strange "U"-like curvature with the molecular weights of the polymer in the end of the reaction very similar to the values observed in the beginning of the reaction. However, the initial increase in the molecular weights (first data point at ~ 10 min. after the beginning of the reaction $M_n \sim 30000$ and $M_w \sim 60000$) is higher than in former experiments. This might be a confirmation of the proposed reason for this increase. If the decomposition of the excess of the free counter radical in the beginning of the reaction, when it is not yet captured by the forming macroradicals, is responsible for it the observed increase in the conversion and molecular weight, thenraising the triazolinyl concentration must provide higher increase as observed in this case (Figure 3.33). The whole rate of the polymerization

slightly decreased by comparison with the previous experiment. Polydispersity was near 2 during the whole polymerization process (Figure 3.30). Conversion reached 45 % when the polymerization was stopped (reaction time 250 minutes).

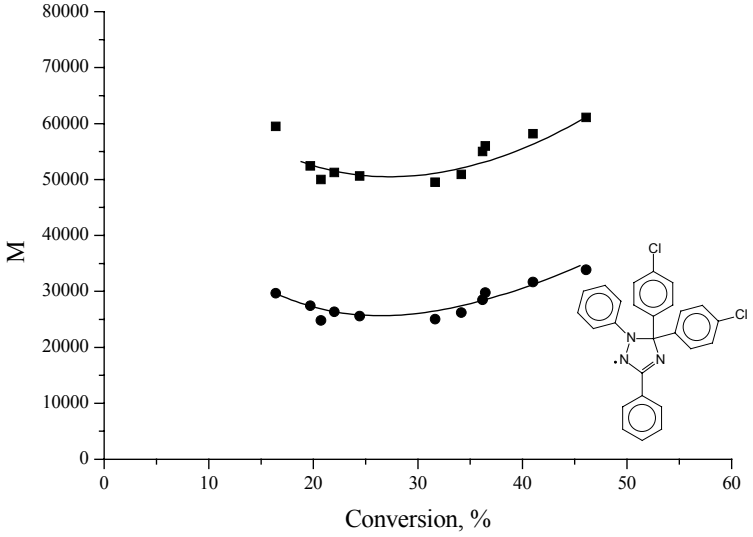

Figure 3.33. Molecular weights (M_w:■; M_n:●) *vs.* conversion plot for the polymerization of styrene in the presence of **77**, styrene/BPO (mol.): 1000, triazolinyl/BPO (mol.): 2, 120°C

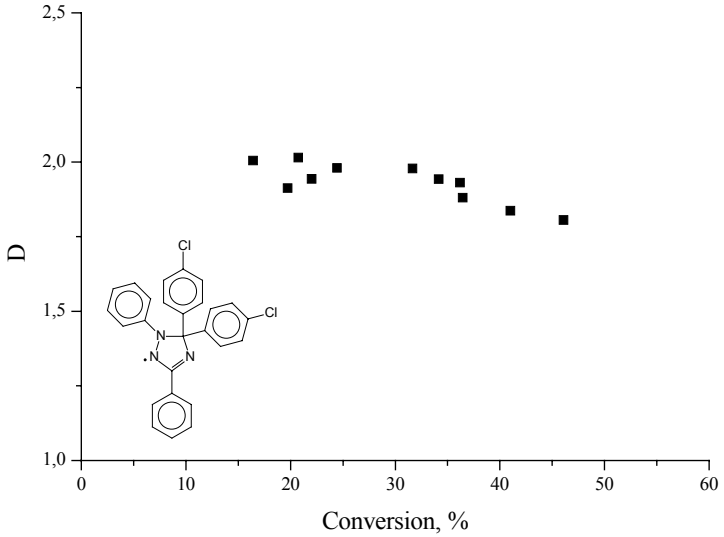

Figure 3.34. Polydispersity (D) *vs.* conversion plot for the polymerization of styrene in the presence of **77**, styrene/BPO (mol.): 1000, triazolinyl/BPO (mol.): 2, 120°C

Attempts to lower the decomposition rate by running the polymerization at 110°C while keeping the triazolinyl/initiator ratio 2 led to a complete loss of control over the polymerization. The $\ln([M]_0/[M])$ *vs.* time plot is "root" like and no increase in number average molecular weight was observed (Figures 3.35 – 3.37). The polymerization rate dropped in comparison to previous experiments and 40 % conversion was achieved when polymerization was quenched after a

reaction time of 250 minutes. The polydispersity of the polymer was higher than 2 during whole polymerization process (Figure 3.37).

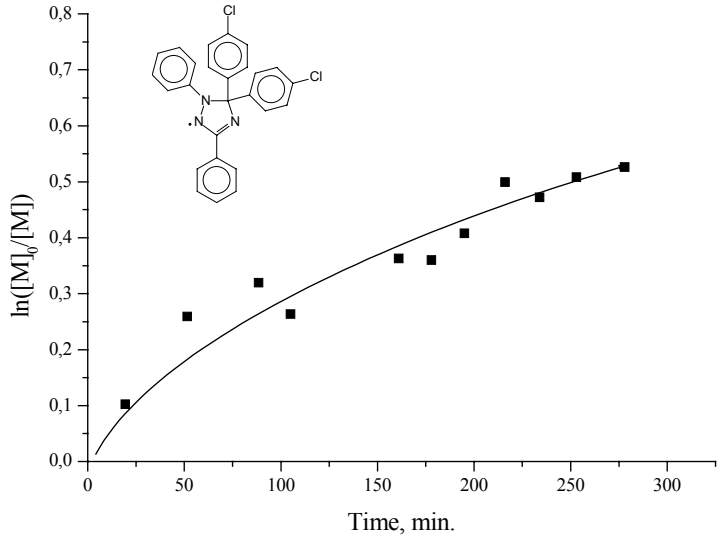

Figure 3.35. ln([M]$_0$/[M]) *vs.* time plot for the polymerization of styrene in the presence of **77**, styrene/BPO (mol.): 1000, triazolinyl/BPO (mol.): 2, 110°C

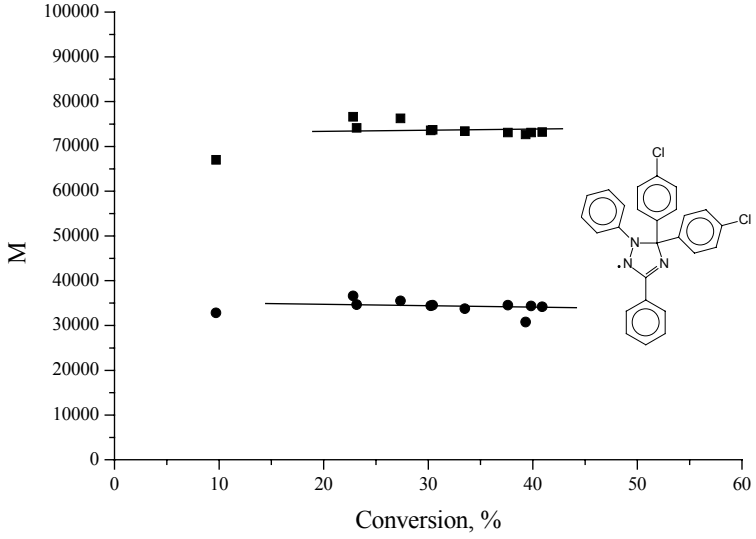

Figure 3.36. Molecular weights (M_w:■; M_n:●) *vs.* conversion plot for the polymerization of styrene in the presence of **77**, styrene/BPO (mol.): 1000, triazolinyl/BPO (mol.): 2, 110°C

As a common result of the attempts to realize controlled radical polymerization of styrene in the presence of **77**, significantly less controlled polymerization of the styrene was observed in this case as compared to earlier performed polymerization in the presence of **81** and **84**. This radical is relatively less stable in comparison to the previously used ones and the loss of the control is in good accordance with the original proposition of the lower efficiency of the less

stable triazolinyls when they are used as additives in controlled radical polymerization of styrene. In order to confirm this, polymerization in the presence of other poor stable triazolinyl - 1,3–diphenyl-5,5-di(4-bromophenyl)-Δ^3-1,2,4-triazolin-2-yl (**79**) was performed.

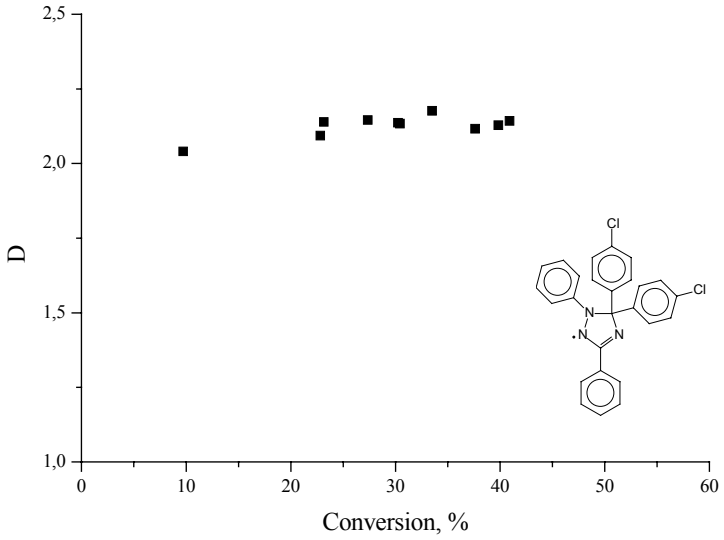

Figure 3.37. Polydispersity (D) *vs.* conversion plot for the polymerization of styrene in the presence of **77**, styrene/BPO (mol.): 1000, triazolinyl/BPO (mol.): 2, 110°C

Polymerization in the presence of 1,3–diphenyl-5,5-di(4-bromophenyl)-Δ^3-1,2,4-triazolin-2-yl (**79**) was expected to show a behavior similar to the case of **77**. As the radical **79** is even less stable than the previously used **77** it should have shown even worse or at least similar results, when applied as counter radical in the polymerization of styrene. Realization of the experiment showed that, as in the case of radical **77**, the control over the polymerization process in the presence of **79** was poor. The linearity of $\ln([M]_0/[M])$ *vs.* time is considerably better than in the case when **77** was used as counter radical (Figure 3.38). However, after three hours of reaction the polymerization rate dropped considerably. The increase in the number average molecular weight with time was very small (Figure 3.39). The polydispersity was near 2 during the whole polymerization (Figure 3.40), which was very similar to the cases of the polymerization with **77**. 45 % conversion was achieved within 250 minutes.

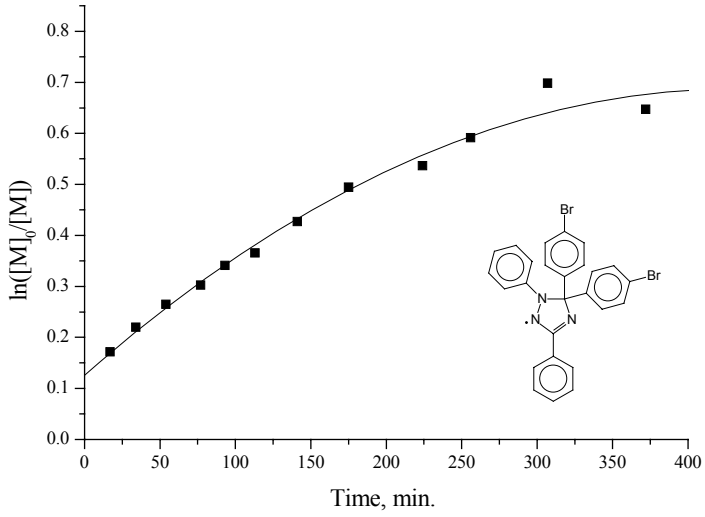

Figure 3.38. ln([M]$_0$/[M]) *vs.* time plot for the polymerization of styrene in the presence of **79**, styrene/BPO (mol.): 1000, triazolinyl/BPO (mol.): 1.5, 120°C.

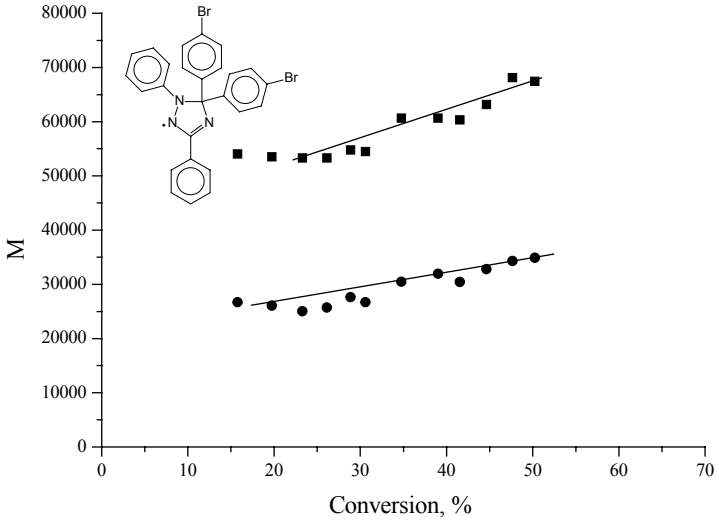

Figure 3.39. Molecular weights (M_w:■; M_n:●) *vs.* conversion plot for the polymerization of styrene in the presence of **79**, styrene/BPO (mol.): 1000, triazolinyl/BPO (mol.): 1.5, 120°C.

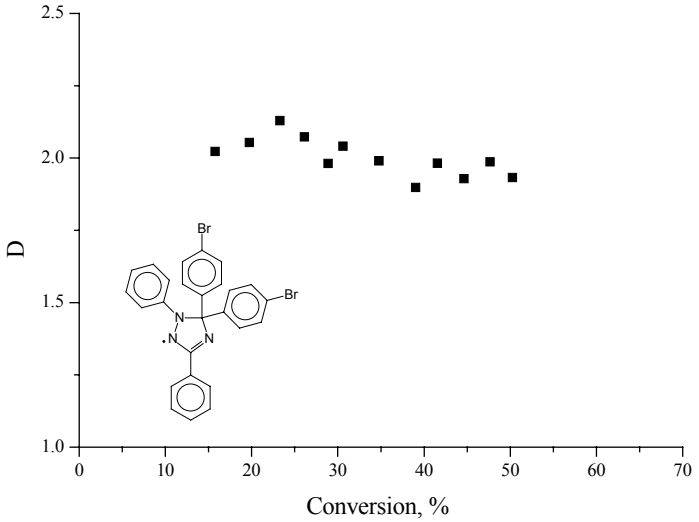

Figure 3.40. Polydispersity (D) *vs*. conversion plots for the polymerization of styrene in the presence of **79**, styrene/BPO (mol.): 1000, triazolinyl/BPO (mol.): 1.5, 120°C.

Both experiments with poorly stable triazolinyls **77** and **79** showed that although there were very minor changes in the polymerization behavior between the cases when triazolinyls **33**, **81**, and **84** were applied, further decrease in the triazolinyl stability lowered the control over the polymerization. The changes within each of the groups of the radicals in the polymerization process were not big enough to reveal the tendency of the influence of the stability of a radical on the control over the polymerization in its presence. However the comparison of these groups shows that less stable ones provide worse control. Therefore, the even more stable radical **82** was used as a counter radical. It might have permitted to find out the differences, brought by more stable radicals in the system, such as increased control over the polymerization process. Due to the higher stability of this derivative the previously observed initial rapid growth of conversion and molecular weights must be less pronounced or even not seen at all. If it is the case, the proposed earlier reason for the initial overinitiation, provided by the excess of counter radical in the beginning of the polymerization will become first confirmation.

1,3-Diphenyl-5,5-bis(4-dimethylaminophenyl)-Δ^3-1,2,4-triazolin-2-yl (**82**) was one of the most stable triazolinyl radicals synthesized during this work. It is of course not as stable as spiro-triazolinyl radical **40** discussed in Section 1.7.1, because it still can cleave the substituent at the 5-position, however its stability is significantly higher than that of any triazolinyls used in previous styrene polymerization experiments. Since the results obtained for less stable radicals have shown worse control of the polymerization, better control in the case of more stable radicals as **82** was expected. The results confirmed this expectation.

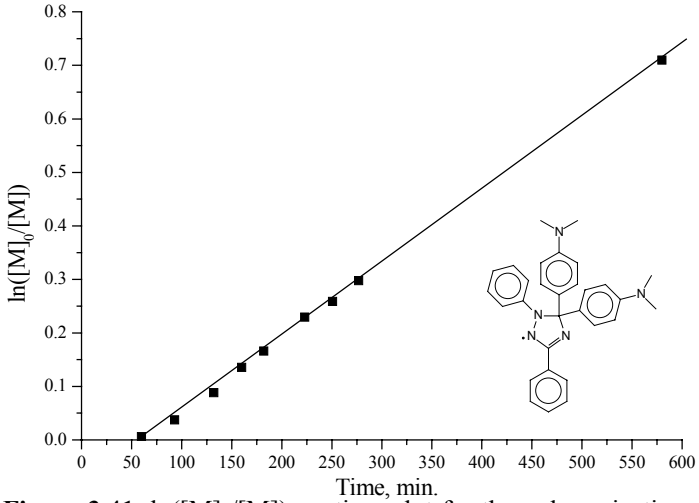

Figure 3.41. ln([M]$_0$/[M]) *vs.* time plot for the polymerization of styrene in the presence of **82**, styrene/BPO (mol.): 1000, triazolinyl/BPO (mol.): 1.5, 120°C

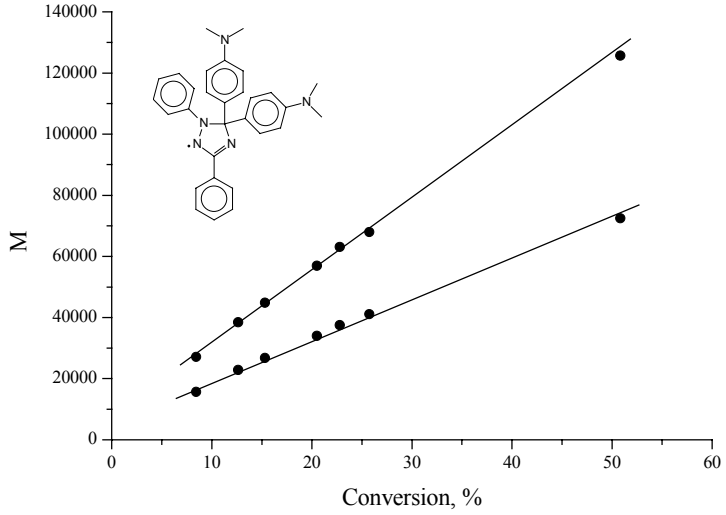

Figure 3.42. Molecular weights (M_w:■; M_n:●) *vs.* conversion plot for the polymerization of styrene in the presence of **82**, styrene/BPO (mol.): 1000, triazolinyl/BPO (mol.): 1.5, 120°C

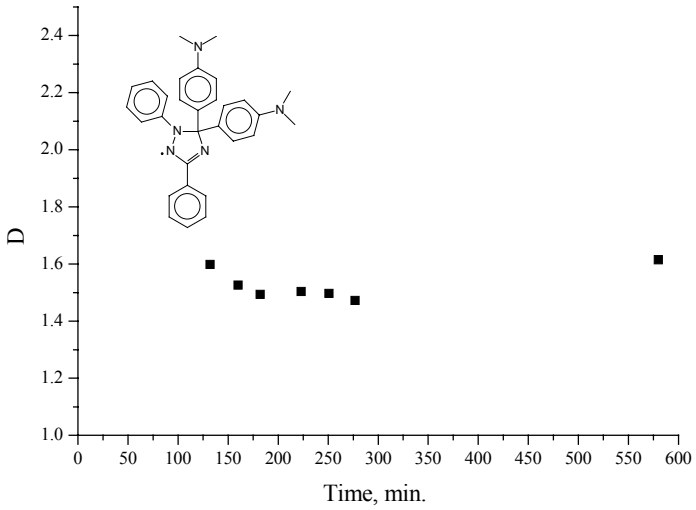

Figure 3.43. Polydispersity (D) *vs.* conversion plot for the polymerization of styrene in the presence of **82**, styrene/BPO (mol.): 1000, triazolinyl/BPO (mol.): 1.5, 120°C

Well controlled polymerization of styrene was observed in this case. Obtained results were better than with any other triazolinyl radical within derivatives used in this work. The characteristic plots were perfectly linear (Figures 3.41 – 3.43). The polymerization had an inhibition period lasting for about an hour. This is very different from the other polymerizations of styrene with triazolinyl counter radicals. The reason for this is not fully understood. Possibly, due to the higher stability of the radical, at the beginning of the polymerization the additional initiation, provided by decomposition of the triazolinyl radicals, is lowered. This does not lead to the previously observed rapid increase in conversion of the monomer and molecular weights of the polymer. This again confirms the proposition of the major role of the decomposition of the

free triazolinyl radicals for the previously observed effect in the beginning of the polymerization. The less stable radicals used, the faster decomposition leads to a relatively higher amount of initiated chains in the beginning of the polymerizations as was observed in previous cases when **33**, and other radicals were used. The excess of the initiating species is not captured by the triazolinyls and gives the quick increase of molecular weights and conversion in the beginning of the polymerization. But in the case of **82**, having increased stability, decomposition of the radical does not provide the system with that excess of the initiating species, which even lead to the inhibition period in the beginning of the polymerization. Interestingly an intermediate behavior *i.e.* either shorter inhibition period or small increase in conversion and molecular weights was not observed. The methoxy triazolinyl derivative **81** having moderate stability, which is lower than **82** but higher than all other mentioned triazolinyls. However, in this case increase of conversion and molecular weights of the polymer was quite high. This does not fit perfectly to the proposed explanation. A possible proof of the given hypothesis might be to start of the polymerization, not by the common radical initiator in the presence of triazolinyl but from the triazolinyl derivative which is formed as the result of addition of the triazolinyl to the formed initiating species (Figure 3.44). In this case the excess of the radical is absent and the kinetic plots of the polymerization must go through zero point without both initial increase of the conversion and molecular weights and inhibition period, independent of the structure of the radical.

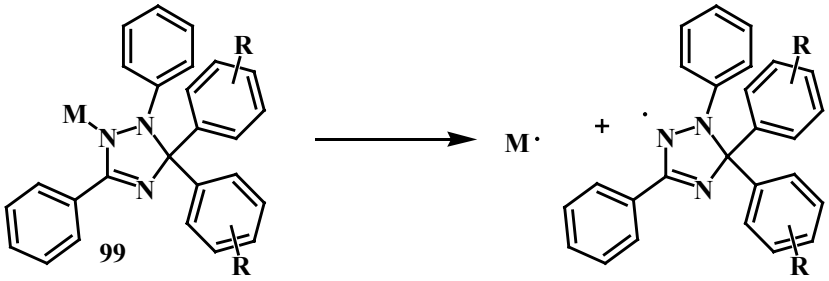

Figure 3.44. Possible initiator, which might reveal the influence of the excess of triazolinyl at early stage of the polymerization on the presence/absence of inhibition period and rapid growth of conversion and molecular weights of formed polymer.

The polydispersity was 1.47 at a reaction time of 280 minute and increased to 1.6 at a reaction time of 600 minutes (Figure 3.43). This is also lower than in the cases of other triazolinyl derivatives used in this work, however, still higher than in the cases when TEMPO is used as counter radical. At the time when the reaction was quenched (600 minutes), molecular weights have reached 115000 and 70000 for M_w and M_n respectively. These values were almost two times higher than in the case of any other triazolinyls used. This can be useful when high

molecular weights have to be prepared by triazolinyl mediated polymerization. Polymerization was considerably slower than usual.

3.5.2. Discussion of the styrene polymerization experiments

The stability of the triazolinyl derivatives used to control the polymerizations of styrene varies over a wide range. The behavior of the polymerization is also quite different, especially in the cases of significant variation from the average stability of the triazolinyl radical used. It was observed that in the cases when less stable radicals such as **77** and **79** were used the polymerization showed less controlled character. When the stability of the radical increases the polymerization of styrene is better controlled. In the case of the most stable radical **82**, the polymerization was very well controlled. Generally, the increase in stability of the triazolinyl used as additive improved the control over the polymerization of styrene. The influence of stability of the counter radical on the character of the polymerization of styrene in its presence is shown schematically in Figure 3.45. Surprisingly the change of the polymerization behavior from well controlled in the case of **82** to poorly controlled or uncontrolled does not proceed gradually. Instead, the control over of the polymerizations in the presence of the two least stable radicals **77** and **79** is comparable. Results obtained in the presence of the second group of the radicals: **33**, **81** and **84** are also similar. However, the stability of the radical **81** is sufficiently higher than stability of the radicals **33** and **84**. And finally the polymerization behavior of radical **82** is well controlled while the radical is the most stable within used in the polymerization experiments. The rates of the polymerizations, calculated using Equation 3.5 were similar (in the range 1.1 – 1.5 $mol \cdot l^{-1} \cdot s^{-1}$) for all traizolinyl radicals except for triazolinyl **82** (Table 3.7). In the case when triazolinyl **82**, which was more stable than other derivatives, was used as additive the polymerization was significantly slower.

Table 3.7. Propagation rates for polymerizations of styrene in the presence of triazolinyls with various stability; styrene/BPO (mol.): 1000, triazolinyl/BPO (mol.): 1.5, 120°C

Triazolinyl (stability decreases in the column)	Propagation rate V_p x10^4 (mol l^{-1} s^{-1})
79 (*p*-Br)	1.13
77 (*p*-Cl)	1.28
33	1.71
84 (*p*-C_6H_5)	1.49
81 (*p*-OCH3)	1.48
82 (*p*-$N(CH_3)_2$)	0.97

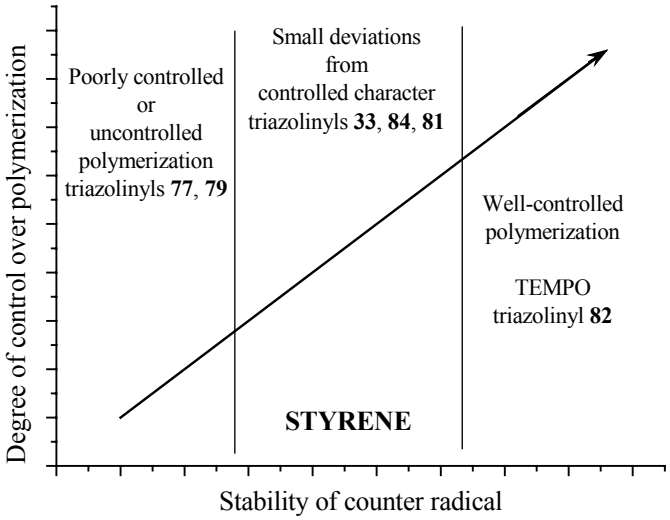

Figure 3.45. Dependence of control over polymerization of styrene on the stability of triazolinyl radical used as additive.

$V_p = -\frac{d[M]}{dt}$, **Equation 3.5**, where [M] is concentration of monomer.

Plots of $\ln([M]_0/[M])$ *vs.* time and M_n *vs.* conversion, which serve as indicators for estimation of the degree of control over the polymerization are linear or close to linear in most cases (Figures 3.46 – 3.49). Considerable deviations from the linearity could be observed only when less stable radicals **77** and **79** are used as additives. The polydispersities of the polymers obtained range from 1.4 to 2 (Figures 3.50 - 3.51). In most cases the polydispersity was decreasing during the polymerization. For the experiments with the less stable radicals as additives, polydispersity was considerably higher indicating loss of control over the process fully confirming the initial expectations. A polydispersity of 2 is close to the values usually obtained by conventional radical polymerization. The polydispersity of the polymers obtained using more stable triazolinyl radicals reaches values as low as 1.4, which is lower than the theoretical limit for the conventional free radical polymerization (1.5). However, the polydispersity is considerably higher than in the cases when nitroxides are used as additives. This is possibly due to the relatively lower energy of the C-N (72.8 Kcal/mol)[195] bond, which is formed as a result of coupling of the active macroradical and the triazolinyl, in comparison to the C-O (85.5 Kcal/mol) bond formed in the reaction between the nitroxide and the macroradical. The bond strength influences the equilibrium between the active and the dormant species. A weaker bond should lead to a shift of the equilibrium towards the active side. As a result the rate of termination increases and the control becomes worse. Another possible reason is over-initiation provided by triazolinyl radical. The styrene is known to be able to initiate polymerization by

[195] J. D. Roberts; M. C. Caserio, ***Osnovy Organicheskoi Khimii***, Mir: Moscow, *1*, 94, **1978**.

itself (autoinitiation).[196,197] In this way autoinitiation provides the polymerization in the presence of nitroxides with necessary active species to keep the polymerization far from dying caused by the termination reactions. Since the triazolinyls are unstable under the reaction conditions, they decompose throughout the polymerization process forming new active species. It seems that the amount of the initiating species formed by the combination of these two processes is higher than necessary. This is confirmed by the fact that the less initiating species are produced by the triazolinyl decomposition the better control over the polymerization is. The increased amount of initiating species in comparison to the TEMPO for example leads to lower control over the polymerization process. Both factors express themselves in a broadening of molecular weight distribution, a deviation from linearity of the characteristic plots and worse end-functionalization, especially at high conversions.

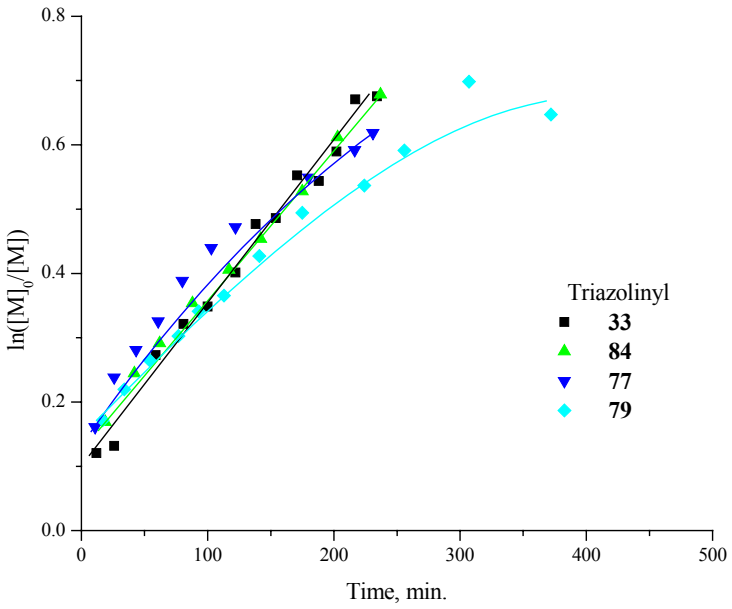

Figure 3.46. Summarized $\ln([M]_0/[M])$ *vs*. time plots for the polymerizations of styrene in the presence of less stable triazolinyl counter radicals, deviations from linearity for triazolinyls **77** and **79** are clearly seen; styrene/BPO (mol.): 1000, triazolinyl/BPO (mol.): 1.5, 120°C

[196] F. R. Mayo, Polym. Prepr. (Am. Chem. Soc., Div. Polym. Chem.), *2*, 55, **1961**.
[197] G. Moad; D. H. Solomon, ***The chemistry of free radical polymerization***, Pergamon: Oxford, 93, **1995**.

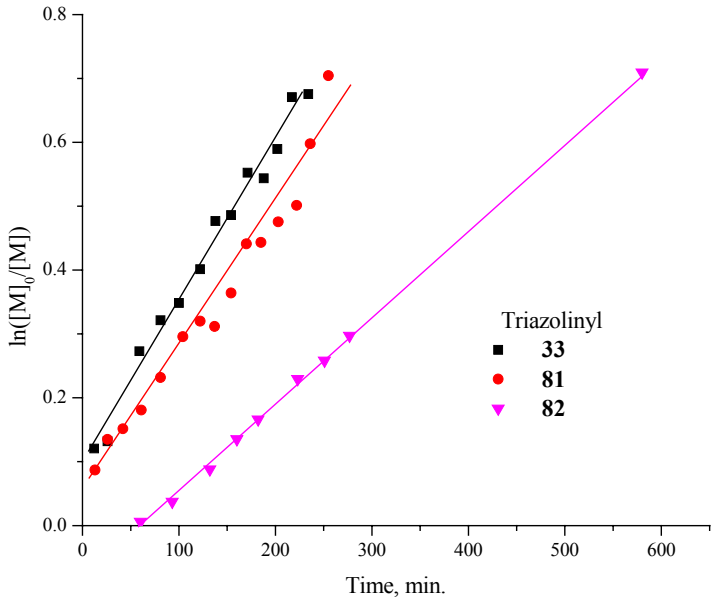

Figure 3.47. Summarized $\ln([M]_0/[M])$ *vs*. time plots for the polymerizations of styrene in the presence of more stable triazolinyl counter radicals, linear plots indicate controlled character of the polymerization; styrene/BPO (mol.): 1000, triazolinyl/BPO (mol.): 1.5, 120°C

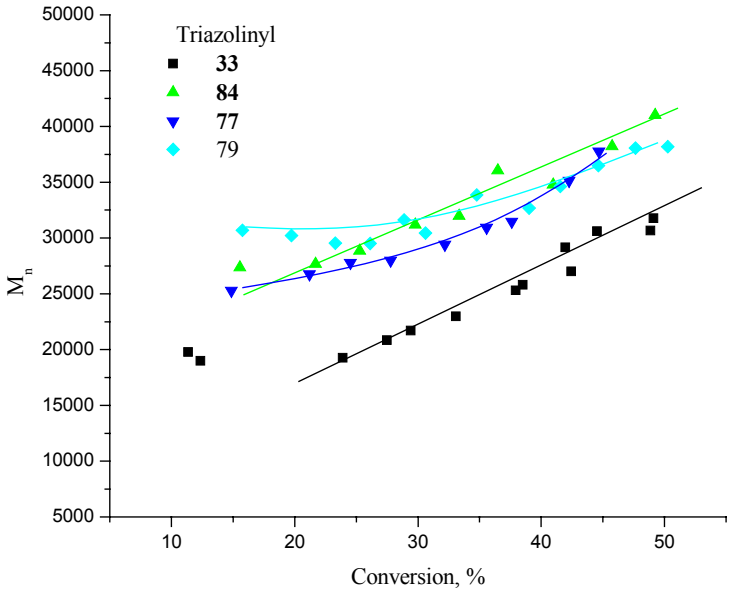

Figure 3.48. Summarized number average molecular weights (M_n) *vs*. conversion plots for the polymerizations of styrene in the presence of less stable triazolinyl counter radicals, deviations from linear increase in the case of **77** and **79** are well pronounced, styrene/BPO (mol.): 1000, triazolinyl/BPO (mol.): 1.5, 120°C

In conclusion, triazolinyl radicals are able to induce polymerization of styrene in a controlled fashion. However, as indicated by the properties of the obtained polymer (polydispersity) and kinetic parameters (increase of $\ln([M]_0/[M])$ with time and M_n with conversion) the control is worse than in the case of TEMPO where polydispersity in best cases can reach as low as 1.05 together with perfectly linear characteristic plots. Some features of the

polymerization can be tuned by changing the properties of the radical. Less stable radicals worsen the controlled character of the polymerization of styrene, while more stable radicals provide better control. Of all used radicals, dimethylamino derivative **82** showed the best results when used as the counter radical. At certain conditions, when less stable radicals were used, loss of control was observed. This phenomenon can be easily explained by the over-initiation during the polymerization.

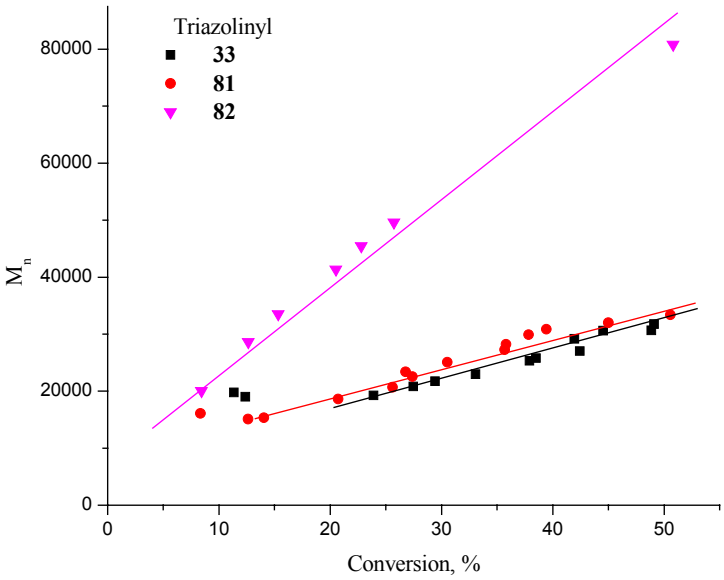

Figure 3.49. Summarized number average molecular weights (M_n) *vs*. conversion plots for the polymerizations of styrene in the presence of more stable triazolinyl counter radicals, styrene/BPO (mol.): 1000, triazolinyl/BPO (mol.): 1.5, 120°C

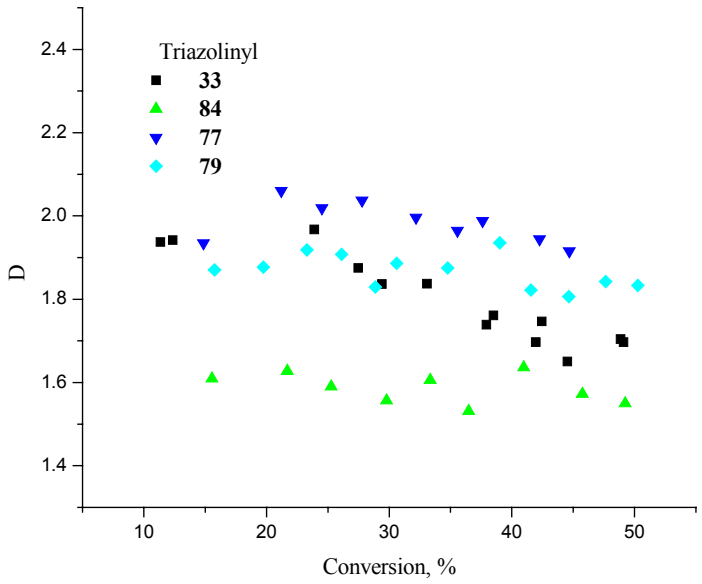

Figure 3.50. Summarized polydispersity (D) *vs*. conversion plots for the polymerizations of styrene in the presence of less stable triazolinyl counter radicals, polydispersity is higher than 1.75 for both **77** and **79**, styrene/BPO (mol.): 1000, triazolinyl/BPO (mol.): 1.5, 120°C

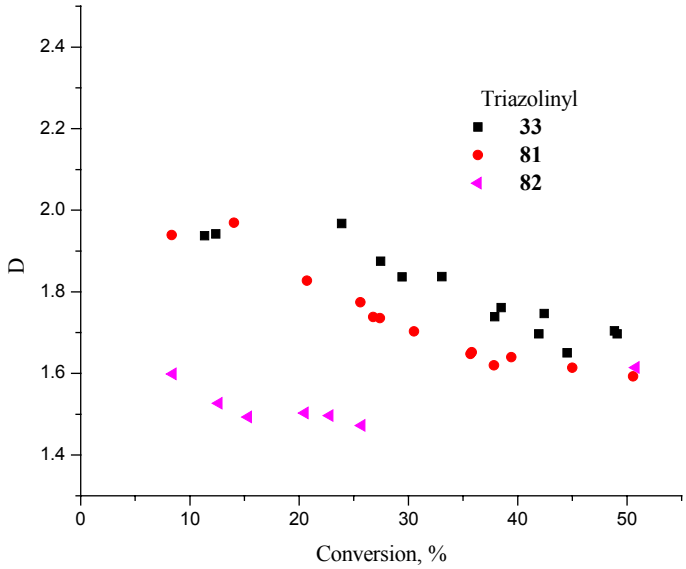

Figure 3.51. Summarized polydispersity (D) *vs*. conversion plots for the polymerizations of styrene in the presence of more stable triazolinyl counter radicals, styrene/BPO (mol.): 1000, triazolinyl/BPO (mol.): 1.5, 120°C

One of the main conclusion, which can be extracted from the whole series of the experiments is that all phenomena observed are in full agreement with the self-regulation concept discussed above (see Section 1.9.1). As expected the more stable radicals are more suitable for the polymerization of styrene. The decrease in stability of the radical leads to overinitiation, which though undesirable, however confirms the importance of this process for the whole polymerization process. Since the concept has received these confirmations, the use of the triazolinyls was attempted to be extended for methacrylates where the counter radical stability factor must play different and more important role, which will be discussed in the next section.

3.5.3. Polymerization of methylmethacrylate (MMA) in the presence of triazolinyl radicals

Stable free radical approach to polymerization of methacrylates has been a problematic objective in the polymer science up-to-now. Controlled radical polymerization of methacrylates does not proceed in the presence of the most investigated counter radicals - nitroxides. Only oligomers can be isolated if for instance TEMPO is used as the additive. This is due to the stop of the polymerization caused by incompletely suppressed termination reactions (see Section 1.9). Of course, due to these problems the preparation of methacrylates containing block copolymers by the stable free radical technique is also limited. The only possibility is the use of this technique for the preparation of one of the blocks (*e.g.* PS), followed by change of the strategy

for the preparation of another block made of methacrylates. However, recently stable free radical polymerization of MMA in the presence of triazolinyl radicals has proven very promising. The use of **33** as additive in controlled radical polymerization of MMA has already been reported[198] (see Section 1.7.2). The instability of the triazolinyl radical must be the key-feature permitting the controlled radical polymerization of MMA. Therefore, it is of interest to find out the influence of the stability of the radical on the behavior of the controlled radical polymerization of this simplest methacrylate monomer. In order to investigate this influence polymerizations of MMA in the presence of various triazolinyls were performed. The setup (Section 6.10) of the polymerization was similar to the previously described styrene polymerization experiments. Similarly to the polymerizations of styrene, comparisons of the polymerization kinetics were made. Developments of conversion, molecular weights and polydispersity indexes were followed as the polymerization proceeded. In contrast to the styrene polymerization where the most stable radical showed the best results, in the case of MMA, such a situation was not expected. The more stable triazolinyl radical is the more "nitroxide-like" it behaves in the polymerization. Therefore, in the case of MMA such more stable radicals must lead to the stop of the polymerization. The more stable the radical, the earlier the stop of the MMA polymerization should appear. From the other side, the very unstable radicals must lead to loss of control, as in this case the process approximates to the conventional free radical polymerization. Therefore, a certain instability of the triazolinyl, determined by its decomposition rate, must be the best realization of the controlled radical polymerization process. From another point of view, since the stop of the polymerization is caused by the loss of the active species due to the termination reactions, the rate of the decomposition of the radical must be such that it compensates for the loss of those active species but does not overproduce them in order to avoid loss of control.

Polymerization of MMA in the presence of 1,3,5,5-tetraphenyl-Δ^3-1,2,4-triazolin-2-yl (**33**) was performed by Steenbock.[199] The results obtained by Steenbock are given in Figures 3.52 – 3.54. The plot $\ln([M]_0/[M])$ *vs.* time has a linear region. Similarly to most polymerizations of styrene, the line does not go through zero indicating rapid polymerization at the beginning of the process. After approximately 200 minutes of reaction, deviations from linearity were observed (Figure 3.52). This is possibly due to the gradual stopping of the polymerization due to the loss of the active species, which was discussed above. The plot M_n *vs.* conversion is also linear and number average molecular weights grow with time (Figure 3.53). In this plot, again, similarities to the styrene polymerizations are well pronounced. The rapid increase of the molecular weights in the beginning confirms quick polymerization at this stage. The reason for

[198] M. Steenbock; M. Klapper; K. Müllen, Macromol. Chem. Phys., 199, 763 – 769, **1998**.
[199] M. Steenbock; ***Ph.D. thesis***, Johannes Gutenberg University: Mainz, **1998**.

that is probably the same as was suggested for the similar effects observed in the case of the polymerization of styrene. Both characteristic graphs indicate controlled character of the polymerization. The polydispersity varied between 1.25 – 2 depending upon the degree of conversion (Figure 3.54). Unlike the styrene polymerization where polydispersities either decreased during the polymerization or stayed almost constant, a different behavior is observed. Initially the polydispersity index increases from 1.25 in the beginning of the polymerization to almost 2 at 20 % conversion. Further, the polydispersity decreases, so a pronounced maximum is observed. These results are used in this work as a comparison. The following experiments are set similarly in order to compare the polymerization results obtained from the use of other triazolinyl radicals as additives.

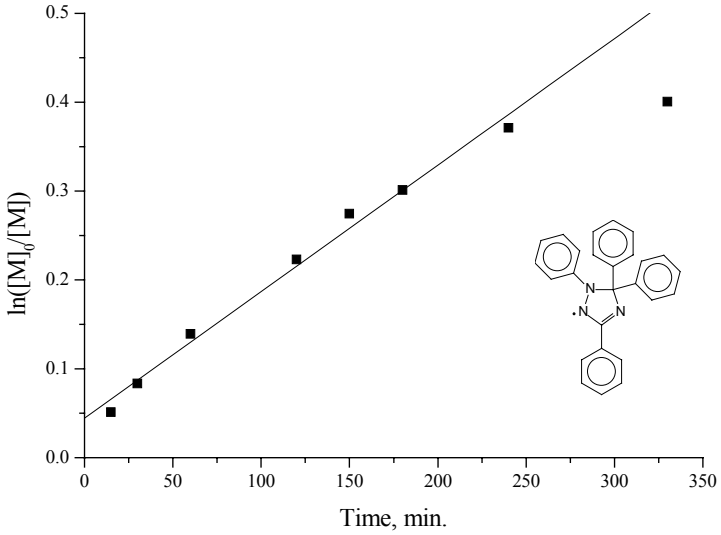

Figure 3.52. ln([M]$_0$/[M]) *vs.* time plot for the polymerization of MMA in the presence of **33**, MMA/BPO (mol.): 1000, triazolinyl/BPO (mol.): 1.5, 70°C.

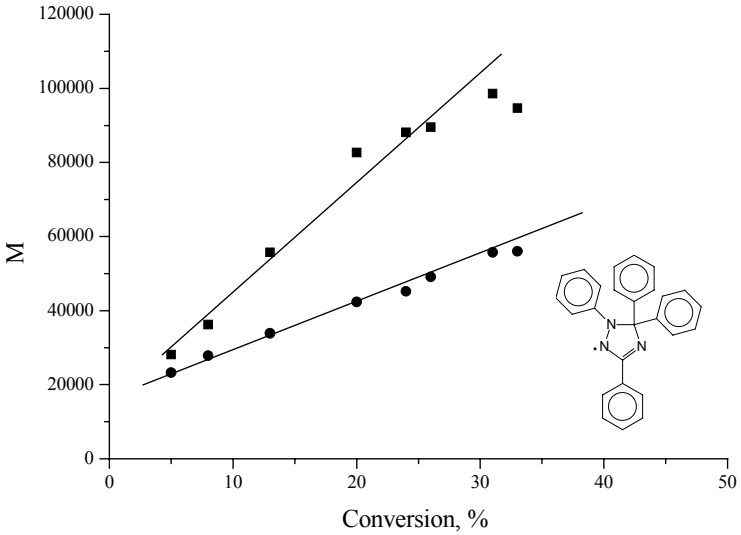

Figure 3.53. Molecular weights (M_w:■; M_n:●) *vs.* conversion plots for the polymerization of MMA in the presence of **33**, MMA/BPO (mol.): 1000, triazolinyl/BPO (mol.): 1.5, 70°C.

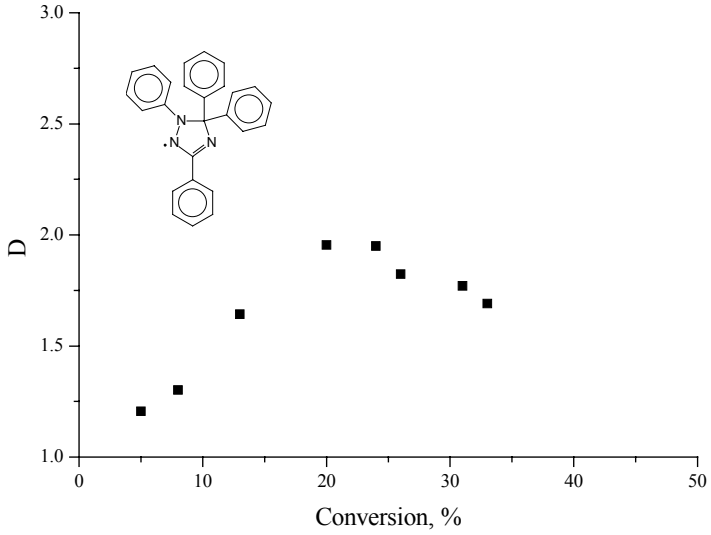

Figure 3.54. Polydispersity (D) *vs.* conversion plot for the polymerization of MMA in the presence of **33**, MMA/BPO (mol.): 1000, triazolinyl/BPO (mol.): 1.5, 70°C.

As 1,3–diphenyl-5,5-di(4-chlorophenyl)-Δ^3-1,2,4-triazolin-2-yl (**77**) is less stableradical, the polymerization of styrene in its presence was less controlled or even uncontrolled (Section 3.5.1). However, as the instability of the radical is more important for the realization of the polymerization of MMA, better results with additive were possible. From the other side, if the rate of decomposition of **33** discussed above was already matching the decay in the loss of the active species, the increased instability might have also lead to a less controlled process. In this case, it would mean that at these polymerization conditions **33** is the best candidate for providing

control over the polymerization of MMA. However, the results can possibly be improved by tuning the affinity of the triazolinyl to the growing PMMA macroradicals, *i.e. via* the change of equilibrium constant *K* between the active and the dormant species. This can possibly be realized by variation of the substituents at the 1- and 3-positions of the triazolinyl ring (see below: Section 4). Therefore, definite expectations of the results could not yet be figured out before this experiment. The results obtained from kinetic investigation of polymerization of MMA in the presence of **77** are shown in Figures 3.55 – 3.57.

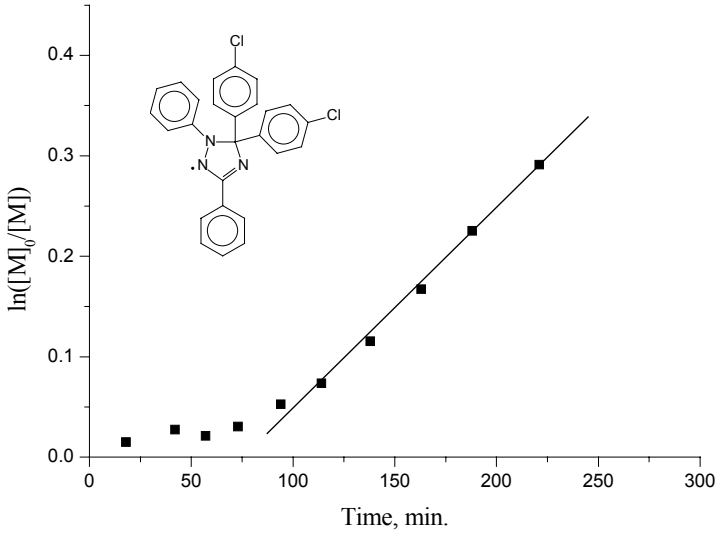

Figure 3.55. ln([M]$_0$/[M]) *vs.* time plot for the polymerization of MMA in the presence of **77**, MMA/BPO (mol.): 1000, triazolinyl/BPO (mol.): 1.5, 70°C.

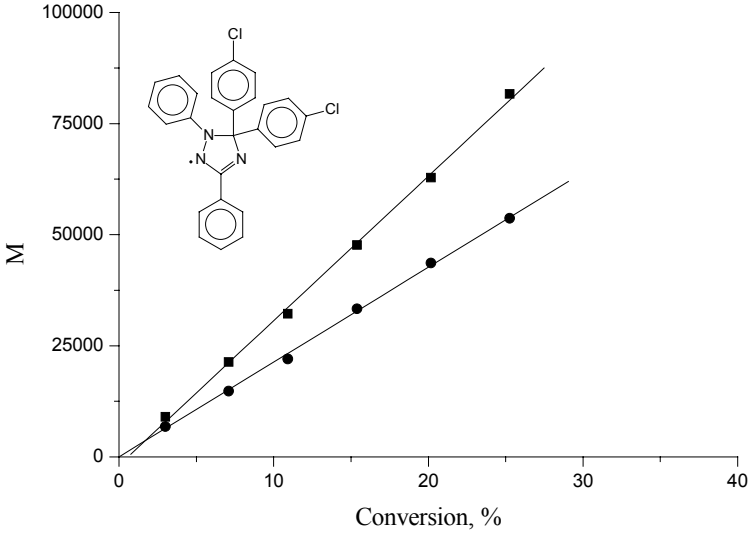

Figure 3.56. Molecular weights (M_w:■; M_n:●) *vs.* conversion plot for the polymerization of MMA in the presence of **77**, MMA/BPO (mol.): 1000, triazolinyl/BPO (mol.): 1.5, 70°C.

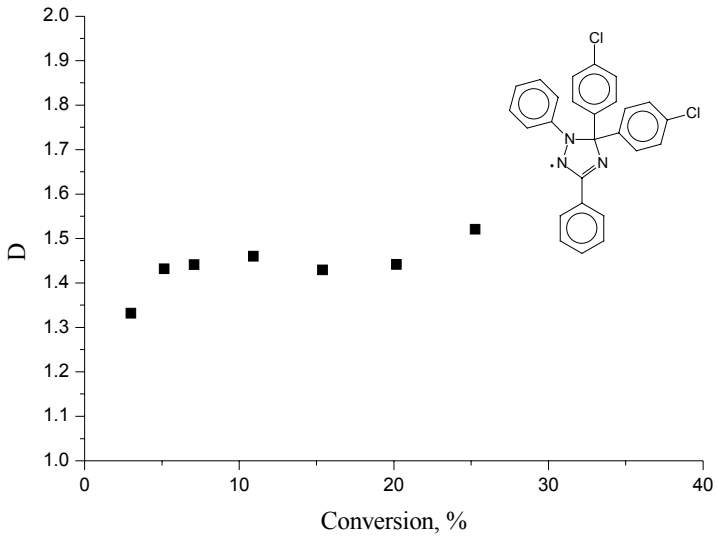

Figure 3.57. Polydispersity (D) *vs.* conversion plot for the polymerization of MMA in the presence of **77**, MMA/BPO (mol.): 1000, triazolinyl/BPO (mol.): 1.5, 70°C.

An inhibition period similar to that in the case of polymerization of styrene in the presence of **82** is observed in the beginning of the polymerization. This was a good indication that the polymerization of styrene in the presence of **82** was best controlled among all the triazolinyl derivatives tested in this work. The characteristic plots are perfectly linear indicating very well controlled character of the polymerization process (Figures 3.55 - 3.56). This means that decomposition rate of the triazolinyl **77** better fits to the rate of the disappearance of the active species caused by the termination reactions in the case of polymerization of MMA. Obviously, this polymerization of MMA in the presence of **77** behaved differently from the polymerization of styrene with the same counter radical (compare: Section 3.5.1). The reason is that in the case of styrene the additional initiation provided by the triazolinyl decomposition adds to the styrene self-initiation process. Here the self-initiation is absent and as the result the total amount of newly appearing radicals is lower than in the styrene case. In the beginning of the polymerization the often-observed rapid growth of the molecular weights and conversion is absent, and even short inhibition period is seen. The polydispersity of the polymer obtained varied from 1.4 to 1.5 (Figure 3.57). The development of the polydispersity is similar to that observed when **33** was used as additive: again the polydispersity increases in the beginning and decreases in the end of the polymerization.

For further investigation of the possible use of poorly stable triazolinyl for controlling the polymerization of MMA, even less stable radical: 1,3–diphenyl-5,5-di(4-bromophenyl)-Δ^3-1,2,4-triazolin-2-yl (**79**) was utilized as additive. Since the results obtained with more stable derivative **77** showed well controlled polymerization behavior, some loss of the control was expected in

this case. The experiment showed that polymerization of methylmethacrylate in the presence of **79** was also controlled. This is very much in contrast to the case of the polymerization of styrene, again confirming the importance of the reinitiation process for the efficient controlled radical polymerization of MMA. However, a few signs of poorer control than in the case of polymerization with **77** as additive appeared, as seen in the plots given in Figures 3.58 – 3.60.

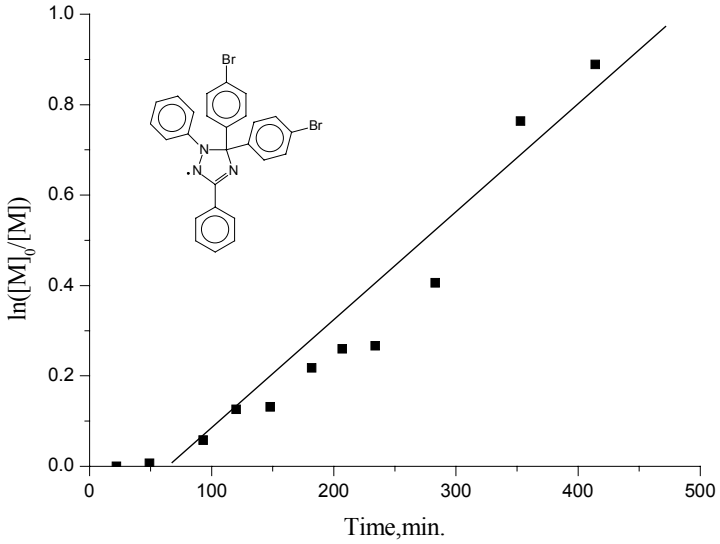

Figure 3.58. $\ln([M]_0/[M])$ *vs*. time plots for the polymerization of MMA in the presence of **79**, MMA/BPO (mol.): 1000, triazolinyl/BPO (mol.): 1.5, 70°C.

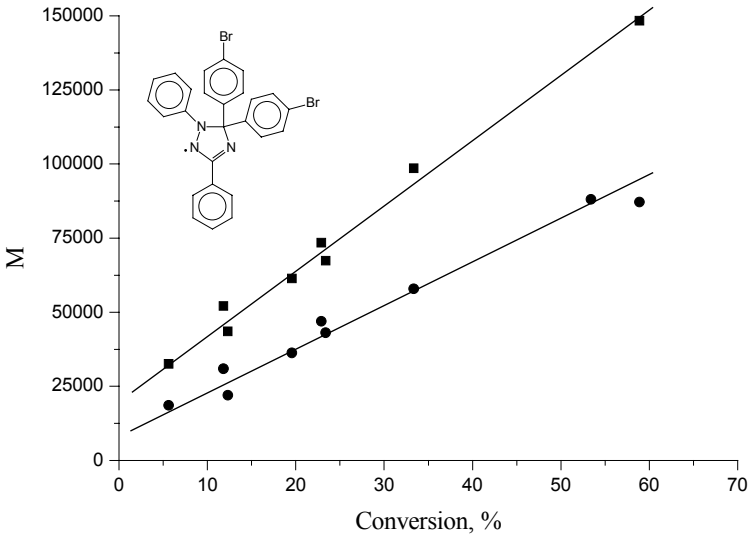

Figure 3.59. Molecular weights (M_w:■; M_n:●) *vs*. conversion plots for the polymerization of MMA in the presence of **79**, MMA/BPO (mol.): 1000, triazolinyl/BPO (mol.): 1.5, 70°C.

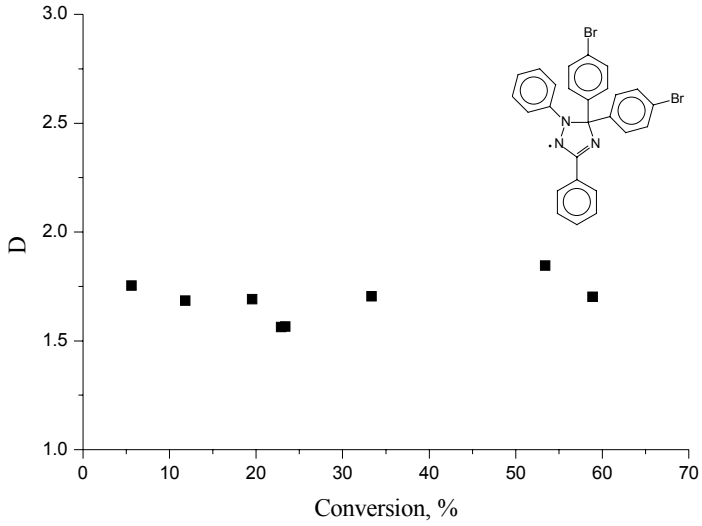

Figure 3.60. Polydispersity (D) *vs*. conversion plots for the polymerization of MMA in the presence of **79**, MMA/BPO (mol.): 1000, triazolinyl/BPO (mol.): 1.5, 70°C.

The plots M_n *vs.* conversion and $\ln([M]_0/[M])$ *vs.* time are linear indicating control over the process (Figures 3.58 – 3.59). The initial increase in the molecular weights was again observed. However, in this case it was present together with short inhibition period, which suggests that the decomposition rate of this radical is not far from the optimal rate and not all features previously seen in the cases of worse controlled polymerizations take place in the presence of this radical. However, the results obtained in the presence of this triazolinyl are slightly worse than in the case of **77**. Polydispersity of the obtained polymer varied between 1.5 and 1.85 depending on the conversion, which is higher than for the case of **77** discussed above (Figure 3.60). Kinetic investigations show that polymerization had a controlled character up to conversions as high as 60 % when the polymerization was quenched due to the high viscosity of the reaction mixture (after 415 minutes of polymerization). At high conversions, the appearance of a low molecular weight "tail" in the molecular weight distribution appeared. This indicates the presence of a large amount of reinitiated chains, which led to a loss of end-functionalization (Figure 3.61). At high conversions, the accumulated amount of chains, reinitiated by the triazolinyl decomposition in this case, can reach considerable values. This is an undesired side effect of the triazolinyl-mediated polymerizations, which effects further block copolymer syntheses. Here as the reaction was allowed to run longer than usual, this effect is well seen. Therefore, in the cases when end-functionalization is an essential feature (*e.g.* preparation of macroinitiators), the polymerization should be stopped at an earlier stage or more stable radicals should be used.

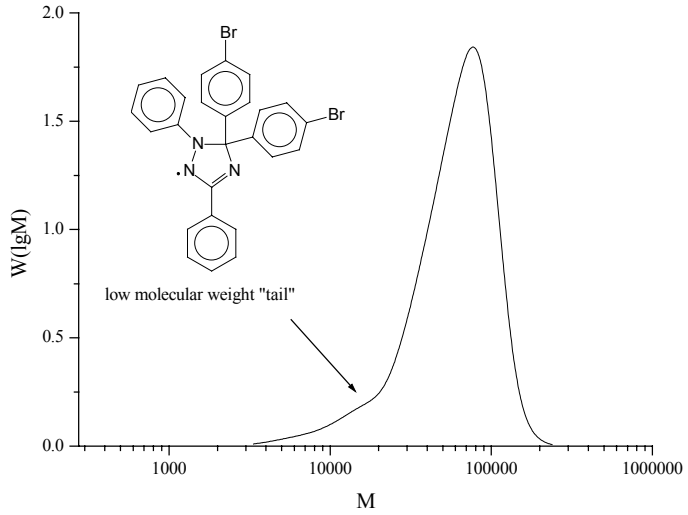

Figure 3.61. Appearance of low molecular weight "tail" at high conversion (55 %) in polymerization of MMA in the presence of **79**, MMA/BPO (mol.): 1000, triazolinyl/BPO (mol.): 1.5, 70°C.

As the less stable triazolinyl radicals showed better control over the polymerization of MMA, the more stable triazolins are expected to cause a stop of the polymerization. Therefore, three triazolinyls with increasing stability were used as additives in order to confirm this expectation. The first of those was 1,3–diphenyl-5,5-di(4-fluorophenyl)-Δ^3-1,2,4-triazolin-2-yl (**78**), which had a higher stability than **33**, **77** and **79**. The kinetic measurements are shown in Figures 3.62 – 3.64.

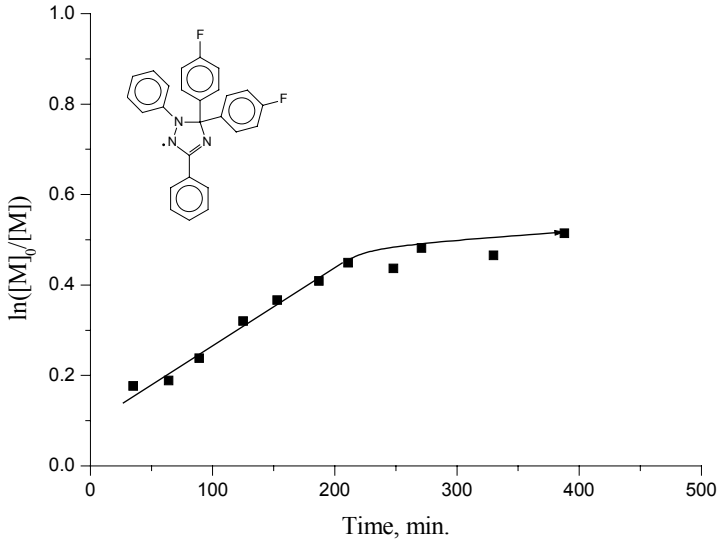

Figure 3.62. ln($[M]_0$/[M]) *vs*. time plot for the polymerization of MMA in the presence of **78**, MMA/BPO (mol.): 1000, triazolinyl/BPO (mol.): 1.5, 70°C.

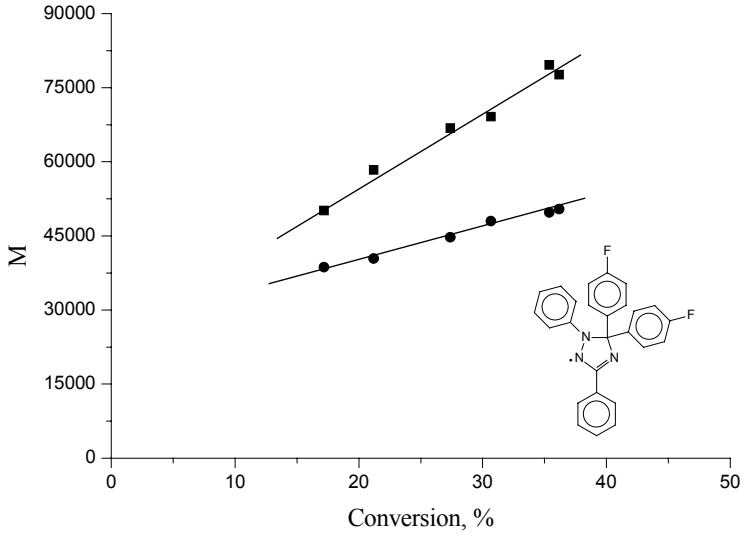

Figure 3.63. Molecular weights (M_w:■; M_n:●) *vs*. conversion plots for the polymerization of MMA in the presence of **78**, MMA/BPO (mol.): 1000, triazolinyl/BPO (mol.): 1.5, 70°C.

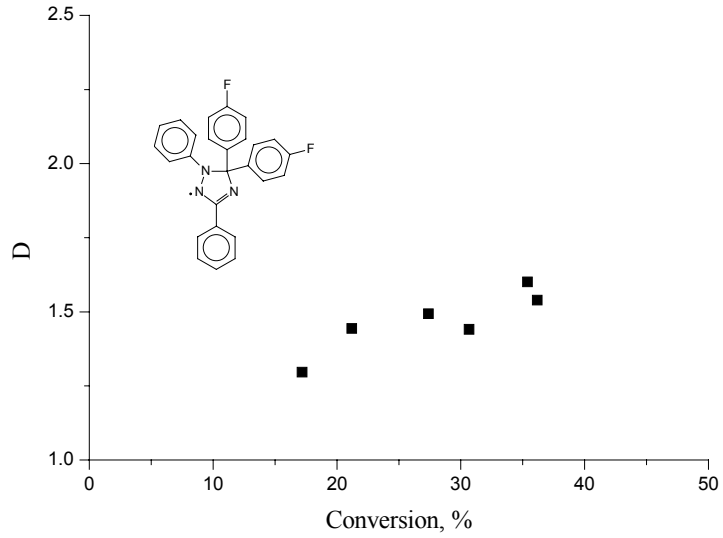

Figure 3.64. Polydispersity (D) *vs*. conversion plots for the polymerization of MMA in the presence of **78**, MMA/BPO (mol.): 1000, triazolinyl/BPO (mol.): 1.5, 70°C.

The polymerization showed a well-controlled character to yield monomer conversion of 40 % after 200 minutes of reaction time (Figure 3.62). After that the polymerization stopped. No increase in the molecular weights and conversion was observed after that time. This result is in good accordance with the expectations. The stop of the polymerization at a certain point has been observed previously when stable radicals are used as counter radicals in polymerization of MMA. For example, when TEMPO or spiro-triazolinyl **40** were used as counter radicals only oligomers could be isolated. This indicates that the reaction stopped at a very early stage of the

polymerization. As mentioned above, it happens due to the loss of active species in the polymerization. As the result, the equilibrium shifts to the dormant side and the reaction stops (see Section 1.9). However, unlike the TEMPO radical, which is completely stable under the polymerization conditions, **78** is unstable and allows polymerization to proceed to a relatively high conversion. Therefore, as predicted by the self-regulation concept, with increasing stability of the radical, the polymerization will stop at an earlier point. The polydispersity was between 1.3 and 1.76 depending on the degree of conversion (Figure 3.64). During the time when the polymerization was yet running it showed all features of a controlled process, such as linear characteristic plots (Figures 3.62 and 3.63).

In order to follow this tendency, polymerization of MMA in the presence of 1,3–diphenyl-5,5-di(4-methoxyphenyl)-Δ^3-1,2,4-triazolin-2-yl (**81**) was carried out. This compound is an even more stable radical than the triazolinyl **78** described above and its use led to a slowing down of the polymerization at even earlier stage than in the case of **78** (Figure 3.65).

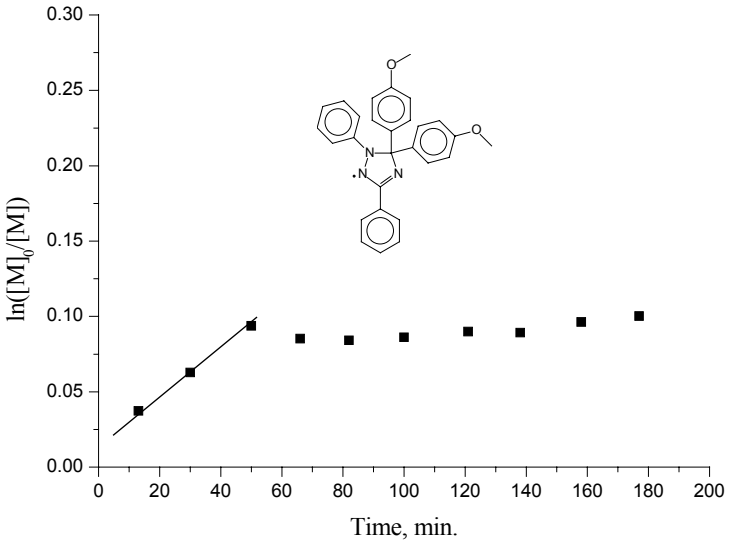

Figure 3.65. ln([M]$_0$/[M]) *vs*. time plot for the polymerization of MMA in the presence of **81**, MMA/BPO (mol.): 1000, triazolinyl/BPO (mol.): 1.5, 70°C

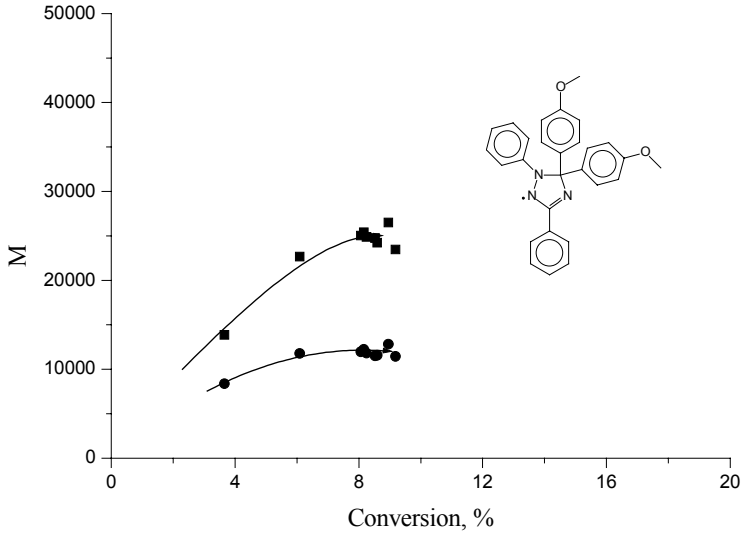

Figure 3.66. Molecular weights (M_w:■; M_n:●) *vs*. conversion plots for the polymerization of MMA in the presence of **81**, MMA/BPO (mol.): 1000, triazolinyl/BPO (mol.): 1.5, 70°C

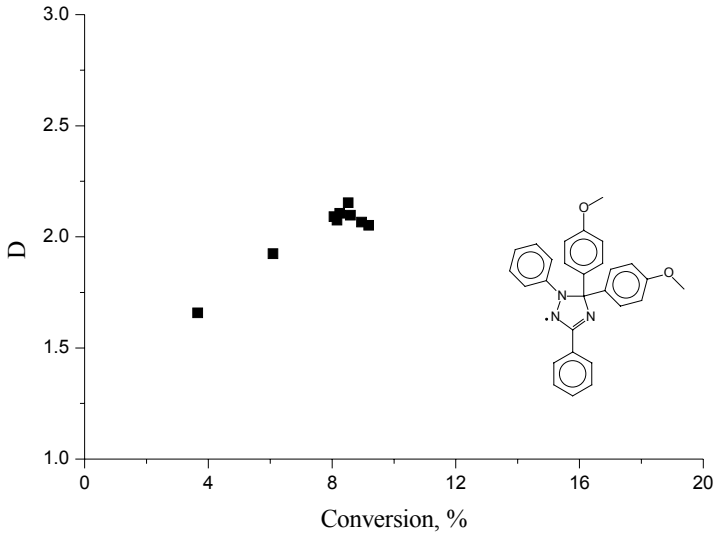

Figure 3.67. Polydispersity (D) *vs*. conversion plot for the polymerization of MMA in the presence of **81**, MMA/BPO (mol.): 1000, triazolinyl/BPO (mol.): 1.5, 70°C

The reaction stopped when conversion reached 8 %. Molecular weights achieved at that conversion were 12000 and 25000 for M_n and M_w, respectively (Figure 3.66), and the polydispersity changed from 1.7 to 2 (Figure 3.67). Generally the behavior of the polymerization in this case is very similar to the previous case of **78**. However, as the stability of the radical increased, the polymerization stops earlier. Since this radical is more stable, it cannot provide the polymerization with sufficient initiating species. As the result the equilibrium shifted and the polymerization stopped as predicted by the self-regulation concept. Again, this confirmed the

great importance of the reinitiation process during the controlled radical polymerization of MMA.

1,3-Diphenyl-5,5-bis(4-dimethylaminophenyl)-Δ^3-1,2,4-triazolin-2-yl (**82**) was the most stable among the radicals used as additives in the polymerizations of MMA. It showed the best results when used as counter radical in the polymerization of styrene. However, the polymerization of MMA in its presence was completely inhibited. No polymer was isolated after the reaction mixture was held in the thermostat heated to 70°C over 15 hours. The result is similar to the attempts to polymerize MMA in the presence of TEMPO radical: the high stability of **82** causes inhibition of the polymerization at such early stage that no polymer is formed. Comparing all three radicals with increasing stability: **78**, **81** and **82**, it is clearly seen that the increase in the stability leads to the stop of the polymerization at earlier stage. The most important finding is that this behavior is in good agreement with the expectations, which were made on the basis of the self-regulation concept. Therefore, the self-regulation concept confirms its validity.

3.5.4. Discussion of MMA polymerization experiments

TEMPO and other nitroxides cannot be used in controlled radical polymerization of methacrylates. By contrast, triazolinyl radicals due to their instability are good candidates for carrying out the controlled radical polymerization of these monomers. The character of the polymerization varies widely depending on minor changes in the stability of the radical used as additive, unlike the corresponding polymerizations of styrene. This is possibly due to the absence of the self-initiation process in the case of MMA. The self-initiation of styrene might play a role in supplying of a “background” amount of the initiating species in the polymerization of this monomer. The minor differences in the amount of newly produced phenyl radicals, provided by slight differenes in the stability of triazolinyls, hence are possibly hidden by that background. Therefore, remarkable changes in the polymerization behavior in the case of styrene can be observed only if a great change in the stability of used triazolinyls is introduced. More stable radicals cause the polymerizations of MMA to stop. As shown by the experiments described in the previous section, the more stable radical is, the earlier polymerization of MMA stops in its presence. The rates of the polymerizations, also unlike the styrene case (see Section 3.5.2) show a dependance on the stability of the radical being used as an additive (Table 3.8). The more stable radicals not only lead to a stop of the polymerization at an earlier point but also decrease the rate of the polymerization of the monemer at the stage before this stop occurs. Whereas polymerization of styrene was best controlled when more stable radicals are added to the

polymerization mixture, unstable radicals allowed controlled polymerization of MMA. However, when the stability of the radical is decreased dramatically as in the case of **79** indications of a loss of control of the polymerization begins to appear. By contrast, polymerization of styrene in the presence of less stable radicals shows large deviations from controlled character.

Table 3.8. Propagation rates for polymerizations of MMA in the presence of triazolinyls with various stability; for those radicals, which cause stopping of the polymerization the rates are calculated for the period of the reaction before the cessation occurs; MMA/BPO (mol.): 1000, triazolinyl/BPO (mol.): 1.5, 70°C

Triazolinyl (stability decreases in the column)	Propagation rate V_p x10^4 (mol l^{-1} s^{-1})
79 (*p*-Br)	1.7
77 (*p*-Cl)	1.56
33	1.28
78 (*p*-F)	1.36
81 (*p*-OCH_3)	0.93
82 (*p*-$N(CH_3)_2$)	0

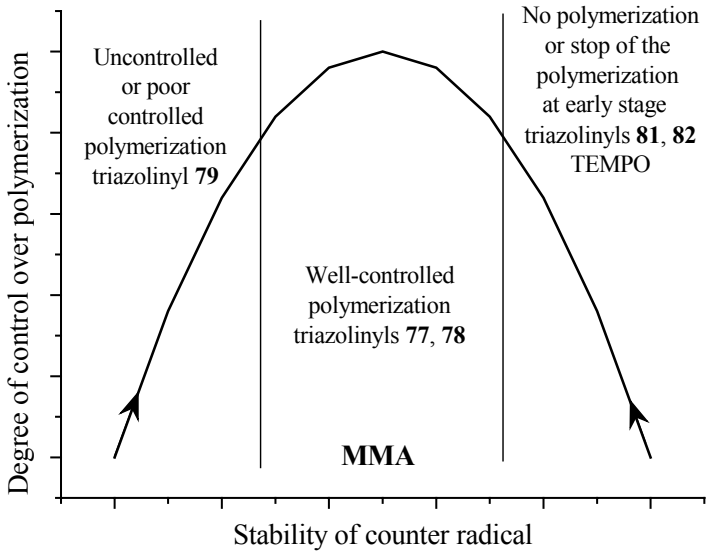

Figure 3.68. Dependence of control over polymerization of MMA on the stability of triazolinyl radical used as additive.

A certain rate of decomposition of the triazolinyl radical is needed to compensate for the loss of active species by termination reactions. When the triazolinyl decay matches this rate in the polymerization conditions, the polymerization is well controlled. However, if the rate of decomposition is different from the optimal one, deviations appear. If the rate is too high, control of the polymerization is worse as indicated by broadening of the molecular weight distribution and by deviation of the characteristic plots from linearity. In the case of lower decomposition rates in comparison to optimal one, the polymerization comes to stop. Obviously the greater the difference between the actual rate of decomposition of the radical and the optimal one is the more significant is the change in the process behavior observed. Therefore, similar to the Figure

drawn for the polymerizations of styrene (Figure 3.45), an influence of the stability of the triazolinyl on the degree of the control of the polymerization of MMA can be schematically displayed as in Figure 3.68.

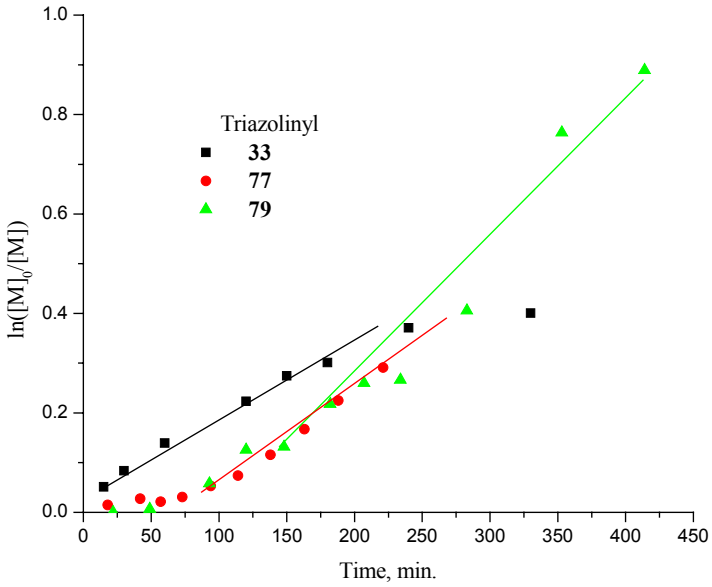

Figure 3.69. Summarized $\ln([M]_0/[M])$ *vs.* time plots for the polymerizations of MMA in the presence of less stable triazolinyl radicals, MMA/BPO (mol.): 1000, triazolinyl/BPO (mol.): 1.5, 70°C

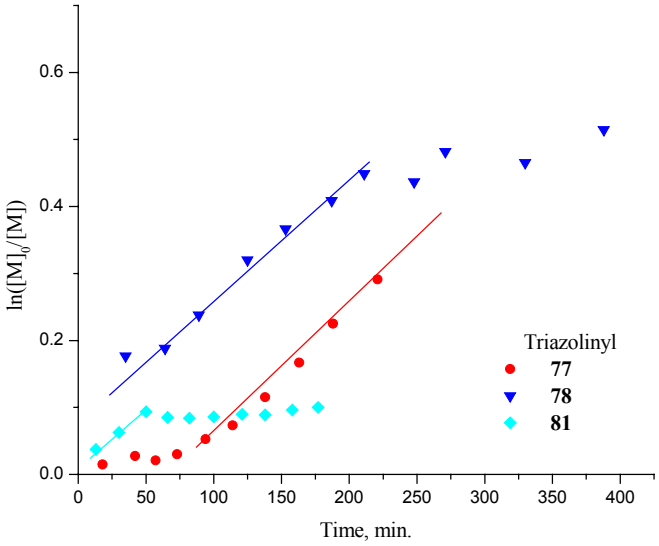

Figure 3.70. Summarized $\ln([M]_0/[M])$ *vs.* time plots for the polymerizations of MMA in the presence of more stable triazolinyl counter radicals, cessation of the polymerization in the case of 78 and 81 is observed, MMA/BPO (mol.): 1000, triazolinyl/BPO (mol.): 1.5, 70°C

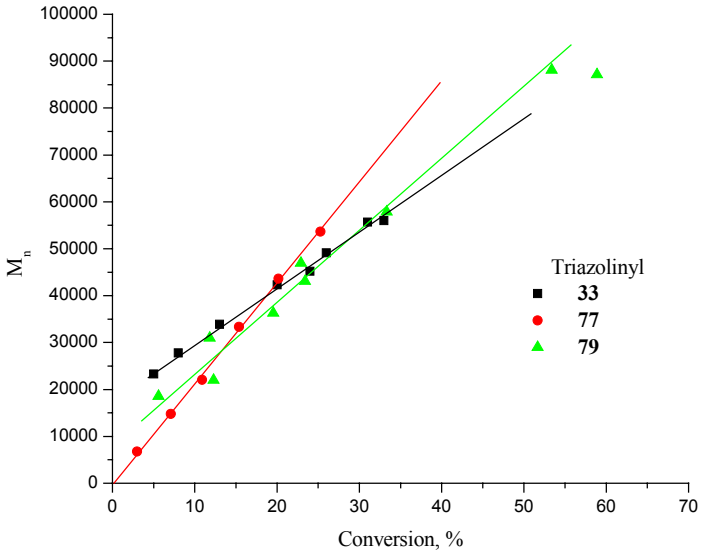

Figure 3.71. Summarized number average molecular weights (M_n) *vs.* conversion plots for the polymerizations of MMA in the presence of less stable triazolinyl counter radicals, perfectly linear plots indicate good control over polymerization, MMA/BPO (mol.): 1000, triazolinyl/BPO (mol.): 1.5, 70°C

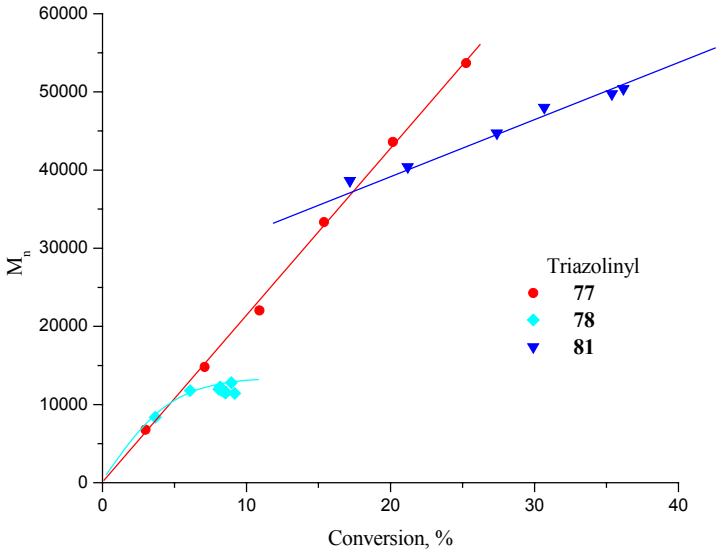

Figure 3.72. Summarized number average molecular weights (M_n) *vs.* conversion plots for the polymerizations of MMA in the presence of more stable triazolinyls as compared to **77**, MMA/BPO (mol.): 1000, triazolinyl/BPO (mol.): 1.5, 70°C

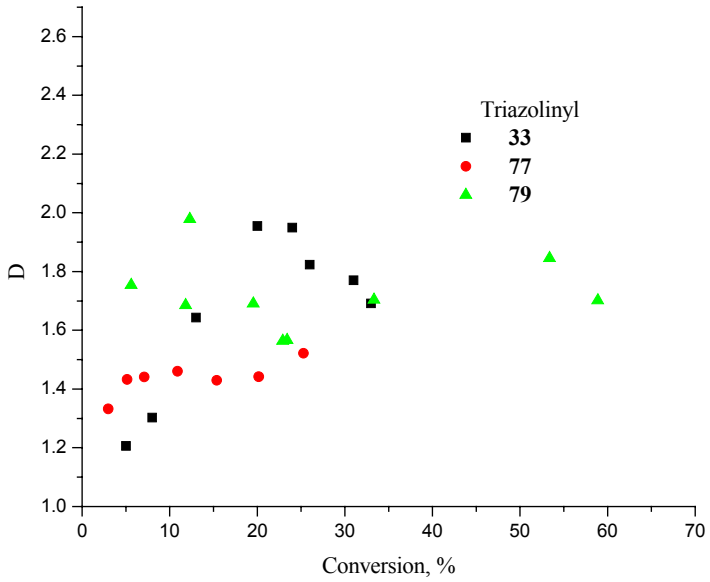

Figure 3.73. Summarized polydispersity (D) *vs.* conversion plots for the polymerizations of MMA in the presence of less stable triazolinyl counter radicals, polydispersities in the case of **77** below 1.5 during whole polymerization, MMA/BPO (mol.): 1000, triazolinyl/BPO (mol.): 1.5, 70°C

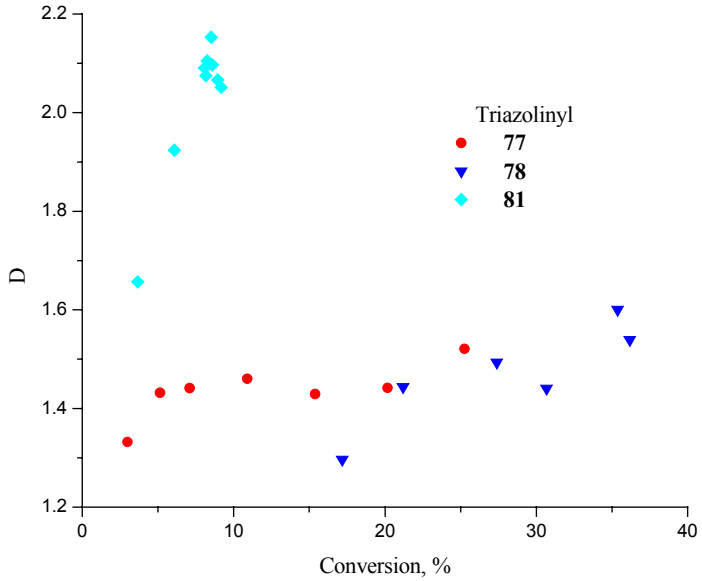

Figure 3.74. Summarized polydispersity (D) *vs.* conversion plots for the polymerizations of MMA in the presence of more stable triazolinyl counter radicals, MMA/BPO (mol.): 1000, triazolinyl/BPO (mol.): 1.5, 70°C

So, the highly stable triazolinyl **82** and TEMPO do not allow polymerization of MMA. Tuning of the optimal decomposition rate can be achieved by changing the substituent at 5-position of the triazolinyl, as was shown in Section 3.4.2. In the range of the triazolinyl radicals utilized in polymerizations of MMA, **77** performed the best for controlling the polymerization. However, all the radicals used except **82** and **81**, allow controlled radical polymerization of MMA as indicated by linear kinetic plots shown in Figures 3.69 – 3.72. The experiment with **79** showed that reinitiation at high conversion and a high triazolinyl decomposition rate can lead to

the appearance of a low molecular weight "tail". This indicates a considerable amount of "dead" polymer in the obtained polymer sample and as a result a loss of end-functionalization, which must be taken into account when attempting syntheses of block copolymers. Polydispersity of the polymers obtained with different triazolinyls also vary one from another (Figures 3.73 – 3.74). The triazolinyls, which allow good control over the polymerizations, are also able to mediate the polymerization for obtaining polymers with polydispersity as low as 1.4 (*e.g.* **77**). However, in other cases polydispersity can reach values higher than 2 as for instance in the case of **79**.

3.6. Polymerizations of other monomers (non styrene and MMA) in the presence of triazolinyl radicals

3.6.1. Polymerization of ethylmethacrylate (EMA) in the presence of 1,3–diphenyl-5,5-di(4-chlorophenyl)-Δ^3-1,2,4-triazolin-2-yl (77)

77 was the best triazolinyl radical for controlling the polymerization of MMA. As the side chain in the methacrylate monomers should not change the polymerization behavior of the monomer significantly it was promising to try to apply the radical **77** for controlling polymerizations of other methacrylates. The first chosen monomer was ethylmethacrylate (EMA), which has one extra methylene group in the side chain in comparison to MMA (Figure 3.19). The polymerization was investigated in the same way as the previously described polymerizations of MMA. The results obtained were similar to the MMA polymerization experiment in the presence of the same radical (Figures 3.75 – 3.77).

As in the case of MMA, the polymerization has an inhibition period. However, unlike the polymerization of MMA, the molecular weights showed a remarkable rapid growth at the beginning of the polymerization (Figure 3.76). This is similar to the polymerization of MMA in the presence of **79**, where control over the polymerization was concluded to be slightly worse than in the presence of **77**. The polymerization was well controlled as indicated by the linear characteristic plots (Figures 3.75 – 3.76). Polydispersity was around 1.5 at any point during the polymerization (Figure 3.77). After 320 minutes conversion was above 60 % and molecular weights reached 114000 and 183000 for M_n and M_w, respectively. These results confirmed the expectation of the applicability of the same effective radical in the case of MMA for the case of EMA. The change of the ester group just slightly influences the polymerization behavior. Since use of **77** as a counter radical was efficient for controlling the polymerization of both MMA and

EMA, other methacrylates with variations in the side chain such as *n*-butylmethacrylate and 2,2,2-trifluoroethylmethacrylate were tested in order to check the universality of the radical.

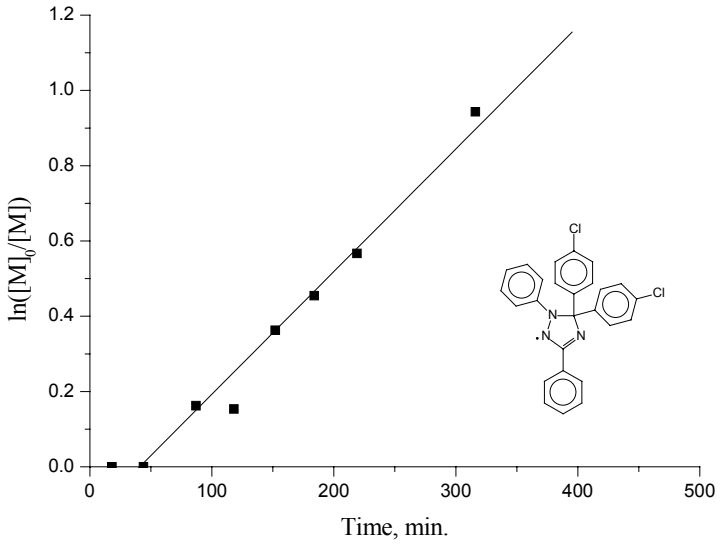

Figure 3.75. ln([M]$_0$/[M]) *vs*. time plot for the polymerization of EMA in the presence of **77**, EMA/BPO (mol.): 1000, triazolinyl/BPO (mol.): 1.5, 70°C

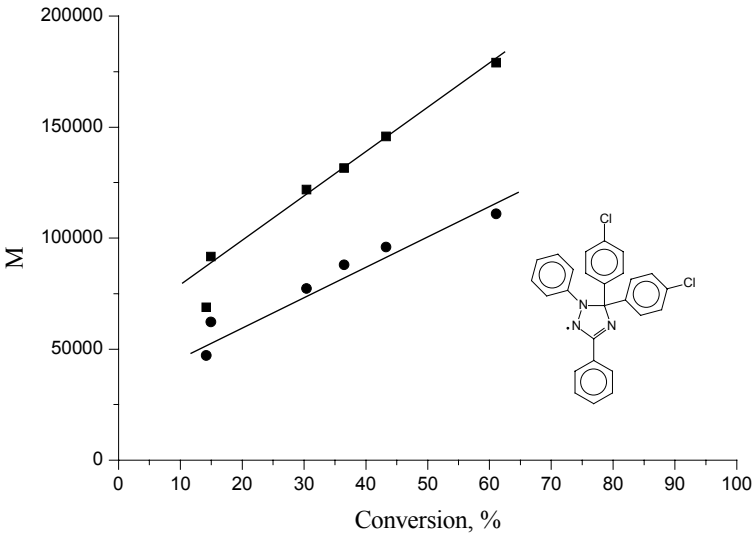

Figure 3.76. Molecular weights (M_w:■; M_n:●) *vs*. conversion plots for the polymerization of EMA in the presence of **77**, EMA/BPO (mol.): 1000, triazolinyl/BPO (mol.): 1.5, 70°C

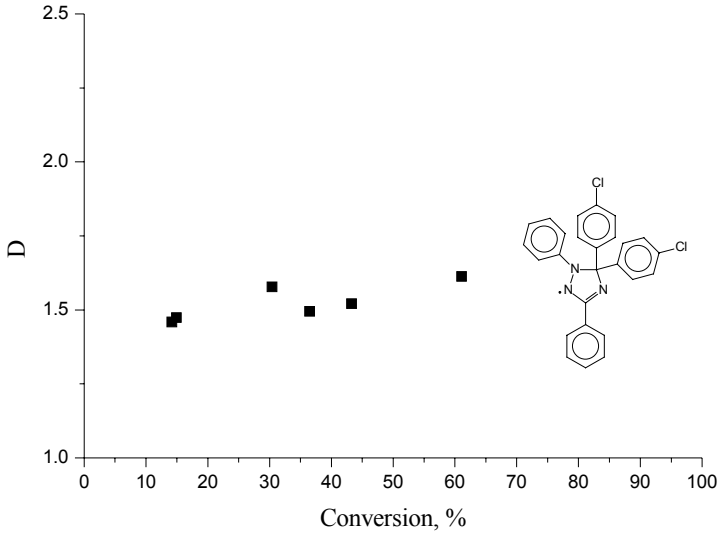

Figure 3.77. Polydispersity (D) *vs*. conversion plot for the polymerization of EMA in the presence of **77**, EMA/BPO (mol.): 1000, triazolinyl/BPO (mol.): 1.5, 70°C

3.6.2. Polymerization of 2,2,2-trifluoroethylmethacrylate (FEMA) in the presence of triazolinyl radicals 77 and 86

There is considerable academic and industrial interest in fluorine containing polymers due to their unusual properties such as chemical inertness, low refractive index, *etc.* In order to test the application of controlled polymerization to such monomers, FEMA was used as monomer in polymerizations in the presence of **77** and **86**. The advantage of **77** is the very good control over polymerizations of methacrylates, while **86** contains two CF_3 groups in the molecular structure, which provide better solubility of the radical in this monomer.

The polymerization of FEMA in the presence of **86** in bulk was very slow (Figures 3.78 – 3.79). Conversion of only 10 % was observed when the polymerization was carried out for 400 minutes. However, the polymerizations showed features of a controlled process during this time. Polydispersity increased from 1.5 to 1.8 during the final period of the polymerization (Figure 3.80).

Simultaneously, the polymerizations of FEMA were carried out in supercritical CO_2 under high pressure in the presence of **86** and **78**. Description of the used method regarding the polymerizations in critical CO_2 is given in Section 6.19. This part of the work was performed in cooperation with Nagarajan Vedaraman and Axel Schlewing. The choice of the radicals was based on their solubility in supercritical carbon dioxide. The polymerizations in both cases produced only oligomers and conversions did not exceed 20 % in any experiment. Both bulk

polymerization and polymerization in supercritical CO_2 approaches suggest that triazolinyl **86** is not a good counter radical for realization of controlled radical polymerization of FEMA.

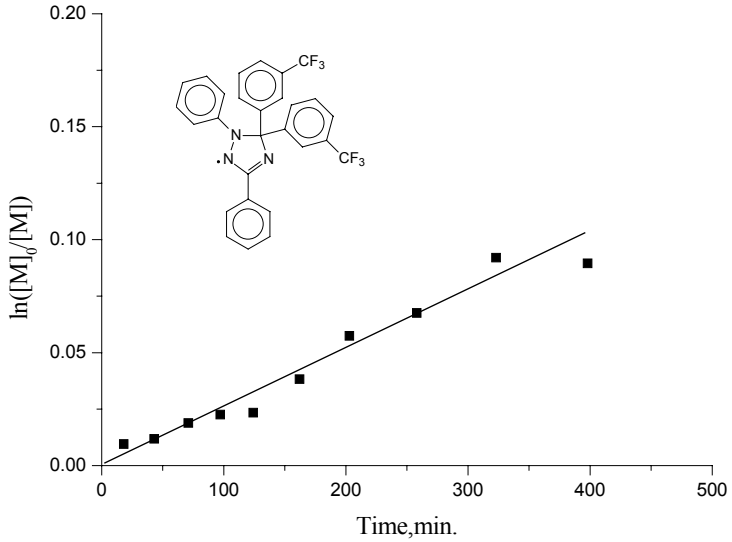

Figure 3.78. ln($[M]_0$/[M]) *vs*. time plot for the polymerization of FEMA in the presence of **86**, FEMA/BPO (mol.): 1000, triazolinyl/BPO (mol.): 1.5, 70°C.

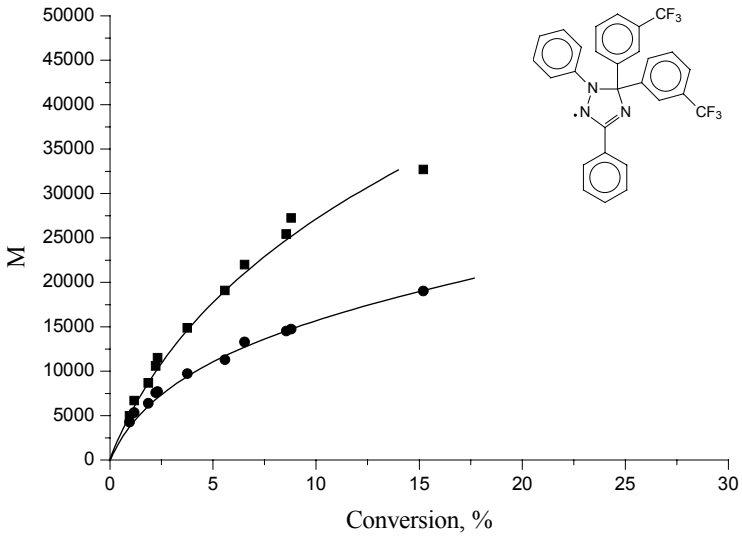

Figure 3.79. Molecular weights (M_w:■; M_n:●) *vs*. conversion plots for the polymerization of FEMA in the presence of **86**, FEMA/BPO (mol.): 1000, triazolinyl/BPO (mol.): 1.5, 70°C.

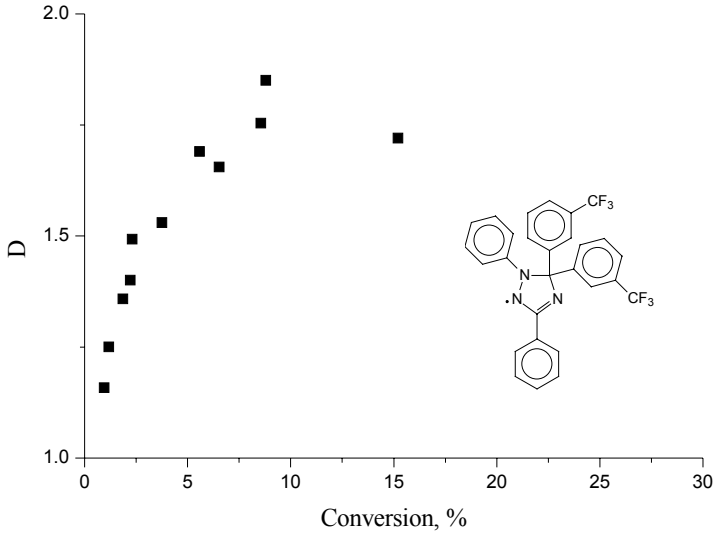

Figure 3.80. Polydispersity (D) *vs*. conversion plot for the polymerization of FEMA in the presence of **86**, FEMA/BPO (mol.): 1000, triazolinyl/BPO (mol.): 1.5, 70°C.

The low polymerization degrees obtained in all polymerization experiments when the fluorinated radicals were employed suggested further investigations. Since the radical **77** showed best results when used in the controlled radical polymerizations of EMA and MMA, polymerization of FEMA in its presence was also carried out. Unfortunately, solubility of this radical in the monomer at room temperature is poor. Attempts to solubilize the radical at the temperature of the polymerization reaction (75°C) showed that at these conditions and in the concentration range used in the polymerization experiments the radical dissolves completely. However, it is possible that solubility of the radical formed during the reaction in the polymer-monomer mixture will be worse as is often the case. Therefore, the expectations for this experiment were not clear: the possibility of poor solubilization of the radical might lead to worse reproducible results. In order to provide better and faster solubilization of the radical upon heating, its suspension in the monomer was reduced to very fine particles using an ultrasound bath and polymerization started. After being heated for a minute in the thermostat at the reaction temperature, the solution became clear indicating complete dissolution. Since the time necessary for dissolving is short, the influence of poor solubility of the radical at room temperature was considered negligible. The conversion for this polymerization was measured by gas chromatography as described in Section 6.8. The polymerization was controlled until conversion reached 30 % (Figures 3.81 and 3.82), after which the increase in the number average molecular weight stopped. Molecular weights at that reaction time (220 minutes) were 49000 and 68000 for M_n and M_w, respectively (Figure 3.82). This is very unusual in comparison to all previous polymerization experiments. In the cases where control over the polymerization was worse during the polymerization (compare: polymerization of styrene in the presence of **77** (Section

3.5.1) or the polymerization was slowing down (compare: polymerization of MMA in the presence of **81** or **78** (Section 3.5.3)) the changes were observed in the development of both M_n and M_w. The reason for such a behavior can be explained by the expected poor solubility of the triazolinyl in the formed polymer-monomer mixture, especially at higher polymerization degrees when the ratio polymer/monomer increases. Another indirect confirmation of this is the relatively poor reproducibility of the obtained results as especially well seen at the D *vs.* conversion plot. Polydispersity of the obtained polymer varied in the range of 1.25 – 1.9 depending on conversion (Figure 3.83). The results show that controlled polymerization of FEMA could be performed when **77** was used as counter radical. However, the control of the polymerization was lost when conversion reached 30 %. Probably the solution for the problem might be the proper choice of a solvent, which would simultaneously provide good solubility for all components of the polymerization mixture: monomer, polymer and radical.

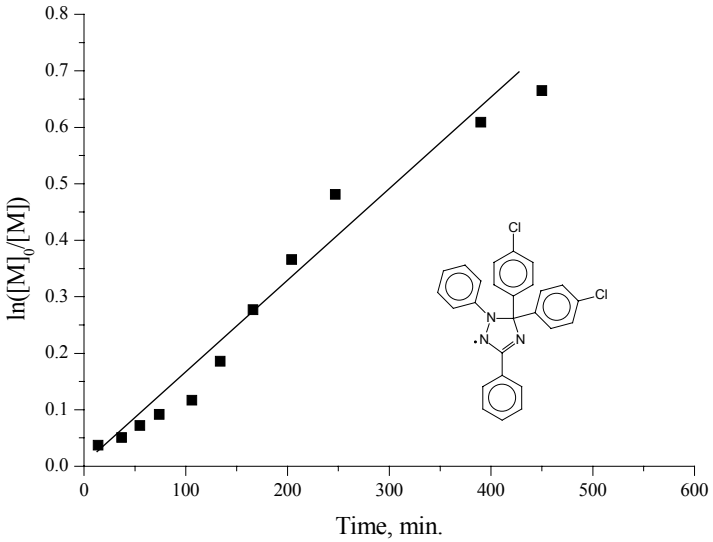

Figure 3.81. ln([M]$_0$/[M]) measured by GC chromatography *vs.* time plot for the polymerization of FEMA in the presence of **77**, FEMA/BPO (mol.): 1000, triazolinyl/BPO (mol.): 1.5, 70°C.

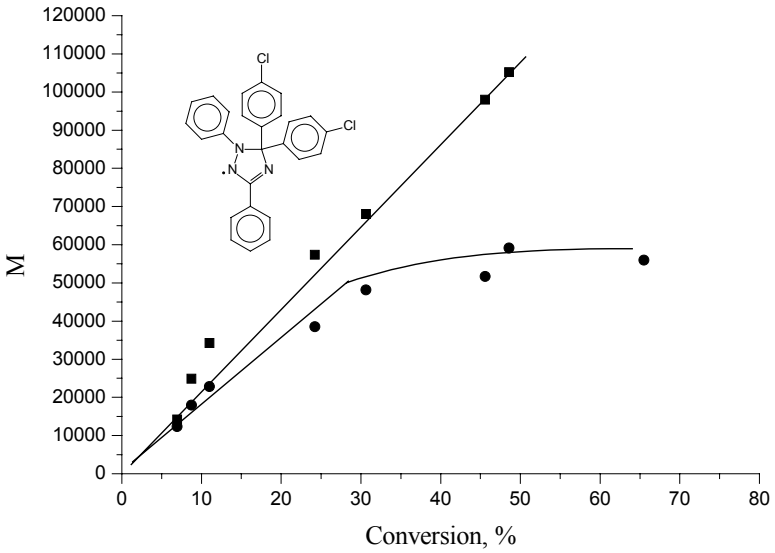

Figure 3.82. Molecular weights (M_w:■; M_n:●) *vs*. conversion plots for the polymerization of FEMA in the presence of **77**, FEMA/BPO (mol.): 1000, triazolinyl/BPO (mol.): 1.5, 70°C.

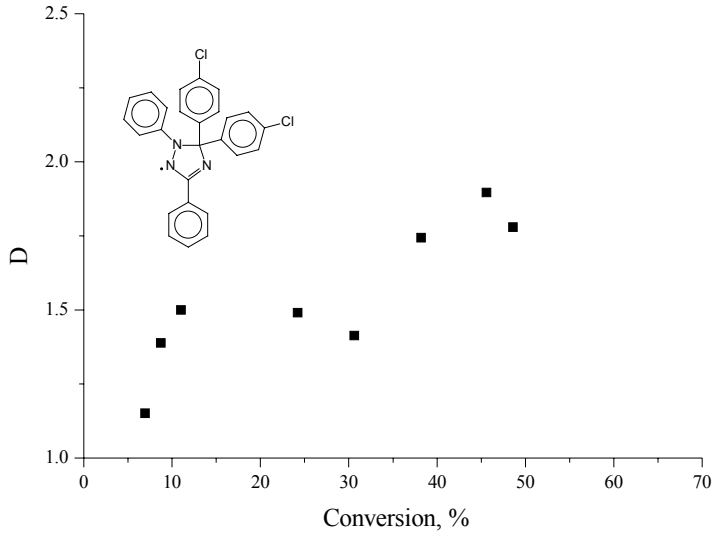

Figure 3.83. Polydispersity (D) *vs*. conversion plot for the polymerization of FEMA in the presence of **77**, FEMA/BPO (mol.): 1000, triazolinyl/BPO (mol.): 1.5, 70°C.

3.6.3. Polymerization of *n*-butylmethacrylate (*n*-BMA) in the presence of 1,3–diphenyl-5,5-di(4-chlorophenyl)-Δ^3-1,2,4-triazolin-2-yl (77)

n-Butylmethacrylate is another methacrylate, which in comparison to previously polymerized MMA and EMA, has an even more extended side ester chain. Comparing the results obtained during the polymerizations of the MMA and EMA in the presence of **77** one can see that the changes were very insignificant. Therefore, it was promising to attempt the use of this radical for polymerization of this methacrylate. As is revealed by the experiment, the

polymerization of *n*-BMA in the presence of **77** was another example of controlled polymerization of methacrylate derivatives. The characteristic plots were perfectly linear showing good control over the polymerization (Figures 3.84 – 3.85).

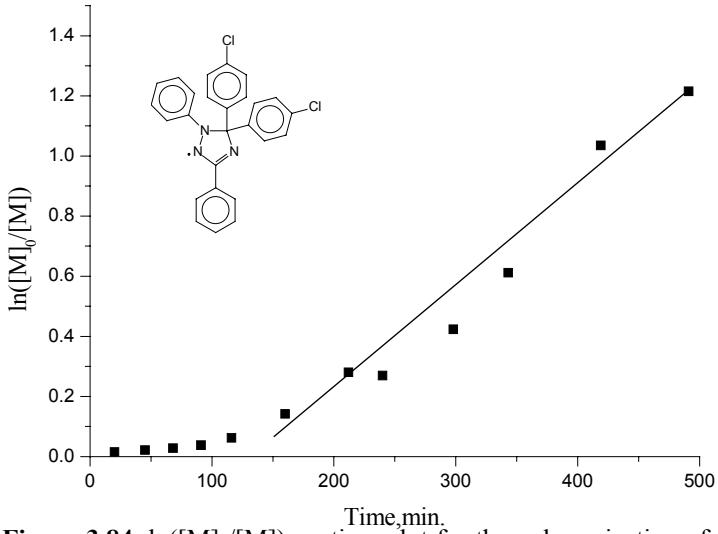

Figure 3.84. ln($[M]_0$/[M]) *vs*. time plot for the polymerization of *n*-BMA in the presence of **77**, *n*-BMA/BPO (mol.): 1000, triazolinyl/BPO (mol.): 1.5, 70°C.

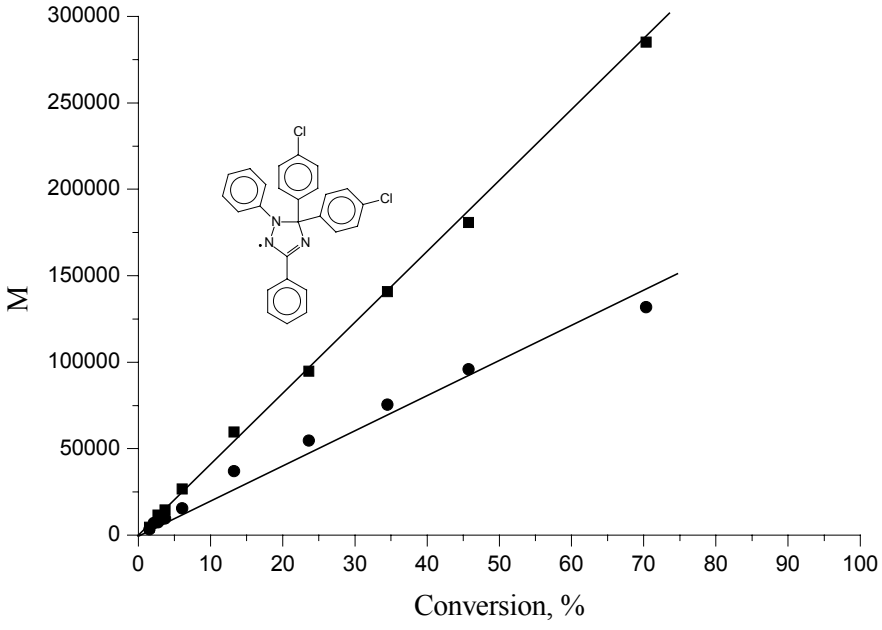

Figure 3.85. Molecular weights (M_w:■; M_n:●) *vs*. conversion plot for the polymerization of *n*-BMA in the presence of **77**, *n*-BMA/BPO (mol.): 1000, triazolinyl/BPO (mol.): 1.5, 70°C.

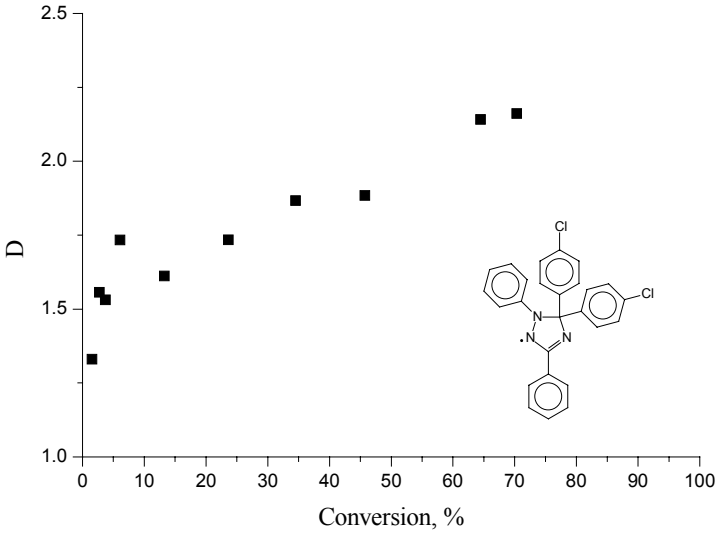

Figure 3.86. Polydispersity (D) *vs*. conversion plot for the polymerization of *n*-BMA in the presence of **77**, *n*-BMA/BPO (mol.): 1000, triazolinyl/BPO (mol.): 1.5, 70°C.

Again as in the case of the previous polymerizations of MMA and EMA the polymerization process had an inhibition period, which seems to be a constant property of well controlled triazolinyl mediated polymerization (in all cases when the best results were achieved it took place). Conversion of 70 % was reached within 490 minutes. The molecular weights of the polymer obtained with this reaction time were 134000 and 285000 for M_n and M_w, respectively. This is a relatively high value, which is very difficult to achieve using for instance the common ATRP technique. As in the cases when the best results were obtained so far, the linear dependence of the M_n *vs.* conversion goes straight through zero point. Initially polydispersity varied in the range of 1.3 – 1.75, however, at high conversions, the polydispersity increased considerably and reached 2.15 (Figure 3.86). This might be caused by the increased viscosity of the polymerization mixture leading to worse mixing of the reaction mixture. However, it also might have been an effect of the longer ester side-chain. Similarly to the case of polymerization of MMA in the presence of **79** (Section 3.5.3) at high conversions the amount of dead polymer can increase significantly, and therefore the use of such a polymer as a macroinitiator for following block copolymer syntheses might lead to low degree of reinitiation. Therefore, if the following block copolymer syntheses are the goal of the triazolinyl mediated polymerization, the polymerization must be quenched at lower conversions.

3.6.4. Polymerization of 4-vinylpyridine (4-VP) in the presence of 1,3-diphenyl-5,5-bis(4-dimethylaminophenyl)-Δ^3-1,2,4-triazolin-2-yl (82)

Vinyl pyridines (4- and 2-isomers) are examples of monomers which can, with difficulty[200,201], be polymerized by the commonly used ATRP technique. Therefore, it was of interest to find out whether the triazolinyl mediated polymerization technique can be extended to this monomer. Successful polymerization of this monomer could allow the syntheses of interesting copolymer structures, especially considering the possible formation of polypyridinium polycations in acidic media. Polymerization of 4-VP was performed using **82** as counter radical. The choice of the radical was based on very good results obtained in the polymerization experiments of styrene (formally similar monomer) with this radical. The characteristic plots are linear showing the controlled character of the polymerization (Figures 3.87 – 3.88). Unlike the polymerization of styrene in the presence of this radical, an inhibition period was not observed in this case. However, the plot $\ln([M]_0/[M])$ *vs.* time still goes through zero indicating the absence of the rapid growth of conversion observed in several polymerization experiments. The molecular weights at the end of the polymerization (40 % conversion, 470 minutes) achieved values of 65000 and 110000, respectively for M_n and M_w (Figure 3.88). Again as in the case of the plot $\ln([M]_0/[M])$ *vs.* time plots go through zero point and no initial increase in the molecular weights is observed. The polydispersity varied in the range 1.55 – 1.75 (Figure 3.89). The results show that the use of the radical **82** showed promising results in controlled radical polymerization of styrene can be easily extended to similar monomers as *e.g.* 4-VP. In comparison to the ATRP technique, much higher molecular weights can be easily achieved and possibility to polymerize this monomer with the same or similar counter radicals as styrene and methacrylates opens the way to block copolymers of these monomers.

[200] X. S. Wang; R. A. Jackson; S. P. Armes, Macromolecules, *33*, 255, **2000**.
[201] J. T. Rademacher; M. Baum; M. E. Pallack; W. J. Brittain; W. J. Simonsick, Jr., Macromolecules *33*, 284, **2000**.

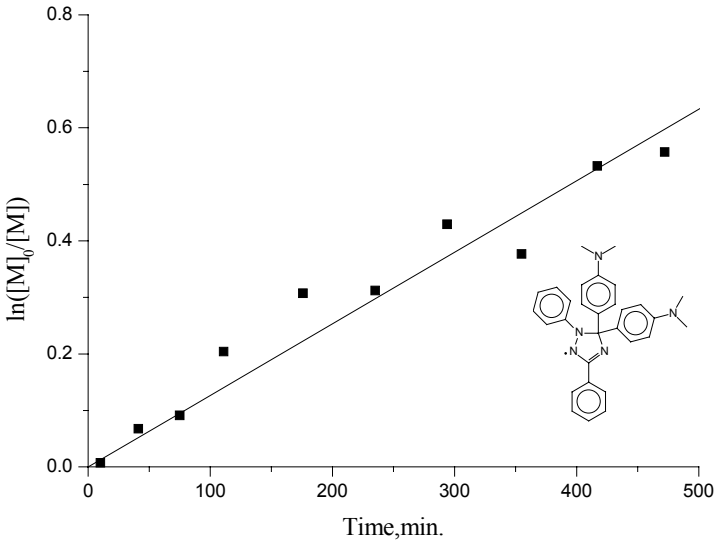

Figure 3.87. ln([M]$_0$/[M]) *vs*. time plot for the polymerization of 4-VP in the presence of **82**, 4-VP/AIBN (mol.): 1000, triazolinyl/AIBN (mol.): 1.5, 120°C

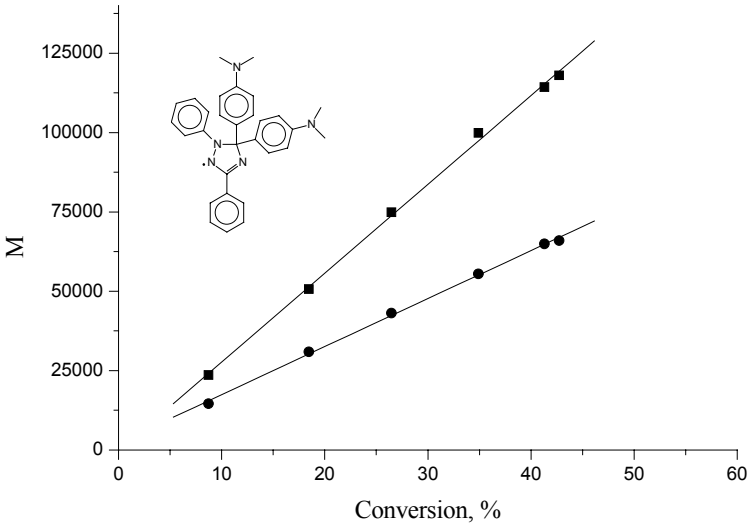

Figure 3.88. Molecular weights (M_w:■; M_n:●) *vs*. conversion plots for the polymerization of 4-VP in the presence of **82**, 4-VP/AIBN (mol.): 1000, triazolinyl/AIBN (mol.): 1.5, 120°C

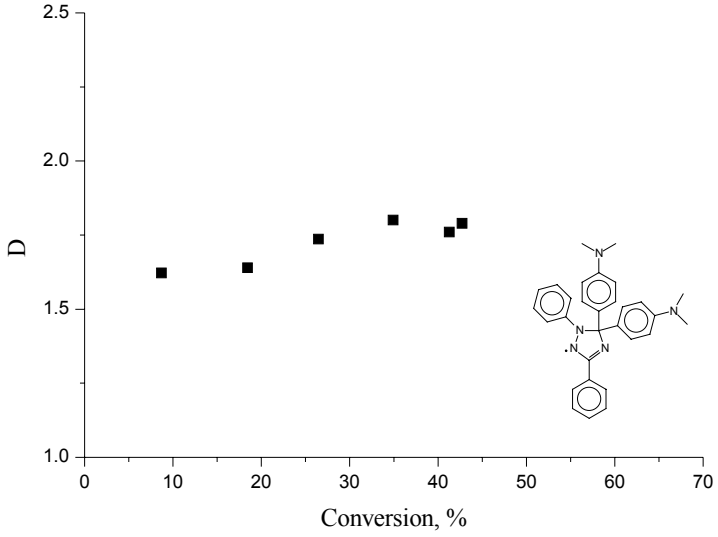

Figure 3.89. Polydispersity (D) *vs*. conversion plot for the polymerization of 4-VP in the presence of **82**, 4-VP/AIBN (mol.): 1000, triazolinyl/AIBN (mol.): 1.5, 120°C

3.6.5. Summary of the application of the triazolinyl radicals 77 and 82 for the controlled radical polymerization of the methacrylates and 4-VP

One of the promising features of the triazolinyl radicals discussed in the Section 1.9.1 is their possible applicability to different monomers. As shown above, one aspect of this approach is the possibility to tune the radical for a specific monomer. So the less stable radicals such as **77** can be used for better control over the polymerization of MMA. At the same time the use of more stable radical allows well controlled polymerization of styrene. In the cases when the perfectness of the polymerization can be sacrificed to ensure better compatibility of the method, meaning widening range of the applicable monomers and reaction conditions, radicals not showing the best results with each of two different monomers but still allowing controlled radical polymerization of both of them can be useful. So, for example, the use of the radical **33**, which does not give the best results in both polymerizations of styrene and MMA, however allows controlled polymerization of both monomers and can be efficiently used when control over polymerization of both monomers is an important feature (possibly controlled statistical copolymer syntheses and soon). This feature of the triazolinyls might become an important and useful tool in polymer chemistry.

Another feature of the radicals observed during the polymerizations of EMA, n-BMA, and 4-VP is the possibility to extend effective use of one radical for a series of similar compounds. This extension, however, has some limitations such as, the solubility factors, which might play an important role as shown in polymerization experiments with FEMA. By combining these two features of the triazolinyl radicals, it might be possible to realize syntheses of a large variety of materials using a few counter radicals. All mentioned above is possible only by changing the stability of the radicals without consideration of the possible changes to the electronic features of the radicals, which can be additionally tuned by substitution at 1- and 3-positions. Use of both approaches simultaneously would of course further widen the abilities of the triazolinyl-mediated controlled radical polymerization.

During this work attempts to polymerize acrylic monomer such as *tert*-butyl acrylate and acrylic acid in the presence of different triazolinyl radicals were made. However, in all cases extremely quick polymerization with simultaneous gelation of the reaction mixture was observed. This behavior was similar independently to the stability of triazolinyls used as additives. A possible explanation for such a behavior might be the high values of the propagation rate constants in the case of polymerization of acrylates.[202] A possible solution for this problem might be the synthesis of triazolinyl derivatives having higher affinity to the active

macro(acrylate)radical. This might be realized by changing the substituents at the 1- and 3-positions of the triazolinyl ring directly influencing the electronic properties of the radical center, responsible for this affinity.

3.7. Syntheses of block copolymers

End-functionalization of the polymers obtained by controlled radical polymerization allows syntheses of block copolymers. At the ends of the polymer chains there are certain functionalities provided by the controlled radical polymerization mechanism. So, for example, in the case of the ATRP such functionalities are the halogen groups. In the case of the triazolinyl mediated polymerization at the end of the polymerization process the reaction is usually quenched by deep freezing of the polymerization mixture. At low temperature the shift of the equilibrium between dormant and active species occurs leading to formation of the dormant species. These dormant species can be processed (isolated, purified, and so on). At the end of the polymer chains obtained in such a way there are triazolinyl moieties attached. Upon heating these dormant species can again be activated to form the active species. If another monomer is added in the system it might lead to formation of block copolymers. The existence of the triazolinyl moieties at the ends of the polymers obtained by triazolinyl mediated stable free radical polymerization was demonstrated earlier.[203] However, as mentioned in Sections 1.9 and 3.6, there are significant limitations in the applicability of the controlled radical polymerization for the syntheses of block copolymers. In the anionic polymerization, which is the most used tool for obtaining such molecular structures, the electrostatic repulsion between the active macroions, prevents possible termination reaction between themselves, providing very high degree of end functionalization, if the polymerization setup has been done carefully (see Section 1.3). Unlike the ionic polymerizations, in a controlled radical polymerization process the termination reactions cannot be suppressed completely even if the polymerization vessel and all reactants are prepared extremely carefully. Due to the reactions between the active macroradicals the "dead" polymer is formed while the reaction proceeds. This leads to no-quantitative end-functionalization of the resulting polymer. It is important to notice that the appearance of the non-functionalized polymer is not due to practical errors, but is a direct consequence of the mechanism of controlled radical polymerization. Of course, when the reinitiation of such polymer sample containing certain amount of the "dead" polymer is attempted the reinitiation is not complete. However, from the material point of view the sample containing small amounts of

[202] M. Buback; A. Feldermann; C. Barner-Kowollik, Macromolecules, *34*, 5439 – 5448, **2001**.
[203] M. Steenbock; M. Klapper; K. Müllen, Macromol. Chem. Phys., *199*, 763 – 769, **1998**.

homopolymer might have similar or even the same properties as the block copolymer alone. Therefore, in many cases the simplicity of syntheses of block copolymers by controlled radical polymerization, still allowing the preparation of materials with given properties is more acceptable than the syntheses of block copolymers with ideal structure, which however, demands complex practical conditions. This is similar to the homopolymerization case where the absence of the "perfectness" of the living ionic polymerization is compromised by the possibility to synthesize larger variety of polymers by controlled radical polymerization with greater simplicity. The amount of the non-end-functionalized "dead" polymer increases during the reaction. This was observed during the preparation of the polymers with triazolinyls as additives when the conversion was allowed to increase to high values (see Section 3.5.3, *e.g.* polymerization of MMA in the presence of **79**). As the result, the later the polymerization is quenched at the stage of preparation of macroinitiator the worse the reinitiation is expected to be on the following stage of the synthesis of block copolymer. The second block can be prepared by both controlled mechanism and uncontrolled radical polymerization. In the first case the polymerization of the second block proceeds *via* a mechanism similar to that of the polymerization of the first monomer. Of course in this case the additive used in the polymerization must permit controlled polymerization of both monomers. Since triazolinyl radicals proved to be able to provide control over polymerizations of different monomers it its promising to attempt syntheses of the block copolymers consisting of various monomers. In the cases when the second monomer in the presence of the additive polymerizes in "uncontrolled way" the second block of the resulting block copolymer will be prepared *via* conventional radical polymerization.

Direct investigation of the end-functionalization of high polymers is often difficult, since the absolute amount of the end-groups of the chains is very low in comparison to the amount of the polymer itself. Hence, only very sensitive methods can be used for the determination of the end-groups of high polymers. In the case of triazolinyl end-functionalized polymers, the triazolinyl moiety can be detected by ^{1}H-NMR spectrometry as peaks near 7 ppm caused by phenyl protons and by UV-Vis spectrometry as specific absorption in range of 200 - 300 nm caused by absorption by electrons in the π-systems of the phenyl rings. Unfortunately, aromatic rings of monomers like styrene and 4-VP and phenyl rings left from BPO initiator show peaks in the same region in NMR and UV-Vis spectra. BPO was used as initiator in all polymerizations in order to permit direct comparison of the obtained data with the polymerizations performed earlier. Therefore, direct investigation of the end-functionalization of the polymers obtained in this work was complex. The goal of the determination of the degree of end-functionalization is an even more difficult target, since it requires the following of those parameters during the

reaction. This is also due to the low intensity values of the investigated parameters used to determine the end groups (e.g. NMR signals or UV-Vis absorption of the end-group). Therefore, these investigations require intensive experimental work, which lies outside the field of the current work, but might be a subject of separate follow-up project. As the result, the attempts to synthesize block copolymers were made without determination of the degree of end-functionalization, but where possible, conclusions about the end-functionalization based on the amount of reinitiated polymer were made. This can be estimated from the GPC curves. In the cases when the reinitiation is not very effective, the residual peak corresponding to the homopolymer precursor can be observed in the GPC of the block copolymers. In order to permit such comparison, all GPC measurements of the block copolymers were performed under the same conditions as the macroinitiators (see Method 6.11). This estimation does not give the exact amount of the reinitiated chains, but provides a rough estimate of the efficiency of the block copolymer formation, which can give an idea about the relative degree of end-functionalization in each particular case.

3.7.1 Syntheses of block copolymers started from polystyrene (PS) macroinitiator

Polystyrene samples obtained by controlled radical polymerization in the presence of various triazolinyl radicals (**33**, **77**, **81**, **82**, **84**) were used as precursors for block copolymer syntheses. The prepared polystyrene samples were processed by usual methods as described in Section 6.7. Also, the polymer precursors were taken at different conversions of the polymerization of styrene. This might allow estimation of the end-functionalization. In the cases when the polymer precursor was taken at the higher degree of polymerization the amount of the non-reinitiated polymer should be higher (see Section 3.5.3). In Table 3.9, the results obtained from block copolymer syntheses started from PS macroinitiators with various monomers for the second block formation are summarized. The PS macroinitiators were prepared by triazolinyl-mediated controlled radical polymerization with a variety of triazolinyls with different stabilities. As described in Sections 3.5.1 and 3.5.3 the stability of the radicals influences the degree of control over the polymerization process. This should also influence the degree end functionalization, which is key-feature for efficient block copolymer syntheses.

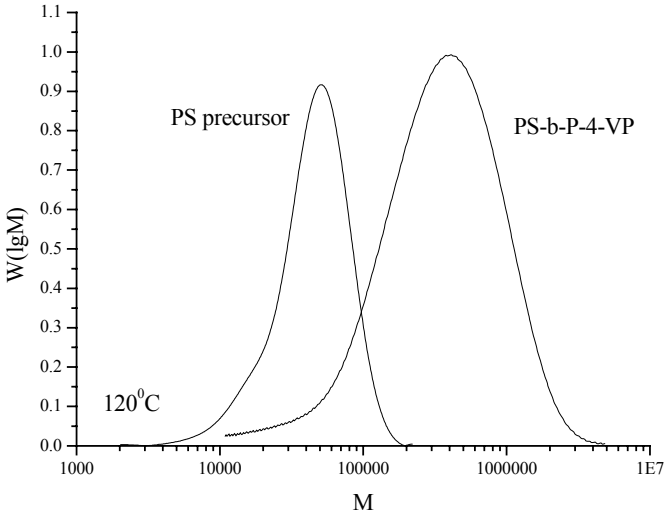

Figure 3.90. Increase of molecular weight during PS-*b*-P-4-VP block copolymer synthesis using **81**-end-capped PS macroinitiator at 120°C in bulk.

The possibility of elongating triazolinyl capped PS chains by reinitiation in the presence of styrene was reported previously.[204] PS-*b*-P-4-VP copolymer was successfully synthesized by reinitiating polystyrene samples obtained by triazolinyl mediated controlled radical polymerization at 120°C. In comparison to the homo PS, the block copolymer PS-*b*-P-4-VP has much poorer solubility in common organic solvents, which complicated the goal of obtaining GPC results. A typical example of the increase in the molecular weight of the block copolymer produced from PS macroinitiator obtained by GPC is shown in Figure 3.90. The molecular weights of the obtained block copolymers show insignificant dependence on the nature of the counter radical and conversion, at which the macroinitiator was taken. So for instance the block copolymers PS-*b*-P-4-VP synthesized from PS macroinitiators obtained by polymerization of styrene in the presence of **82** and **77** gave very similar increase in molecular weights, polydispersity of the final sample and conversion of 4-VP. This is despite the fact that the conversions of the initial PS macroinitiator were different (23 % in the case of **82** and 36 % in the case of **77**), and that the stability of these radicals varied over a wide range: **77** is one of the least stable radicals synthesized, while **82** is one of the most stable triazolinyls. In all cases the polydispersity of the block copolymer samples increased during the block copolymer preparation and was slightly higher than 2 for all used triazolinyls. This might indicate a relative loss of control on the second stage of the block copolymer synthesis in comparison to the stage of the preparation of the macroinitiator. The relative loss of control, independent of the type of the employed triazolinyl might then explain the similarities in the properties of the obtained block copolymers. The control over the polymerization of the second monomer was also worse in

comparison to the homo polymerization of 4-VP, which is discussed in Section 3.6.4. This might be due to less efficient initiation provided by the macroinitiator, as the result of the presence of certain amount of "dead" chains. That amount, however, is not as high as the peak on the GPC trace corresponding to the molecular weight of the PS macroinitiator is absent.

The block copolymer syntheses in the cases when the first block was made of PS and *tert*-butylacrylate (*tert*-BA) and MMA were used for formation of the second block at moderate temperatures (70 – 85°C) were unsuccessful. No increase in the polymer weights was observed in these cases. Typical GPC curves are given in Figures 3.91 – 3.92. However, earlier it was reported[205] that syntheses of block copolymers started from triazolinyl-terminated PS with MMA, as a second monomer were successful at 120°C. The temperature used in that case is higher than MMA's boiling point and is close to the temperatures at which decomposition of PMMA obtained by triazolinyl mediated controlled radical polymerization starts (140 - 150°C). High temperature used for these syntheses also excludes the possibility to run the polymerization in a controlled way (for this, temperatures ~ 70°C in the case of MMA are required).

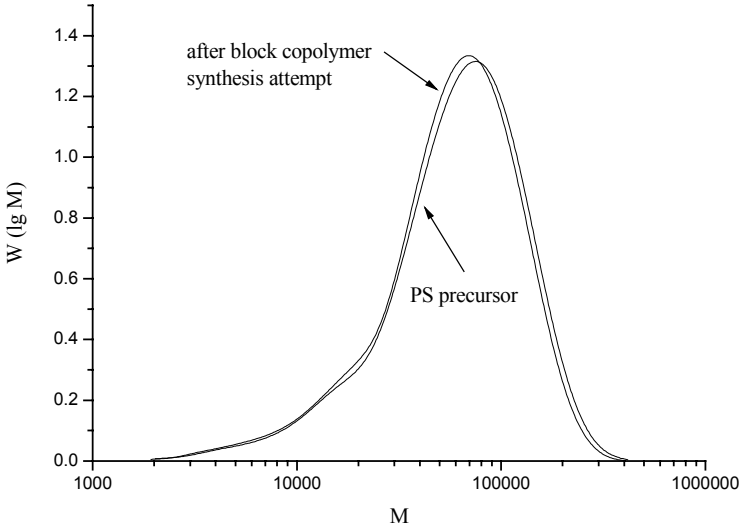

Scheme 3.91. Absence of increase in molecular weights during attemting PS-*b*-PMMA copolymer preparation started from **81** end-functionalized PS precursor.

[204] M. Steenbock; M. Klapper; K. Müllen, Macromol. Chem. Phys., *199*, 763 – 769, **1998**.
[205] D. Colombani; M. Steenbock; M. Klapper; K. Müllen, Macromol. Rapid Commun. *18*, 243 – 251, **1997**.

Table 3.9. Datasheet of block copolymer syntheses using PS macroinitiators.

Block copolymer	Triazolinyl	M_n	M_w	Initial M_n	Initial M_w	Polydispersity	Conversion at which macroinitiator was taken, %	Formation of block copolymer	Temperature, °C	Reaction time, min	Macroinitiator weight, g	Monomer weight, g	Copolymer weight, g
PS-b-PMMA	Cl (**77**)	37300	72300	39200	76700	1.9	46	-	70	1395	0.0430	1.5000	0.0628
PS-b-PMMA	OCH_3 (**81**)	33700	75900	34500	53600	2.3	>50	-	70	1400	0.0444	1.5016	0.2492
PS-b-PMMA	H (**33**)	37800	63300	33800	55700	1.7	49	-	70	1397	0.0471	1.6580	0.0641
PS-b-PMMA	C_6H_5 (**84**)	35400	63500	349100	58600	1.8	>50	-	70	1405	0.0429	1.5042	0.058
PS-b-PMMA	$N(CH_3)_2$ (**82**)	39500	65500	41100	67900	1.7	25.7	-	70	1412	0.0415	1.5069	0.0644
PS-b-P-*tert*-BA	Cl (**77**)	25500	66900	39200	76700	2.6	46	-	85	1398	0.0407	1.5084	0.9219
PS-b-P-*tert*-BA	OCH_3 (**81**)	32600	43500	34500	53600	1.3	>50	-	85	1401	0.0456	1.5051	1.5121
PS-b-P-*tert*-BA	H (**33**)	25900	54400	33800	55700	2.1	49	-	85	1401	0.0460	1.5022	1.7585
PS-b-P-*tert*-BA	C_6H_5 (**84**)	11900	53700	34900	58600	4.5	>50	-	85	1401	0.0405	1.5064	0.8264
PS-b-P-*tert*-BA	$N(CH_3)_2$ (**82**)	68800	120500	80800	130500	1.7	50.8	-	85	1401	0.0457	1.5120	0.660
PS-b-P-4-VP	$N(CH_3)_2$ (**82**)	238800	545900	45500	68100	2.3	22.8	+	120	142	0,0167	1,4963	0.1759
PS-b-P-4-VP	OCH_3 (**81**)	241000	574100	27300	44900	2.4	35.7	+	120	142	0,0064	1,1441	0.1985
PS-b-P-4-VP	Cl (**77**)	255700	609100	30900	60800	2.4	35.6	+	120	142	0,0115	1,4589	0.21
PS-b-P-4-VP	H (**33**)	254700	616500	25300	44000	2.4	38	+	120	142	0,0145	1,4572	0.3052
PS-b-P-4-VP	C_6H_5 (**84**)	242700	576800	24100	42100	2.4	29.8	+	120	142	0,0078	1,3194	0.1952

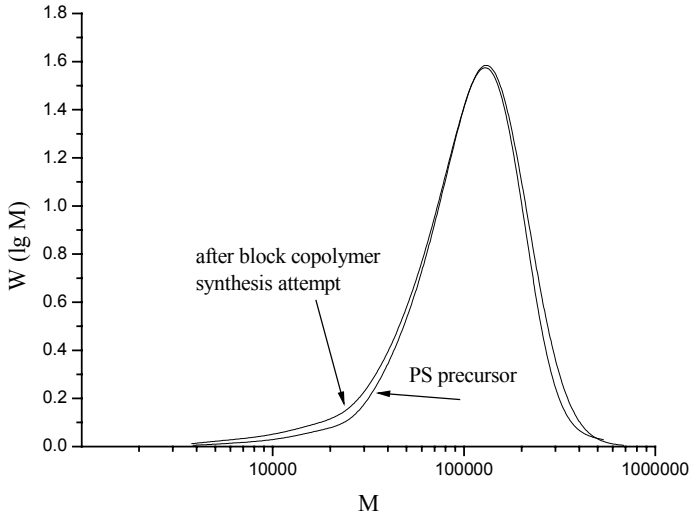

Scheme 3.92. Absence of increase in molecular weights during attemting PS-*b*-P-*tert*-BA copolymer preparation started from **81** end-functionlized PS precursor.

Experiments showed that PS macroinitiators can be successfully reinitiated in the presence of 4-VP at high temperature (120°C). Earlier it was also reported that the PS macroinitiators obtained by triazolinyl-mediated controlled radical polymerization could be reinitiated in the presence of styrene at the same temperature.[206] Taking into account that during homopolymerization experiments it was observed that the triazolinyl radicals have relatively high flexibility and permit controlled polymerization of similar monomers, it should be possible to synthesize other block copolymers with various other styrene-like monomers. More in-depth investigations of the behavior of the polymerization process at the stage of the preparation of the second block is required to clear possible ways to overcome the problem of use of other non-styrene-like monomers. For instance kinetic investigations similar to those performed for homopolymerization experiments might reveal the reasons of the failure of the block copolymer syntheses with MMA and *tert*-BA.

Surprisingly the nature of the radical does not influence the behavior of the system as it was in the case of homopolymerization experiments. For instance the PS-*b*-P-4-VP copolymers obtained from PS macroinitiators prepared in the presence of **77** and **45** are very similar (see Table 3.9): polydispersities of the final products are 2.3 and 2.4 correspondingly. The increase in molecular weights is in the same range and the conversions of the 4-VP are very close one to another. This shows that the features (including stability) of the triazolinyl radical play a relatively insignificant role in comparison to the homopolymerization of styrene (compare: Section 3.5.1, polymerization of styrene in presence of **77** and **82**). Therefore, the choice of the radical for further block copolymer syntheses must be mainly based on the criteria of the

providing better control and consecutively end functionalization of the macroinitiator. The experimental data obtained so far suggests that triazolinyl radical **82** is most suitable for this purpose.

3.7.2. Syntheses of block copolymers started from polymethylmethacrylate (PMMA) macroinitiator

The polystyrene macroinitiators allowed block copolymer formation with only 4-VP, therefore attempts to use PMMA precursors for the block copolymer syntheses were carried out. Similarly to the block copolymers syntheses initiated by polystyrene samples, polymethylmethacrylate samples end-functionalized with triazolinyl moieties have been used in order to obtain block copolymers. Similarly to the PS macroinitiators, the PMMA samples were taken at different conversions and from the polymerizations with various counter radicals to reveal possible influence of these factors on the efficiency of the block copolymer syntheses, which have been discussed in the previous section. The block copolymers were successfully prepared when styrene, FEMA, *n*-BMA and *tert*-BA were used as monomers for formation of the second block. This is very from block copolymer syntheses starting from PS precursors. The results are summarized in Table 3.10. Unlike the experiments with PS macroinitiators, here the dependence on the type of the counter radical was clearly seen in several cases.

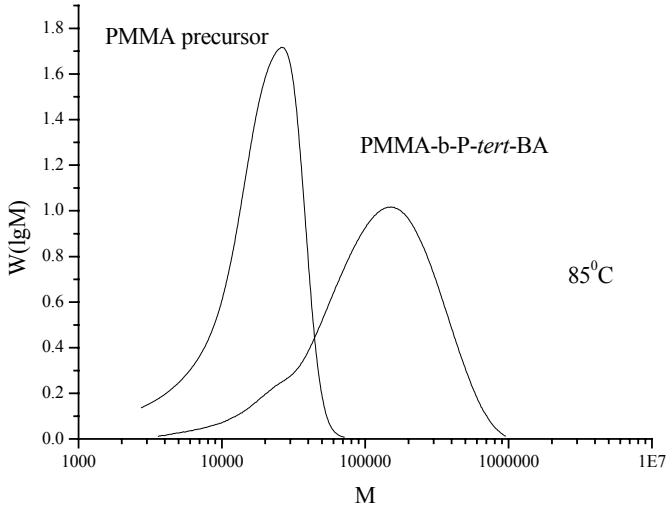

Figure 3.93. Increase of molecular weight during PMMA-*b*-P-*tert*-BA block copolymer synthesis using **78**-end-capped PMMA macroinitiator at 85°C in bulk.

The first monomer, which was attempted to be polymerized from PMMA precursor, was *tert*-butyl acrylate (*tert*-BA). As it was mentioned in the Section 3.6.5, homopolymerization of

[206] M. Steenbock; M. Klapper; K. Müllen, Macromol. Chem. Phys., *199*, 763 – 769, **1998**.

this monomer in the presence of triazolinyls was uncontrolled. Therefore, the formation of the second block of the block copolymers is prepared *via* conventional radical polymerization. The PMMA precursors in this case play the role of initiator and the cleaved triazolinyl moiety should not influence the polymerization behavior. Freed triazolinyls at higher temperature can undergo decomposition simultaneously generating initiating species. Therefore, the obtained block copolymers must also contain *tert*-BA homopolymer. Confirming this proposition, very high polydispersities of the obtained block copolymers were observed (up to 4.5 in the case of **79** counter radical). Possibly chain transfer occurs in the system in this case as well, leading to such a high value of the polydispersity index. An example of the GPC curve of the obtained PMMA-*b*-P-*tert*-BA copolymer as compared to the initial PMMA precursor is shown in Figure 3.93. A shoulder corresponding to the molecular weight of PMMA precursor is observed in the GPC of the obtained copolymer. This confirms the mentioned "imperfectness" of the block copolymer syntheses *via* controlled radical polymerization in comparison to ionic polymerizations. The non-end-functionalized "dead" polymer formed *via* termination reactions is responsible for incomplete reinitiation. As in the case of the homopolymerization where the "perfectness" of the process is decreased in order to simplify the polymerization conditions here, the "perfectness" of the final product is not achieved. The final product contains homopolymers of both monomers used in the two stages of the preparation of the block copolymer. However, the procedure of the preparation, in the comparison to more precise ionic polymerization is much simpler. Therefore, the main point in the preparation of the block copolymers by triazolinyl-mediated polymerization is the goal to keep the amount of the homopolymers at the level where their presence does not worsen the properties of the final material. It depends, first of all, on the application where such materials will be used. As was already mentioned in order to improve the results, the macroinitiator must be taken at lower degree of polymerization. The controlled character of the polymerization at the stage of the preparation of the second block is very desired. Therefore, there is an interest in looking for new, especially 1- and 3-substituted triazolinyls, which might allow controlled radical polymerization of acrylates. Having such triazolinyl radicals, it would be possible to perform more efficient syntheses of PMMA-*b*-P-*tert*-BA copolymer, where both monomers are polymerized in a controlled manner.

After failure of extension of the PS macroinitiator by MMA, preparation of PMMA-*b*-PS copolymer was attempted starting from PMMA precursor. The experiments showed (Table 3.10) that in this case the formation of the block copolymer could be successfully achieved. The block copolymers were obtained from PMMA macroinitiators obtained with different triazolinyls. In all cases polydispersities of the obtained block copolymers were close to 2, showing relatively good reinitiation in this case (Figure 3.94). No well-pronounced shoulder, corresponding to the

initial PMMA precursor is observed in this case. This shows that the amount of "dead" polymer is not very high. The increase in molecular weights and polydispersities of the obtained copolymer samples are comparable one with another without consideration of the counter radical. Comparing the results obtained after quenching of the block copolymer preparation after 188 minutes and 995 minutes, simultaneous increase in the conversions and molecular weights is observed. This is a good indication of the controlled process, which however, needs more detailed kinetic studies for further confirmation. In order to prove homogenety of the obtained block copolymers HPLC chromatography of a typical block copolymer was performed. The chromatogram shows only one peak confirming efficient reinitiation and formation of block copolymer in this case (Figure 3.95). Possible controlled polymerization of styrene at the stage of the preparation of the second block of the copolymer is very promising and is a big advantage of this system. This is the result of the flexibility of the triazolinyl radicals, which permits controlled radical polymerization of various monomers in the presence of the same radical.

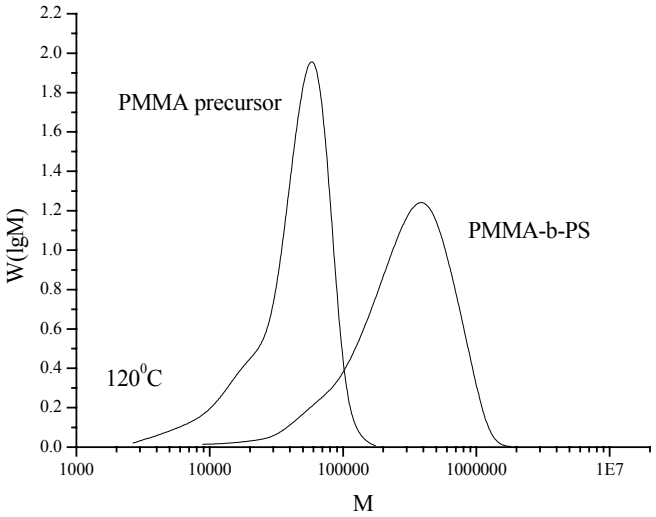

Figure 3.94. Increase of molecular weight during PMMA-*b*-PS block copolymer synthesis using **33**-end-capped PMMA macroinitiator at 120°C in bulk.

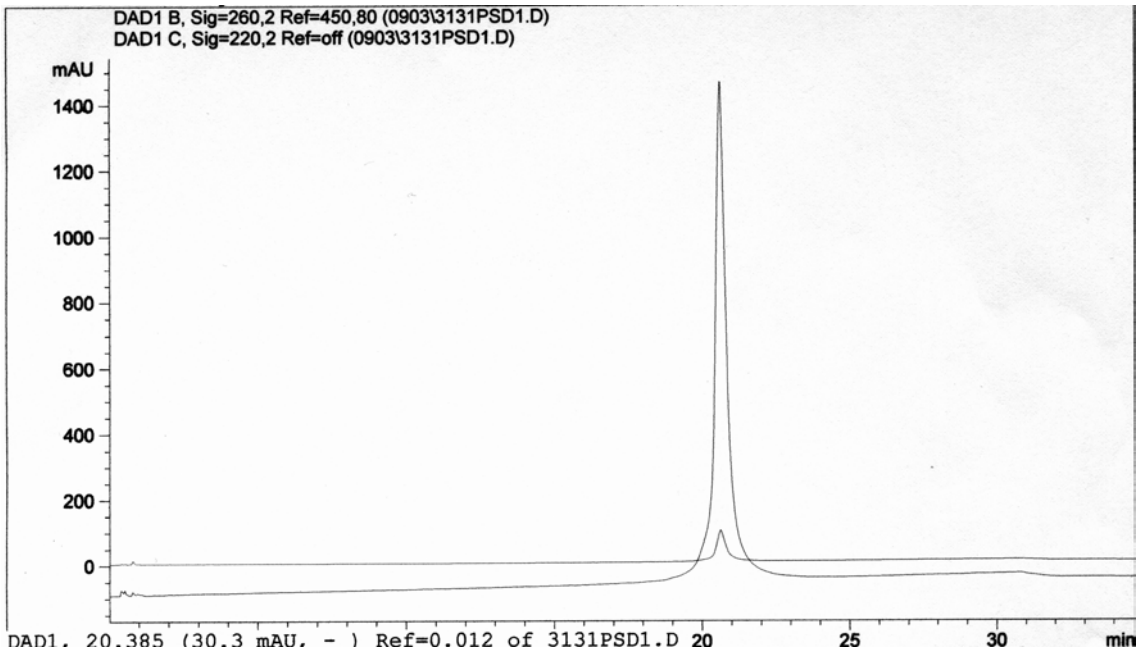

Figure 3.95. HPLC using THF/water as a liquid phase showing presence of only block copolymer in the sample obtained by reinitiation of **78**-end-capped PMMA macroinitiator in the presence of styrene at 120°C in bulk.

Table 3.10. Datasheet for block copolymer syntheses started from PMMA macroinitiator.

Block copolymer	Triazolinyl	M_n	M_w	Initial M_n	Initial M_w	Polydispersity	Conversion at which macroinitiator was taken, %	Block copolymer formation	Temperature, °C	Reaction time, min	Macroinitiator weight, g	Monomer weight, g	Copolymer weight, g
PMMA-b-PFEMA	H (**33**)	43100	66700	31800	51400	1.5	25	+	70 to 85	1545	0.0199	0.8451	0.0281
PMMA-b-PFEMA	Cl (**77**)	34100	60200	14800	21300	1.7	7	+	70 to 85	1545	0.0118	1.0763	0.0384
PMMA-b-PFEMA	Br (**79**)	12700	26600	16500	26000	2.1	9	-	70 to 85	1545	0.0082	0.6059	0.0134
PMMA-b-PFEMA	C_6H_5 (**84**)	32100	67300	25300	42200	2.1	14	+	70 to 85	1545	0.0069	1.2675	0.0136
PMMA-b-PFEMA	OCH_3 (**81**)	27700	45900	11500	24700	1.6	9	+	70 to 85	1545	0.0157	1.0768	0.0205
PMMA-b-PFEMA	mono-Br (**80**)	55900	91300	35100	58900	1.6	-	+	70 to 85	1545	0.0106	0.757	0.0197
PMMA-b-P-*n*-BMA	C_6H_5 (**84**)	202200	1193200	25300	42200	5.9	14	+	70	2674	0.0115	0.6945	0.0879
PMMA-b-P-*n*-BMA	Cl (**77**)	55500	98100	43600	62900	1.7	25.3	+	70	4250	0.0108	0.5542	0.0172
PMMA-b-P-*n*-BMA	Br (**79**)	301600	1097100	57900	98600	3.6	33	+	70	1715	0.0082	0.9344	0.0989
PMMA-b-P-*n*-BMA	OCH_3 (**81**)	235000	456600	11500	24700	1.9	9	+	70	4250	0.0084	0.9272	0.0097
PMMA-b-P-*n*-BMA	H (**33**)	516000	922500	31800	51400	1.8	25	+	70	4250	0.0101	0.5521	0.0563
PMMA-b-P-*n*-BMA	mono-Br (**79**)	101400	249000	35100	58900	2.5	-	+	70	4250	0.0097	0.6060	0.0269
PMMA-b-P-*n*-BMA	F (**78**)	752900	1309300	59800	86900	1.7	41	+	70	2674	0.0076	0.5565	0.0972

Table 3.10. (continued) Datasheet for block copolymer syntheses started from PMMA macroinitiator.

Block copolymer	Triazolinyl	M_n	M_w	Initial M_n	Initial M_w	Polydispersity	Conversion at which macroinitiator was taken, %	Block copolymer formation	Temperature, °C	Reaction time, min	Macroinitiator weight, g	Monomer weight, g	Copolymer weight, g
PMMA-b-PS	OCH_3 (**81**)	149700	329200	11400	23500	2.2	9	+	120	995	0.0608	1.5423	1.3053
PMMA-b-PS	H (**33**)	166200	344100	30100	48100	2.1	23	+	120	995	0.0540	1.5124	1.3775
PMMA-b-PS	Cl (**77**)	112200	279300	33300	47700	2.5	15	+	120	995	0.0122	1.5660	1.3175
PMMA-b-PS	OCH_3 (**81**)	123000	248100	11400	23500	2	9	+	120	188	0.0141	1.0183	0.2320
PMMA-b-PS	H (**33**)	148600	312500	29800	49000	2.1	24	+	120	188	0.0221	1.0120	0.2602
PMMA-b-PS	Cl (**77**)	128100	250400	22000	32200	1.9	11	+	120	188	0.0121	1.0403	0.2728
PMMA-b-PS	Br (**79**)	147800	298300	10500	18800	2	5	+	120	188	0.0192	1.2026	0.5166
PMMA-b-P-*tert*-BA	Cl (**77**)	161100	582200	22100	32200	3.6	11	+	85	227	0.0136	1.1712	0.1223
PMMA-b-P-*tert*-BA	C_6H_5 (**84**)	37200	126300	25300	42200	3.4	14	+	85	227	0.0109	0.8811	0.0260
PMMA-b-P-*tert*-BA	H (**33**)	45500	149800	30100	48100	3.3	23	+	85	227	0.0097	1.0252	0.0251
PMMA-b-P-*tert*-BA	Br (**79**)	16300	77000	9880	17900	4.7	5	+	85	227	0.0107	0.9163	0.0235
PMMA-b-P-*tert*-BA	OCH_3 (**81**)	26300	57700	11400	23500	2.2	9	+	85	227	0.0179	1.1761	0.06
PMMA-b-P-*tert*-BA	F (**78**)	78200	103100	59800	86900	1.3	41	+	85	1275	0.0062	1.0060	0.0768
PMMA-b-P-*tert*-BA	Cl (**77**)	66000	166200	14800	21300	2.2	7	+	85	2462	0.0064	0.6710	0.0414
PMMA-b-P-*tert*-BA	Br (**79**)	942900	1565900	57900	98600	2.1	33	+	85	959	0.0057	0.6133	0.5055
PMMA-b-P-*tert*-BA	C_6H_5 (**84**)	416000	1397400	25300	42200	2.5	14	+	85	2459	0.0096	0.6118	0.9998
PMMA-b-P-*tert*-BA	OCH_3 (**81**)	26900	48600	11500	24700	2	9	+	85	2460	0.0078	0.5278	0.011
PMMA-b-P-*tert*-BA	H (**33**)	64500	152100	31800	51400	2.4	25	+	85	2462	0.0111	0.5895	0.0265

As the preparation of PMMA-*b*-PS copolymer showed promising results indicating possible controlled character of the polymerization of styrene at the second stage, the preparation of the blocks started from PMMA precursors with other methacrylates as monomers for the second block was expected to work well. Two methacrylates 2,2,2-trifluoroethylmethacrylate and *n*-butylmethacrylate, were chosen for block copolymerization experiments. The first methacrylate was successfully polymerized in a controlled manner using triazolinyl **77**. This monomer has interesting physical properties (*e.g.* solubility, optical properties), which in combination with easy processability of PMMA could give interesting properties of the copolymers. Initially the reaction was set at 70°C, but at this temperature no visible signs of the block copolymer formation were observed. Therefore, the temperature was elevated to 85°C, and at this temperature in the presence of several triazolinyl radicals (**33**, **77**, **80**, **81**, **84**), the syntheses of block copolymers were successfully achieved. The amount of the reacted FEMA was considerably less than in the cases when other monomers were used for the preparation of the second block (Table 3.10). One of the possible reasons for this is the poor miscibility of the PMMA precursor and FEMA leading to phase separation of the reagents. This was also one of the possible reasons during the strange behavior of molecular weights during the homopolymerization of this monomer in the presence of triazolinyl **77**. For the realization of the efficient block copolymer syntheses a proper solvent should be found, allowing solubilization of macroinitiator and fluorinated monomer, and formed block copolymer. In the case when **79** end-capped PMMA precursors were used as macroinitiators, the synthesis of the block copolymer was not successful. The low degrees of conversion in the homopolymerization of FEMA in the presence of triazolinyls **86** and **78** (the latter in supercritical CO_2) might suggest that proper choice of counter radical is very important for the efficient polymerization of this monomer.

The second methacrylate used for block copolymer syntheses was *n*-BMA, which has a longer ester side chain. Similar to MMA, this monomer was polymerized in the presence of **77** in controlled manner. The control over the homopolymerization was very good (see Section 3.5.3), however the polydispersities were relatively high in comparison to the polymerization of MMA. When it was introduced as the monomer for the formation of the second block, copolymers were formed in all cases. Molecular weight distributions of the copolymers obtained were in the range 1.7 – 3.6, which is relatively broad. Again it is similar to the homopolymerization of this monomer in the presence of **77**, where despite the linear characteristic plots ($\ln([M]_0/[M])$ *vs.* time and M_n *vs.* conversion), relatively high polydispersities were observed. In the case of the **84** end-capped PMMA precursor, the polydispersity reached extremely high value of 5.6.

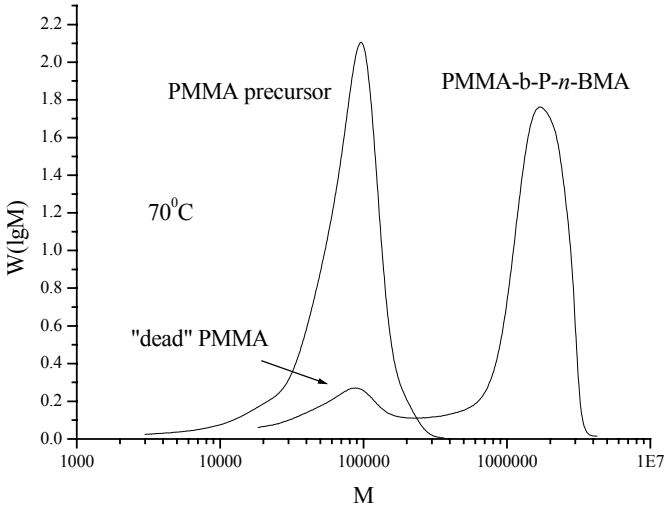

Figure 3.96. Increase of the molecular weight during PMMA-*b*-P-*n*-BMA block copolymer synthesis using **78**-end-capped PMMA macroinitiator at 70°C in bulk; incomplete reinitiation caused by "dead" PMMA is observed.

In contrast to the PS macroinitiator which was reinitiated completely, several PMMA samples show a residual amount of polymer which was not reinitiated. For example, presence of "dead" polymer can be clearly seen in the GPC of PMMA-*b*-P-*n*-BMA copolymer (Figure 3.96). This confirms the proposition that under certain conditions (especially when macroinitiator is taken at a high degree of conversion of the first monomer, or the counter radical used at the first stage is too unstable), a significant amount of dead polymer can be formed during macroinitiator syntheses leading to incomplete reinitiation at the second step of block copolymer synthesis. Similar to the block copolymers started from PS macroinitiator, for efficient block copolymer formation, the macroinitiators should be taken from the polymerization at lower conversions. The polymerizations started from PMMA precursors showed a dependence on the type of the radical, which was used for the preparation of the first block. Block copolymers started from **79**, and **84** end-capped PMMA samples in several cases gave very high polydispersities (up to 5.9) indicating loss of control and bad reinitiation. This of course, leads to worse properties of the obtained materials, which contain significant amounts of homopolymer. An example of a GPC curve obtained for PMMA-*b*-P-*n*-BMA copolymer obtained from **79**-capped PMMA macroinitiator is shown in Figure 3.97. Poor reinitiation together with bimodality of the molecular weight distribution can be clearly seen in this case.

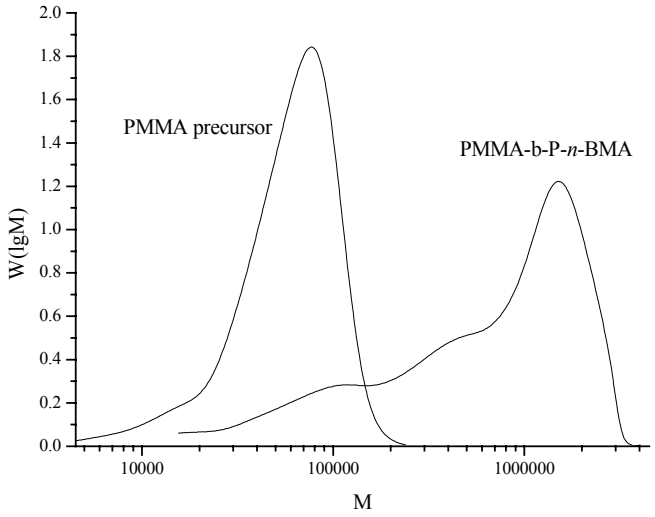

Figure 3.97. Increase of molecular weight during PMMA-*b*-P-*n*-BMA block copolymer synthesis using **79**-end-capped PMMA macroinitiator at 70°C in bulk.

Similar to the preparation of the block copolymers started from PS precursor, the choice of the counter radical for the polymerization of the MMA is very important if further block copolymer preparation is planned. The counter radicals which have moderate stability, such as **33** and **77,** as in the case of homopolymerization of MMA, are more suitable for this purpose. On the one hand, they permit better-controlled homopolymerization of MMA. On the other, the block copolymers prepared with these radicals have better properties, which is partially determined by better end-functionalization as a result of a more controlled process at the first stage. More unstable radicals lead to the formation of "dead" polymer in the macroinitiator sample, while more stable radicals do not allow controlled radical polymerization of MMA.

More detailed investigations of the block copolymer syntheses, including kinetic studies and determination of the influence of the counter radical on the polymerization process, are indeed required for better understanding of the processes going on during the block copolymer formation in this system.

4. Conclusions and outlook

During the realization of the work it was found that the syntheses of triazolinyl radicals and investigations of controlled radical polymerizations in their presence are a challenging, though often complicated subject. From the point of view of synthetic organic chemistry, the instability of the radicals complicates the goal of isolation and purification of these compounds. The complexity of the processes involved in controlled radical polymerization in general and even more in the case of the self-regulation concept, make it difficult to find out the veritable reasons for the behavior of the system in a particular case. However, efforts to overcome these problems were made and this work is an attempt to bring more understanding in this field. On the basis of the work discussed in previous sections the following key conclusions can be formulated.

1. Fourteen triazolinyl radicals (twelve of which are new) having various substituents at the 5-position have been synthesized and characterized during this work for further use as additives in controlled radical polymerizations (Figure 4.1). As the substituents at the 5-position proved to be important for the stability of the radicals (Section 3.4.2), the synthesized radicals include electron poor (**77**, **78**, **79**, **86**, **83**, **87**, **89**, and **88**) and electron-rich aromatic systems (**82**, **81**, and **85**) in order to reveal the possible influence of electronic effects on the stability of the radicals. Radicals **86** and **83** have perfluroalkyl substituted phenyl rings in their structure, improving their solubility in supercritical CO_2, which might improve future results for polymerizations in this promising (especially on an industrial scale) solvent. The developed synthetic route allowed the synthesis of most of the radicals starting from cheap, commercially available benzophenone derivatives (all except **89** and **87**). The radicals **88** and **89** were unstable at room temperature and this did not permit their isolation.

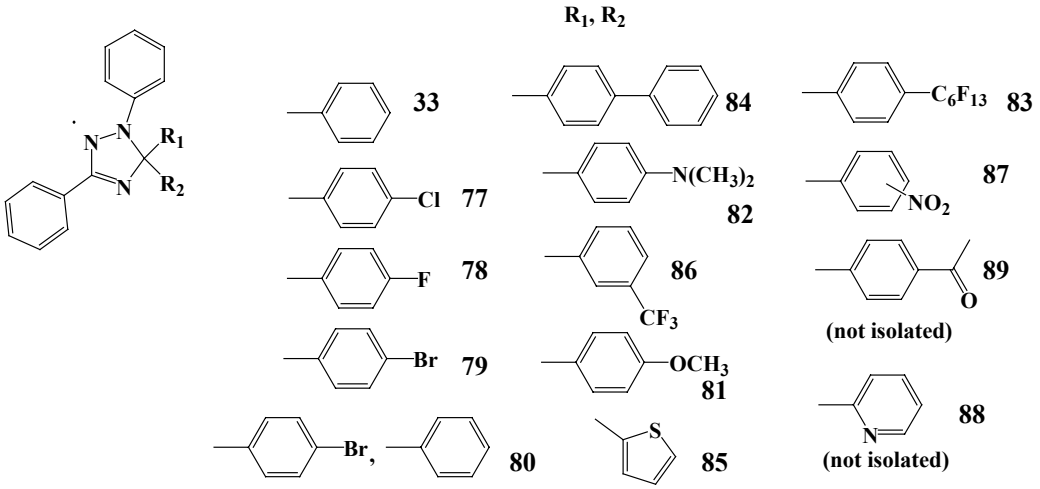

Figure 4.1. Synthesized triazolinyl radicals. Radicals **88** and **89** are unstable at room temperature and were not isolated.

2. The importance of the substituents at the 5-position of the triazolinyl on its stability has been proven and investigated by ESR technique. It was found that electron-poor aromatic substituents at this position destabilize the radical (*e.g.* **77**) and conversely electron-rich aromatic substituents increase stability (*e.g.* **81**) (Section 3.4.2).
3. Kinetic investigations of the polymerizations of styrene and MMA using a variety of triazolinyls with different stabilities (Styrene: **33**, **77**, **79**, **81**, and **82**; MMA: **33**, **77**, **78**, **79**, **81**, and **82**) have been performed. The results showed that in the case of styrene, the more stable radicals provide better control over the polymerization. In particular, **82** showed the best results of the radicals used to control the polymerizations of styrene. In the case of MMA, there is a certain stability of the triazolinyl, which gives the best results in controlled radical polymerization. More and less stable radicals in comparison to the optimal one lead to decrease in the control over the polymerization of MMA. The best results were obtained when **77** was used as a counter radical. Using the radical **82** as additive (which is able to provide control over the polymerization of styrene), controlled radical polymerization of the structurally similar monomer: 4-VP was successfully carried out. Similarly, using the radical showing good performance in the controlled radical polymerization of MMA, control over polymerizations of other methacrylates such as EMA, *n*-BMA and 2,2,2-trifluoroethylmethacrylate (FEMA) were achieved. This demonstrates that efficient use of the triazolinyl radicals in controlled radical polymerization can be spread over the

polymerizations of the series structurally similar monomers; for styrene-like monomers using **82** as additive and for other methacrylates for **77**.

4. The experimental results obtained during this work confirmed predictions made on the basis of the self-regulation concept, thus supporting the self-regulation concept itself. So, the behavior of the system in the case of polymerizations of styrene using less stable radicals **77** and **79** was less controlled, following the expected behavior (Section 3.5.1). At the same time based on the results obtained during the polymerization of styrene and initial polymerizations of MMA with **33** and **77** as additives, and taking into account the stability of the used radicals the behavior of the polymerizations of MMA in the presence of all other triazolinyl radicals was exactly the same as expected. This is an important point for future developing the strategy of controlled radical polymerization, since it allows synthesizing the best performing radicals for a particular monomer.
5. The labile bond between the terminal triazolinyl moieties at the end of the PS and PMMA polymer chains obtained by controlled radical polymerization in the presence of triazolinyls allowed reinitiation of the chains at elevated temperature. This permitted the syntheses of PS-*b*-P-4-VP, PMMA-*b*-PS, PMMA-*b*-P-*tert*-BA, PMMA-*b*-PFEMA, and PMMA-*b*-P-*n*-BMA copolymers. In the same time syntheses of block copolymers PS-*b*-PMMA and PS-*b*-P-*tert*-BA at 70°C and 85°C failed. The results showed that structurally perfect block copolymers is not achieved, due to the presence of the homopolymers in the block copolymer samples. This is due to the "dead" polymer formed at the stage of the formation of the first block and reinitiation caused by the decomposition of the triazolinyls at the stage of the formation of the second block. However, as shown by GPC chromatography in most cases (all except PMMA-*b*-P-*tert*-BA and use of highly unstable radicals such as **79**) the amount of homopolymer is relatively low. It was found that for further decreasing the amount of the homopolymers in the resulting copolymer when (i) the macroinitiator must be taken out of the polymerization at the lowest possible conversion; (ii) the polymerization of the monomer for the formation of the second block must be controlled by the same triazolinyl as used for the preparation of the polymer precursor.

Synthesized triazolinyls with different substituents at the 5-position permitted investigation of the stability of the radical without influencing the properties of the radical center. This is confirmed by the UV-Vis spectra where all triazolinyls have similar shape in the

long wavelength 300 – 500 nm region caused by absorption of the unpaired electron. However, at the same time great changes in the shape of the spectra were observed in the short wavelength region 200 –300 nm when different substituents were introduced. The delocalization of the unpaired electron is not spread over the aromatic substituents at the 5-position as there are two single bonds between the π-systems of the aromatic substituents at this position and of the triazolinyl ring. Moreover, as shown earlier by X-ray scattering,[207] the planes of the phenyl rings at the 5-position of **33** lie almost perpendicularly to the plane of the triazolinyl ring. All those results indicate the very small effect of the substituents at the 5-position on the nature of the radical center. This is important for the self-regulation concept where the stability of the radicals is one of the key features of the process. As the properties of the radical center are not influenced by this structural change it allowed the investigation of the process of reinitiation separately from the other processes going on in the system. The stability of the synthesized radicals changed in a wide range: the least stable radicals, such as **88** and **89**, were not isolated due to instability at room temperature and at the same time the most stable radicals, such as **82** and **85**, have half-life times at 80°C of more than 10 hours. Such a wide range allows the tuning of the rate of the reinitiation to the required value, which is determined by the rate of the termination reactions in the system and is generally variable for each monomer.

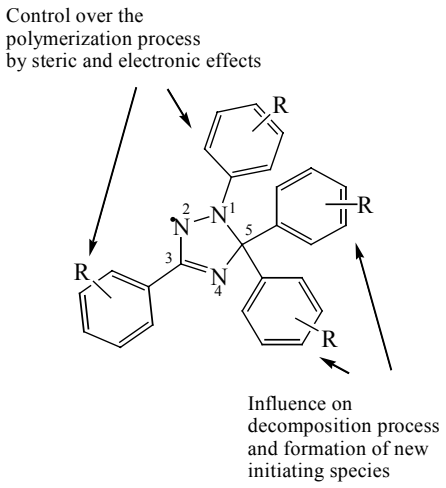

Figure 4.2. General possibilities of tuning of the triazolinyl radical for use in controlled radical polymerizations.

For better performance in CRP, two major factors should be taken into account. From one side, the equilibrium between the dormant and the active species should be adjusted at such level that the polymerization proceeds in reasonable time (several hours). At the same time, if the equilibrium is too much on the active side the reaction time becomes shorter, but simultaneously

[207] F. A. Neugebauer; H. Fischer; C. Krieger, Angew. Chemie, *101*, *4*, 486 – 488, **1989**.

the level of termination reactions increases leading to the formation of "dead" polymer and loss of control over the process. Since all monomers have a different affinity to the coupling with the counter radical to form the dormant species and different termination rates, it is difficult to use the same counter radicals with a variety of monomers. Similarly to the possibilities discussed in this work, to change the decomposition rate of the triazolinyls by variation of the substituents at the 5-position, the affinity of the triazolinyl radical to the growing chain can be changed by substitution at the 1- and 3- positions of the triazolinyl ring (Figure 4.2). There are two ways to modify the affinity of the triazolinyl to the macroradical. First is the change of the electrophilicity/nucleophilicity of the radical *via* electronic factors such as introducing electron donating and withdrawing groups at these positions. This is because, unlike the substituents at the 5-position, here the aromatic groups participate in the delocalization of the unpaired radical. Therefore, introducing, for example, strongly electron-donating groups such as $N(CH_3)_2$ on the phenyl rings at the positions 1 and 3 would lead to a more nucleophilic radical center (Figure 4.3). Such a more nucleophilic triazolinyl should better bind relatively electron deficient macroradicals as in the case of the polymerization of acrylates. Converesely if the substituents are electron-withdrawing groups such as NO_2, this will lead to a more electrophilic radical center, improving binding to more electron rich macroradicals (e.g. the case of vinyl acetate) (Figure 4.3). Another possibility to manipulate the binding of the macroradical to the electron center is introducing of bulky groups, such as *iso*-Pr or *tert*-But as substituents at the positions 1 and 3 (Figure 4.3). They may hinder access of the growing chain to the radical center, leading to worse binding of the triazolinyl to macroradical, shifting in such way the equilibrium from the dormant to the active species. Unfortunately the alkyl 1- and 3- substituted triazolinyls are poorly stable, so the exchange of the phenyl rings by less space demanding groups is difficult in this case. An interesting approach could be the introduction of a chiral substituent at the 1- and 3- positions, which might lead to formation of the polymer with a certain tacticity if during the activation-deactivation equilibrium counter radical stays in a close proximity to the growing macroradical.

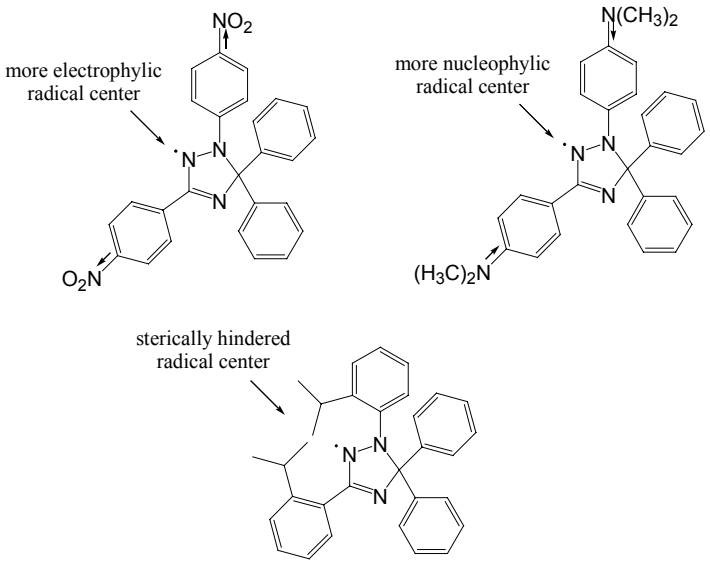

Figure 4.3. Tuning of the radical center in the triazolinyl.

As the two approaches, change in the stability *via* 5-position substituents and variation of the affinity of the radical to the macroradical, are independent one or the other and can be achieved simultaneously by using 1-, 3-, 5- differently substituted triazolinyls, it opens the way for a large library of the compounds. Such combination of the substituents at different positions simultaneously may provide the radicals with features, which are required for the realization of the controlled polymerization of a certain monomer in the most efficient way. Besides performing syntheses of new triazolinyls with their following testing in the kinetic investigations of the polymerization experiments, such tuning might possibly be done *via* computer simulations of the triazolinyl-mediated polymerizations on the basis of dependencies of the stability of the radical *vs.* Hammett constants in such a way lowering the required time and research costs for achieving the required results. The matching of termination rates of a certain monomer with the rate of decomposition of triazolinyl should lead to the optimal conditions for achieving the control over the polymerization. This would become a very powerful tool if the influence of the substituents in the series of 1-, 3-substituted triazolinyls on the equilibrium between the active and dormant species could be rationalized on the basis of, for example, Hammett constants for electronic effects or of size of the substituent in the case of steric hindrance.

In this work, it has been demonstrated that various monomers such as different methacrylates, 4-vinylpyridine, and styrene could be efficiently polymerized using triazolinyl radicals as additives. However, the list of the monomers can probably be extended. Monomers

such as vinyl acetate, acrylates, (meth)acrylamides, acrylonitrile and acrolein, which are of particular industrial interest, are the targets for future development of the method. This is especially important because by this method, which allows polymerization of various monomers with the same counter radical, block copolymers of various compositions could be prepared more easily.

The preparation of advanced macromolecules such as block copolymers and even more complex structures is one of the major targets of triazolinyl mediated radical polymerization as well as other controlled radical polymerization techniques. In this work it has been shown that the polymers obtained by triazolinyl mediated controlled radical polymerization can be efficiently reinitiated at elevated temperature and reacted further leading to block copolymers, giving the possibility for further widening of applications of the method. It was shown that in some cases (especially for the block copolymers prepared from PMMA macroinitiator), the formation of the second block of the block copolymer strongly depends on the counter radical used on the first stage (preparation of the macroinitiator). Therefore, it is of interest to determine the influence of counter radicals on the polymerization of the second monomer. Kinetic investigations of the polymerization on the stage of extension of the polymer precursor may help to understand the processes influencing the properties of the obtained copolymers in greater depth. Unfortunately, due to the imperfect character of the triazolinyl-mediated controlled radical polymerization, the amount of the homopolymers in the obtained copolymers might be significant. It was shown that the efficiency of reinitiation depends on the conversion of the monomer, at which the polymer precursor for block copolymer synthesis was taken from the reaction. This, of course, influences the properties of the final material. Therefore, systematic investigation of the reinitiating abilities of the macroinitiator depending on the conversion of the monomer at the first stage is an important target for future studies.

Recent intensive development of the controlled radical polymerization techniques shows the great prospects of the method for future laboratory and industrial applications. Among many other approaches to the controlled radical polymerization, use of triazolinyls as counter radicals, lying at the foundation of the self-regulation concept seems to be one of the most promising ideas in the field to date.

5. Experimental part: syntheses

5.1. Synthesis of N-phenylbenzenecarbohydrazonoyl chloride

N-phenylbenzenecarbohydrazonoyl chloride was synthesized *via* a published procedure[208] from phenylhydrazine and benzoyl chloride as shown in Scheme 5.1.

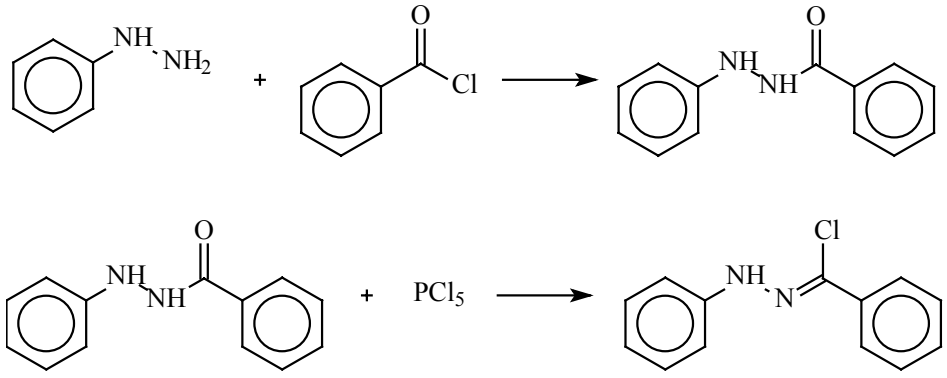

Scheme 5.1. Synthetic route to N-phenylbenzenecarbohydrazonoyl chloride.

Step 1. Synthesis of N'-phenylbenzohydrazide (101)

The first step was synthesis of N'-phenylbenzohydrazide (**101**), which was realized as shown in Scheme 5.2.

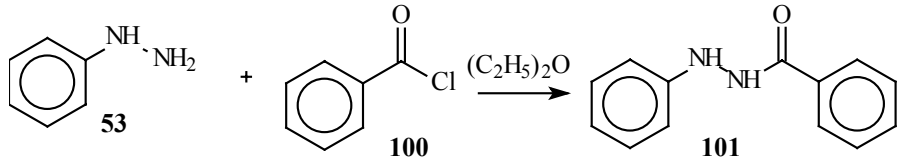

Scheme 5.2. Synthesis of N'-phenylbenzohydrazide (**101**).

A 1000 ml three-necked round-bottom flask equipped with a reflux condenser, a dropping funnel, and an effective magnetic stirrer bar allowing mixing of viscous suspensions was dried as described in Section 6.1. A thermometer with temperature range -30 – 30°C was inserted into one of the necks and the vessel filled with argon. A solution of 29.5 ml (32.4 g, 0.3 mol) of phenylhydrazine (**53**) (Merck) in 300 ml of diethyl ether dried over molecular sieves (Riedel-de Haen) was added to the flask and cooled down to 5°C in an ice bath. A solution of 12.7 ml (15.5 g, 0.11 mol) of benzoyl chloride (**100**) (Aldrich) in 100 ml of dry diethyl ether was

[208] R. Huisgen; M. Seidel; G. Wallbillich; H. Knupfer, Tetrahedron, *17*, 3, **1962**.

added dropwise using a dropping funnel, at a rate such that the temperature of the reaction mixture did not exceed 15°C. After the addition of **100** was complete, the resulting suspension was stirred for 3 hours at temperatures below 15°C. The solid was collected by filtration, washed with plenty of petroleum ether (Fluka) and dried at the pump.

The solid was collected from the filter and transfered into a Soxhlet extraction cartridge. Continuous Soxhlet extraction according to the method given in Section 6.2 with dichloromethane (Riedel-de Haen) was carried out over 48 hours. Dichloromethane was removed under reduced pressure and the resulting solid recrystallized from ethanol to give N'-phenylbenzohydrazide (**101**) as a colorless crystalline solid substance. The yield = 70 %.

Analysis:

Melting point: 167 - 168°C

^{1}H-NMR spectra (D_6-DMSO (Cambridge Isotope Laboratories), 250 MHz) δ [ppm]: 10.4 (br. s, 1H, CONH); 6.7 – 7.9 (m, 11H, NH, phenyl protons)

Mass spectra (FD): m/z: 212.5 (M^+) (only peak)

Elemental analyses: calculated: C: 73.6 %; H: 5.7 %; N: 13.2 %

found: C: 73.4 %; H: 5.8 %; N: 13.0 %

Step 2. Synthesis of N-phenylbenzenecarbohydrazonoyl chloride (37)

The second step was the nucleophilic substitution of oxygen of carbonyl group by chlorine with simultaneous migration of double bond to nitrogen (Scheme 5.3).

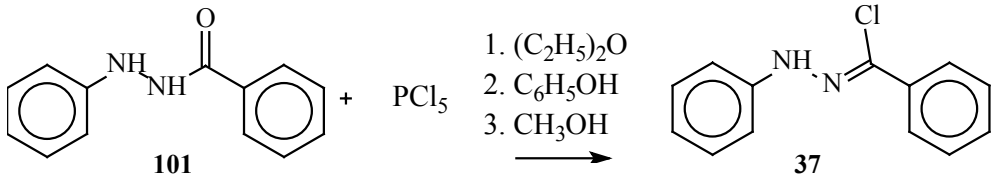

Scheme 5.3. Synthesis of N-phenylbenzenecarbohydrazonoyl chloride (**37**).

A 250 ml two-necked round-bottom flask, equipped with a reflux condenser and magnetic stirrer bar was dried (Method 6.1). The second neck of the flask was capped. 10.65 g (0.046 mol) of **101**, 12.5 g (0.06 mol) of phosphorous pentachloride (Merck) and 100 ml of dry diethyl ether were mixed in the flask under argon atmosphere. The reaction was performed by two different methods.

Method 1. The reactants were stirred at room temperature over 72 hours.

Method 2. The flask was heated in an oil bath with temperature 65°C, and the mixture was stirred under reflux over 8 hours.

In both methods, after completion of the reaction the mixture was cooled by putting the reactor into an ice bath. In the second neck, a 100 ml dropping funnel was installed and a solution of 1.7 g (0.018 mol) of phenol (Riedel-de Haen) in 20 ml of diethyl ether and 20 ml (15.8 g, 0.49 mol) of methanol (Riedel-de Haen) were added consecutively dropwise. The addition rate had to be carefully controlled, due to the highly exothernic reaction. The ice bath was removed and both diethyl ether and unreacted methanol were removed under reduced pressure. Yellow amorphous solid or oil was purified *via* column chromatography on silica gel 60 (Macherey - Nagel) to give N-phenylbenzenecarbohydrazonoyl chloride (**37**) as a grainy, slightly beige crystalline solid. The yield was around 50 % from both methods.

Analyses:

Melting point: 133 – 134°C

^{1}H-NMR spectra (D_6-DMSO, 250MHz) δ [ppm]: 10.4 (broad s, 1H, NH); 6.7 – 7.9 (m, 10H, phenyl protons)

Mass spectra (FD): m/z: 230.0 (M^+) (only peak)

Element analyses: calculated: C: 67.7 %; H: 4.8 %; N: 12.1 %

found: C: 67.8 %; H: 4.9 %; N: 12.3 %

** The substance seems to be able to cause allergic reactions and is possibly toxic*

5.2. Synthesis of 1,3,5,5-tetraphenyl-Δ^3-1,2,4-triazolin-2-yl

1,3,5,5-Tetraphenyl-Δ^3-1,2,4-triazolin-2-yl was prepared *via* a published procedure from N-phenylbenzenecarbohydrazonoyl chloride (**37**) and benzhydrylamine (**38**).[209,210,211] The method of the synthesis is shown in Scheme 5.4.

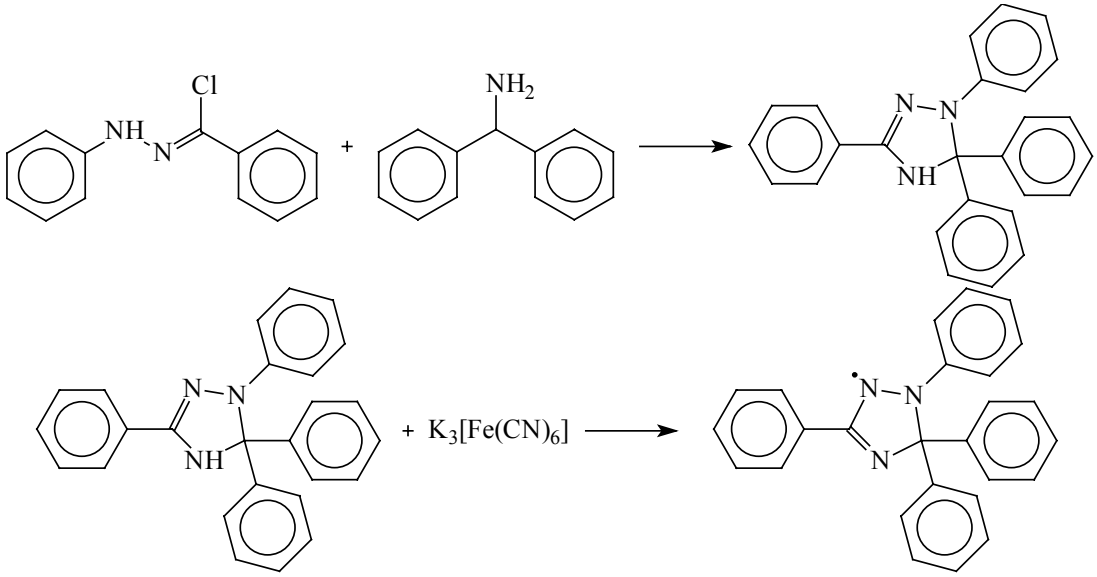

Scheme 5.4. Synthetic route to 1,3,5,5-tetraphenyl-Δ^3-1,2,4-triazolin-2-yl.

Step 1. Synthesis of 1,3,5,5-tetraphenyl-Δ^2-1,2,4-triazolin (39)

The first step is a [2 + 3] cyclization leading to formation of 5-membered triazolin heterocycle (Scheme 5.5).

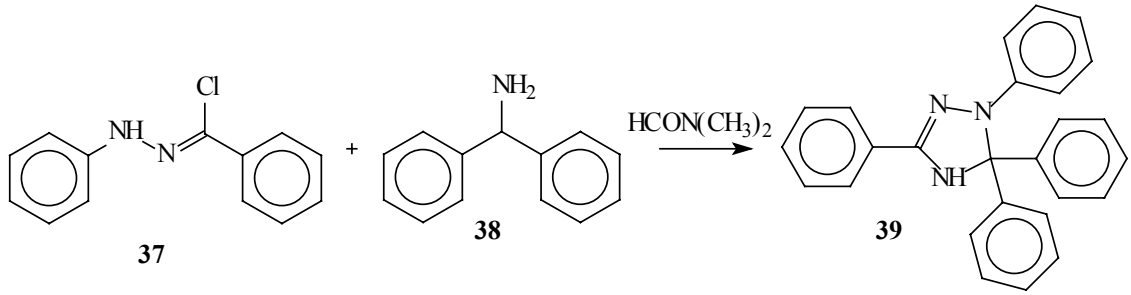

Scheme 5.5. Synthesis of 1,3,5,5-tetraphenyl-Δ^2-1,2,4-triazolin (**39**)

A one-necked 250 ml round-bottom flask, equipped with a reflux condenser and magnetic stirrer bar was dried (Section 6.1). 7.69 g (0.033 mol) of **37** and 11.45 ml (0.066 mol, 12.25 g) of benzhydrylamine (**38**) (Aldrich) were dissolved in 150 ml of DMF (Merck). Under

[209] F. A. Neugebauer; H. F. Fisher; C. Krieger, Angewante Chemie, *101*, 486, **1989**.
[210] F. A. Neugebauer; H. Fisher, Tetrahedron, *51*, 12883, **1995**.

argon the solution was heated to 180°C for 40 minutes. The resulting bright orange solution was cooled to room temperature, and an excess of water was added. The product was extracted with diethyl ether untill the aqueous layer became almost colorless. The organic extracts were collected, washed several times with brine and water, and dried above $MgSO_4$ (Deutero GmbH). Afterwards, the solvent was removed under reduced pressure. The resulting orange-brown oil was purified by column chromatography on silica gel 60 with dichloromethane/petroleum ether mixture as eluent and the product obtained was recrystallized from hexane (Fisher) to give 1,3,5,5-tetraphenyl-Δ^2-1,2,4-triazolin (**39**) isolated as a yellow-orange solid. The yield was 56 %. **39**, as well as, other triazolins are very easily oxidized by air during handling and purification. The process can be easily monitored by thin layer chromatography. The color of the substance changes due to formation of triazolinyl radical (see below) from yellow-orange to brown and leads to a decrease in the melting point, *i.e.* samples which were exposed to air for longer periods showed lower melting points. Hence, the observed melting points may be lower than their actual values as the triazolins may contain traces of the corresponding radical.

Analysis:

Melting point: 192 – 193°C

^{1}H-NMR spectra (D_6-DMSO, 250MHz) δ [ppm]: 8.5 (s, 1H, N<u>H</u>); 6.5 – 7.9 (m, 20H, phenyl protons)

Mass spectra (FD): m/z: 375.1 (M^+) (only peak)

Elemental analysis: calculated: C: 83.2 %; H: 5.6 %; N: 11.1 %

found: C: 83.1 %; H: 5.9 %; N: 11.0 %

Step 2. Synthesis of 1,3,5,5-tetraphenyl-Δ^3-1,2,4-triazolin-2-yl (33)

The second step is oxidation of the 1,3,5,5-tetraphenyl-Δ^2-1,2,4-triazolin (**39)** to the corresponding triazolinyl radical **33** (Scheme 5.6).

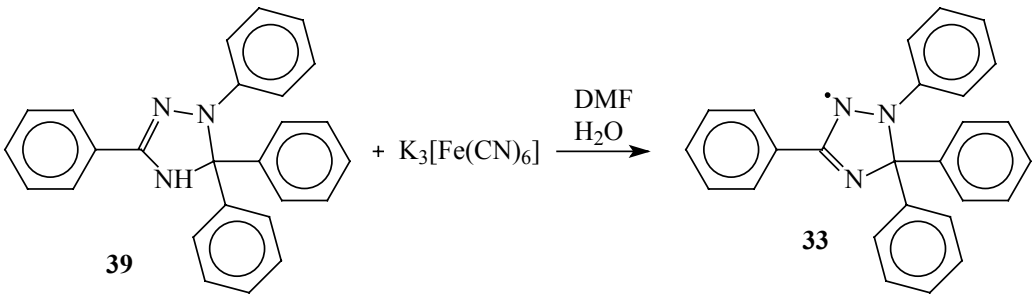

Scheme 5.6. Synthesis of 1,3,5,5-tetraphenyl-Δ^3-1,2,4-triazolin-2-yl (**33**).

[211] F. A. Neugebauer; H. F. Fisher; C. Krieger, Angewante Chemie International Edition, *28*, 491, **1989**.

In a 500 ml Erlenmeyer flask equipped with magnetic stirrer bar 5.24 g (0.014 mol) of **39** were dissolved in 200 ml of DMF and the solution cooled in a dry ice/acetone bath. 6.92 g (0.021 mol) of potassium hexacyanoferrate (III) (Organic Chemistry Faculty of Johannes Gutenberg University, Mainz) and 1.59 g (0.015 mol) of sodium carbonate (Riedel-de Haen) were dissolved in 100 ml of water. The mixture was added dropwise to a stirred solution of **58**. Reagents were mixed over 3 hours. Temperature of the reaction mixture was kept below – 10°C at all times. 200 ml of water were then added dropwise to the solution and the resulting dark-brown precipitate was collected by filtration and washed with water. The completeness of the reaction was checked by TLC on silica gel plates (Merck) with a mixture of dichloromethane and petroleum ether as eluent, and in the case of incompleteness, the procedure was repeated until no **39** was present in the solid. 1,3,5,5-Tetraphenyl-Δ^3-1,2,4-triazolin-2-yl (**33**) was obtained as an almost black powder. Decomposition can take place during handling or preparation. In this case, **33** can be purified by column chromatography on silica gel 60 with dichloromethane/petroleum ether as eluent. The yield = 99 %.

Analysis:

Melting point: 140°C

Mass spectra (FD): m/z: 374.2 (M^+) (only peak)

Elemental analysis: calculated: C: 83.4%; H: 5.4%; N: 11.2%

found: C: 83.4%; H: 5.2%; N: 11.4%

The UV-Vis spectrum at room temperature in dichloromethane is shown in Figure 5.1.

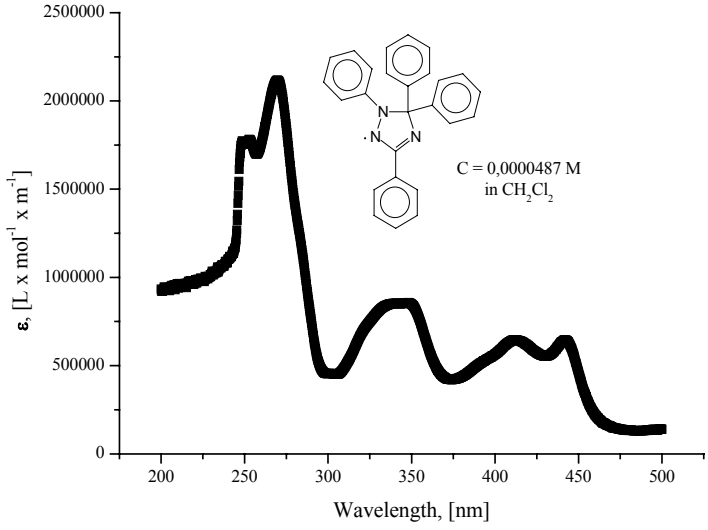

Figure 5.1. UV-Vis spectra of 1,3,5,5-tetraphenyl-Δ^3-1,2,4-triazolin-2-yl (**33**) in CH_2Cl_2.

5.3. Synthesis of 1,3–diphenyl-5,5-di(4-methoxyphenyl)-Δ^3-1,2,4-triazolin-2-yl

1,3–Diphenyl-5,5-di(4-methoxyphenyl)-Δ^3-1,2,4-triazolin-2-yl was synthesized from 4,4′-dimethoxybenzophenone *via* synthetic route shown in Scheme 5.7.

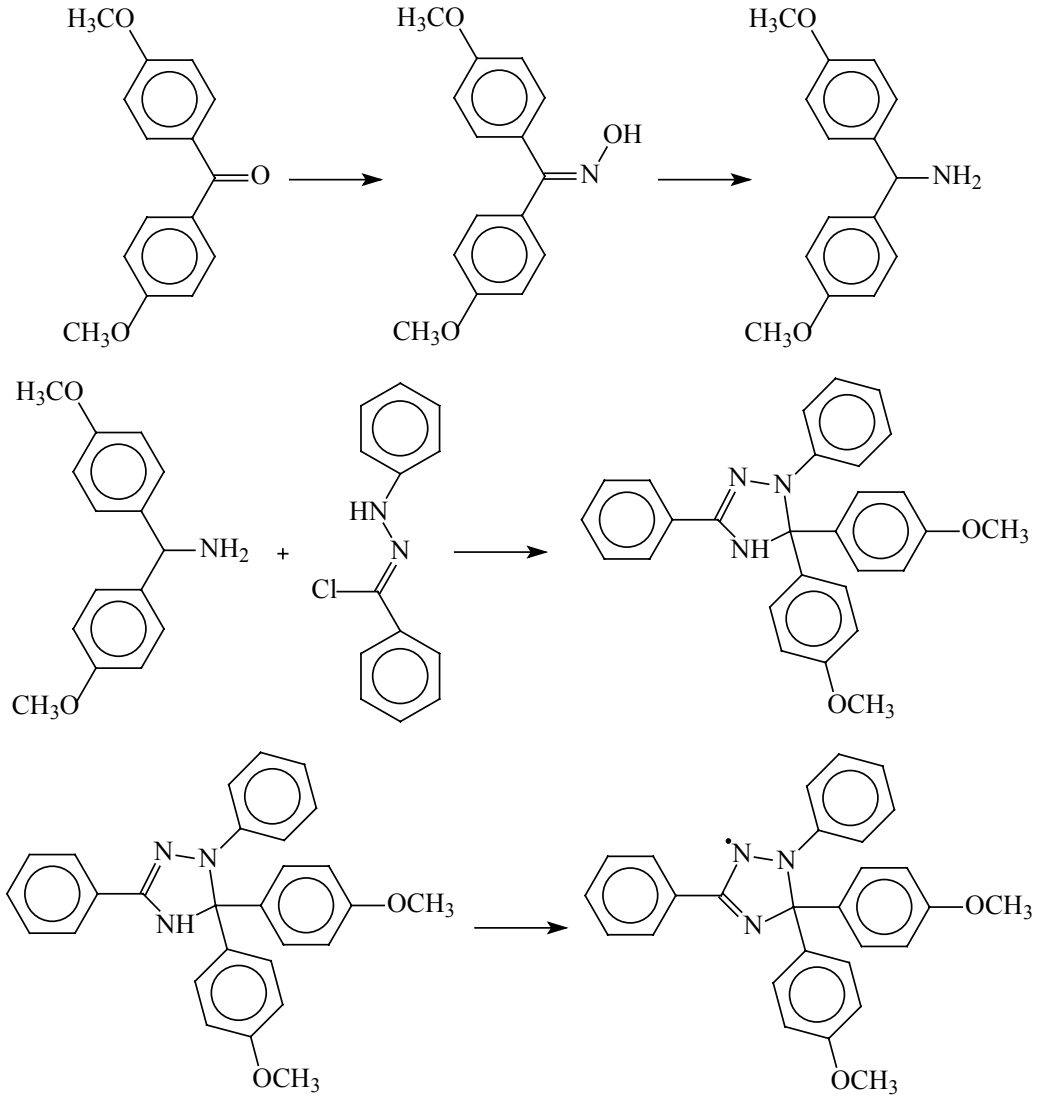

Scheme 5.7. Synthetic route to 1,3-diphenyl-5,5-di(4-methoxyphenyl)-Δ^3-1,2,4-triazolin-2-yl.

Step 1. Synthesis of 4,4`-dimethoxybenzophenone oxime (102)

On the first step 4,4`-dimethoxybenzophenone oxime (**102**) was prepared by reaction of 4,4`-dimethoxybenzophenone (**63**) with hydroxylamine (Scheme 5.8).

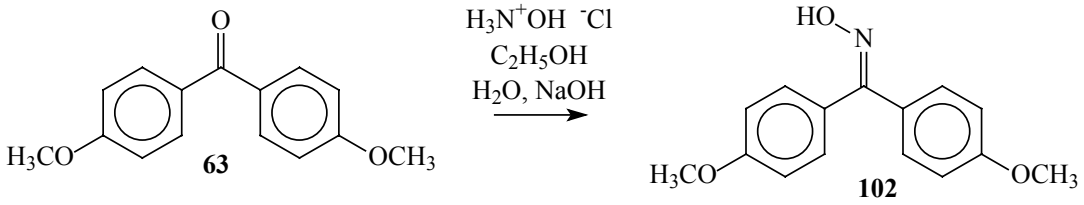

Scheme 5.8. Synthesis of 4,4`-dimethoxybenzophenone oxime (**102**).

In a two-necked 250 ml round-bottom flask equipped with removable septum, reflux condenser and magnetic stirrer bar, 13.32 g (0.055 mol) of 4,4`-dimethoxybenzophenone (**63**) (Lancaster) were mixed with 8.96 g (0.130 mol) of hydroxylamine hydrochloride (Acros). 8 ml of water and 40 ml of ethanol (Riedel-de Haen) were added and 6.33 g of sodium hydroxide (0.158 mol) (Riedel-de Haen) was added in portions at room temperature to the stirred suspension. The flask was then put into an oil bath and the temperature of the bath elevated to 100°C. The mixture was refluxed over two hours. The slightly yellow clear solution was then cooled to room temperature and poured into diluted hydrochloric acid (Riedel-de Haen). The resulting solid was collected by filtration and washed with water to give 4,4`-dimethoxybenzophenone oxime (**102**) as a colorless crystalline solid. The yield was quantitative.

Analysis:

Melting point: 132 – 133°C

^{1}H-NMR spectra (D_6-DMSO, 250MHz) δ [ppm]: 3.77 (s, 3H, OC<u>H</u>$_3$); 3.81 (s, 3H OC<u>H</u>$_3$); 6.91 - 7.34 (m, 8H, phenyl protons); 11.05 (s, 1H, NO<u>H</u>)

Mass spectra (FD): m/z: 257.2 (M^+) (only peak)

Elemental analysis: calculated: C: 70.02 %; N: 5.44 %; H: 5.88 %

found: C: 69.74 %; N: 5.52 %; H: 6.22 %

Step 2. Synthesis of 4,4`-dimethoxybenzhydrylamine (64)

Reduction of **102** in order to obtain 4,4`-dimethoxybenzhydrylamine (**64**) was realized using sodium in *iso*-propanol (Scheme 5.9).

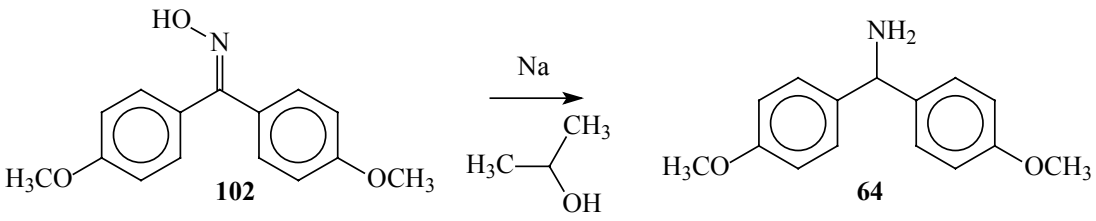

Scheme 5.9. Synthesis of 4,4`-dimethoxybenzhydrylamine (**64**).

In a dried (Section 6.1), one liter two-necked round-bottom flask equipped with magnetic stirrer bar, reflux condenser and removable septum 13.44 g (0.052 mol) of 4,4`-dimethoxybenzophenone oxime (**102)** were dissolved in 550 ml of *iso*-propanol (Riedel-de Haen) and the mixture was heated until boiling in an oil bath. Sodium (14 g, 0.609 mol) (Aldrich) was added as small pieces to the stirred solution. After addition of all the sodium, the reaction mixture was refluxed for 10 hours. The yellow solution was cooled down to room temperature and several small portions of water were added to the mixture and the *iso*-propanol removed under reduced pressure. The yellow oil obtained was separated from the water by extraction with diethyl ether; combined organic layers were washed several times with water and dried over anhydrous magnesium sulfate. HCl gas (Section 6.5) was then bubbled through the ether solution and resulting precipitate collected by filtration and washed with diethyl ether. The washed solid was then stirred with 500 ml of water and basified with sodium carbonate (Riedel-de Haen) until the pH exceeded 7. The slightly yellow oil was extracted with diethyl ether, and the extract was washed with water and dried over $MgSO_4$. The solvent was removed under reduced pressure to give 4,4`-dimethoxybenzhydrylamine (**64**) as a yellow amorphous solid. The yield was 65 %.

Analysis:

Melting point: 58 – 59°C

^{1}H-NMR spectra (CD_2Cl_2 (Deutero GmbH), 250MHz) δ [ppm]: 1.57 (broad s, 2H, $N\underline{H}_2$); 3.67 (s, 6H, $OC\underline{H}_3$); 5.03 (s, 1H, C<u>H</u>); 6.74 (d, J = 8.66 Hz, 4H, 3 & 5 phenyl protons); 7.19 (d, J = 8.66 Hz, 4H, 2 & 6 phenyl protons)

Mass spectra (FD): m/z: 243.0 (M^+) (only peak)

Elemental analysis: calculated: C: 74.05 %; N: 5.76 %; H: 7.04 %

found: C: 74.19 %; N: 5.63 %; H: 7.00 %

Step 3. Synthesis of 1,3–diphenyl-5,5-di(4-methoxyphenyl)-Δ^2-1,2,4-triazolin (103)

The third step was preparation of 1,3–diphenyl-5,5-di(4-methoxyphenyl)-Δ^2-1,2,4-triazolin (**103**) *via* cyclization, by a procedure similar to that described in Section 5.2 (Scheme 5.9).

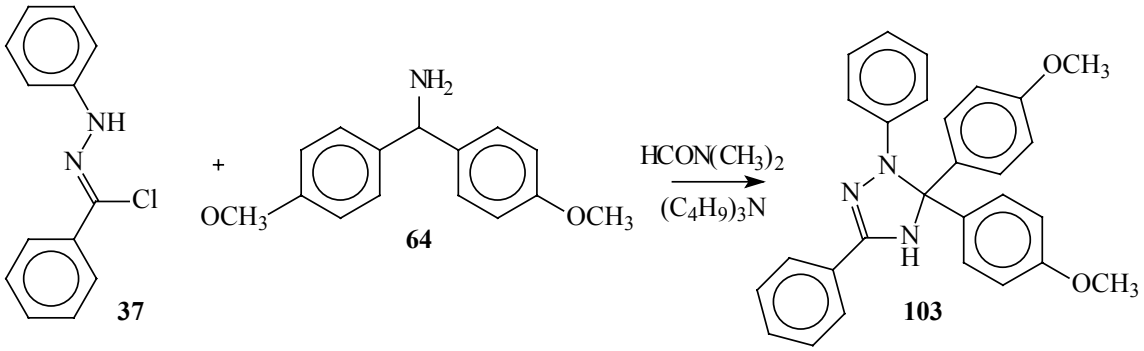

Scheme 5.9. Synthesis of 1,3–diphenyl-5,5-di-4-methoxyphenyl-Δ^2-1,2,4-triazolin (**103**).

In an one-necked 250 ml round-bottom flask equipped with a reflux condenser and magnetic stirrer bar, 4.54 g (0.019 mol) of 4,4`-dimethoxybenzhydrylamine (**64**), 4.3 g **(**0.019 mol) of N-phenylbenzenecarbohydrazonoyl chloride (**56**) and 4.77 ml (3.7 g, 0.02 mol) of tri-*n*-butylamine (Fluka) were mixed with 150 ml of DMF, and an argon atmosphere introduced. The reactor was put into an oil bath heated to 180°C and the mixture stirred at this temperature for 40 minutes. The resulting bright orange solution was cooled down to room temperature and **64** was isolated by a similar method as **39** (Section 5.2) to give a yellow-orange solid with 35 % yield.

Analysis:

Melting point: 145 – 146°C (may be lowered by presence of the corresponding radical)

^{1}H-NMR spectra (D_6-aceton (Deutero GmbH), 300MHz) δ [ppm]: 3.70 (s, 3H, OC<u>H</u>$_3$); 3.85 (s, 3H OC<u>H</u>$_3$); 6.72 – 7.57 (m, 18H, phenyl protons); 7.99 (s, 1H, N<u>H</u>).

Mass spectrum (FD): m/z: 435.3 (M^+) (only peak)

Elemental analysis: calculated: C: 77.22 %; N: 9.65 %; H: 5.79 %

found: C: 77.46 %; N: 9.52 %; H: 6.11 %

Step 3. Synthesis of 1,3–diphenyl-5,5-di(4-methoxyphenyl)-Δ^3-1,2,4-triazolin-2-yl (81)

Oxidation of **103** to the corresponding radical **81** (Scheme 5.10) was performed by a similar method to the step 2 described in Section 5.2. As in the case of **33**, oxidation could occur very easily and was observed during the processing of **103**.

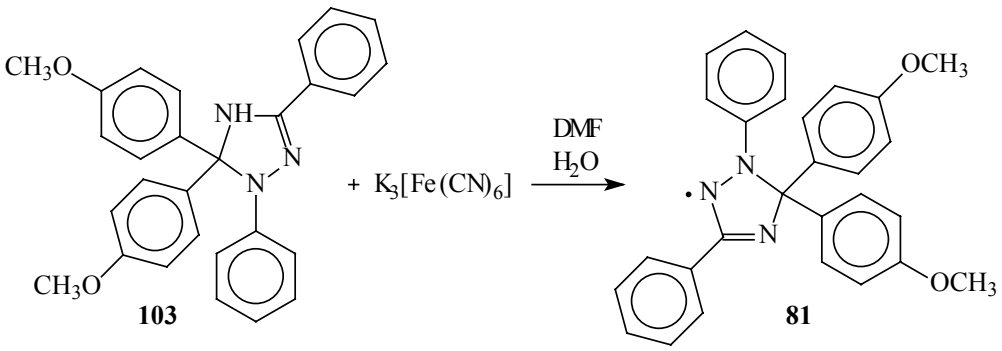

Scheme 5.10. Synthesis of 1,3–diphenyl-5,5-di(4-methoxyphenyl)-Δ^3-1,2,4-triazolin-2-yl (**81**).

1,3-Diphenyl-5,5-di-4(methoxyphenyl)-Δ^3-1,2,4-triazolin-2-yl (**81**) was obtained by treatment of 1.4 g (0.0032 mol) of 1,3-diphenyl-5,5-di-4(methoxyphenyl)-Δ^2-1,2,4-triazolin (**103**) in 50 ml of DMF with a solution of 1.59 g (0.0048 mol) of $K_3[Fe(CN)_6]$ and 0.25 g of Na_2CO_3 (0.0024 mol) in 24 ml of water at temperatures below – 10°C. **81** thus obtained was pure, but in the case of decomposition could be purified by column chromatography on silica gel 60 with a mixture of petroleum ether and dichloromethane as eluent. **81** was obtained as a black fine powder, forming solutions of a dark red-red color. The yield was 90 %.

Analyses:

Melting point: 130 – 131°C

Mass spectra (FD): m/z: 433.9 (M^+) (only peak)

Elemental analysis: calculated: C: 77.40 %; N: 9.67 %; H: 5.57%

found: C: 77.67 %; N: 9.56 %; H: 5.72 %

The UV-Vis spectrum at room temperature in dichloromethane is shown in Figure 5.2.

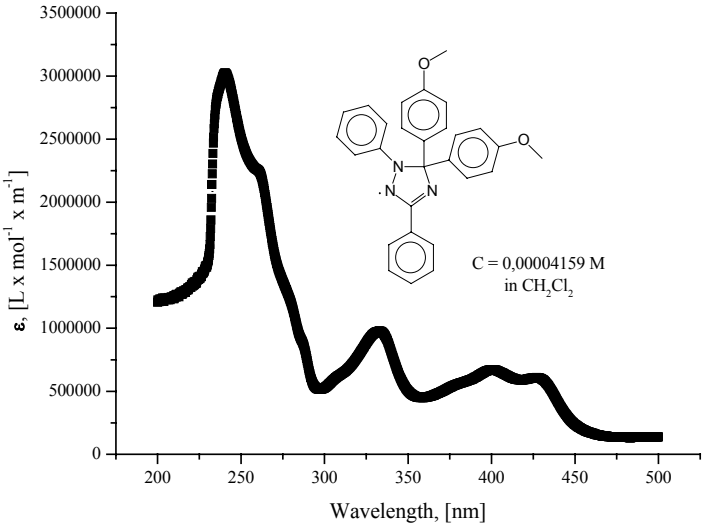

Figure 5.2. UV-Vis spectra of 1,3-diphenyl-5,5-di(4-methoxyphenyl)-Δ^3-1,2,4-triazolin-2-yl (**81**) in CH_2Cl_2.

5.4. Synthesis of 1,3–diphenyl-5,5-di(4-chlorophenyl)-Δ^3-1,2,4-triazolin-2-yl

The synthetic route developed for 1,3-diphenyl-5,5-di(4-methoxyphenyl)-Δ^3-1,2,4-triazolin-2-yl (**77**) was also used for synthesis of 1,3–diphenyl-5,5-di(4-chlorophenyl)-Δ^3-1,2,4-triazolin-2-yl (Scheme 5.11).

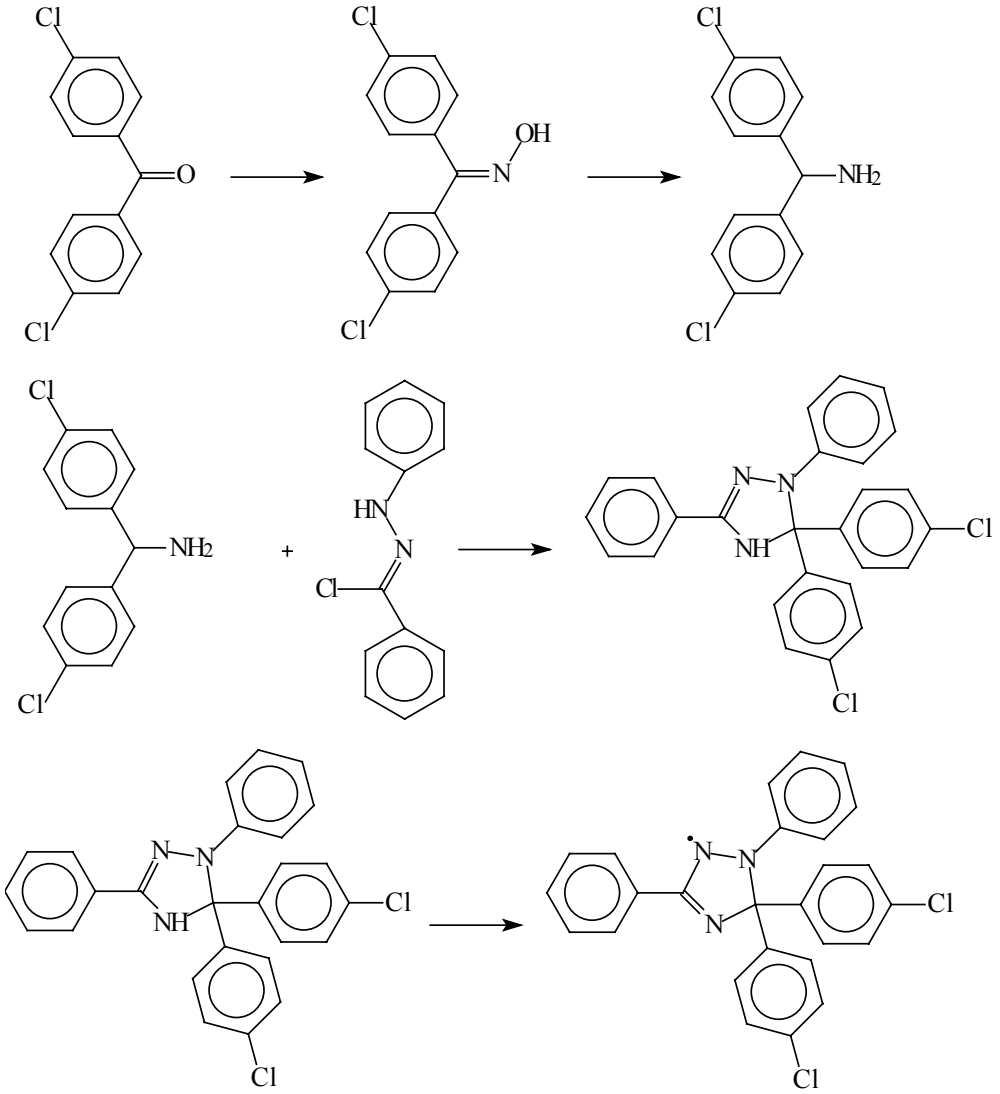

Scheme 5.11. Synthetic route to 1,3–diphenyl-5,5-di-4(chlorophenyl)-Δ^3-1,2,4-triazolin-2-yl.

Step 1. Synthesis of 4,4`-dichlorobenzophenone oxime (104)

The first step was preparation of 4,4`-dichlorobenzophenone oxime (**104**) from the 4,4`-dichlorobenzophenone (**61**) as shown in Scheme 5.12.

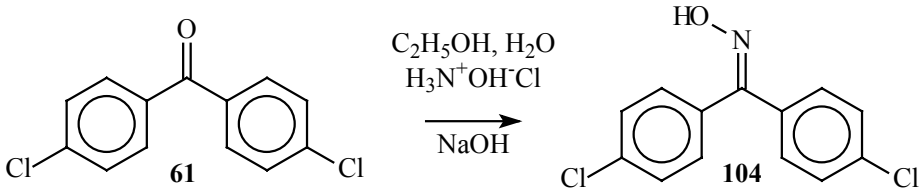

Scheme 5.12. Synthesis of 4,4`-dichlorobenzophenone oxime (**104**)

4,4`-Dichlorobenzophenone oxime (**104)** was obtained by a procedure similar to that described for **60**. In a 250 ml two-necked round-bottom flask, equipped with magnetic stirrer bar and reflux condenser, 12 g (0.048 mol) of 4,4`-dichlorobenzophenone, 6.9 g (0.1 mol) of hydroxylamine hydrochloride, 8 ml of water and 40 ml of ethanol were mixed. The flask was placed in an oil bath set at 100°C. Then 4.8 g (0.12 mol) of NaOH pellets was added in portions and the suspension refluxed for 3 hours. On completion of the reaction, the yellow solution was cooled down and poured into diluted hydrochloric acid. A colorless residue formed immediately. To complete the precipitation the solution was cooled down and the precipitate collected by filtration to give **104** as a colorless crystalline solid, which was purified by recrystallization from ethanol/water. The yield was 93 %.

Analysis:

Melting point: 135 – 136°C

^{1}H-NMR spectra (D_6-DMSO, 250 MHz) δ [ppm]: 7.33 - 7.58 (m, 8H, phenyl protons); 11.68 (s, 1H, NO<u>H</u>)

Mass spectra (FD): m/z: 265.2 (M^+) (only peak)

Elemental analysis: calculated: C: 58.67 %; N: 5.26 %; H: 3.41 %;

found: C: 58.63 %; N: 5.27 %; H: 3.47 %

Step 2. Synthesis of 4,4`-dichlorobenzhydrylamine (62)

Reduction of **104** to 4,4`-dichlorobenzhydrylamine (**62**) was carried out as shown in Scheme 5.13.

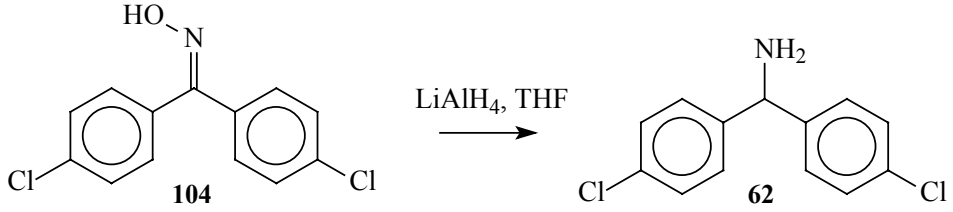

Scheme 5.13. Synthesis of 4,4`-dichlorobenzhydrylamine (**62**).

In a dry (Method 6.1) 500 ml three-necked round-bottom flask, equipped with magnetic stirrer bar 10.34 g (0.272 mol) of lithiumaluminiumhydride (Fluka) under continous flow of nitrogen was mixed with 100 ml of THF (Fluka). A solution of 13.64 g of **104** (0.051 mol) in 100 ml of THF was then added dropwise with a rate of addition such that the mixture was close to boiling, but did not boil. After addition of all the reagent, the flask was placed in an oil bath and refluxed for 14 hours. It was then cooled down and the excess of lithiumaluminiumhydride was destroyed by cautious addition of water. **62** was separated from aluminium hydroxide by repeated addition of diethyl ether and decantation. The combined organic layers were washed with brine and water. In order to remove non-basic impurities, the amine was converted into its hydrochloric salt as previously described for **55**, and, after washing of the salt by diethyl ether, converted back to the free amine form. **62** was isolated by column chromatography on silica gel 60 with dichloromethane as eluent as yellow crystals. The yield was 70 %.

Analysis:

Melting point: 59 – 60°C

^{1}H-NMR spectra (D_6-DMSO, 250 MHz) δ [ppm]: 2.41 (broad s, 2H, N<u>H</u>$_2$); 5.14 (s, 1H, C<u>H</u>); 7.38 (d, J = 8.61 Hz, 4H, 2 & 6 phenyl protons); 7.45 (d, J = 8.61 Hz, 4H, 3 & 5 phenyl protons)

Mass spectra (FD): m/z: 250.8 (M^+) (only peak)

Elemental analysis: calculated: C: 61.93 %; N: 5.56 %; H: 4.40 %

found: C: 62.22 %; N: 5.57 %; H: 4.57 %

Step 3. Synthesis of 1,3-diphenyl-5,5-di(4-chlorophenyl)-Δ^2-1,2,4-triazolin (105)

1,3-Diphenyl-5,5-di(4-chlorophenyl)-Δ^2-1,2,4-triazolin (**105**) was prepared by cyclization of **37** and **62** as shown in Scheme 5.14.

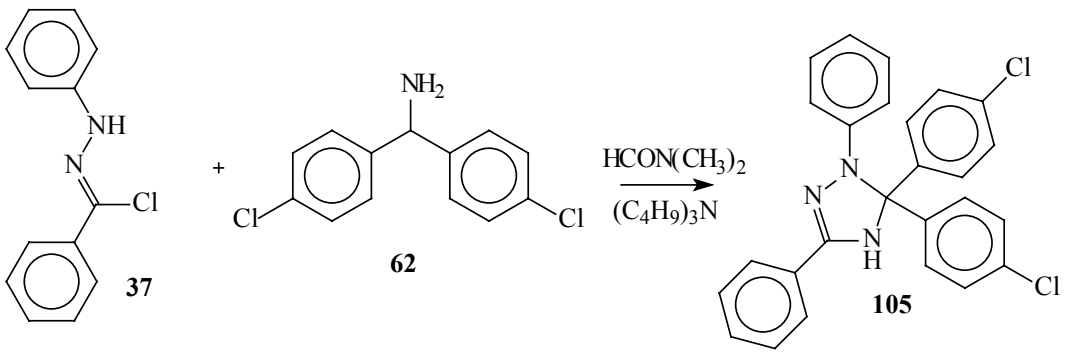

Scheme 5.14. Synthesis of 1,3-diphenyl-5,5-di(4-chlorophenyl)-Δ^2-1,2,4-triazolin (**105**).

1,3-Diphenyl-5,5-di(4-chlorophenyl)-Δ^2-1,2,4-triazolin (**105**) was obtained by a procedure similar to that described for **58** from 8.87 g (0.035 mol) of 4,4`-

dichlorobenzhydrylamine (**62**), 8.09 g (0.035 mol) of N-phenylbenzenecarbohydrazonoyl chloride (**37**) and 8.93 ml (6.94 g, 0.037 mol) of tri-*n*-butylamine in 105 ml of DMF. **105** was obtained as a yellow-orange solid and purified by column chromatography on silica gel 60 with a mixture of petroleum ether and dichloromethane as eluent. The yield was 38 %.

Analysis:

Melting point: 153 – 154°C (may be lowered by the presence of the corresponding radical)

^{1}H-NMR spectra (D_6-DMSO, 250 MHz) δ [ppm]: 6.59 - 7.88 (m, 18H, phenyl rings); 8.68 (s, 1H, N<u>H</u>)

Mass spectra (FD): m/z: 444.8 (M^+) (only peak)

Elemental analysis: calculated C: 70.28 %; N: 9.46 %; H: 4.31 %

found: C: 70.29 %; N: 9.35 %; H: 4.29 %

Step 4. Synthesis of 1,3-diphenyl-5,5-di(4-chlorophenyl)-Δ^3-1,2,4-triazolin-2-yl (77)

1,3-Diphenyl-5,5-di(4-chlorophenyl)-Δ^2-1,2,4-triazolin (**105**) was oxidized to yield the corresponding triazolinyl radical **77** as shown in Scheme 5.15.

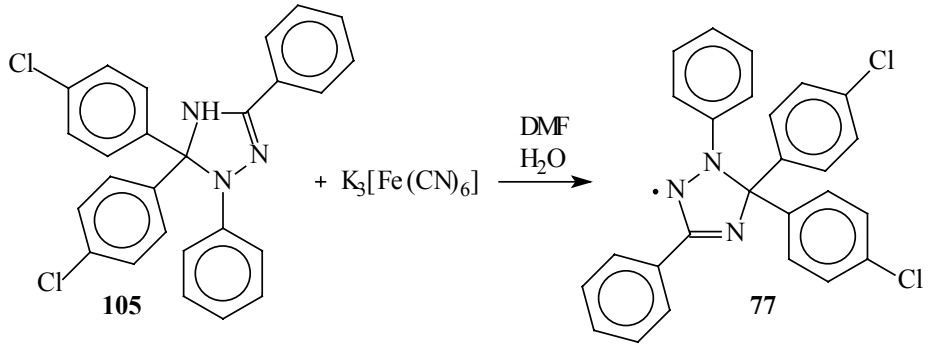

Scheme 5.15. Synthesis of 1,3-diphenyl-5,5-di(4-chlorophenyl)-Δ^3-1,2,4-triazolinyl (**77**)

66 (0.58 g, 0.0013 mol) was dissolved in 20 ml of DMF and poured into a 250 ml Erlenmeyer flask equipped with a magnetic stirrer bar. The solution was cooled down by placing the flask into acetone/dry ice bath. The triazolin **105** was oxidized to 1,3-diphenyl-5,5-di(4-chlorophenyl)-Δ^3-1,2,4-triazolin-2-yl (**77**) by dropwise addition of 10 ml water solution of $K_3[Fe(CN)_6]$ (0.7 g, 0.0021 mol) and Na_2CO_3 (0.1 g, 0.0009 mol) in a similar manner as described above for **81**. On completion of the reaction, the mixture was diluted with water. **77** was isolated by filtration as a fine black powder. The substance was pure without any further processing. The yield was 99 %.

Analysis:

Melting point: 134 – 135°C

Mass spectra: (FD) m/z: 442.8 (M^+) (only peak)

Elemental analysis: calculated: C: 70.44 %; N: 9.48 %; H: 4.09 %

found: C: 70.16 %; N: 9.41 %; H: 4.42 %

The UV-Vis spectrum at room temperature in dichloromethane is shown in Figure 5.3.

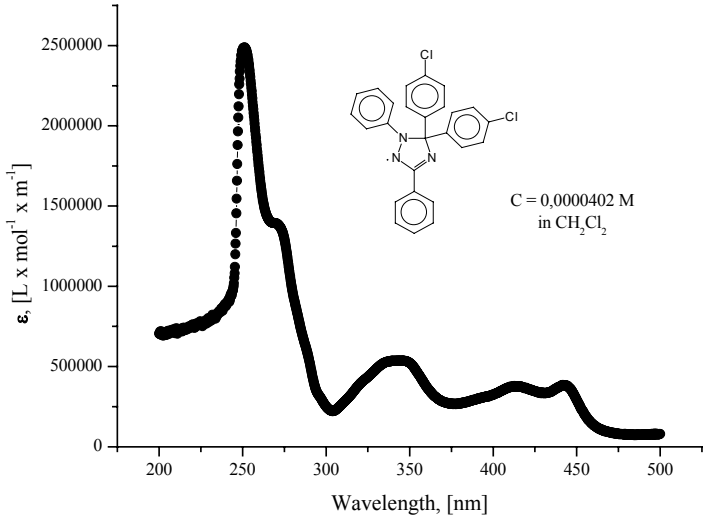

Figure 5.3. UV-Vis spectra of 1,3-diphenyl-5,5-di-4-chlorophenyl-Δ^3-1,2,4-triazolin-2-yl (**77**) in CH_2Cl_2.

5.5. Synthesis of 1,3-diphenyl-5,5-bis(4-dimethylaminophenyl)-Δ^3-1,2,4-triazolin-2-yl

1,3-Diphenyl-5,5-bis(4-dimethylaminophenyl)-Δ^3-1,2,4-triazolin-2-yl was synthesized *via* the synthetic route shown in Scheme 5.16.

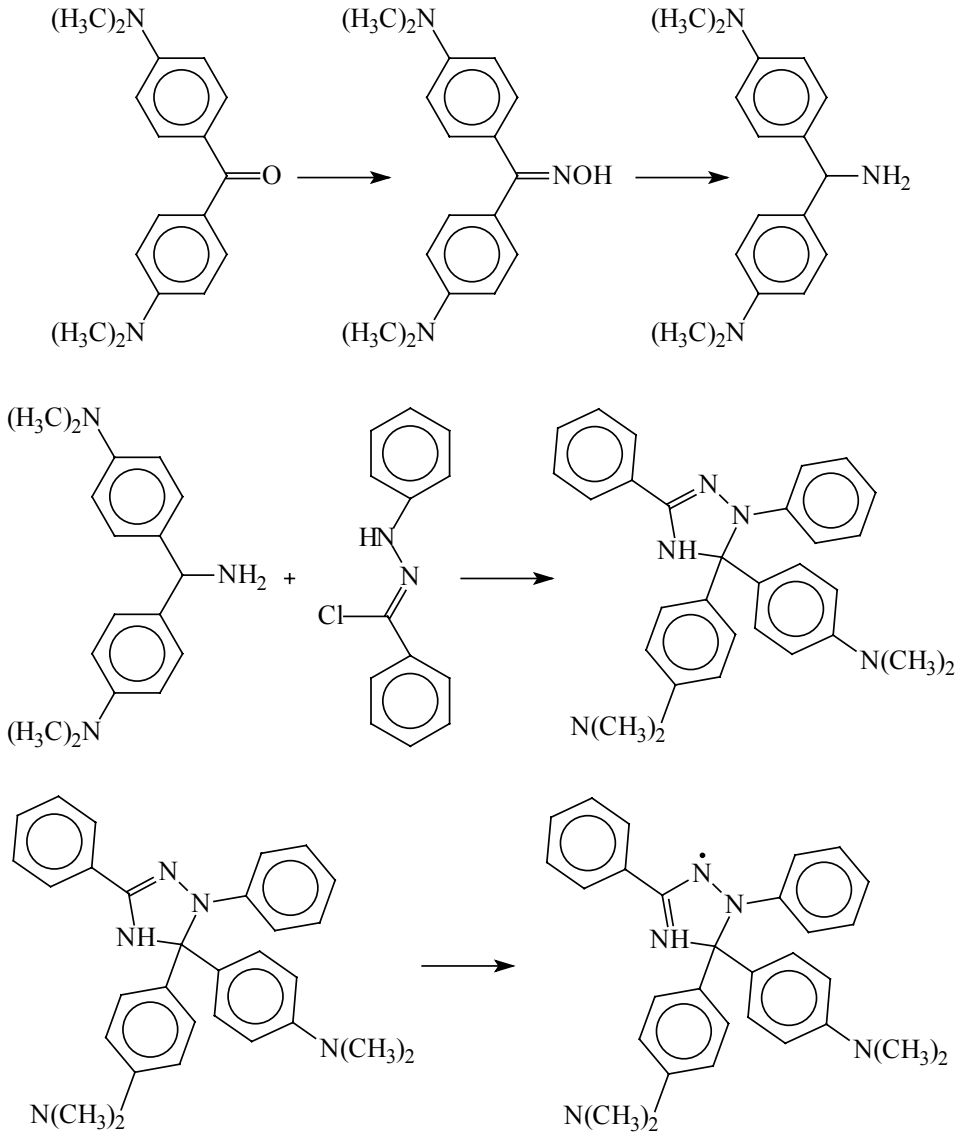

Scheme 5.16. Synthetic route to 1,3-diphenyl-5,5-bis(4-dimethylaminophenyl)-Δ^3-1,2,4-triazolin-2-yl.

Step 1. Synthesis of 4,4`-bis(dimethylamino)benzophenone oxime (107)

4,4`-Bis(dimethylamino)benzophenone oxime (**107**) was prepared using the standard procedure (Scheme 5.17).

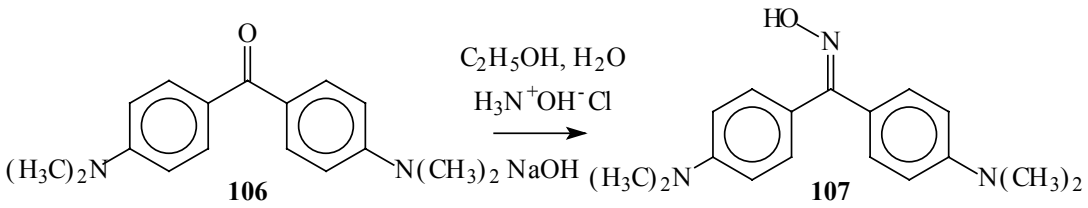

Scheme 5.17. Synthesis of 4,4`-bis(dimethylamino)benzophenone oxime (**107**).

4,4`-Bis(dimethylamino)benzophenone oxime (**107**) was obtained by treatment of 4.91 g (0.018 mol) of 4,4`-bis(dimethylamino)benzophenone (**106**) with 2.99 g (0.043 mol) of hydroxylamine hydrochloride and 2.11 g (0.053 mol) of NaOH pellets in a refluxing water (2.7 ml)/ethanol (13.3 ml) mixture for 15 hours. The procedure was similar to that used for the preparation of **102**. However, prolonged reaction time was needed in order to complete the reaction. **107** was purified by recrystallization from a water/ethanol mixture to give 4,4`-bis(dimethylamino)benzophenone oxime (**107**) as a colorless powder. The **107** rapidly turned a violet color in the presence of acids. The yield was 95%.

Analysis:

Melting point: 209 – 210°C

^{1}H-NMR spectra (D_6-DMSO, 250 MHz) δ [ppm]: 2.91 (s, 6H, $N(C\underline{H}_3)_2$); 2.94 (s, 6H, $N(C\underline{H}_3)_2$); 6.65 - 7.23 (m, 8H, phenyl protons); 10.64 (s, 1H, NO<u>H</u>)

Mass spectra (FD): m/z: 283.4 (M^+) (only peak)

Elemental analysis: calculated: C: 72.06 %; N: 14.83 %; H: 7.47 %

found: C: 71.87 %; N: 14.62 %; H: 7.54 %

Step 2. Synthesis of 4,4`-bis(dimethylamino)benzhydrylamine (108)

Reduction of **107** to 4,4`-bis(dimethylamino)benzhydrylamine **108** was realized according to Scheme 5.18.

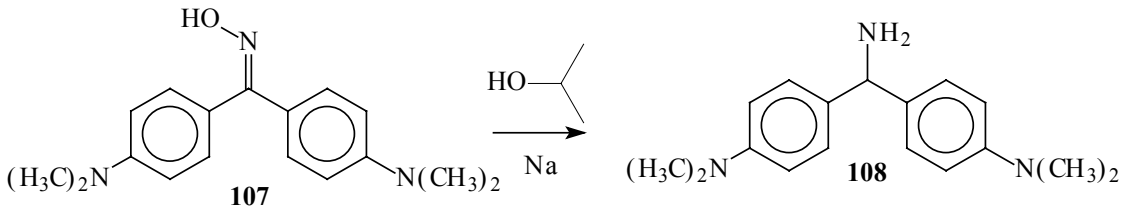

Scheme 5.18. Synthesis of 4,4`-bis(dimethylamino)benzhydrylamine (**108**).

The procedure was similar to the one used for the preparation of **64**. 15.63 g (0.055 mol) of 4,4`-bis(dimethyl)aminobenzophenone oxime (**107**) were dissolved in 600 ml of *iso*-propanol and 20 g (0.87 mol) of sodium were added in pieces to the refluxing solution. Afterwards, the

solution was allowed to reflux for 24 hours with constant stirring. At the end of the reaction the mixture was diluted with water and the *iso*-propanol was removed under reduced pressure. The 4,4`-bis(dimethylamino)benzhydrylamine (**108**) was collected by filtration and washed with water. The resulting **108** contained about 10 % of unreacted **107** (detected by mass spectroscopy), and in order to complete the reduction the whole procedure had to be repeated. Pure **108** was finally isolated as a colorless powder, which rapidly changed color to violet in the presence of acids. The yield was 83 %.

Analysis:

Melting point: 128 – 129°C

^{1}H-NMR spectra (D_6-DMSO, 250 MHz) δ [ppm]: 2.01 (broad s, 2H, $N\underline{H}_2$); 2.83 (s, 12H, $N(C\underline{H}_3)_2$); 4.89 (s, 1H, C<u>H</u>); 6.64, d, J = 8.69 Hz, 4H (3 & 5 phenyl protons); 7.16, d, J = 8.69 Hz; 4H (2 & 6 phenyl protons)

Mass spectra (FD): m/z: 269.2(M^+) (only peak)

Elemental analysis: calculated: C: 75.80 %; N: 15.60 %; H: 8.61 %

found: C: 75.70%; N: 15.52 %; H: 8.71 %

Step 3. Synthesis of 1,3-diphenyl-5,5-bis(4-dimethylaminophenyl)-Δ^2-1,2,4-triazolin (109)

1,3-Diphenyl-5,5-bis(4-dimethylaminophenyl)-Δ^2-1,2,4-triazolin (**109**) was obtained by cyclization of **37** and **108** (Scheme 5.19).

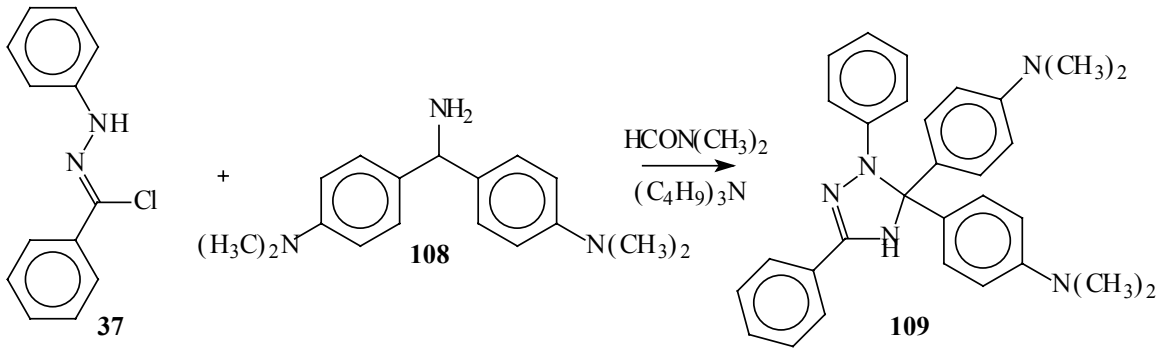

Scheme 5.19. Synthesis of 1,3-diphenyl-5,5-bis(4-dimethylaminophenyl)-Δ^2-1,2,4-triazolin (**109**).

1,3-Diphenyl-5,5-bis(4-dimethylaminophenyl)-Δ^2-1,2,4-triazolin **(109)** (30 %) was obtained by the same method as previously described for compound **103** from 1.54 g (0.0057 mol) of 4,4`-bis(dimethylamino)benzhydrylamine (**108)**, 8.09 g (0.0057 mol) of N-phenylbenzenecarbohydrazonoyl chloride (**37**) and 1.5 ml (1.17 g, 0.0063 mol) of tri-*n*-butylamine in 50 ml of DMF. On completion of the reaction, the mixture was cooled down to

room temperature and diluted with water. Sodium carbonate and sodium chloride (Riedel-de Haen) were added to the mixture and the crude product was extracted with a mixture of THF and diethyl ether. As the solubility of the product in pure diethyl ether is limited, it could not be used for the extraction. The combined organic layers were washed with brine and sodium carbonate solution and dried over magnesium sulfate. The resulting brown oil was purified by column chromatography on silica gel 60 with a mixture of petroleum ether, diethyl ether and triethylamine (Merck) as eluent. Recrystallization from diethyl ether gave **109,** as a yellow solid. The yield = 26 %.

Analysis:

Melting point: 209 – 210°C

^{1}H-NMR (300MHz, D_6-DMSO) δ [ppm]: 2.76 (s, 12H, N($C\underline{H}_3$)$_2$); (6.37 – 7.73, m, 18H, phenyl protons); 8.05 (s, 1H, N$\underline{H}$)

Mass spectra: (FD) m/z: 461.8 (M^+)

Elemental analysis: calculated: C: 78.06 %; N: 15.17 %; H: 6.77 %

found: C: 78.00 %; N: 15.20 %; H: 6.78 %

Step 3. Synthesis of 1,3-diphenyl-5,5-bis(4-dimethylaminophenyl)-Δ^3-1,2,4-triazolin-2-yl (82)

The standard procedure for the oxidation of triazolins to triazolinyls was used for conversion of **109** to **82** (Scheme 5.20).

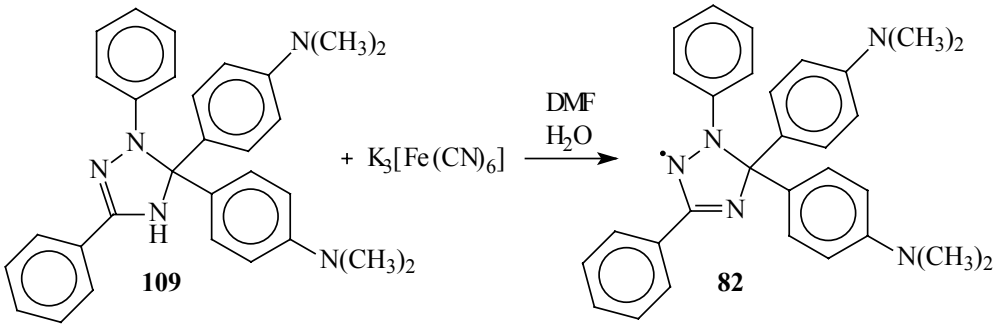

Scheme 5.20. Synthesis of 1,3-diphenyl-5,5-bis(4-dimethylaminophenyl)-Δ^3-1,2,4-triazolin-2-yl (**82**).

To a solution of 2.5 g (0.0054 mol) of **70** in 150 ml of DMF, solution of $K_3[Fe(CN)_6]$ (3 g, 0.009 mol) and Na_2CO_3 (0.45 g, 0.005 mol) in 30 ml of water was added dropwise keeping the temperature below – 10°C. On the completion of the reaction the solution was diluted with water and residue formed was collected by filtration to give the radical 1,3-diphenyl-5,5-bis(4-dimethylaminophenyl)-Δ^3-1,2,4-triazolin-2-yl (**82**) as a red-black fine powder. The yield = 94 %.

Analysis:

Melting point: 168 – 169°C

Mass spectra: (FD) m/z: 460.5 (M^+) (only peak)

Elemental analysis: calculated: 78.23 %; N: 15.20 %; H: 6.56 %

found: C: 78,06 %; N: 14.95 %; H: 6.91 %

UV-Vis spectrum at room temperature in dichloromethane is shown in Figure 5.4.

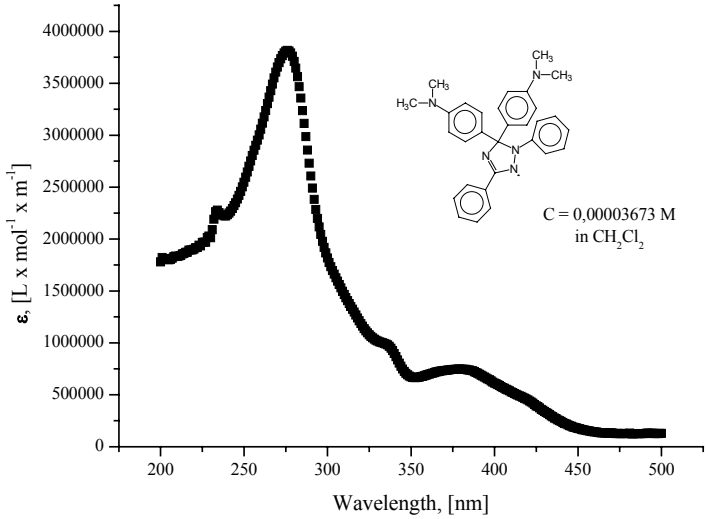

Figure 5.4. UV-Vis spectra of 1,3-diphenyl-5,5-bis(4-dimethylaminophenyl)-Δ^3-1,2,4-triazolin-2-yl (**82**) in CH_2Cl_2.

5.6. Synthesis of 1,3-diphenyl-5, 5-di(4-biphenyl)-Δ^3-1,2,4-triazolin-2-yl

The synthetic route to 1,3-diphenyl-5,5-di(4-biphenyl)-Δ^3-1,2,4-triazolin-2-yl is shown in Scheme 5.21.

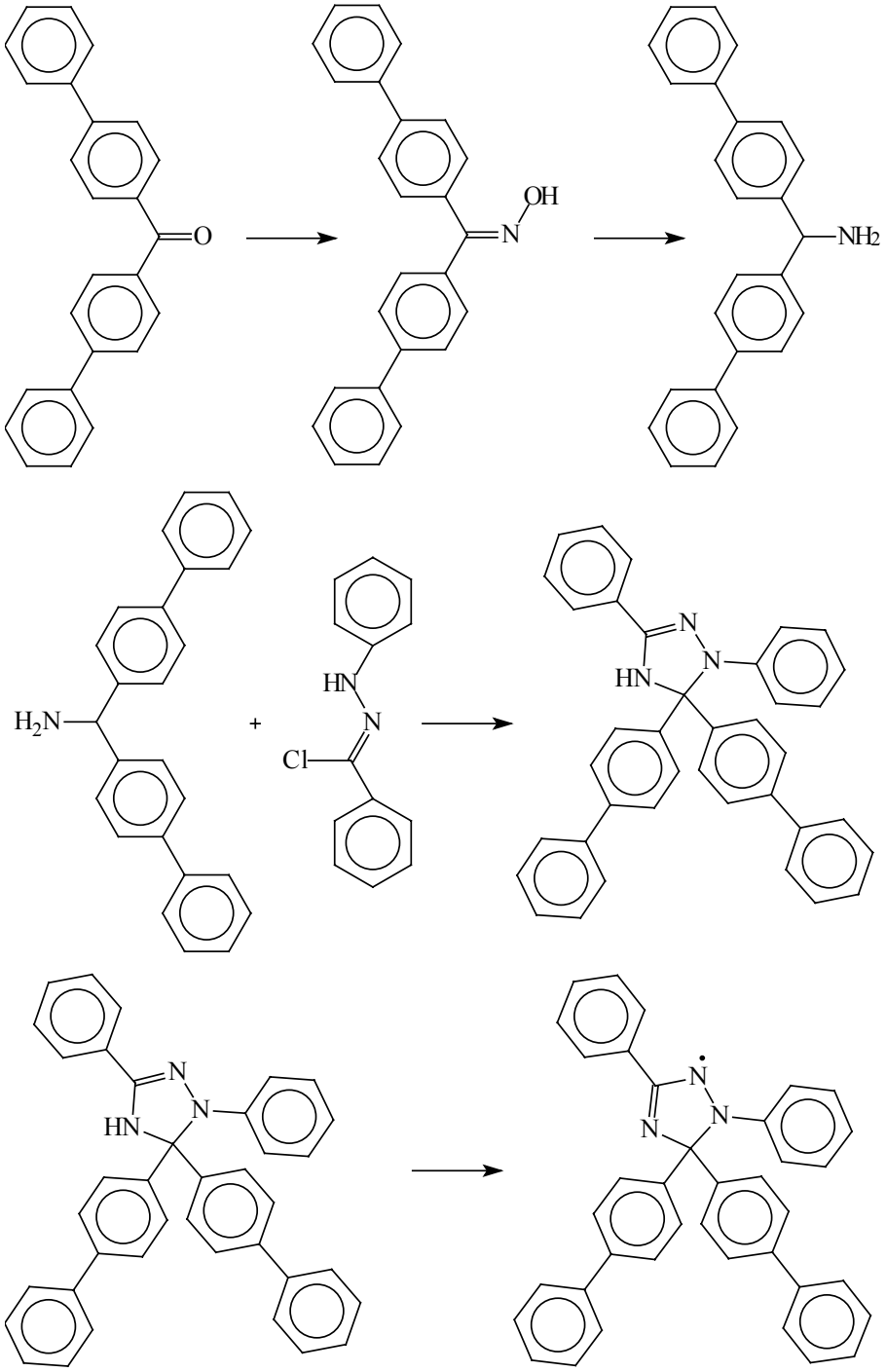

Scheme 5.21. Synthetic route to 1,3-diphenyl-5,5-di(4-biphenyl)-Δ^3-1,2,4-triazolin-2-yl.

Step 1. Synthesis of 4,4`-diphenylbenzophenone oxime (111)

In the first step 4,4`-diphenylbenzophenone oxime (**111**) was obtained *via* reaction shown in Scheme 5.22.

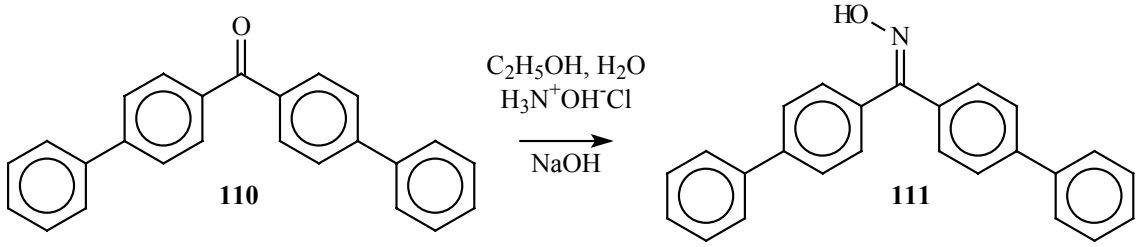

Scheme 5.22. Synthesis of 4,4`-diphenylbenzophenone oxime (**111**).

4,4`-Diphenylbenzophenone (**110**) (6.10 g, 0.018 mol) was twice treated with hydroxylamine hydrochloride (5.9 g, 0.085 mol)/NaOH (4.37 g, 0.109 mol) in ethanol (40 ml)/water (6 ml) media by a procedure similar to that previously used to obtain **102**. 4,4`-diphenylbenzophenone oxime (**111**) was isolated by precipitation from diluted hydrochloric acid and purified by column chromatography on silica gel 60 with dichloromethane, to give a colorless solid which is poorly soluble in most solvents. The yield was 60 %.

Analysis:

Melting point: 231 – 232°C

^{1}H-NMR spectra (D_8-THF (Cambridge Isotope Laboratories), 250 MHz) δ [ppm]: 7.31-7.86 (m, 18H, phenyl protons); 10.56 (s, 1H, NO<u>H</u>)

Mass spectra (FD): m/z = 349.0 (M^+) (only peak)

Elemental analysis: calculated: C: 85.92 %; N: 4.01 %; H: 5.48 %

found: C: 85.65 %; N: 3.80 %; H: 5.64 %

Step 2. Synthesis of 4,4`-diphenylbenzhydrylamine (112)

The reduction of the oxime **111** to 4,4`-diphenylbenzhydrylamine (**112**) was performed in a way similar to the synthesis of **64** (Scheme 5.23).

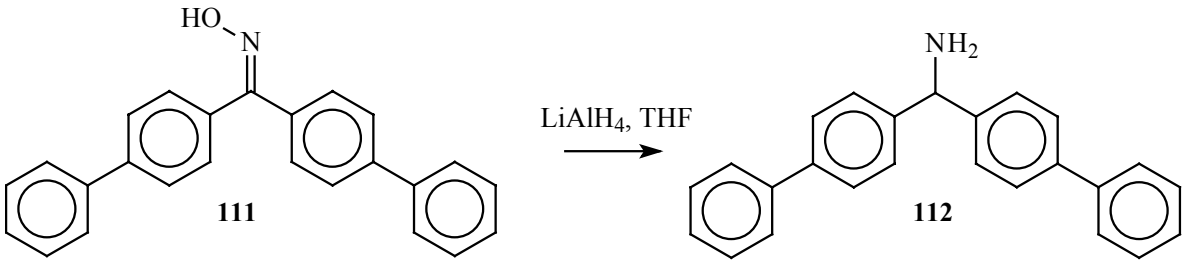

Scheme 5.23. Synthesis of 4,4`-diphenylbenzhydrylamine (**112**).

A three-necked round-bottom 1000 ml flask was dried according to Method 6.1. A magnetic stirrer bar, reflux condenser and dropping funnel were attached and a nitrogen atmosphere was introduced to the reaction vessel. A solution of 6.7 g (0.019 mol) of **111** in 450 ml of THF was added dropwise to stirred suspension of 5 g (0.132 mol) of lithiumaluminiumhydride in 150 ml of tetrahydrofuran. After addition of all the reagent, the reaction vessel was immersed in an oil bath, and the mixture was stirred under reflux over 24 hours. During the reaction, the mixture became a dark-blue in color. After cooling in an ice bath, the excess lithiumaluminiumhydride was destroyed with water. The product was separated from aluminium hydroxide *via* repeated decantation of a solution in THF/diethyl ether mixture. The organic layers were combined, washed with brine and dried over magnesium sulfate. The solvent was removed under reduced pressure and the resulting 4,4`-diphenylbenzhydrylamine (**112**) was purified by column chromatography on silica gel 60 with dichloromethane as eluent. **112** was isolated as a colorless powder in a yield of 45 %.

Analysis:

Melting point: 181 – 182°C

^{1}H-NMR spectra (CD_2Cl_2 (Deutero GmbH), 250 MHz) δ [ppm]: 1.67 (s, 2H, NH_2); 5.22 (s, 1H, CH, overlaps with signal from CD_2Cl_2, also observed in D_6-DMSO); 7.23- 7.50 (m, 18H, phenyl protons)

Mass spectra (FD): m/z: 335.1 (M^+) (only peak)

Elemental analysis: calculated: C: 89.51 %; N: 4.18 %; H: 6.31 %

found: C: 89.38 %; N: 4.15 %; H: 6.53 %

Step 3. Synthesis of 1,3-diphenyl-5,5-di(4-biphenyl)-Δ^3-1,2,4-triazolin-2-yl (84)

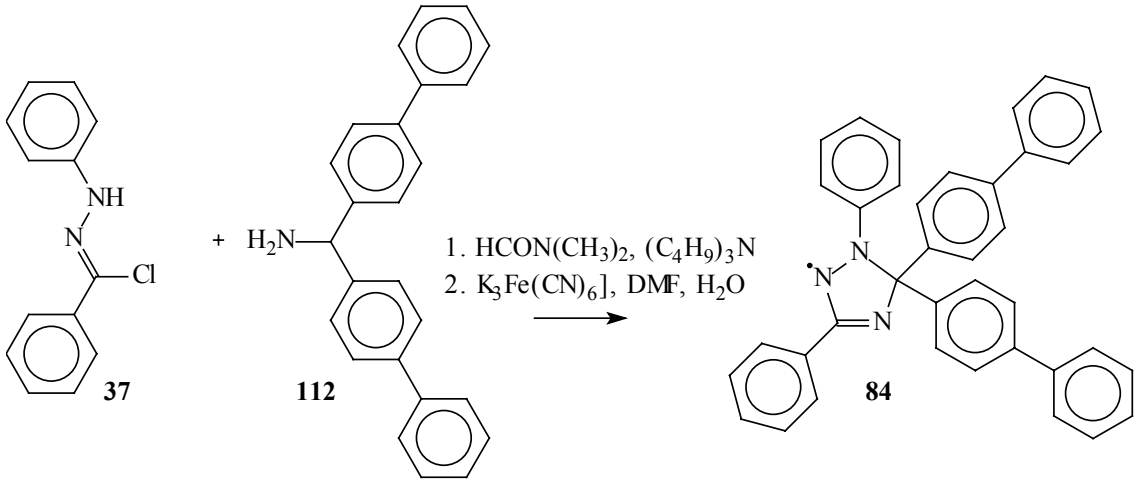

Scheme 5.24. Synthesis of 1,3-diphenyl-5,5-di(4-biphenyl)-Δ^3-1,2,4-triazolin-2-yl (**84**).

Preparation of 1,3-diphenyl-5,5-di(4-biphenyl)-Δ^3-1,2,4-triazolin-2-yl (**84**) was conducted without isolation of the intermediate triazolin, due to its continual decomposition during attempted purification. The reaction consequence is shown in Scheme 5.24.

1,3-Diphenyl-5,5-di(4-biphenyl)-Δ^2-1,2,4-triazolin was obtained from 4,4`-diphenylbenzhydrylamine (**112**) (6.23 g, 0.019 mol), N-phenylbenzenecarbohydrazonoyl chloride (**37**) (4.37 g, 0.019 mol) and tri-*n*-butylamine (11.21 ml, 8.7 g, 0.047 mol) in 120 ml of DMF, using a similar method to that described above for **103**. All attempts of purification failed due to decomposition during processing. Therefore, the crude product obtained by extraction with dichloromethane was dissolved in 100 ml of DMF and treated with an excess of $K_3[Fe(CN)_6]/Na_2CO_3$ (ratio of salts 3:1 by mass) water solution to form 1,3-diphenyl-5,5-di(4-biphenyl)-Δ^3-1,2,4-triazolin-2-yl (**84**), which was isolated by extraction with diethyl ether and purified by column chromatography on silica gel with petroleum ether/dichloromethane mixture as eluent, to give a black amorphous solid substance The yield was 6.7 % (calculated from the amine **112**).

Analysis:

Melting point: 131 – 133°C

Mass spectra (FD): m/z: 526.6 (M^+) (only peak)

Elemental analysis: calculated: C: 86.66 %; N: 7.98 %; H: 5.36 %

found: C: 86.80 %; N: 7.64 %; H: 5.58 %

UV-Vis spectrum at room temperature in dichloromethane is shown in Figure 5.5.

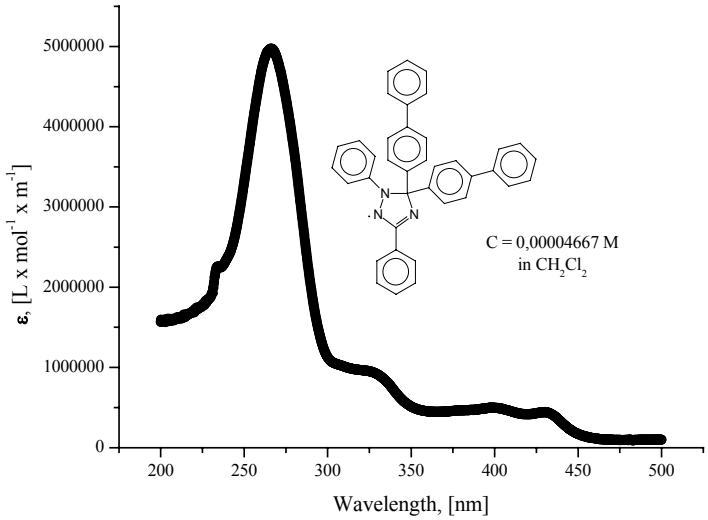

Figure 5.5. UV-Vis spectra of 1,3-diphenyl-5,5-di(4-biphenyl)-Δ^3-1,2,4-triazolin-2-yl (**84**) in CH_2Cl_2.

5.7. Synthesis of 1,3–diphenyl-5,5-di(4-fluorophenyl)-Δ^3-1,2,4-triazolin-2-yl

The synthesis of 1,3–diphenyl-5,5-di(4-fluorophenyl)-Δ^3-1,2,4-triazolin-2-yl is similar to the synthesis of **77** described above (Scheme 5.25).

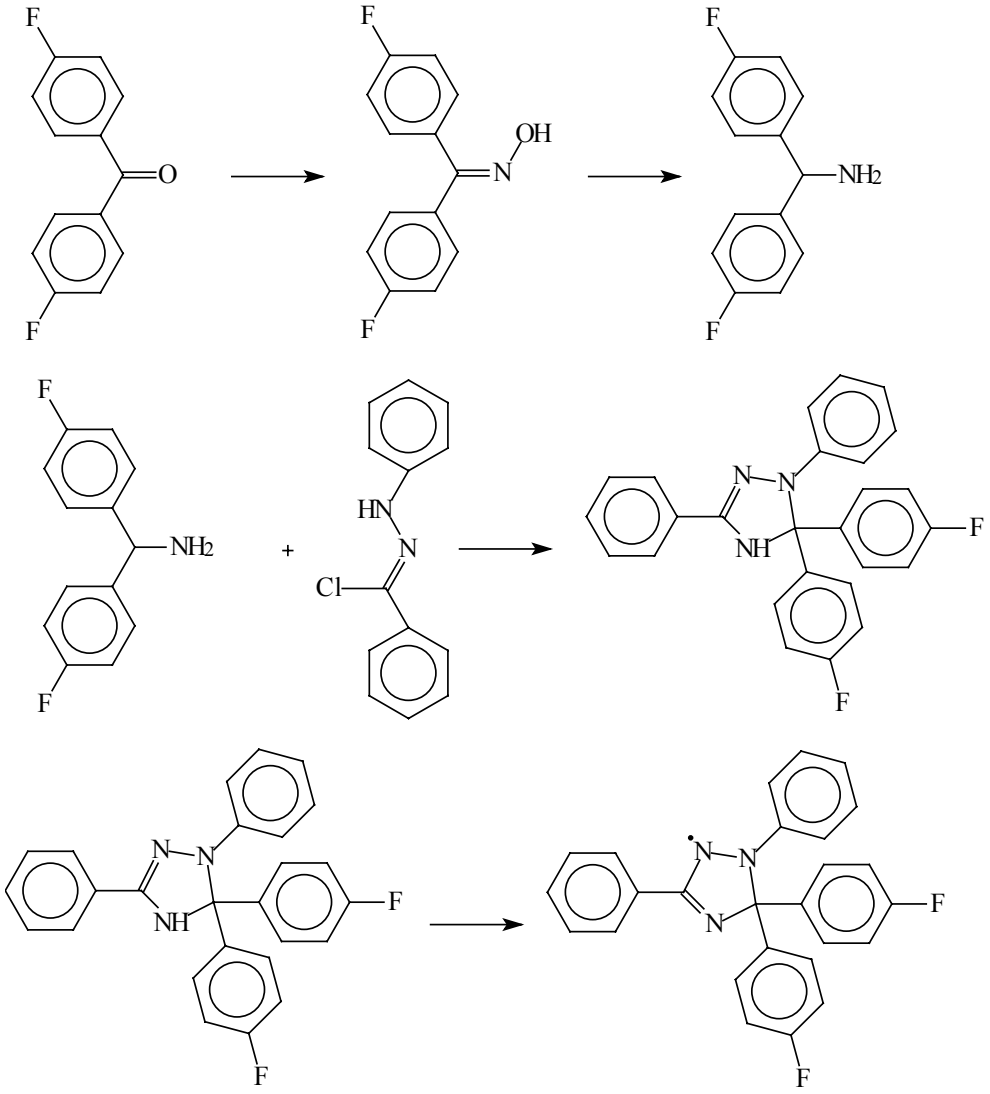

Scheme 5.25. Synthetic way to 1,3–diphenyl-5,5-di(4-fluorophenyl)-Δ^3-1,2,4-triazolin-2-yl.

Step 1. Synthesis of 4,4`-difluorobenzophenone oxime (114)

4,4`-Difluorobenzophenone oxime (**114)** was obtained as the product from the reaction of 4,4`-difluorobenzophenone (**113**) and hydroxylamine (Scheme 5.26).

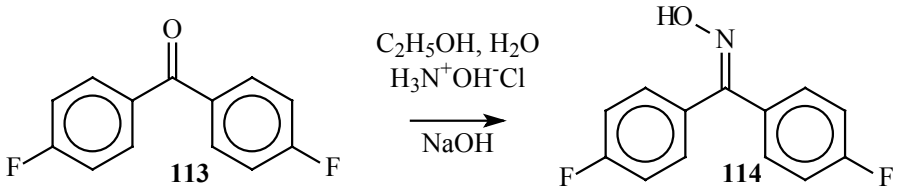

Scheme 5.26. Synthesis of 4,4`-difluorobenzophenone oxime (**114**).

4,4`-Difluorobenzophenone oxime (**114**) was prepared by a procedure similar to the one used for preparation of **102**. 2 g (0.0092 mol) of 4,4`-difluorobenzophenone (**113**), 0.56 g (0.014 mol) of sodium hydroxide and 1 g (0.014 mol) hydroxylamine hydrochloride were refluxed in a mixture of 8 ml ethanol and 2 ml water for 3 hours. The temperature was then lowered to 40°C and reaction was continued for a further 20 hours. The yellow solution obtained was poured into diluted hydrochloric acid. The precipitate was collected by filtration and washed with water. The crude **114** was purified by recrystallization from ethanol/water mixture to give a colorless crystalline powder. The yield was 90 %.

Analysis:

Melting point: 138 – 139°C

^{1}H-NMR spectra (D_6-DMSO, 250MHz) δ [ppm]: 11.51 (s, 1H, NOH); 7.20 - 7.51 (m, 8H, phenyl protons)

Mass spectra (FD): m/z: 233.1 (M^+) (only peak)

Elemental analysis: calculated: C: 66.95 %; N: 6.01 %; H: 3.89 %

found: C: 67.00 %; N: 5.83 %; H: 3.64 %

Step 2. Synthesis of 4,4`-difluorobenzhydrylamine (58)

4,4`-Difluorobenzhydrylamine **(58)** was obtained by a procedure similar to the synthesis of **62** (Scheme 5.27).

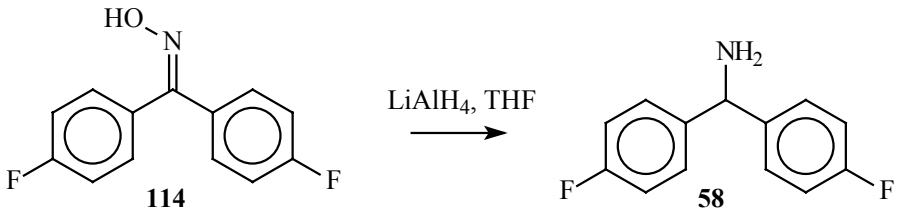

Scheme 5.27. Synthesis of 4,4`-difluorobenzhydrylamine (**58**).

10 g (0.043 mol) of **114** were dissolved in 100 ml of THF and the solution was added dropwise to a stirred suspension of 7 g (0.2 mol) of lithiumaluminiumhydride in 200 ml of THF. After addition of all the oxime, the mixture was refluxed for 20 hours. The excess of lithiumaluminiumhydride was then destroyed with water and the amine **58** was isolated by

decantation of an ether solution from an aqueous suspension of aluminium hydroxide. The amine was transformed to its hydrochloric salt, washed with diethyl ether and converted back to the free base form. **58** was isolated as a slightly yellow oily liquid after purification by column chromatography on silica gel 60 with dichloromethane as eluent. The yield was 86 %.

Analysis:

Melting point: oily liquid at room temperature.

^{1}H-NMR spectra (250MHz, D_6-DMSO) δ [ppm]: 7.40 - 7.46 (m, 4H, phenyl protons 2&6); 7.08 - 7.15 (m, 4H, phenyl protons 3&5); 5.13 (s, 1H, C<u>H</u>), 2.29 (s, 2H, N<u>H</u>$_2$)

Mass spectra (FD): m/z: 218.8 (M+) (only peak)

Elemental analysis: calculated: C: 71.22 %; N: 6.39 %; H: 5.06 %

found: C: C: 71.01 %; N: 6.63 %; H: 5.04 %

Step 3. Synthesis of 1,3–diphenyl-5,5-di(4-fluorophenyl)-Δ^2-1,2,4-triazolin (115)

1,3–Diphenyl-5,5-di(4-fluorophenyl)-Δ^2-1,2,4-triazolin (**115**) was obtained by the usual triazolin synthesis procedure (Scheme 5.28).

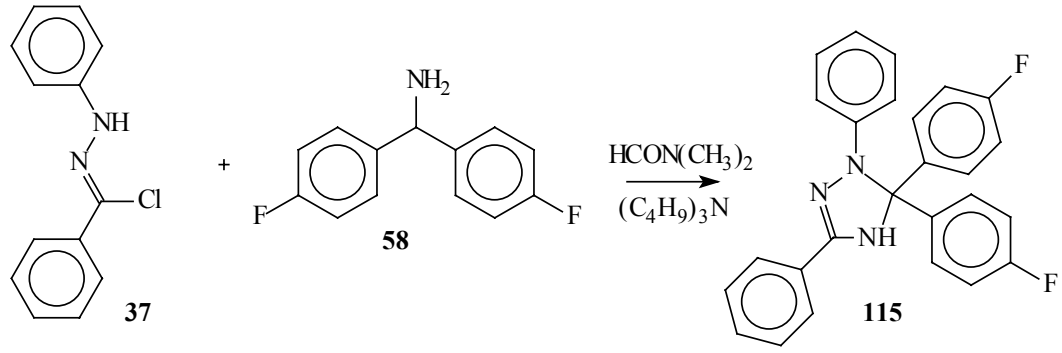

Scheme 5.28. Synthesis of 1,3–diphenyl-5,5-di(4-fluorophenyl)-Δ^2-1,2,4-triazolin (**115**).

8.75 g (0.04 mol) of **58**, 9.2 g (0.04 mol) of **37** and 9.5 ml (7.5 g, 0.04 mol) of tri-*n*-butylamine were dissolved in 150 ml of DMF and the solution was heated to 180°C in an oil bath. After 1 hour, the mixture was cooled and diluted with an excess of water. Extraction by diethyl ether and subsequent evaporation of solvent gave an orange oil, which was purified by column chromatography on silica gel 60 with dichloromethane/petroleum ether mixture as eluent. 1,3–Diphenyl-5,5-di(4-fluorophenyl)-Δ^2-1,2,4-triazolin (**115**) was isolated as a yellow solid. The yield = 24 %.

Analysis:

Melting point: 139 – 140°C

^{1}H-NMR spectra (D_6-DMSO, 250MHz) δ [ppm]: 6.56-7.89 (m, 18H, phenyl protons); 8.64 (s, 1H, N<u>H</u>)

Mass spectra (FD): m/z: 411.4 (M^+) (only peak)

Elemental analysis: calculated: C: 75.9 %; H: 4.7 %; N: 10.2 %

found: C: 75.8 %; H: 5.0 %; N: 10.5 %

Step 4. Synthesis of 1,3-diphenyl-5,5-di(4-fluorophenyl)-Δ^3-1,2,4-triazolin-2-yl (78)

The fourth step of the synthesis was the oxidation of the triazolin **115** to the corresponding radical **78** (Scheme 5.29) by a standard procedure.

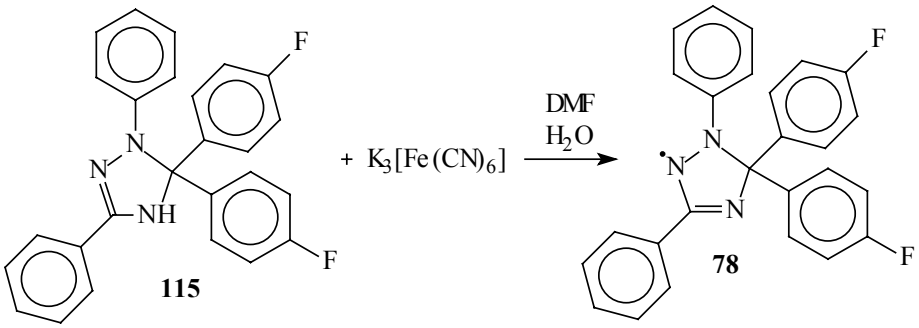

Scheme 5.29. Synthesis of 1,3-diphenyl-5,5-di(4-fluorophenyl)-Δ^3-1,2,4-triazolin-2-yl (**78**).

In a 250 ml Erlenmeyer flask 1 g (0.0024 mol) of **115** was dissolved in 100 ml of DMF and cooled down in a dry ice/acetone bath. A solution of 2 g (0.0061 mol) of potassium hexacyanoferrate (III) and 1 g (0.012 mol) of sodium carbonate in 20 ml of water was added dropwise to the stirred mixture, and the mixture stirred at temperatures below – 10°C for 4 hours. An excess of water was added to the mixture and the radical **78** was collected by filtration as black fine powder. **78** was purified by column chromatography on silica gel 60 with petroleum ether/dichloromethane mixture as eluent. The yield was 95 %.

Analysis:

Melting point: 128 – 129°C

Mass spectra (FD): m/z: 410.2 (M^+) (only peak)

Elemental analysis: calculated: C: 76.1%; H: 4.4%; N: 10.2%

found: C: 75.7 %; H: 4.7 %; N: 10.5 %

UV-Vis spectrum at room temperature in dichloromethane is shown in Figure 5.6.

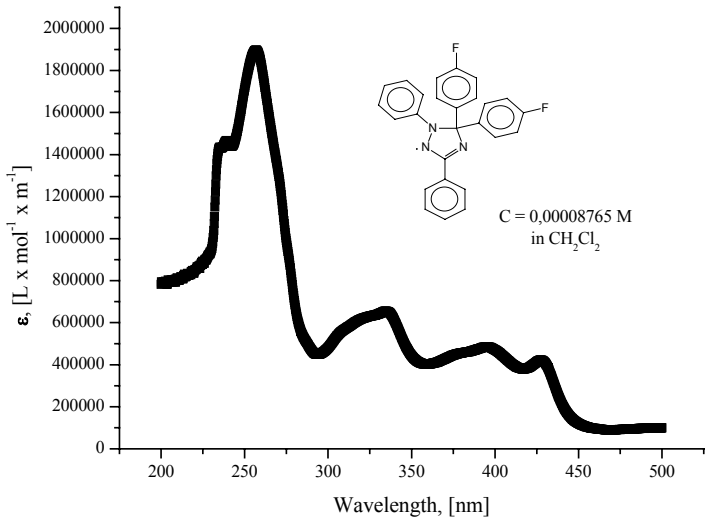

Figure 5.6. UV-Vis spectra of 1,3-diphenyl-5,5-di(4-fluorophenyl)-Δ^3-1,2,4-triazolin-2-yl (**78**) in CH_2Cl_2.

5.8. Syntheses of 1,3–diphenyl-5,5-di(4-bromophenyl)-Δ^3-1,2,4-triazolin-2-yl and 1,3,5–triphenyl-5-(4-bromophenyl)-Δ^3-1,2,4-triazolin-2-yl

1,3–Diphenyl-5,5-di(4-bromophenyl)-Δ^3-1,2,4-triazolin-2-yl and 1,3,5–triphenyl-5-(4-bromophenyl)-Δ^3-1,2,4-triazolin-2-yl were synthesized in the same experiment. Bromine cleavage was observed during the synthesis, which permitted the simultaneous preparation of both derivatives and their subsequent separation. The general synthetic route was the same as for triazolinyls described above (Scheme 5.30).

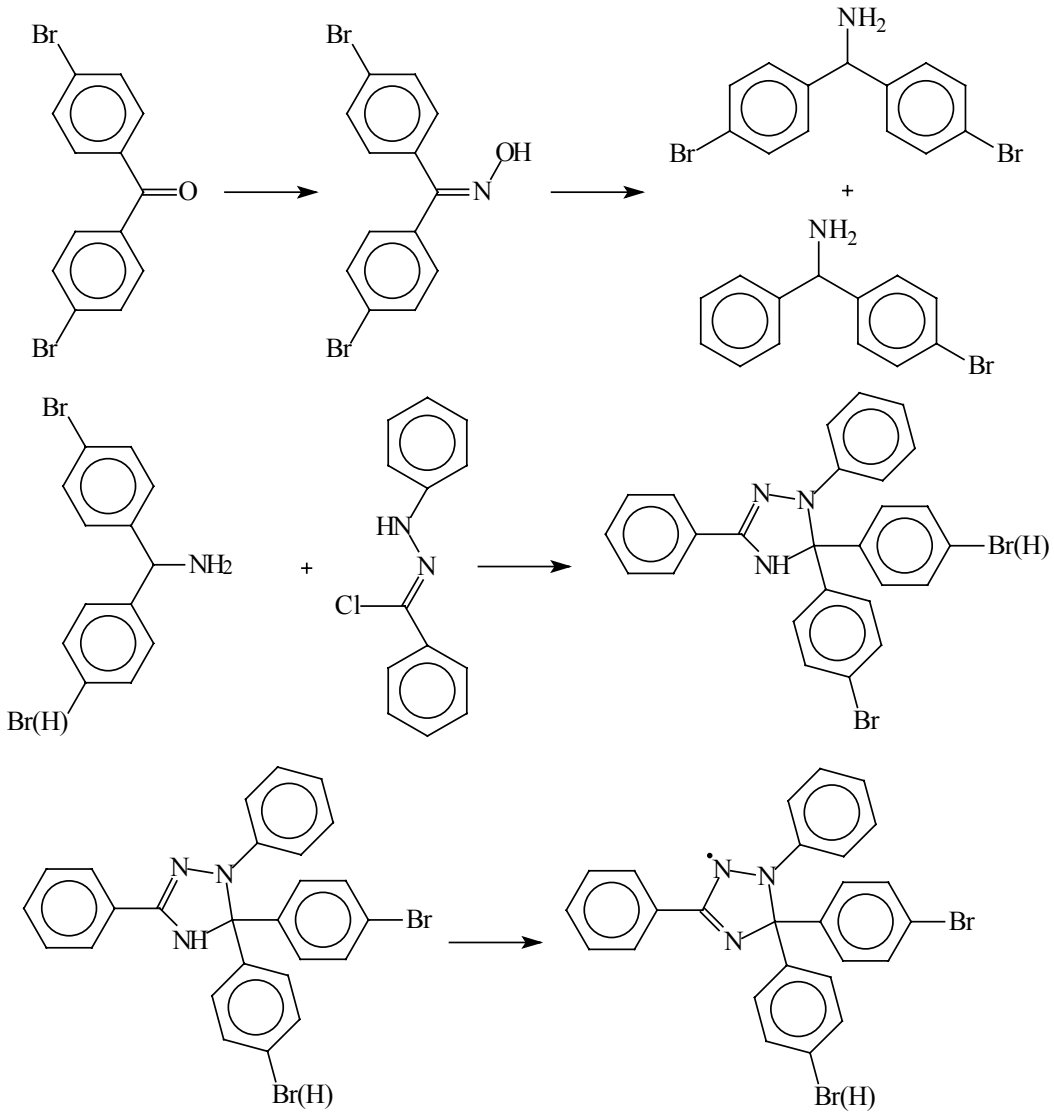

Scheme 5.30. Synthetic route to 1,3–diphenyl-5,5-di(4-bromophenyl)-Δ^3-1,2,4-triazolin-2-yl and 1,3,5–triphenyl-5-(4-bromophenyl)-Δ^3-1,2,4-triazolin-2-yl.

Step 1. Synthesis of 4,4`-dibromobenzophenone oxime (116)

4,4`-dibromobenzophenone (**72**) was converted to 4,4'-dibromobenzophenone oxime (**116**) using hydroxylamine (Scheme 5.31).

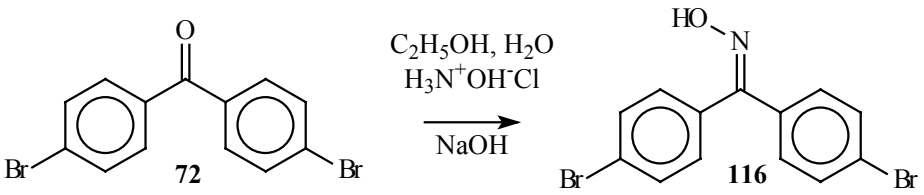

Scheme 5.31. Synthesis of 4,4`-dibromobenzophenone oxime (**116**).

In a 250 ml round-bottom two-necked flask 13.6 g (0.04 mol) of 4,4´-dibromobenzophenone (**77**), 6.8 g (0.098 mol) of hydroxylamine hydrochloride were mixed in ethanol (40 ml)/water (8 ml). A reflux condenser and magnetic stirrer bar were attached and the reaction vessel was immersed in an oil bath. 5 g (0.125 mol) of sodium hydroxide pellets was added by portions to the stirred suspension. The temperature was raised and the suspension was refluxed over a period of 5 hours. The resulting solution was poured into dilute hydrochloric acid. The precipitate was collected by filtration and washed with of water. The crude **116** was purified by recrystallization from water/ethanol mixture. The yield was 98 %.

Analysis:

Melting point: 153 – 154°C

^{1}H-NMR spectra (D_6-DMSO, 250MHz) δ [ppm]: 7.25-7.70 (m, 8H, phenyl protons); 11.65 (s, 1H, NO<u>H</u>).

Mass spectra (FD): m/z: 354.8 (M^+) (only peak)

Elemental analysis: calculated: C: 43.98 %; N: 3.95 %; H: 2.56 %

found: C: 43.91 %; N: 3.64 %; H: 2.07 %

Step 2. Syntheses of 1,3–diphenyl-5,5-di(4-bromophenyl)-Δ^2-1,2,4-triazolin (119) and 1,3,5–triphenyl-5-(4-bromophenyl)-Δ^2-1,2,4-triazolin (120)

The reduction of the oxime **116** gave 4,4`-dibromobenzhydrylamine (**117**), which however, lost bromine continuously during purification, drying and other processing. Hence, the isolation of this compound was not achieved. Mixture of amines **117**, **118** and **38** was used as the reagent in the following cyclization stage. The synthetic route is given in Scheme 5.32.

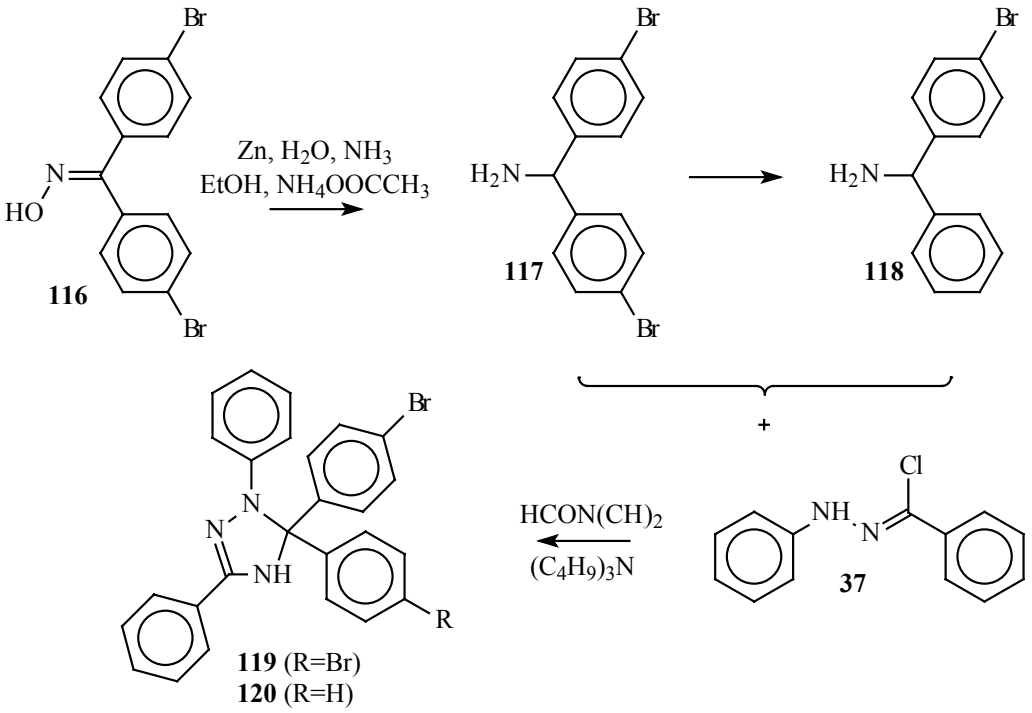

Scheme 5.32. Syntheses of 1,3–diphenyl-5,5-di-4(bromophenyl)-Δ^2-1,2,4-triazolin (**119**) and 1,3,5–triphenyl-5-(4-bromophenyl)-Δ^2-1,2,4-triazolin (**120**).

In a 250 two-necked round-bottom flask equipped with a reflux condenser and a magnetic stirrer bar 1 g (0.0028mol) of **116**, 0.37 g (0.0048 mol) of ammonium acetate (Aldrich) were dissolved in a mixture of 16 ml of ammonia solution (25 %) (Riedel-de Haen), 12 ml of water and 30 ml of ethanol. The mixture was heated until boiling and 0.8 g (0.12 mol) of Zn powder (Merck) were added by portions.[212] After addition of all the Zn, the mixture was stirred under reflux for 5 hours. Then the suspension was cooled down, diluted with water and ammonia solution until formed zinc hydroxide had completely dissolved. Unreacted zinc was removed by filtration and **117** was extracted with diethyl ether. The combined ether portions were washed several times with brine and water and dried over magnesium sulfate. The solvent was then removed under reduced pressure. During drying cleavage of Br was observed leading to formation of **118** and **38**. Due to the failure of all attempts of further purification, a mixture of the three amines was used in the next stage.

In a 250 ml one-necked round-bottom flask equipped with reflux condenser and magnetic stirrer bar 0.57 g of the mixture of amines, 0.4 g (0.0022 mol, 0.5 ml) of tri-*n*-butylamine and 0.386 g (0.0017 mol) of **37** were dissolved in 70 ml of DMF. Argon atmosphere was mounted and flask was put in oil bath heated to 80°C, and the mixture was stirred for 14 hours. The cooled mixture was diluted with water and the products were extracted with diethyl ether. The organic layers were collected, washed with brine and water and dried over magnesium sulfate. The resulting mixture of triazolins was separated from other impurities by column chromatography

on silica gel 60 with dichloromethane/petroleum ether mixture as eluent. Afterwards the triazolins were separated by column chromatography on silica gel 60 with toluene (Fisher)/petroleum ether mixture as eluent. Isolated **119** contained about 5 % of **120**. Isolated **120** contained about 8 % of **119** and 8 % of **39**. The joint yield of both triazolins calculated from oxime used was 15 %.

*Analysis: (**119**)*

Melting point was not measured, since the substance contains a noticeable amount of **120**

^{1}H-NMR spectra (D_6-DMSO, 250MHz) δ [ppm]: 8.52 (s, 1H, NH); 6.46 - 7.74 (m, 18H, phenyl protons)

Mass spectra (FD): m/z: 533.3 (M^+) (100 %); 453.3 (M^+) (**120**) (5 %)

Elemental analysis: calculated: C: 58.56 %; N: 7.88 %; H: 3.59 %

found: C: 59.11 %; N: 6.98 %; H: 3.78 %

*Analysis: (**120**)*

Melting point was not measured, due to the presence of **119** and **33**

^{1}H-NMR spectra (D_6-DMSO, 250MHz) δ [ppm]: 8.44 (s, 1H, NH); 6.38 - 7.70 (m, 19H, phenyl protons)

Mass spectra (FD): m/z: 455.3 (M^+) (100%), 375.3 (M^+) (**39**) (10 %); 533.3 (M^+) (**119**) (10 %)

Elemental analysis: calculated: C: 68.73 %; N: 9.25 %; H: 4.44 %

found: C: 68.81 %; N: 8.72 %; H: 5.08 %

Step 3a. Synthesis of 1,3-diphenyl-5,5-di(4-bromophenyl)-Δ^3-1,2,4-triazolin-2-yl (79)

Oxidation of 1,3–diphenyl-5,5-di(4-bromophenyl)-Δ^2-1,2,4-triazolin (**119**) to the corresponding radical **79** was performed by a standard procedure (Scheme 5.33).

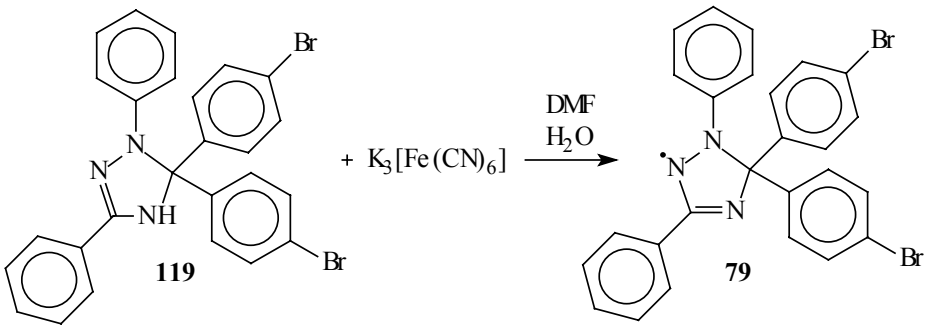

Scheme 5.33. Synthesis of 1,3-diphenyl-5,5-di(4-bromophenyl)-Δ^3-1,2,4-triazolin-2-yl (**79**).

[212] Caution: addition of first portion can cause extremely vigorous boiling.

In a 250 ml Erlenmeyer flask, 1 g (0.0019 mol) of **119** was dissolved in 50 ml of DMF and the solution was cooled down in a dry ice/acetone bath. A solution of 2 g (0.0061 mol) of potassium hexacyanoferrate (III) and 0.35 g (0.0033 mol) of sodium carbonate in 15 ml of water was added dropwise and the mixture stirred at temperature below – 10°C for 4 hours. The solution was diluted with an excess of water and the resulting precipitate collected by filtration and washed with water. 1,3-Diphenyl-5,5-di(4-bromophenyl)-Δ^3-1,2,4-triazolin-2-yl (**79**) containing about 5 % of **80** was obtained free of other impurities without further processing as a very dark red fine powder. The yield was 99 %.

Analyses:

Melting point was not measured, since the substance contains about 5 % of **80**

Mass spectra (FD): m/z: 532.2 (M^+) (only peak)

Elemental analysis: calculated: C: 58.67 %; N: 7.89 %; H: 3.41 %

found: C: 59.17 %; N: 7.17 %; H: 3.93 %

UV-Vis spectrum at room temperature in dichloromethane is given in Figure 5.7.

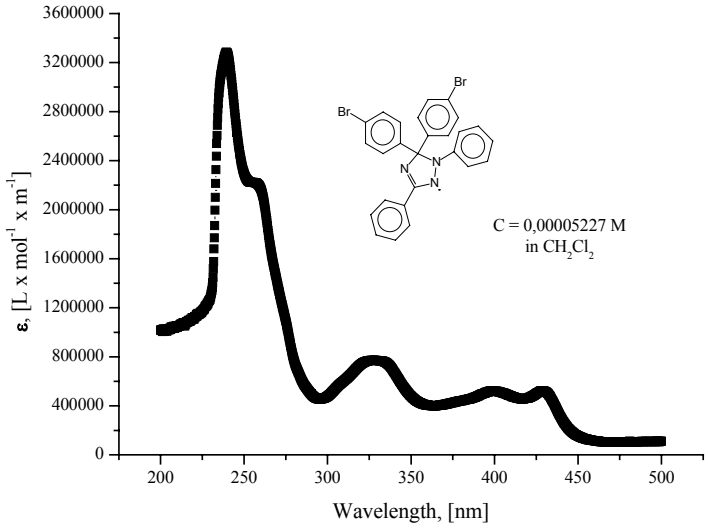

Figure 5.7. UV-Vis spectrum of 1,3-diphenyl-5,5-di(4-bromophenyl)-Δ^3-1,2,4-triazolin-2-yl (**79**) in CH_2Cl_2.

Step 3b. Synthesis of 1,3,5-triphenyl-5-(4-bromo phenyl)-Δ^3-1,2,4-triazolin-2-yl (80)

The standard oxidation procedure was used also in this case (Scheme 5.34).

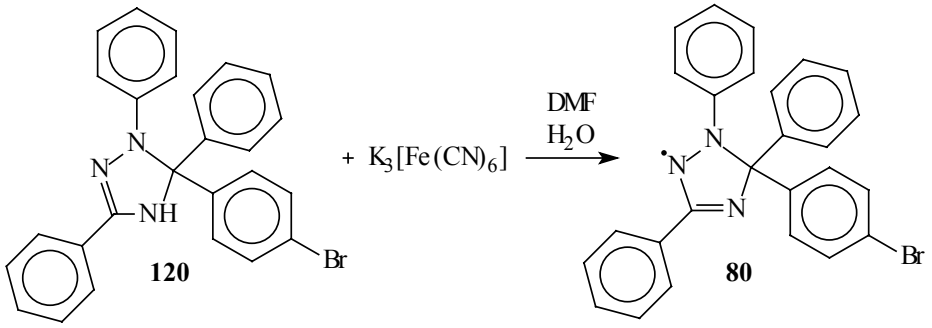

Scheme 5.34. Synthesis of 1,3,5-triphenyl-5-(4-bromophenyl)-Δ^3-1,2,4-triazolin-2-yl (**80**).

In a 250 ml Erlenmeyer flask, 0.8 g (0.0018 mol) of **120** were dissolved in 50 ml of DMF. 2 g (0.0061 mol) of potassium hexacyanoferrate (III) and 0.35 g (0.0033 mol) of sodium carbonate in 15 ml of water were added dropwise and the mixture was stirred at temperature below – 10°C for 4 hours. An excess of water was added to the solution, and the resulting precipitate collected by filtration and washed with water to give the radical **80** as very dark red-brown fine powder. It contained about 15 % of **119** and **33** and was free of other impurities. The yield was quantitative.

Analysis:

Melting point was not measured, since the substance contains noticeable amount of **33** and **79**

Mass spectra (FD): m/z: 454.4 (M^+) (100 %); 532.5 (M^+) (**42**) (12 %)

Elemental analysis: calculated: C: 68.88 %; N: 9.27 %; H: 4.22 %

found: C: 68.94 %; N: 8.79 %; H: 4.99 %

UV-Vis spectrum at room temperature in dichloromethane is given in Figure 5.8.

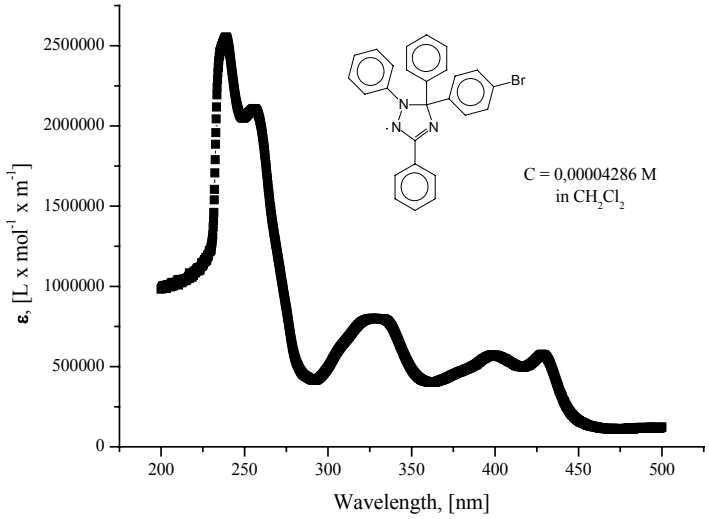

Figure 5.8. UV-Vis spectrum of 1,3,5-triphenyl-5-(4-bromophenyl)-Δ^3-1,2,4-triazolin-2-yl (**80**) in CH_2Cl_2.

5.9. Synthesis of 1,3-diphenyl-5,5-di(nitrophenyl)-Δ^3-1,2,4-triazolin-2-yl (mixture of isomers)

1,3-Diphenyl-5,5-di(nitrophenyl)-Δ^3-1,2,4-triazolin-2-yl was synthesized by the synthetic route shown on Scheme 5.35.

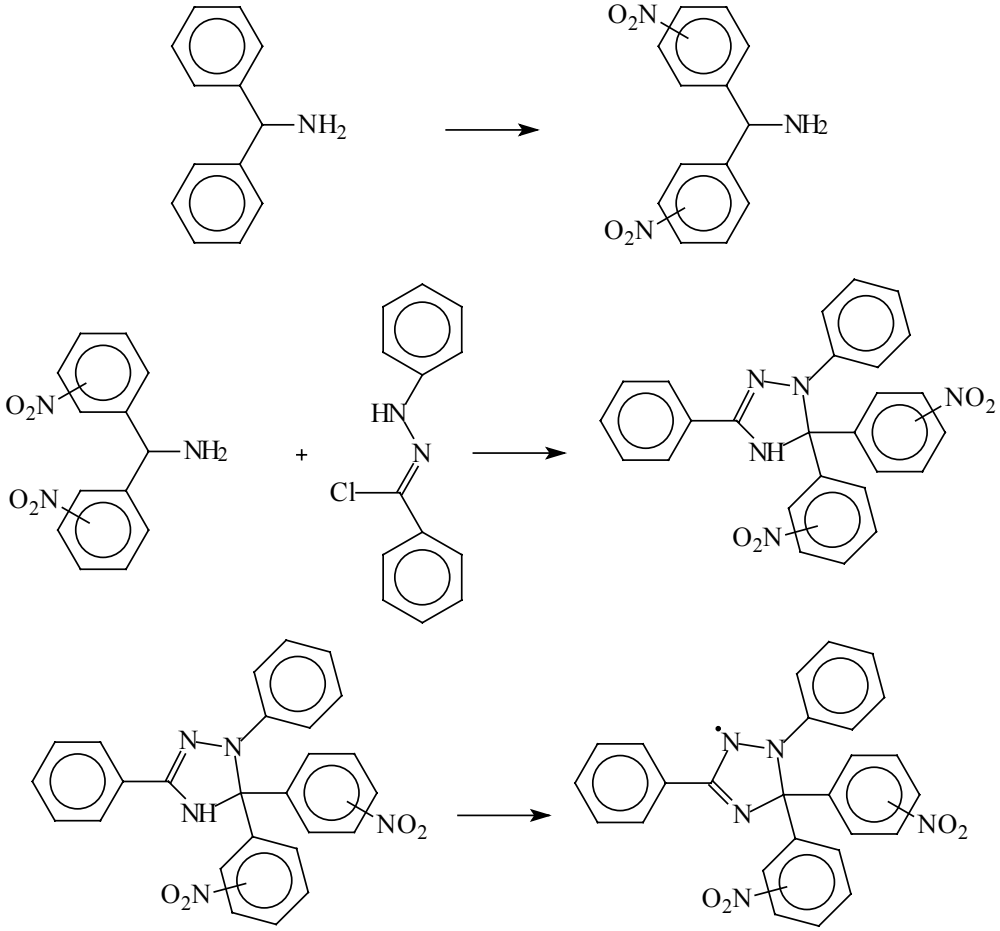

Scheme 5.35. Synthetic route to 1,3-diphenyl-5,5-di(nitrophenyl)-Δ^3-1,2,4-triazolin-2-yl.

Step 1. Synthesis of dinitrobenzhydrylamine (76) (mixture of isomers)

Dinitrobenzhydrylamine (**76**) has been synthesized as a mixture of isomers by direct nitration of benzhydrylamine in sulfuric acid (Scheme 5.36).

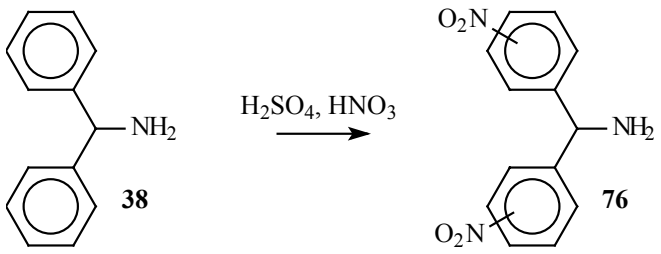

Scheme 5.36. Synthesis of dinitrobenzhydrylamine (**76**) (mixture of isomers).

0.5 g (0.0027 mol, 0.47 mol) of benzhydrylamine (**38**) was placed in a 250 Erlenmeyer flask with thick walls. The flask was cooled down in an ice/sodium chloride bath. 15 ml of concentrated sulfuric acid (Riedel-de Haen) were added to the amine dropwise and the mixture stirred until the amine completely dissolved. Keeping the temperature of the bath below 0°C 5 ml of 68 % nitric acid (Riedel-de Haen) was added slowly dropwise to the mixture with vigorous stirring. After addition of all nitric acid, the mixture was stirred for 40 minutes at 0°C and then 15 minutes at room temperature. Afterwards the reaction was quenched by pouring onto large amount of ice. The pH was raised to 8 by addition of sodium carbonate and the products were extracted by dichloromethane. The organic layers were collected, washed with brine and water and dried over magnesium sulfate. The solvent was removed under reduced pressure and the residue was recrystallized from diethyl ether/ethanol mixture. The product was identified as a mixture of isomers by HPLC and ^{1}H-NMR analyses. The yield = 73 %.

Analysis:

Melting point was not measured because the substance is a mixture of isomers

^{1}H-NMR spectra (D_6-DMSO, 250MHz) δ [ppm]: 2.68 (s, 2H, N<u>H</u>$_2$); 5.44, 5.42 (two peaks with different intensity, 1H, C<u>H</u>); 7.58 - 8.10 (m, 8H, phenyl protons)

Mass spectra (FD): m/z: 273.1 (M^+) (only peak)

Elemental analysis: calculated: C: 57.14 %; N: 15.38 %; H: 4.06 %

found: C: 57.18 %; N: 15.35 %; H: 4.07 %

HPLC on reverse phase column with gradient elution using a pentane/THF mixture showed presence of three very poorly separated compounds. Use of several other eluents did not show any separation. The chromatogram is shown in Figure 5.9.

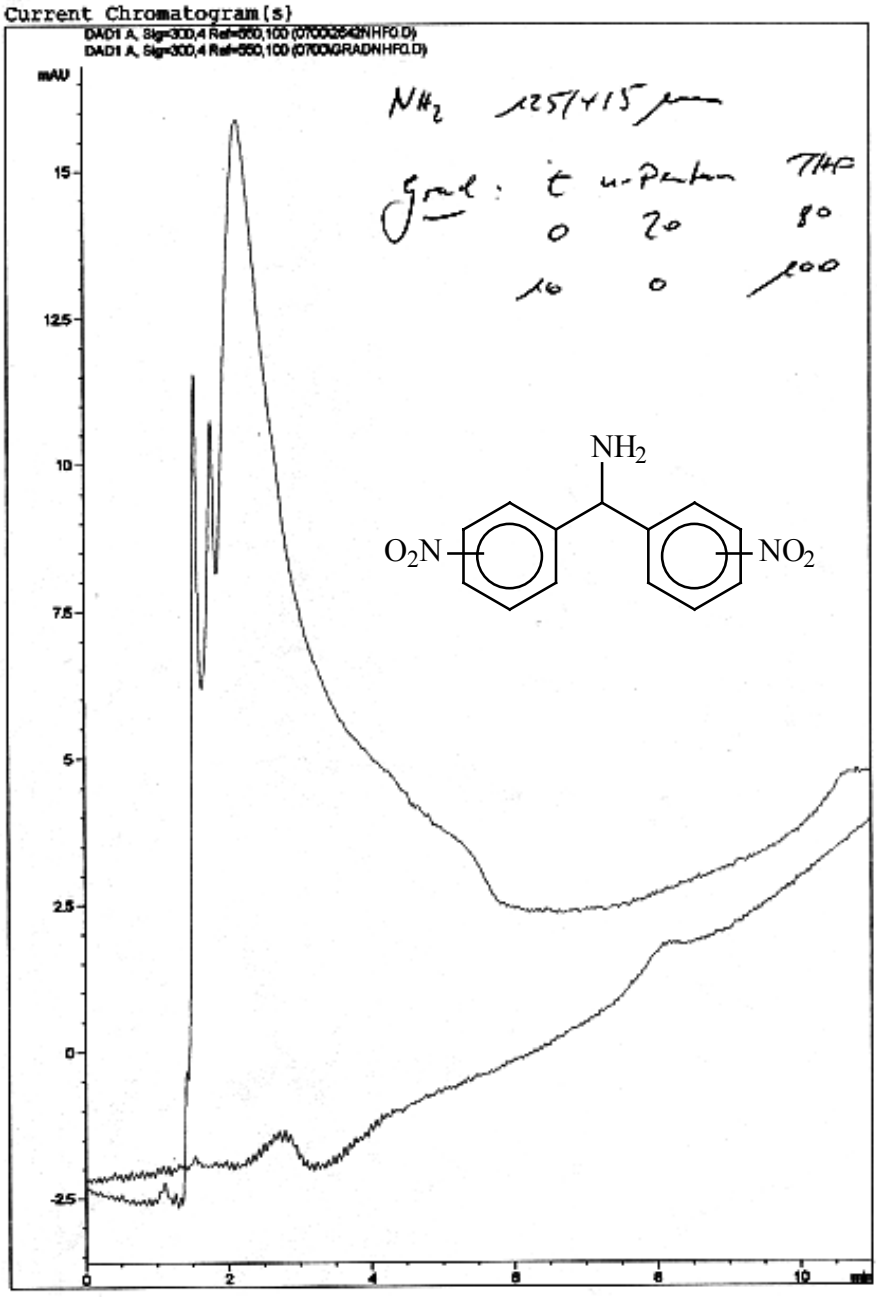

Figure 5.9. High pressure liquid chromatogram of dinitrobenzhydrylamine (**76**), confirming presence of different isomers in the sample.

Step 2. Synthesis of 1,3–diphenyl-5,5-dinitrophenyl-Δ^2-1,2,4-triazolin (121) (mixture of isomers)

1,3–Diphenyl-5,5-di(nitrophenyl)-Δ^2-1,2,4-triazolin was obtained by the standard procedure described above for syntheses of other triazolins (Scheme 5.37).

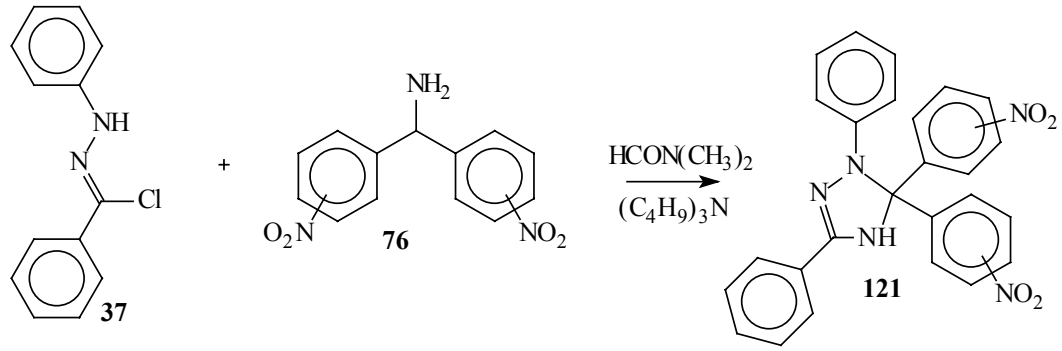

Scheme 5.37. Synthesis of 1,3–diphenyl-5,5-di(nitrophenyl)-Δ^2-1,2,4-triazolin (**121**) (mixture of isomers).

In a round-bottom 50 ml one-necked flask equipped with reflux condenser and magnetic stirrer bar 0.22 g (0.0008 mol) of **76**, 0.19 g (0.00083 mol) of **37** and 0.21 ml (0.16 g, 0.00087 mol) of tri-*n*-butylamine were dissolved in 20 ml of DMF under an argon atmosphere. The mixture was stirred at 180°C for 40 minutes, then the solution cooled down and poured into excess of water and the products extracted with dichloromethane. The combined organic layers were washed with brine and water then dried over magnesium sulfate. Removal of the solvent at reduced pressure gave 1,3–diphenyl-5,5-di(nitrophenyl)-Δ^2-1,2,4-triazolin (**121**), which was purified by column chromatography on silica gel 60 with dichloromethane as eluent, and recrystallization from diethyl ether. The yield = 36 %.

Analysis:

Melting point was not measured because the substance was a mixture of isomers

^{1}H-NMR spectra (D_6-DMSO, 250MHz) δ [ppm]: 6.62 - 8.32 (m, 8H, phenyl protons); 8.96 (s, 1H, N<u>H</u>)

Mass spectra (FD): m/z: 465.4 (M^+) (only peak)

Elemental analysis: calculated: C: 66.98 %; N: 15.05 %; H: 4.11 %

found: C: 67.09 %; N: 14.74 %; H: 4.14 %

Step 3. Synthesis of 1,3–diphenyl-5,5-di(nitrophenyl)-Δ^3-1,2,4-triazolin-2-yl (87)

1,3–Diphenyl-5,5-di(nitrophenyl)-Δ^2-1,2,4-triazolin (**121**) was converted to 1,3–diphenyl-5,5-di(nitrophenyl)-Δ^3-1,2,4-triazolin-2-yl (**87**) by treatment with potassium hexacyanoferrate (III) (Scheme 5.38).

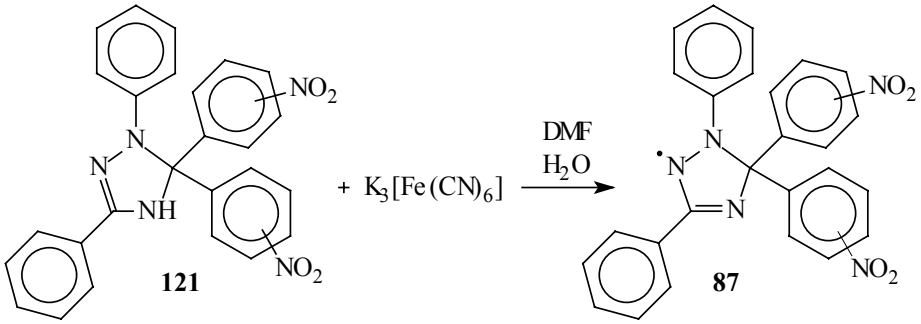

Scheme 5.38. Synthesis of 1,3–diphenyl-5,5-di(nitrophenyl)-Δ^3-1,2,4-triazolin-2-yl (**87**).

In a 250 ml Erlenmeyer flask equipped with magnetic stirrer bar 0.23 g (0.00049 mol) of **121** were dissolved in 100 ml of DMF. The solution was cooled down in a dry ice/acetone bath and a solution of 0.5 g (0.0015 mol) of potassium hexacyanoferrate (III) and 0.1 g (0.00094 mol) of sodium carbonate in 15 ml of water was added dropwise. The solution was stirred for 4 hours at a temperature below – 10°C. An excess of water was added and the resulting precipitate was collected by filtration, washed with water, and dried to give 1,3–diphenyl-5,5-di(nitrophenyl)-Δ^3-1,2,4-triazolin-2-yl (**87**) as a dark red fine powder. The yield was quantitative.

Analysis:

Melting point was not measured because the substance is a mixture of isomers

Mass spectra (FD): m/z = 463.7 (M^+) (only peak)

Elemental analysis: calculated: C: 67.24 %; N: 15.08 %; H: 3.91 %

found: C: 66.93 %; N: 14.74 %; H: 4.20 %

UV-Vis spectrum at room temperature in dichloromethane is given in Figure 5.10.

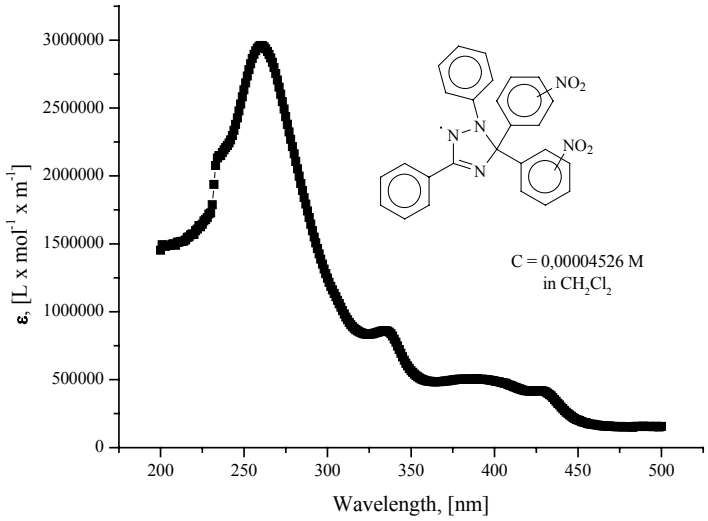

Figure 5.10. UV-Vis spectrum of 1,3–diphenyl-5,5-di(nitrophenyl)-Δ^3-1,2,4-triazolin-2-yl (**87**) in CH_2Cl_2.

5.10. Synthesis of 1,3-diphenyl-5,5-di(3-trifluoromethylphenyl)-Δ^3-1,2,4-triazolin-2-yl

1,3-Diphenyl-5,5-di(3-trifluoromethylphenyl)-Δ^3-1,2,4-triazolin-2-yl was synthesized *via* the synthetic route shown in Scheme 5.39.

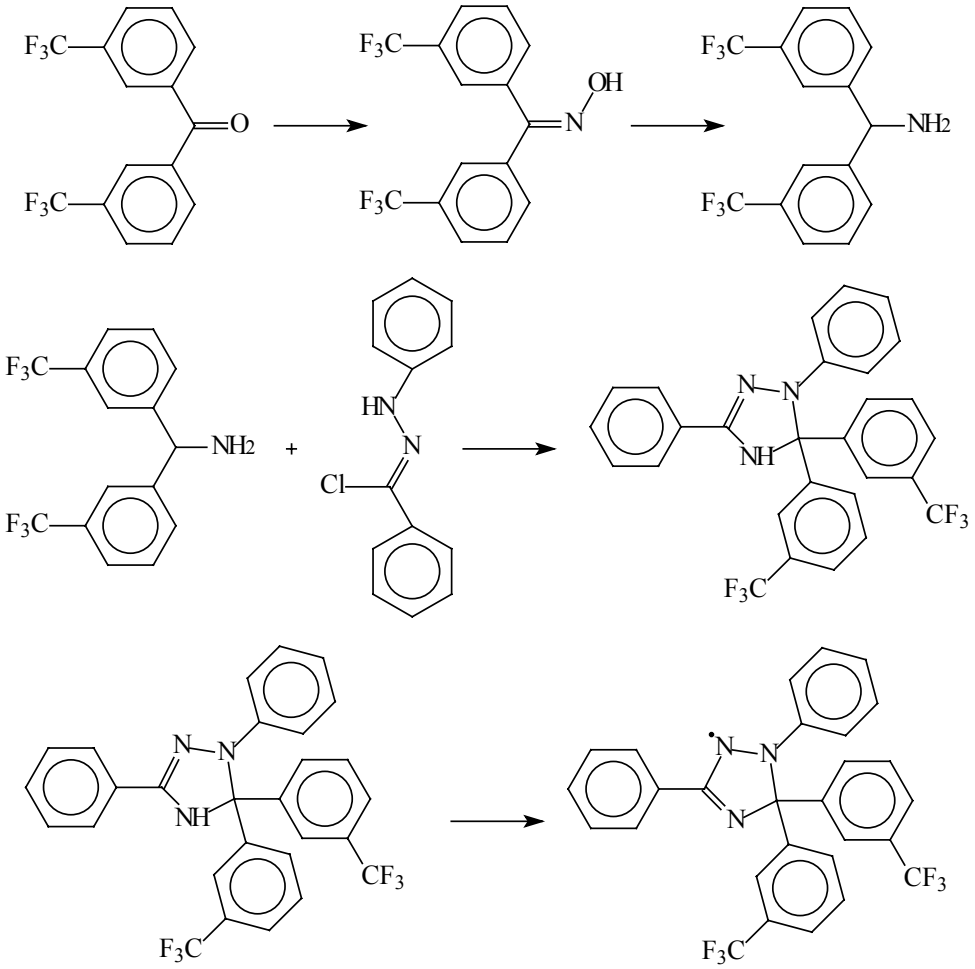

Scheme 5.39. Synthetic route to 1,3-diphenyl-5,5-di-3-trifluoromethylphenyl-Δ^3-1,2,4-triazolin-2-yl.

Step 1. Synthesis of 3,3`-di(trifluoromethyl)benzophenone oxime (123)

3,3`-Di(trifluoromethyl)benzophenone oxime (**123**) was synthesized from 3,3`-di(trifluoromethyl)benzophenone (**122**) by the method shown in Scheme 5.40.

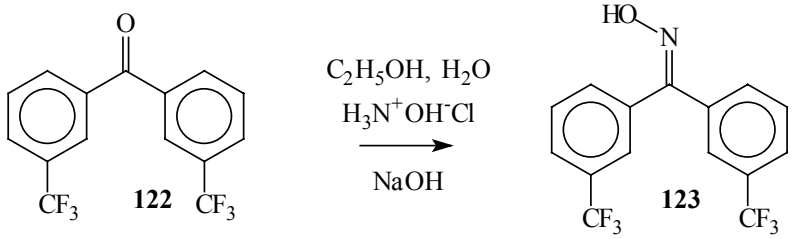

Scheme 5.40. Synthesis of 3,3`-di(trifluoromethyl)benzophenone oxime (**123**).

In a 50 ml two-necked round-bottom flask, equipped with reflux condenser and magnetic stirrer bar 1 g (0.0031 mol) of **122** and 0.51 g (0.0073 mol) of hydroxylamine hydrochloride were mixed with 4 ml of ethanol and 1 ml of water. 0.4 g (0.01 mol) of sodium hydroxide were added to the stirred suspension in small portions. When all the NaOH had been added the reaction flask was put into an oil bath and the temperature was raised to 100°C. After 4 hours, the flask was removed from the bath. The resulting yellow solution was cooled down and poured into an excess of dilute hydrochloric acid. Oil, which was denser than water formed immediately. The emulsion was cooled down to 0°C. The oil which had solidified at this temperature, was collected by filtration and washed with water. Recrystallization from ethanol/water mixture gave pure 3,3`-di(trifluoromethyl)benzophenone oxime (**123**) as a slightly beige solid. The yield was quantitative.

Analysis:

Melting point: 115 – 116°C

^{1}H-NMR spectra (D_6-DMSO, 250MHz) δ [ppm]: 7.57-7.86 (m, 8H, phenyl protons); 11.94 (s, 1H, NO<u>H</u>).

Mass spectra (FD): m/z: 333.0 (M^+) (only peak)

Elemental analysis: calculated: C: 54.07 %; N: 4.20 %; H: 2.72 %

found: C: 54.02 %; N: 4.20 %; H: 2.63 %

Step 2. Synthesis of 3,3`-di(trifluoromethyl)benzhydrylamine (124)

Reduction of oxime **123** to 3,3`-di(trifluoromethyl)benzhydrylamine (**124**) was carried out using zinc powder in ammonia solution (Scheme 5.41).

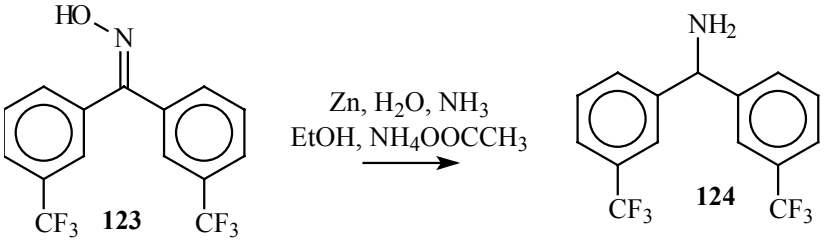

Scheme 5.41. Synthesis of 3,3`-di(trifluoromethyl)benzhydrylamine (**124**).

In a 250 ml two-necked round-bottom flask equipped with reflux condenser and magnetic stirrer bar 1 g (0.003 mol) of **123**, 0.35 g (0.0045 mol) of ammonium acetate, 8 ml of 25 % ammonia solution, 9 ml of ethanol, and 5 ml of water were mixed. The flask was placed into an oil bath and heated to 100°C. Zn powder (0.78 g, 0.012 mol) was added in small portions. After addition of all the zinc the mixture was refluxed for 4 hours. Unreacted zinc was removed by filtration and the mixture was extracted with diethyl ether. The combined organic layers were washed with brine and water and dried over magnesium sulfate. The crude amine was purified by column chromatography on silica gel 60 with dichloromethane as eluent to give 3,3`-di(trifluoromethyl)benzhydrylamine (**124**) as a colorless oil. The yield was 73 %.

Analysis:

Melting point: oil, which forms colorless crystals in the freezer (- 18°C)

^{1}H-NMR spectra (D_6-DMSO, 250MHz) δ [ppm]: 2.63 (s, 2H, N<u>H</u>$_2$); 5.37 (s, 1H C<u>H</u>); 7.53 - 7.90 (m, 8H, phenyl protons)

Mass spectra (FD): no peaks observed

Elemental analysis: calculated: C: 56.43 %; N: 4.39 %; H: 3.47 %

found: C: 56.30 %; N: 4.40 %; H: 3.67 %

Step 3. Synthesis of 1,3–diphenyl-5,5-di(3-trifluoromethylphenyl)-Δ^2-1,2,4-triazolin (125)

1,3–Diphenyl-5,5-di(3-trifluoromethylphenyl)-Δ^2-1,2,4-triazolin (**125**) was synthesized by the standard procedure from 3,3`-di(trifluoromethyl)benzhydrylamine (**124**) and N-phenylbenzenecarbohydrazonoyl chloride (**37**) (Scheme 5.42).

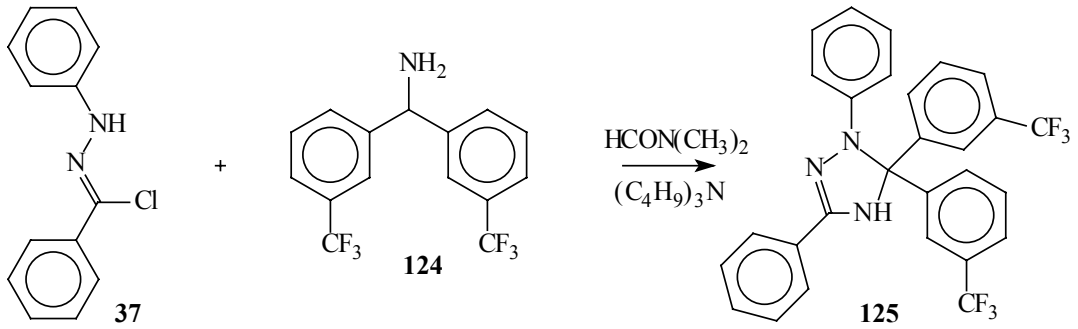

Scheme 5.42. Synthesis of 1,3–diphenyl-5,5-di(3-trifluoromethylphenyl)-Δ^2-1,2,4-triazolin (**125**).

4.8 g (0.015 mol) of **124**, 3.47 g (0.015 mol) of **37** and 3.6 ml (2.8 g, 0.015 mol) of tri-*n*-butylamine were dissolved in 100 ml of DMF in a 250 ml one-necked round-bottom flask (dried by Method 6.1) equipped with magnetic stirrer bar and reflux condenser. An argon atmosphere was introduced to the reactor. The flask was heated up to 180°C in an oil bath and the mixture was stirred for 2 hours. The oil bath was removed and the mixture was stirred for a further 20 hours at room temperature. The bright orange solution was poured into an excess of water and the products were separated by extraction with diethyl ether. The combined organic layers were washed several times with sodium chloride solution and water, then dried over magnesium sulfate, and the solvent was removed in *vacuo*. After purification by column chromatography on silica gel 60 with dichloromethane/petroleum ether mixture as eluent and recrystallization from hexane 1,3–diphenyl-5,5-di(3-trifluoromethylphenyl)-Δ^2-1,2,4-triazolin (**125**) was isolated as a crystalline orange solid. The yield was 12 %.

Analysis:

Melting point: 171 – 172°C

^{1}H-NMR spectra (D_6-DMSO, 250MHz) δ [ppm]: 6.63 - 7.92 (m, 18H, phenyl protons); 8.88 (s, 1H, N<u>H</u>)

Mass spectra (FD): m/z: 511.3 (M^+) (only peak)

Elemental analysis: calculated: C: 65.75 %; N: 8.22 %; H: 3.74 %

found: C: 65.57 %; N: 8.22 %; H: 3.96 %

Step 4. Synthesis of 1,3–diphenyl-5,5-di(3-trifluoromethylphenyl)-Δ^3-1,2,4-triazolin-2-yl (86)

1,3–Diphenyl-5,5-di(3-trifluoromethylphenyl)-Δ^2-1,2,4-triazolin (**125**) was oxidized to form 1,3–diphenyl-5,5-di(3-trifluoromethylphenyl)-Δ^3-1,2,4-triazolin-2-yl (**86**) using potassium hexacyanoferrate (III) (Scheme 5.43).

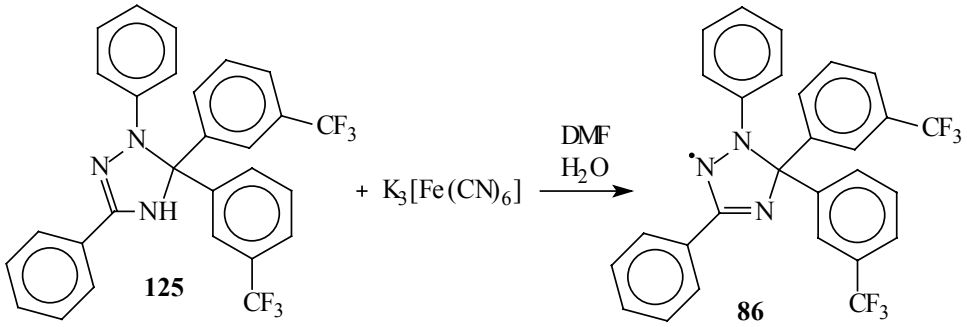

Scheme 5.43. Synthesis of 1,3–diphenyl-5,5-di(3-trifluoromethylphenyl)-Δ^3-1,2,4-triazolin-2-yl (**86**).

In a 250 ml Erlenmeyer flask 0.45 g (0.0009 mol) of **125** were dissolved in 60 ml of DMF. The solution was cooled in a dry ice/acetone bath. A solution of 2 g (0.006 mol) of potassium hexacyanoferrate (III) and 0.5 g (0.005 mol) of sodium carbonate was added dropwise to the stirred solution of **125**. After addition of all reagents, the mixture was stirred for 4 hours at temperature below – 10°C. On completion of the reaction, an excess of water was added to the solution and the resulting solid was collected by filtration and washed by water. 1,3–Diphenyl-5,5-di-3-trifluorothylphenyl-Δ^3-1,2,4-triazolin-2-yl (**86**) was obtained as a very dark red-black fine powder. The yield was quantitative.

Analysis:

Melting point: the substance decomposes; decomposition in bulk starts at ~ 35°C

Mass spectra (FD): m/z: 510.3 (M^+) (only peak)

Elemental analysis: calculated: C: 65.88 %; N: 8.23 %; H: 3.55 %

found: C: 65.57 %; N: 8.19 %; H: 3.80 %

UV-Vis spectrum at room temperature in dichloromethane is given in Figure 5.11.

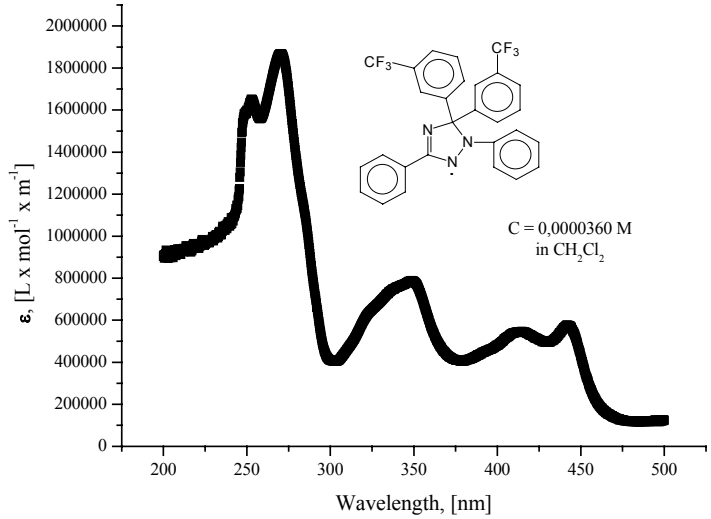

Figure 5.11. UV-Vis spectra of **1,3**–diphenyl-5,5-di(3-trifluoromethylphenyl)-Δ^3-1,2,4-triazolin-2-yl (**86**) in CH_2Cl_2.

5.11. Synthesis of 1,3-diphenyl-5,5-di(4-(perfluoro-*n*-hexyl)phenyl)-Δ^3-1,2,4-triazolin-2-yl

1,3-Diphenyl-5,5-di(4-(perfluoro-*n*-hexyl)phenyl)-Δ^3-1,2,4-triazolin-2-yl was synthesized by the synthetic route shown in Scheme 5.44.

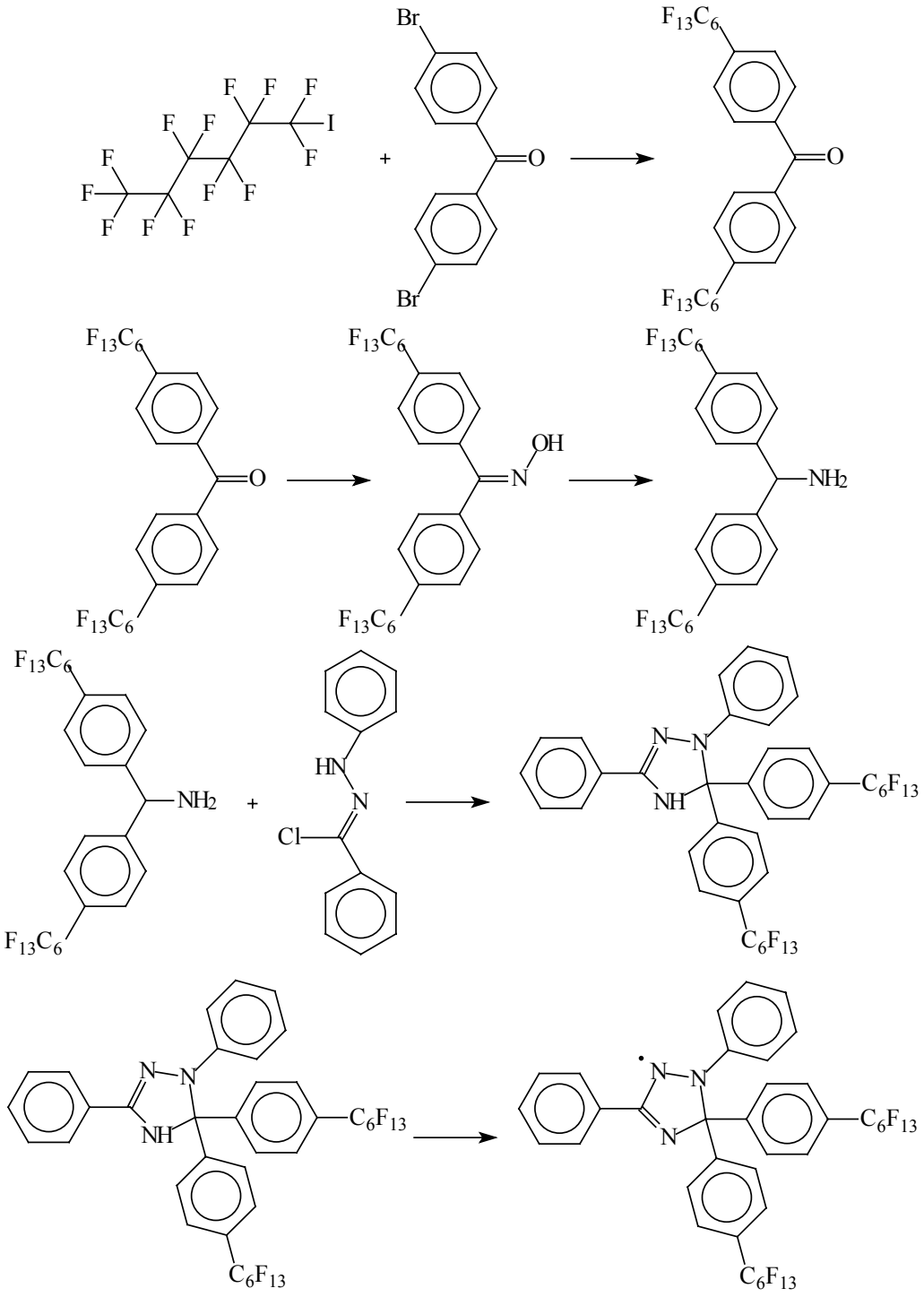

Scheme 5.44. Synthetic route to 1,3-diphenyl-5,5-di(4-(perfluoro-*n*-hexyl)phenyl)-Δ^3-1,2,4-triazolin-2-yl.

Step 1. Synthesis of 4,4`-di(perfluoro-n-hexyl)benzophenone (73)

4,4`-di(perfluoro-*n*-hexyl)benzophenone (**73**) was prepared as shown in Scheme 5.45.

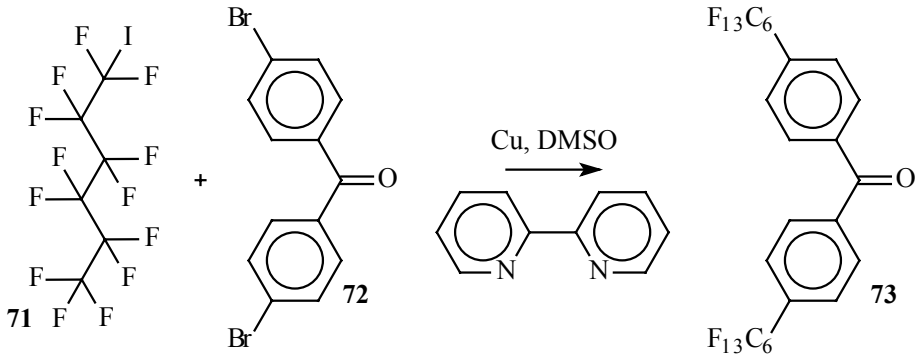

Scheme 5.45. Synthesis of 4,4`-di(perfluoro-*n*-hexyl)benzophenone (**73**).

In a 100 ml round-bottom one-necked flask (dried by the standard Method 6.1) equipped with a magnetic stirrer bar and reflux condenser 0.34 g (0.001 mol) of **72**, 0.98g (0.0022 mol) of perfluoro-*n*-hexyl iodide (**71**) (Lancaster), 0.31 g (0.0048 mol) of cupper fine powder (Aldrich) and 0.0099 g ($6.3*10^{-5}$ mol) of 2,2`-bipyridyl (Aldrich) were mixed in 20 ml of DMSO (Riedel-de Haen) under argon atmosphere. The flask was put in an oil bath heated to 120°C. The mixture was stirred for 48 hours at 120°C, then the resulting suspension was poured into water and the products were extracted with a dichloromethane/hexafluorobenzene (Lancaster) mixture. The combined organic layers were washed with brine and water and dried over magnesium sulfate. The solvent was removed in *vacuo* and the residue recrystallized from methanol to give **73** as a colorless crystalline solid. The yield was 65 %.

Analysis:

Melting point: 97 – 98°C

^{1}H-NMR spectra (D_6-DMSO, 250MHz) δ [ppm]: 7.55 (d, J = 8.04 Hz, 4H, phenyl protons 2 & 6); 7.95 (d, J = 8.04 Hz, 4H, phenyl protons 3 & 5)

Mass spectra (FD): m/z: 818.4(M^+) (only peak)

Elemental analysis: calculated: C: 36.70 %; H: 0.99 %

found: C: 36.60 %; H: 1.20 %

Step 2. Synthesis of 4,4`-di(perfluoro-n-hexyl)benzophenone oxime (126)

4,4`-Di(perfluoro-*n*-hexyl)benzophenone oxime (**126**) was synthesized from 4,4`-di(perfluoro-*n*-hexyl)benzophenone (**73**) as shown in Scheme 5.45.

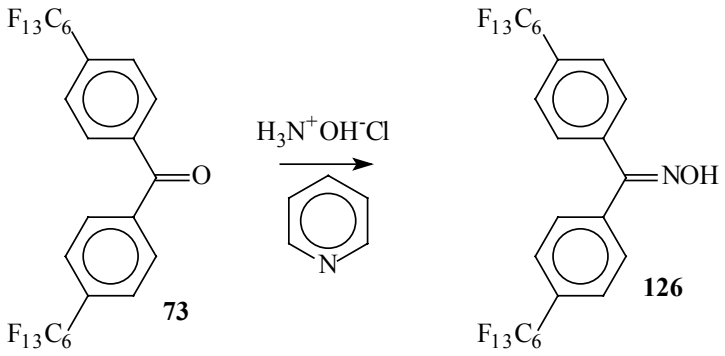

Scheme 5.45. Synthesis of 4,4`-di(perfluoro-*n*-hexyl)benzophenone oxime (**126**).

A 1000 ml three neck round bottom flask equipped with a Dean-Stark apparatus and a magnetic stirrer was dried by the standard procedure (Method 6.1). The outlet of the Dean-Stark trap was filled with dried molecular sieves 4 Å (Karl Roth). 15.7 g (0.019 mol) of 4,4`-di(perfluoro-*n*-hexyl)benzophenone (**73**), 5.2 g (0.075 mol) of hydroxylamine hydrochloride and 550 ml of pyridine (Acros) were mixed under argon atmosphere and the mixture was heated to 130°C. Periodically the pyridine in the Dean-Stark trap was removed and new solvent was added *via* the reflux condenser. After 24 hours excess of pyridine was distilled off and the residue was poured into diluted sulfuric acid. After short period of time a colorless crystalline solid formed. The suspension was cooled down to 0°C in order to complete crystallization and the solid was collected by filtration. Recrystallization from chloroform (Riedel-de Haen) gave 4,4`-di(perfluoro-*n*-hexyl)benzophenone oxime (**126**) as colorless crystalline solid. The yield was 83 %.

Analysis:

Melting point: 138 – 139°C

^{1}H-NMR spectra (D_8-THF, 250MHz) δ [ppm]: 7.56 - 7.94 (m, 8H, phenyl protons); 11.26 (s, 1H, NO<u>H</u>)

Mass spectra (FD): m/z: 833.2 (M^+) (only peak)

Elemental analysis: calculated: C: 36.03 %; N: 1.68 %; H: 1.09 %

found: C: 35.87 %; N: 1.51 %; H: 0.97 %

Step 3. Synthesis of 4,4`-di(perfluoro-n-hexyl)benzhydrylamine (127)

4,4`-Di(perfluoro-*n*-hexyl)benzhydrylamine (**127**) was obtained by reduction of **126** with zinc in ammonia solution (Scheme 5.46).

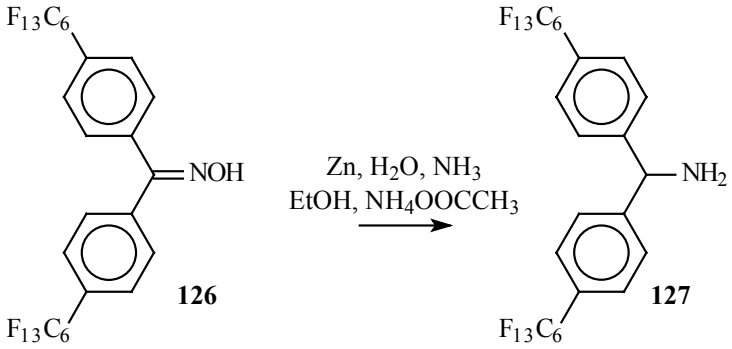

Scheme 5.46. Synthesis of 4,4`-di(4-perfluoro-*n*-hexyl)benzhydrylamine (**127**).

In a 500 ml round-bottom two-necked flask equipped with reflux condenser and magnetic stirrer bar, 2.1 g (0.0025 mol) of **126**, 1g (0.013 mol) of ammonium acetate, 30 ml of 25 % ammonia solution, 50 ml of ethanol, 5 ml of THF and 20 ml of water were mixed (a large flask was used because of intensive foaming during the reaction). The mixture was heated until it refluxed. Zn powder (3 g, 0.046 mol) was added in small portions to the stirred refluxing mixture. After addition of all zinc, the reaction was kept refluxing for 15 hours. On completion of the reaction, the products were extracted with a chloroform/hexafluorobenzene (Lancaster) mixture. The combined organic layers were washed with water and brine and dried over magnesium sulfate. The solvents were removed under reduced pressure. The crude amine was purified by column chromatography with dichloromethane as eluent to give 4,4`-di(perfluoro-*n*-hexyl)benzhydrylamine (**127**) as a colorless crystalline solid. The yield was 67 %.

Analysis:

Melting point: 126 – 127°C

^{1}H-NMR spectra (D_8-THF, 250MHz) δ [ppm]: 2.09 (s, 2H, N<u>H</u>$_2$); 5.25 (s, 1H C<u>H</u>); 7.47 (d, J = 8.36 Hz, 4H, 2 & 6 phenyl protons); 7.57 (d, J = 8.36 Hz, 4H, 3 & 4 phenyl protons)

Mass spectra (FD): no peaks observed

Elemental analysis: calculated: C: 36.65 %; N: 1.71 %; H: 1.35 %

found: C: 36.80 %; N: 1.61 %; H: 1.61 %

Step 4. Synthesis of 1,3–diphenyl-5,5-di(4-perfluoro-n-hexylphenyl)-Δ^2-1,2,4-triazolin (128)

1,3–Diphenyl-5,5-di(4-perfluoro-*n*-hexylphenyl)-Δ^2-1,2,4-triazolin (**128**) has been synthesized *via* the synthetic route shown in Scheme 5.47.

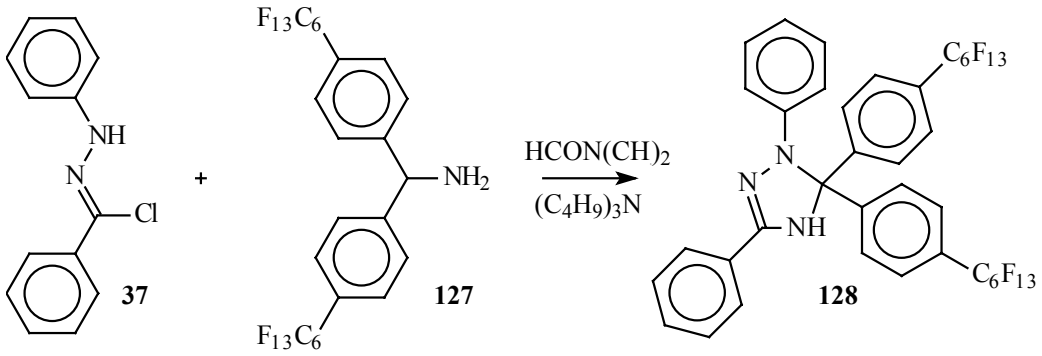

Scheme 5.47. Synthesis of 1,3–diphenyl-5,5-di(4-perfluoro-n-hexylphenyl)-Δ^2-1,2,4-triazolin (**128**).

A 250 ml one-necked round-bottom flask, equipped with reflux condenser and magnetic stirrer bar, was dried as described in Section 6.1. 1.9 g (0.0023 mol) of **127**, 0.55 g (0.0024 mol) of **37** and 1ml (0.78 g, 0.0042mol) of tri-*n*-butylamine were dissolved in 100 ml of DMF under an argon atmosphere and the flask was immersed into an oil bath heated to 180°C. After stirring at 180°C for 100 minutes the oil bath was removed and the mixture stirred for an additional 15 hours at room temperature. The solution was then poured into water and the products extracted with dichloromethane. The organic layers were combined, washed with water, dried over magnesium sulfate, and the solvent removed in *vacuo*. The resulting amorphous solid was purified by column chromatography on silica gel 60, first with dichloromethane/petroleum ether and afterwards with diethyl ether/petroleum ether as eluent. 1,3–Diphenyl-5,5-di(4-perfluoro-*n*-hexylphenyl)-Δ^2-1,2,4-triazolin (**128**) was isolated as a yellow-orange solid, which darkened in air due to oxidation. The yield was 11 %.

Analysis:

Melting point: 171 – 172°C

^{1}H-NMR spectra ($C_2D_2Cl_4$ & C_6F_6, 300MHz) δ [ppm]: peaks were broad, 6.6 – 7.8 (m, phenyl protons & N<u>H</u>); aggregation was reported to cause broadening of NMR peaks for perfluorocompounds[213]

Mass spectra (FD): m/z: 1012.1 (M^+) (100 %); 2023.6 ($2*M^+$) (60 %); 3039.0 ($3*M^+$) (60 %), observation of dimer and trimer of the triazolin in the mass spectra supports the tendency of the compound to agregate

Elemental analysis: calculated: C: 45.12 %; N: 4.15 %; H: 1.89 %

found: C: 45.36 %; N: 3.97 %; H: 2.17 %

Step 5. Synthesis of 1,3–diphenyl-5,5-di(4-perfluoro-n-hexylphenyl)-Δ^3-1,2,4-triazolin-2-yl (83)

Oxidation of the triazolin **128** to the corresponding radical **83** was performed using potassium hexacyanoferrate (III) (Scheme 5.48).

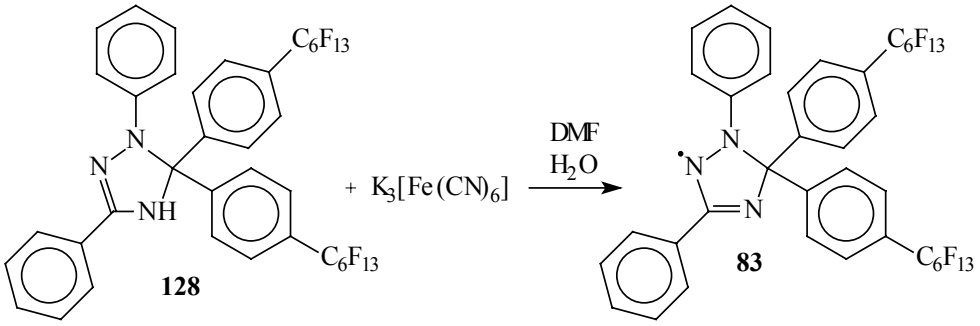

Scheme 5.48. Synthesis of 1,3–diphenyl-5,5-di(4-perfluoro-*n*-hexylphenyl)-Δ^3-1,2,4-triazolin-2-yl (**83**).

1.15 g (0.001 mol) of **128** were dissolved in 150 ml of DMF in a 250 ml Erlenmeyer flask equipped with a magnetic stirrer bar and the flask immersed in a dry ice/acetone bath. At temperatures below – 10°C, a solution of 1 g (0.003 mol) of potassium hexacyanoferrate (III) and 0.2 g (0.0019 mol) of sodium carbonate was added dropwise to the stirred triazolin solution. The reactants were stirred for 4 hours at low temperature after addition was complete. The very dark solution was diluted with an excess of water and the precipitate formed was collected by filtration and washed with water to give 1,3–diphenyl-5,5-di(4-perfluoro-*n*-hexylphenyl)-Δ^3-1,2,4-triazolin-2-yl (**83**) as very dark brown-red fine powder. The yield was quantitative.

Analysis:

Melting point: 112-113°C

Mass spectra (FD): m/z: 1011.0 (M^+) (100 %); 2022.9 ($2*M^+$) (40 %)

Elemental analysis: calculated: C: 45.17 %; N: 4.16 %; H: 1.80 %

found: C: 45.47 %; N: 3.98 %; H: 2.15 %

HPLC on reverse phase column shows one peak, in several eluents used (Figure 5.12). UV-Vis spectrum of the compound, which causes the peak on the HPLC, is identical to the UV-Vis spectrum shown in Figure 5.13.

UV-Vis spectrum at room temperature in dichloromethane is shown in Figure 5.13.

---

[213] I. Huc; R. Oda, Chem. Commun., *20*, 2025 – 2026, **1999**.

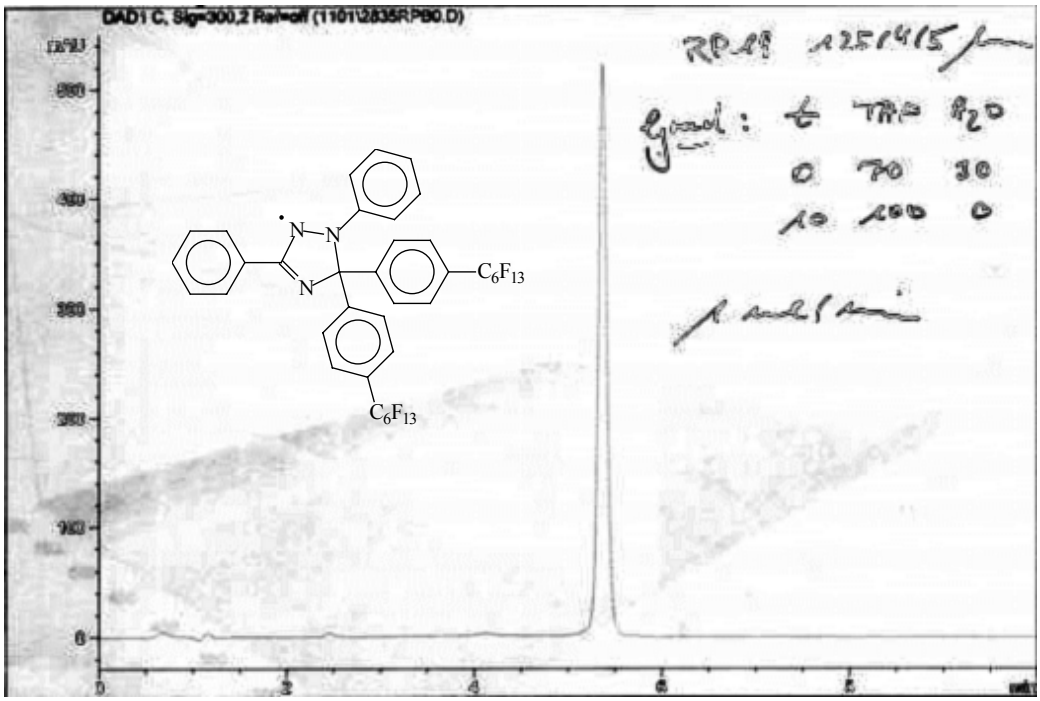

Figure 5.12. High pressure liquid chromatogram of 1,3–diphenyl-5,5-di(4-(perfluoro-*n*-hexylphenyl)-Δ^3-1,2,4-triazolin-2-yl (**83**).

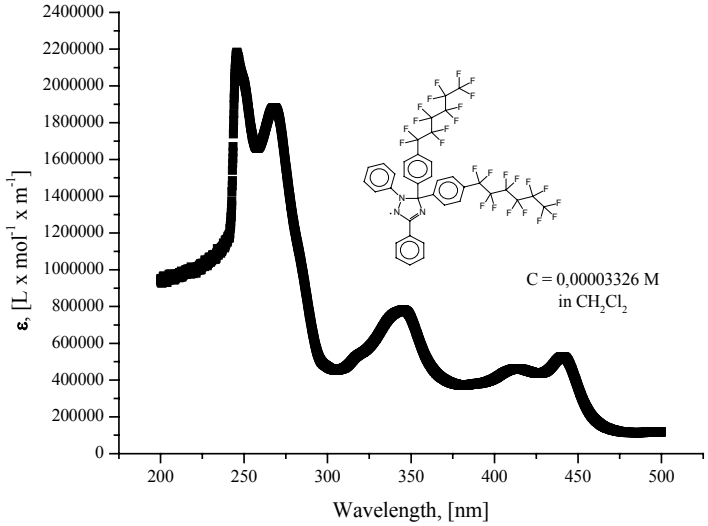

Figure 5.13. UV-Vis spectra of 1,3–diphenyl-5,5-di(4-perfluoro-*n*-hexylphenyl)-Δ^3-1,2,4-triazolin-2-yl (**83**) in CH_2Cl_2.

5.12. Synthesis of 1,3-diphenyl-5,5-di(2-thiophenyl)-Δ^3-1,2,4-triazolin-2-yl

1,3-Diphenyl-5,5-di(2-thiophenyl)-Δ^2-1,2,4-triazolin-2-yl has been synthesized *via* the synthetic route shown in Scheme 5.49.

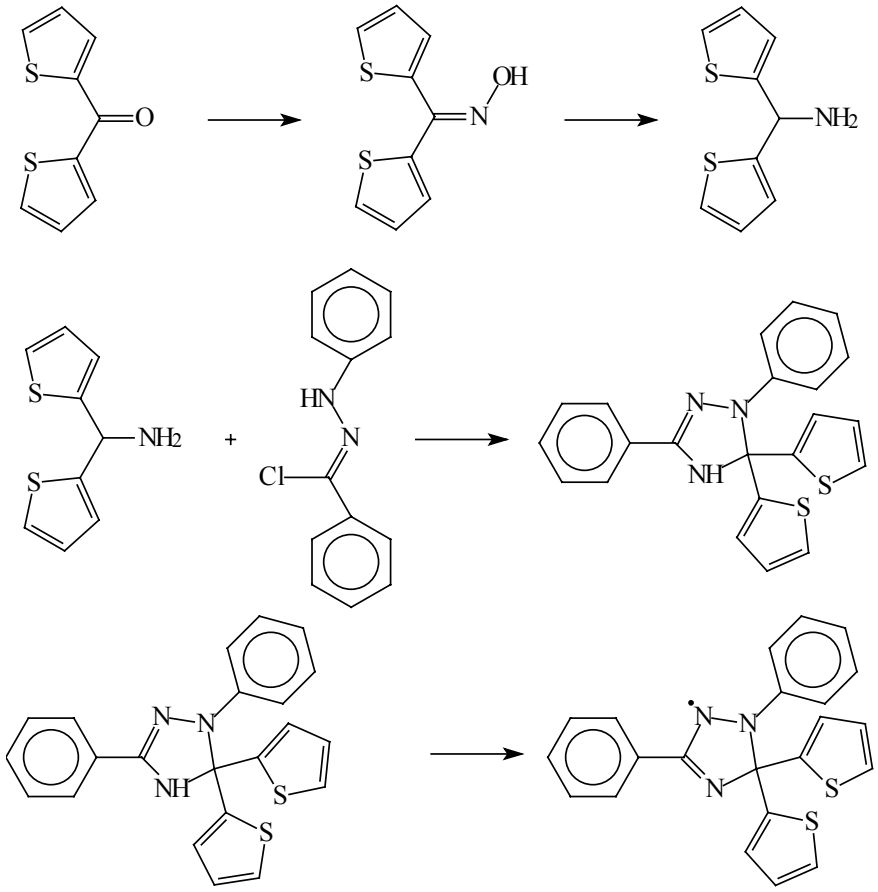

Scheme 5.49. Synthetic route to 1,3-diphenyl-5,5-di(2-thiophenyl)-Δ^2-1,2,4-triazolin-2-yl.

Step 1. Synthesis of di(2-thiophenyl)ketone oxime (130)

Di(2-thiophenyl)ketone oxime (**130**) was obtained by the reaction of di(2-thiophenyl)ketone (**129**) and hydroxylamine in pyridine (Scheme 5.50).

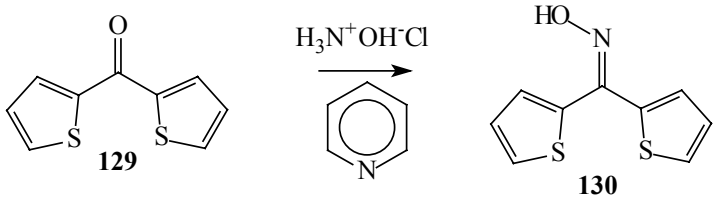

Scheme 5.50. Synthesis of di(2-thiophenyl)ketone oxime (**130**).

3 g (0.015 mol) of di(2-thiophenyl)ketone (**129**) (Aldrich), 4.5 g (0.065 mol) of hydroxylamine hydrochloride were mixed with 90 ml of pyridine in a 250 ml round-bottom two-necked flask, equipped with a Dean-Stark trap and magnetic stirrer bar (previously dried using the standard procedure (Method 6.1)). The outlet of the Dean-Stark trap was filled with dried molecular sieves 4 Å, and the mixture was stirred at 125°C for 10 hours. The cooled solution was poured into diluted sulfuric acid, and the products were extracted by dichloromethane. The organic extracts were washed with water and brine, dried over magnesium sulfate and the solvent was removed under reduced pressure. The crude di(2-thiophenyl)ketone oxime (**130**) was recrystallized from water/ethanol mixture to give a slightly pinky crystalline solid. The yield was quantitative.

Analysis:

Melting point: 133 – 134°C

^{1}H-NMR spectra (D_6-DMSO, 250MHz) δ [ppm]: 7.18 - 7.91 (m, 8H, protons of thiophenyl rings); 11.11 (broad s, 1H, NO<u>H</u>)

Mass spectra (FD): m/z: 211.1 (M^+) (only peak)

Elemental analysis: calculated: C: 51.65 %; N: 6.69 %; S: 30.64 %; H: 3.37 %

found: C: 51.38 %; N: 6.60 %; S: 30.59 %; H: 3.32 %

Step 2. Synthesis of α-aminodi(2-thiophenyl)methane (131)

α-Aminodi(2-thiophenyl)methane (**131**) was obtained by reduction of di(2-thiophenyl)ketone oxime (**130**) with zinc in ammonia solution (Scheme 5.51).

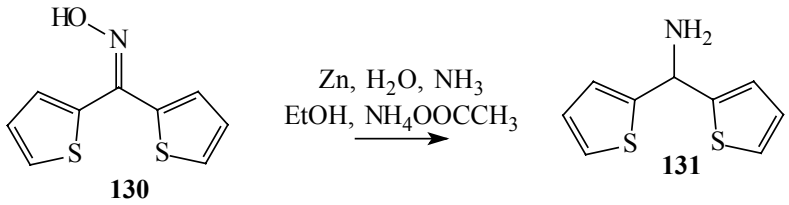

Scheme 5.51. Synthesis of α-aminodi(2-thiophenyl)methane (**131**).

4.1 g (0.02 mol) of **130**, 2.7 g (0.035 mol) of ammonium acetate, 60 ml of 25 % ammonia solution, 60 ml of ethanol and 40 ml of water were mixed in a two-necked 250 ml round-bottom flask equipped with reflux condenser and magnetic stirrer bar. The flask was put into an oil bath and the stirred solution was heated until boiling. 7 g (0.11 mol) of zinc powder were added to the solution in small portions. After addition of all the zinc, the reaction was continued for 16 hours. The suspension was then cooled down and unreacted zinc was removed by filtration. The solution was diluted with ammonia solution and the products extracted by chloroform. The

combined organic layers were washed with brine and water, dried over magnesium sulfate, and the chloroform removed in *vacuo*. α-Aminodi(2-thiophenyl)methane (**131**) was purified by column chromatography on silica gel 60 with dichloromethane as eluent to give a yellow solid compound. The yield was 79 %.

Analysis:

Melting point: 35 – 36°C

^{1}H-NMR spectra (CD_2Cl_4, 250MHz) δ [ppm]: 2.04 (broad s, 2H, N<u>H</u>$_2$); 5.60 (s, 1H C<u>H</u>); 6.84 - 7.21 (m, 8H, thiophenyl protons)

Mass spectra (FD): m/z = 194.9 (M^+) (only peak)

Elemental analysis: calculated: C: 55.35 %; N: 7.17 %; S: 32.84 %; H: 4.64 %

found: C: 55.64 %; N: 7.01 %; S: 32.80; H: 4.56 %

Step 3. Synthesis of 1,3–diphenyl-5,5-di(2-thiophenyl)-Δ^2-1,2,4-triazolin (132)

Condensation of α-aminodi(2-thiophenyl)methane (**131**) with **37** was carried out using the standard procedure as shown in Scheme 5.52.

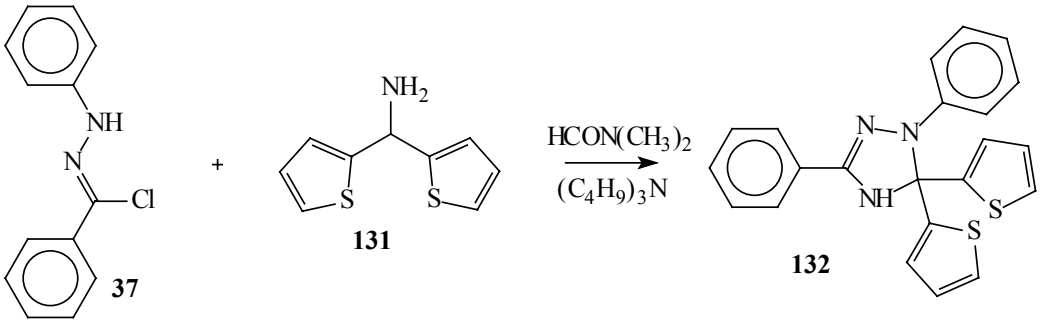

Scheme 5.52. Synthesis of 1,3–diphenyl-5,5-di(2-thiophenyl)-Δ^2-1,2,4-triazolin (**132**).

In a 250 ml one-necked round-bottom flask, equipped with magnetic stirrer bar and reflux condenser, previously dried by standard procedure (Method 6.1), 3.5 g (0.018 mol) of **131**, 4.14 g (0.018 mol) of **37**, 5 ml (3.86 g, 0.021 mol) of tri-*n*-butylamine were dissolved in 100 ml of DMF. Under an argon atmosphere the reaction flask was immersed in an oil bath heated to 180°C. After 40 minutes of stirring at 180°C, the black solution was cooled down and poured into brine and the products were extracted with chloroform. The combined organic layers were washed with brine and water, dried over magnesium sulfate, and the solvent removed in *vacuo*. Column chromatography on silica gel 60 with a mixture of petroleum ether and dichloromethane as eluent gave 1,3–diphenyl-5,5-di(2-thiophenyl)-Δ^2-1,2,4-triazolin (**132**) as a orange solid, which rapidly darkened in air due to oxidation to the corresponding radical. The yield was 12 %.

Analysis:

Melting point: not measured due to rapid oxidation leading to appearance of a large amount of the radical in the sample

^{1}H-NMR spectra (D_6-DMSO, 250MHz) δ [ppm]: 6.69 - 7.92 (m, 18H, phenyl & thiophenyl protons); 8.92 (s, 1H, N<u>H</u>)

Mass spectra (FD): m/z: 389.3 (M^+) (only peak)

Elemental analysis: calculated: C: 68.19 %; N: 10.84 %; S: 16.55; H: 4.42 %

found: C: 67.91 %; N: 10.66 %; S: 16.67; H: 4.47 %

Step 4. Synthesis of 1,3–diphenyl-5,5-di(2-thiophenyl)-Δ^3-1,2,4-triazolin-2-yl (85)

Oxidation of 1,3–diphenyl-5,5-di(2-thiophenyl)-Δ^2-1,2,4-triazolin (**132**) to the corresponding radical **85** was performed using potassium hexacyanoferrate (III) (Scheme 5.53).

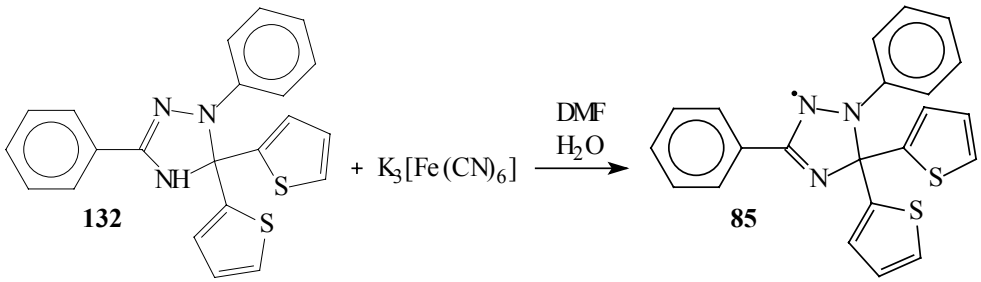

Scheme 5.53. Synthesis of 1,3–diphenyl-5,5-di(2-thiophenyl)-Δ^3-1,2,4-triazolin-2-yl (**85**).

0.5 g (0.0013 mol) of **132** were dissolved in 100 ml of DMF and poured into a 250 ml Erlenmeyer flask. A magnetic stirrer bar was added and the solution was cooled in a dry ice/acetone bath. 1 g (0.003 mol) of potassium hexacyanoferrate (III) and 0.1 (0.001 mol) of sodium carbonate were dissolved in 15 ml of water and added dropwise to the triazolin solution with constant stirring. After addition of all the oxidant, the mixture was stirred for 4 hours at temperatures below – 10°C. On completion of the reaction, the resulting very dark solution was diluted with an excess of water. The resulting precipitate was collected by filtration, washed with water and dried to give 1,3–diphenyl-5,5-di(2-thiphenyl)-Δ^3-1,2,4-triazolin-2-yl (**85**) as a very dark red fine powder. The yield of the reaction was quantitative.

Analysis:

Melting point: 38 – 40°C

Mass spectra (FD): m/z: 386.0 (M^+) (only peak)

Elemental analysis: calculated: C: 68.37 %; H: 4.17 %; N: 10.87 %; S: 16.59 %

found: C: 68.37 %; H: 3.86 %; N: 10.82 %; S: 16.24 %

UV-Vis spectrum at room temperature in dichloromethane is shown in Figure 5.14.

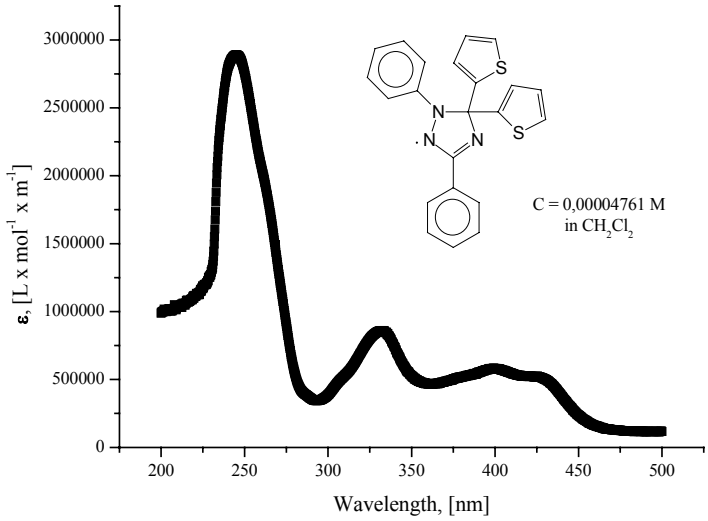

Figure 5.14. UV-Vis spectrum of 1,3–diphenyl-5,5-di(2-thiophenyl)-Δ^3-1,2,4-triazolin-2-yl (**85**) in CH_2Cl_2.

5.13. Synthesis of 1,3-diphenyl-5,5-di(2-pyridyl)-Δ^2-1,2,4-triazolin

An attempt to synthesize 1,3-diphenyl-5,5-di(2-pyridyl)-Δ^3-1,2,4-triazolin-2-yl radical was unsuccessful. During the oxidation step the radical decomposed very rapidly at temperatures above 10°C. However, 1,3-diphenyl-5,5-di(2-pyridyl)-Δ^2-1,2,4-triazolin was synthesized and isolated *via* the synthetic route shown in Scheme 5.54.

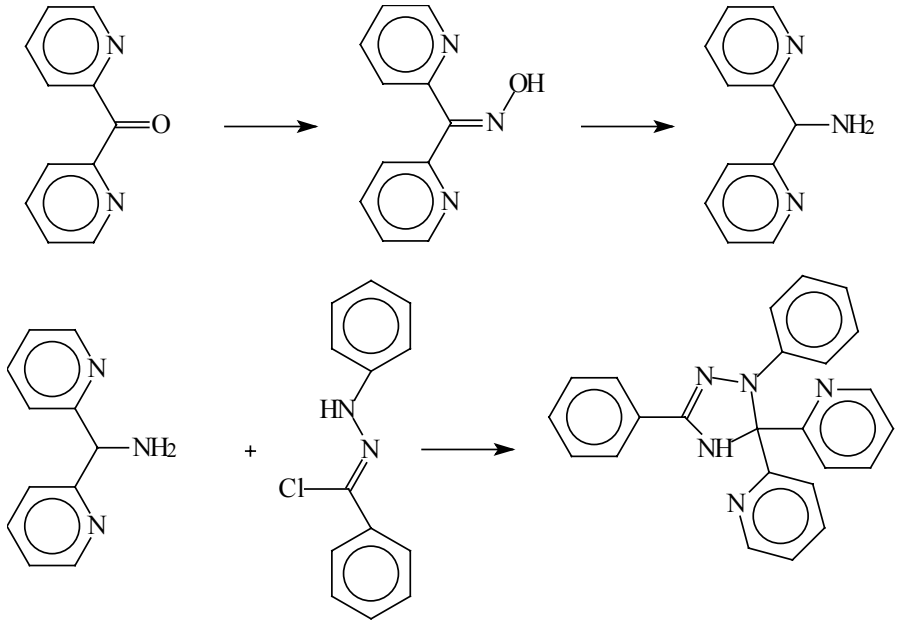

Scheme 5.54. Synthetic route to 1,3-diphenyl-5,5-di(2-pyridyl)-Δ^2-1,2,4-triazolin.

Step 1. Synthesis of di(2-pyridyl)ketone oxime (134)

Di(2-pyridyl)ketone oxime (**134**) is commercially available from Aldrich, however, the price of the oxime is much higher than that of di(2-pyridyl)ketone (**133**). Taking into account the high yields usually achievable in the oxime preparation step, **134** was synthesized as shown in Scheme 5.55.

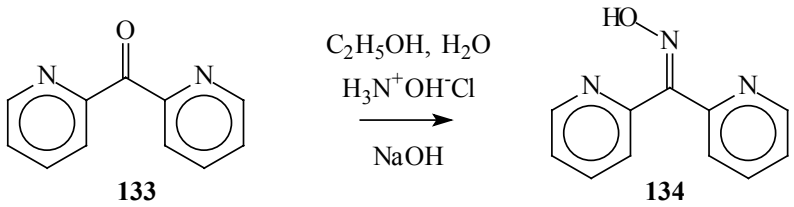

Scheme 5.55. Synthesis of di(2-pyridyl)ketone oxime (**134**).

10.31 g (0.056 mol) of **133** and 5.83 (0.084 mol) of hydroxylamine hydrochloride, 15 ml of water and 50 ml of ethanol were mixed in a 250 ml two-necked round-bottom flask equipped with reflux condenser and magnetic stirrer bar with stirring. 3.6 g (0.09 mol) of sodium

hydroxide pellets were added by small portions. The mixture was refluxed for 4 hours, and the cooled solution poured into water. Crystallization occured when the solution was cooled down to 0°C. The crystals were collected by filtration, washed with cold water and dried to give di(2-pyridyl)ketone oxime (**134**) as a crystalline colorless solid. No further purification was required. The yield was 91 %.

Analysis:

Melting point: 142 – 143°C

^{1}H-NMR spectra (D_6-DMSO, 250MHz) δ [ppm]: 7.35 - 8.46 (m, 8H, pyridyl protons); 11.61 (s, 1H, NO<u>H</u>)

Mass spectra (FD): m/z: 199.2 (M^+) (only peak)

Elemental analysis: calculated: C: 66.83 %; N: 21.09 %; H: 4.55 %

found: C: 66.87 %; N: 20.89 %; H: 4.29 %

Step 2. Synthesis of α-aminodi(2-pyridyl)methane (135)

Reduction of the oxime **134** to α-aminodi(2-pyridyl)methane (**135)** was carried out according to a reported procedure[214, 215] (Scheme 5.56).

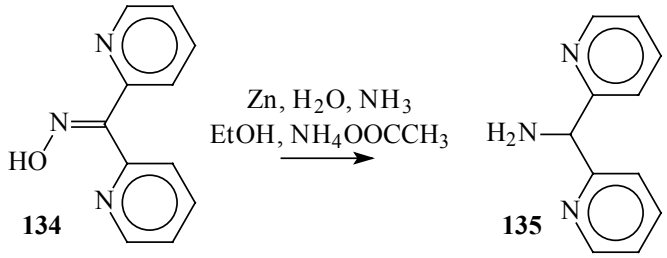

Scheme 5.56. Synthesis of α-aminodi(2-pyridyl)methane (**135**).

11.8 g (0.06 mol) of **134**, 9.37 g (0.12 mol) of ammonium acetate, 240 ml of ethanol, 210 ml of 25 % ammonia solution and 140 ml of water were mixed in a 1000 ml two-necked round-bottom flask equipped with reflux condenser and magnetic stirrer bar, and heated until reflux. Under vigorous stirring, 21 g (0.33 mol) of zinc dust was added in portions to the refluxing solution. After addition of all the zinc, the suspension was stirred under reflux for 20 hours. The unreacted zinc was removed by filtration and the products were extracted with diethyl ether. The combined organic layers were washed with brine and sodium carbonate solution and dried over magnesium sulfate. **135** was isolated by column chromatography on silica gel 60 with ethyl acetate (Acros)/dichloromethane mixture as eluent as a colorless oil. The yield was 67 %.

[214] M. Renz; C. Hemmert; B. Meunier, Eur. J. Org. Chem., 1271 - 1273, **1998**.
[215] E. Niemers; R. Hiltmann, Synthesis, 593 - 595, **1976**.

Analysis:

Melting point: oil

^{1}H-NMR spectra (D_6-DMSO, 250MHz) δ [ppm]: 2.65 (broad s, 2H, N<u>H$_2$</u>); 5.19 (s, 1H C<u>H</u>); 7.20 - 8.47 (m, 8H, protons in pyridyl rings)

Mass spectra (FD): m/z: 185.3 (M^+) (only peak)

Elemental analysis: calculated: C: 71.33 %; N: 22.69 %; H: 5.99 %

found: C: 71.22 %; N: 22.97 %; H: 5.70 %

Step 4. Synthesis of 1,3–diphenyl-5,5-di(2-pyridyl)-Δ^2-1,2,4-triazolin (136)

Condensation of **135** and **37** in order to obtain to obtain 1,3–diphenyl-5,5-di(2-pyridyl)-Δ^2-1,2,4-triazolin (**136**) was performed using the standard procedure described above (Scheme 5.57).

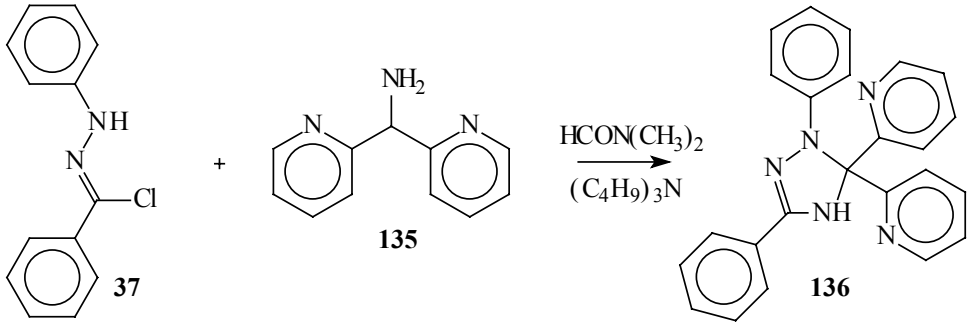

Scheme 5.57. Synthesis of 1,3–diphenyl-5,5-di(2-pyridyl)-Δ^2-1,2,4-triazolin (**136**).

4.17 g (0.023 mol) of **135**, 5.18 g (0.023 mol) of **37**, 10.7 ml (8.3 g, 0.045 mol) of tri-*n*-butylamine and 100 ml of DMF were mixed in a 250 ml one-necked round-bottom flask (dried using Method 6.1) with reflux condenser, magnetic stirrer bar and under argon atmosphere. The mixture was stirred at 180°C for 60 minutes, after which the very dark solution was cooled to room temperature and diluted with water. Sodium chloride and sodium carbonate were added to the solution and the products were extracted with chloroform. The crude 1,3–diphenyl-5,5-di(2-pyridyl)-Δ^2-1,2,4-triazolin (**136**) was purified by column chromatography on silica gel 60 with mixture of diethyl ether, petroleum ether and triethylamine as eluent and by recrystallization from dichloromethane/petroleum ether mixture to give yellow crystalline solid. The yield was 15 %.

Analysis:

Melting point: 158 – 159°C

^{1}H-NMR spectra (D_6-acetone (Deutero GmbH), 250MHz) δ [ppm]: 6.57 - 8.02 (m, 18H, phenyl & pyridyl protons); 8.58 (s, 1H, N<u>H</u>)

Mass spectra (FD): m/z: 377.2 (M^+) (only peak)

Elemental analysis: calculated: C: 76.37 %; N: 18.55 %; H: 5.07 %

found: C: 76.32 %; N: 18.33 %; H: 5.35 %

5.14. Synthesis of 1,3-diphenyl-5,5-di(4-acetylphenyl)-Δ^2-1,2,4-triazolin

Similarly as described in the previous section for the 1,3-diphenyl-5,5-di(2-pyridyl)-Δ^2-1,2,4-triazolin-2-yl radical, 1,3-diphenyl-5,5-di(4-acetylphenyl)-Δ^2-1,2,4-triazolin-2-yl decomposed upon warming to room temperature after oxidation step. 1,3-Diphenyl-5,5-(4-acetylphenyl)-Δ^2-1,2,4-triazolin was, however, prepared *via* the synthetic way shown in Scheme 5.58.

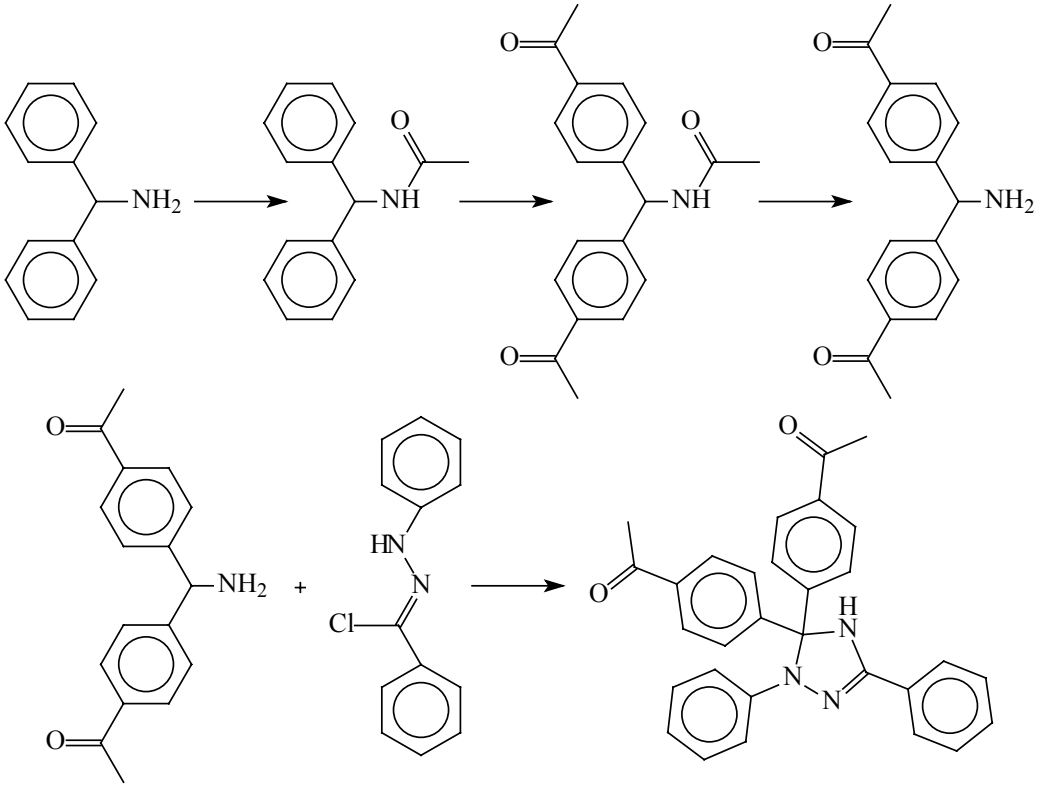

Scheme 5.58. Synthetic route to 1,3-diphenyl-5,5-di(4-acetophenyl)-Δ^2-1,2,4-triazolin.

Step 1. Synthesis of N-benzhydrylacetamide (74)

In order to protect amino group of benzhydrylamine it was converted to its acetamide (Scheme 5.59).

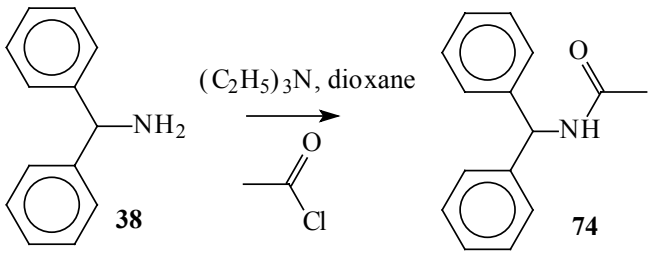

Scheme 5.59. Synthesis of N-benzhydrylacetamide (**74**).

10 ml (10.8 g, 0.059 mol) of benzhydrylamine (**38**) and 11.4 ml (8.32 g, 0.08 mol) of triethylamine were dissolved in 300 ml of dioxane (Riedel-de Haen) in a 500 ml two-necked round-bottom flask equipped with a reflux condenser with a $CaCl_2$ cap on the outlet and a magnetic stirrer bar, dried as described in Method 6.1. The flask was cooled down by immersing in a sodium chloride/ice bath. Then 5.8 ml (6.4 g, 0.008 mol) of acetyl chloride were added dropwise to the stirred solution. After addition of all acetyl chloride, cooling was removed and the reaction continued for 4 hours at room temperature. On completion of the reaction the solution was poured onto ice. Precipitation occurred slowly and the resulting crystalline residue was collected by filtration. After purification by recrystallization from ethanol/water mixture N-benzhydrylacetamide (**74**) was isolated as a colorless crystalline solid. The yield was 86 %.

Analysis:

Melting point: 147 – 148°C

^{1}H-NMR spectra (D_6-DMSO, 250MHz) δ [ppm]: 6.13 (d, J = 8.69 Hz, 1H, C<u>H</u>); 7.23-7.38 (m, 13H, phenyl protons); 8.82 (d, J = 8.69 Hz, 1H, N<u>H</u>)

Mass spectra (FD): m/z: 225.3 (M^+) (only peak)

Elemental analysis: calculated: C: 79.97 %; N: 6.22 %; H: 6.71 %

found: C: 80.17 %; N: 6.16 %; H: 6.78 %

Step 2. Synthesis of 4,4`-di(acetyl)benzhydrylamine (75)

4,4`-Di(acetyl)benzhydrylamine (**75**) was prepared as shown in Scheme 5.60.

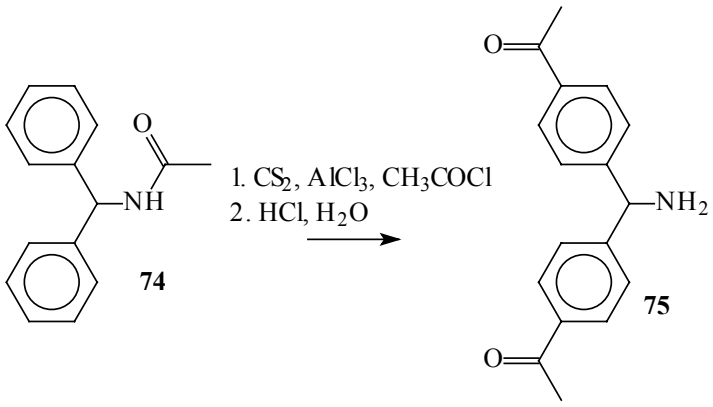

Scheme 5.60. Synthesis of 4,4`-diacetylbenzhydrylamine (**75**).

A 500 ml three-necked round-bottom flask, equipped with dropping funnel, reflux condenser and magnetic stirrer bar allowing mixing of viscous solutions was dried by the usual procedure (Method 6.1). The flask was immersed in an ice bath and 11.57 g (0.052 mol) of **74**, 66 g (0.5 mol) of aluminum chloride (Aldrich) and 100 ml of carbon disulfide (CS_2) (Aldrich)

were added under argon atmosphere. 22 ml (19.9 g, 0.26 mol) of acetyl chloride were added slowly to the stirred suspension, the ice bath was exchanged with an oil bath, and the temperature raised to 65°C. The refluxing solution was stirred for 12 hours, after which the carbon disulfide was removed by distillation. The residue was cooled down and excess of water was carefully added dropwise. The products were extracted with dichloromethane. The combined organic layers were washed with brine and water, dried over magnesium sulfate, and the solvent was removed in *vacuo*. The formation of diacyl-N-benzhydrylacetamide was detected by mass spectrometry, but the amide was hydrolyzed without isolation.

In a 2000 ml two-necked round-bottom flask equipped with magnetic stirrer bar 1200 ml of 6N hydrochloric acid were prepared. In the second neck a dropping funnel was set and the flask was immersed into an oil bath heated to 120°C. The residue of the amide obtained after evaporation of chloroform was dissolved in a minimal amount of ethanol and added dropwise with vigorous stirring to the boiling hydrochloric acid. After refluxing the mixture for 12 hours, the hot yellow solution was filtered to remove side products, insoluble in hot hydrochloric acid. The cooled solution was basified with sodium carbonate and the products were extracted with a mixture of dichloromethane and ethyl acetate. The combined organic layers were washed with sodium chloride and sodium carbonate solutions and dried over magnesium sulfate. The crude products were adsorbed on silica gel 60, which was dried and put into a Soxhlet extractor cartridge. Continuous extraction over 48 hours with diethyl ether as described in Method 6.2 was performed. The resulting product was purified by column chromatography with dichloromethane/ethyl acetate mixture as eluent to give 4,4`-di(acetyl)benzhydrylamine (**75**) as a yellow crystalline solid. The yield = 42 %.

Analysis:

Melting point: 114 – 115°C

^{1}H-NMR spectra (D_6-DMSO, 250MHz) δ [ppm]: 2.07 (broad s, 2H, N<u>H</u>$_2$); 2.61 (s, 6H C<u>H</u>$_3$); 5.26 (s, 1H, C<u>H</u>); 7.55 (d, J = 8,25 Hz, 4H, phenyl protons 2 & 6); 7.88 (d, J = 8,25 Hz, 4H, phenyl protons 3 & 5)

Mass spectra (FD): m/z: 267.5 (M^+) (only peak)

Elemental analysis: calculated: C: 76.38 %; N: 5.24 %; H: 6.41 %

found: C: 76.19 %; N: 4.95 %; H: 6.16 %

Step 4. Synthesis of 1,3–diphenyl-5,5-di(4-acetylphenyl)-Δ^2-1,2,4-triazolin (137)

1,3–Diphenyl-5,5-di(4-acetylphenyl)-Δ^2-1,2,4-triazolin (**137**) was synthesized *via* the standard procedure (Scheme 5.61).

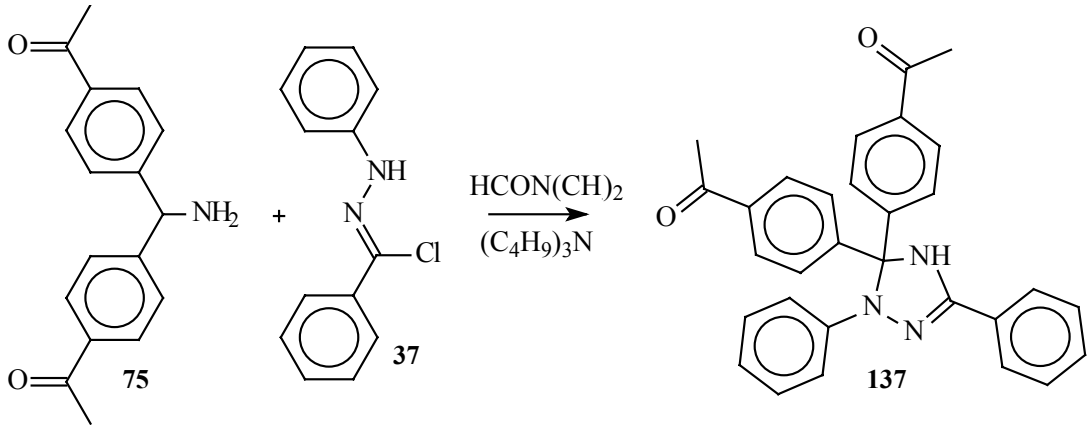

Scheme 5.61. Synthesis of 1,3–diphenyl-5,5-di(4-acetylphenyl)-Δ^2-1,2,4-triazolin (**137**).

2.5 g (0.0094 mol) of **103**, 2.3 g (0.01 mol) of **56**, 2.4 ml (1.85 g, 0.01 mol) of tri-*n*-butylamine were dissolved in 100 ml of DMF in a 250 one-necked round-bottom flask equipped with a magnetic stirrer bar and reflux condenser, previously dried as described in method 6.1 under argon atmosphere. The mixture was heated to 120°C for 90 minutes with stirring. The cooled solution was poured into an excess of sodium chloride solution and the products were extracted with chloroform. The combined organic layers were washed with brine and water and dried over magnesium sulfate. **137** was isolated as a yellow solid after separation by column chromatography on silica gel 60 with dichloromethane/petroleum ether mixture as eluent and subsequently with diethyl ether/petroleum ether as eluent. The yield was 7 %.

Analysis:

Melting point: the substance decomposes, decomposition in bulk starts ~ 90°C

^{1}H-NMR spectra ($C_2D_2Cl_4$, 250MHz) δ [ppm]: 2.59 (s, 6H, C<u>H</u>$_3$); 7.01 – 8.24 (m, 18H, phenyl protons); 8.77 (s, 1H, N<u>H</u>)

Mass spectra (FD): m/z: 459.2 (M^+) (only peak)

Elemental analysis: calculated: C: 78.41 %; N: 9.14 %; H: 5.48 %

found: C: 78.31 %; N: 8.89 %; H: 5.73 %

6. Experimental part: methods

6.1. Removal of moisture from a flask prior to water sensitive reactions

A flask was equipped with all heat tolerant devices (*e.g.* reflux condenser, dropping funnel, Dean-Stark trap *etc.*) necessary for the reaction. A teflon magnetic stirrer bar was not put in the flask in order to avoid its carbonization. In one of the necks of the flask a gas outlet with a tap was set. All other open outlets were closed with glass caps. A vacuum pump was connected to the gas outlet and the pressure was reduced inside the flask. Using a heat-gun (Bosch) adjusted to ~ 630°C, all the apparatus was thoroughly heated under vacuum for *ca.* 10 minutes, then the flask was cooled down to room temperature. The pump was disconnected from the outlet and the cold apparatus was flushed with argon. This procedure was repeated three times in order to ensure moisture exclusion from the reactor. This procedure is performed similarly as that described by Langela.[216]

6.2. Soxhlet extraction

In a one-necked round-bottom flask, the solvent required for the extraction was added. A magnetic stirrer bar and Soxhlet device were attached. Then, the cartridge for the extractor was filled with the substance and placed into the device; on top, a reflux condenser was attached. Depending on the conditions of the extraction and the air-sensitivity of the substance, a balloon filled with argon or water-absorbing cap was installed on the top of the condenser. The apparatus was put in an oil bath and under constant stirring the temperature raised until the solvent boiled. After the desired time of extraction the oil bath was removed and the resulting solution was processed further.

6.3. Melting point measurement

A thin (~ 0.5 mm) capillary was filled by substance to a height of ~ 7 mm. The top of the capillary was sealed with silicone grease (Bayer). The capillary was installed in the melting point automatic measuring machine Buechi Melting Point B-545. The rate of heating was 1°C per minute and the melting point was detected automatically. Obtained values are uncorrected.

[216] M. Langela, ***Diploma thesis***, Johannes-Gutenberg-University/Max-Planck-Institute for Polymer Research: Mainz, **1999**.

6.4. Elemental analyses

Elemental analyses were done by the analytical laboratory of the Johannes Gutenberg University, Mainz.

6.5. Obtaining of HCl gas

HCl gas was obtained from sodium chloride and concentrated sulfuric acid. Sodium chloride was placed in a 250 ml one-necked flask. A dropping funnel with a gas pipe was installed in the neck and filled with concentrated sulfuric acid. A gas outlet was set on the top of the funnel, and an empty trap was connected to the gas outlet. Dropwise addition of the sulfuric acid to the sodium chloride gave HCl gas, which was used without further purification.

6.6. Purification of the chemicals

6.6.1. Dibenzoyl peroxide (BPO) (10)

Dibenzoyl (benzoyl) peroxide (**10**) was purchased from Merck. The substance was dissolved in chloroform. The chloroform solution was stirred in an Erlenmeyer flask using a magnetic stirrer bar and methanol was added dropwise to the solution. A snow-colorless precipitate formed during this procedure. The suspension was cooled down to ~ 0°C in refrigerator and the precipitate was collected by filtration, washed with cold methanol and dried in *vacuo*. The purified benzoyl peroxide was kept at – 18°C. This procedure followed the methods described in literature.[217,218]

6.6.2. Water

Water used in all experiments was deionized by passing through ion-exchange columns in the Max-Planck-Institute for Polymer Research purification system.

6.6.3. Monomers

Monomers include styrene (Aldrich) (**97**), methylmethacrylate (Fluka) (**92**), ethylmethacrylate (Merck) (**94**), 4-vinylpyridine (Merck) (**96**), *tert*-butylacrylate (Aldrich) (**98**),

[217] D. D. Perrin; W. L. F. Armarego, ***Purification of Laboratory Chemicals***, *3rd edition*, Pergamon Press: Oxford, 95, **1988**.
[218] L. F. Fiser; M. Fiser, ***Reagents for Organic Synthesis***, John Wiley and Sons Inc.: New York , 196, **1967**.

2,2,2-trifluoroethylmethacrylate (Acros) (**93**), *n*-bytylmethacrylate (Aldrich) (**95**) (Figure 6.1). Most of the monomers contained inhibitors added by the supplier to prevent self-polymerization. All monomers except **93** were purified in a similar way. First, they were stirred by magnetic stirrer for 12 hours with CaH_2 (Merck) as drying agent in a round-bottom flask. Then, without removal of the additives a dephlegmator with a straight condenser and thermometer were installed. A round-bottom receiving flask was fastened to the outlet of the condenser. A vacuum pump, allowing vacuum down to 10^{-2} mbar with a liquid nitrogen trap was connected to the gas outlet of the straight condenser. The apparatus was put in an oil bath heated slightly above room temperature. The monomer was distilled under reduced pressure and collected in the receiving flask cooled by liquid nitrogen bath. The first and last portions were discarded and the rest was collected. Monomers were kept at – 18°C and checked for presence of the polymer by dropping in a non-solvent each time prior to use. The procedures follow those in the literature.[219] In the case of **93** anhydrous $MgSO_4$ was used as drying agent instead of calcium hydride.

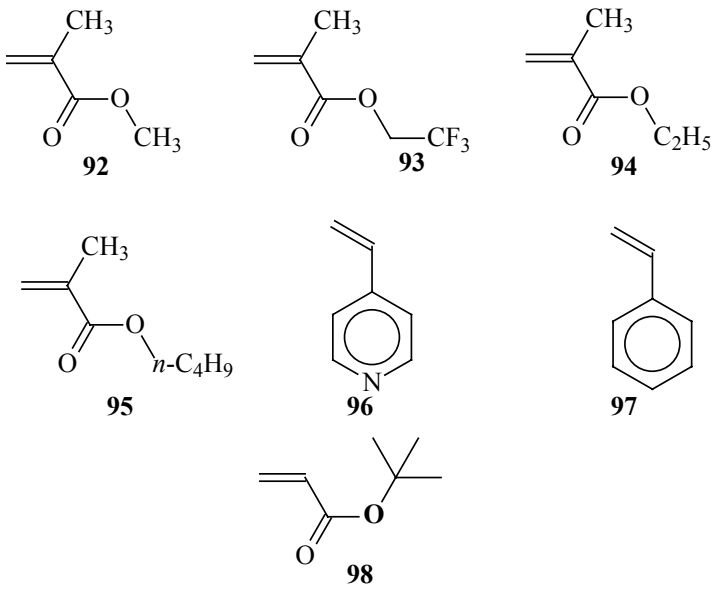

Figure 6.1. Monomers used in the work.

6.6.4. 2,2'-Azobis-*iso*-butyronitrile (AIBN) (9)

AIBN purchased from Merck contained up to 25 % of water. For removal of water and purification it was dissolved in chloroform. The solution was filtered through magnesium sulfate and AIBN was precipitated with petroleum ether. The crystalline residue obtained was collected by filtration and dried in vacuum. Purified AIBN was stored at – 18°C.

[219] D. D. Perrin; W. L. F. Armarego, ***Purification of Laboratory Chemicals***, Pergamon Press: Oxford, **1988**.

6.7. Gravimetrical determination of monomer conversion

Glass filters with porosity 4 were washed with THF and acetone and thoroughly dried at 85°C. Then the filters were cooled down to room temperature and their weight measured several times to ensure reproducibility. The mixture of monomer and polymer taken from the thermostat and cooled in the liquid nitrogen was diluted with an appropriate solvent and the polymer precipitated by a non-solvent. The residue formed was filtered using the filters prepared. The polymer together with filter was dried in a vacuum box at a slightly elevated temperature (35 – 45°C) till constant weight. Afterwards, the weight of polymer on the filter was measured and the conversion was calculated from the known amount of initial monomer in the flask. The weights of the counter radical and the initiator were neglected and not taken in the calculation, due to their insignificant amount.

In the cases when precipitation of the polymer was not successful the procedure used was similar to the one described above. However, instead of the filters, prepared in the same way 50 ml or 100 ml one-necked round-bottom flasks have been used. The polymer solutions were evaporated on the rotor vapor machine. The flasks were dried till constant weight and weight of the polymer was determined as described above.

6.8. GC determination of monomer conversion

Alternatively, monomer conversion could be determined using gas chromatography. Using internal standards, direct determination of the monomer concentration was possible. In the project a Varian 3400 Gas Chromatograph with installed Autosampler 8200CX was used, with a flame-ionization detector. A capillary column “2-4803” 15 m/0.32 mm 0.5 μm film was provided by Supelco. Control over the chromatography process was accomplished using the software Star Chromatography Workstation ver. 4.0, provided by Varian and installed on Compaq DeskPro XL 450. The features of the method used are summarized in Table 6.1.

Isobutyl alcohol (Fluka) was used as standard. Using the method described above the coefficients allowing recalculation of monomers concentration from known concentration of the standard and peak square ratios were determined as follows. A series of solutions containing known amounts of the standard and monomers were prepared. The mixtures were investigated chromatographically, using various conditions. In order to decrease the error of the experiment 10 solutions having different monomer/standard ratios and their concentration in DMF were used for each monomer. Each sample was injected from 5 to 7 times with different injection volumes

(varied in range 0.5 – 2 μl). The values obtained were averaged. The error of the determined values did not exceeded 1 %. The coefficients were calculated by Equation 6.1

Table 6.1. The method used for the GC monomer conversion determination.

Parameter	Value
Evaporator, T°C	220
Column, T°C	gradient from 120 to 180
Column heating rate, °C/min	3
Injection volume, μl	0.5 - 2
Carrier gas (Ar) (Linde) flow, ml/min	40
H_2 (Linde) flow, ml/min	30
Air (synthetic) (Linde) flow, ml/min	200

$f = \frac{s_{mon} m_{st}}{s_{st} m_{mon}}$ **Equation 6.1**, where s_{mon} and s_{st} are the squares of the monomer and the standard peaks on the chromatogram, m_{mon} and m_{st} – weights of the monomer and the standard in the sample, f – the coefficient.

The weight of the monomer in the sample taken from the polymerization was calculated using Equation 6.2.

$$m_{mon} = \frac{s_{mon} m_{st}}{s_{st} f}$$ **Equation 6.2.**

The coefficients for the monomer related to isobutyl alcohol as standard were determined as:

2,2,2-trifluromethylmethacrylate: $f = 0.4814 \pm 0.00194$

methylmethacrylate: $f = 0.7284 \pm 0.0043$

For the determination of the conversion autosampler bottles (Wheaton) were used as polymerization reactors. During the polymerization experiment the bottles were sealed with solid caps, which were exchanged before the chromatography with caps with holes, closed by teflon/*tert*-butylacrylate pads. The weighted amount of the standard was added between the polymerization and the chromatography. In order to homogenize the sample DMF was used as solvent in all cases (including the cases of the coefficient determination).

The values obtained by gravimetrical and GC measurements matched one another within the error range of 5 %.

6.9. Recognition of triazolins spots on TLC plates

In order to determine the triazolin spots on the TLC plates, a solution of $K_3[Fe(CN)_6]$ in water/acetone or water/methanol mixture was used. After the TLC had been run, the plate was dried and then wetted by the $K_3[Fe(CN)_6]$ solution. The triazolin showed itself as a very dark brown or black spot caused by the triazolinyl thus formed. Use of an aqueous solution without addition of organic solvent was less efficient due to poor wettability of the TLC plates.

6.10. Polymer syntheses

The standard polymerization experiment was done as following. In a Schlenk tube the calculated amounts of counter radical, initiator (BPO or AIBN) and monomer were mixed. The solution was degassed 3 - 4 times using the „freeze-thaw“ technique (Method 6.12). Afterwards, in a glove-box the degassed solution was distributed into several reactors. The reactors were weighted prior to filling with the polymerization mixture and after it. This allowed calculation of the weight of the monomer in each reactor, which was required for conversion determination (Sections 6.7 and 6.8). The reactor tubes were put in a thermostat at 120°C in the case of styrene and 4-vinylpyridine. In the case of methacrylates and acrylates the reactors first were put in a thermostat maintained at 95°C and kept there until the initial dark red color changed to a pale yellow, indicating that all the counter radical had been captured by the initiating species formed. Then the reactors were moved to a thermostat at a temperature of 70°C. Polymerizations were quenched after the desired time by putting the sample tube into liquid nitrogen.
Unless stated otherwise molar ratios: monomer/initiator = 1000; counter radial/initiator = 1.5 were used in all polymerization experiments.

6.11. Block copolymer syntheses

All block copolymers were synthesized by a similar method as following. The desired amounts of the polymer precursors (macroinitiators) synthesized by the usual procedure (Method 6.10) were placed in reaction tubes. The opened tubes were carried in a glove-box and kept there over 24 hours. The monomer used for the second block formation was degassed by the “freeze-thaw” technique (Method 6.12). The volume of the monomer required for the block copolymer syntheses was then added to the reactors. The exact amount of the monomer was calculated from the difference between the weights of the filled reactor and the weight of the reactor with the macroinitiator only. The tubes were then put into a thermostat adjusted to the desired

temperature. When the macroinitiator was a PS sample and monomer for second block formation was not styrene or 4-vinylpyridine the tubes were held for ~ 10 minutes in a thermostat heated to 120°C to allow reinitiation prior putting in the thermostat at required temperature. After the desired period of time the reaction was quenched by cooling down in liquid nitrogen and worked up further as described in Sections 6.7 and 6.13.

6.12. "Freeze-thaw" technique

"Freeze-thaw" technique is a method to exclude gases from liquids. A Schlenk tube was filled by a liquid or solution and sealed. The tube was immersed in liquid nitrogen and kept there till complete freezing. Then a vacuum pump, capable of reducing pressure to 10^{-2} mbar, was connected to the Schlenk tube gas outlet and the tube was degassed for 30 – 60 seconds. The outlet was then closed and the liquid allowed to melt. The procedure was repeated three times. After the last cycle the tube was filled with nitrogen or argon.

6.13. Determination of molecular weights of polymers

Molecular weights of polymers and copolymers were determined in the analytical laboratory of the MPI-P using GPC. In all cases except P-4-VP and its copolymers THF was used as eluent, otherwise DMF was used. Standards used were: polymethylmethacrylate for all methacrylates, polystyrene for PS and P-4-VP, poly-*tert*-butylmethacrylate for P-*tert*-BA. In the case of block copolymers, the standard used were the same as were used previously for molecular weight determination of the first block.

6.14. HPLC

HPLC analyses were made in the analytical laboratory of the MPI-P.

6.15. Mass spectroscopy

Mass spectroscopy was performed on a VG (Micromass) ZAB2-SE-FPD instrument. Field desorption ionization was used in all cases. The FD allows ionization without decomposition of the substance and, hence, direct determination of molecular weight from the peak of the molecular ion.

6.16. NMR

NMR measurements were carried out on a Bruker DPX250 (250 MHz) and a Bruker APX300 (300 MHz) NMR spectrometers.

6.17. ESR

ESR spectra were recorded using "Bruker ESP300 amd" equipped with Bruker continuous flow N_2 cryostat at X-Band (9.4 – 9.5 GHz) with 100 KHz modulation frequency. ESR experiments were performed in collaboration with Liletta Chergel.

6.18. UV-Vis spectroscopy

All spectra were recorded in dichloromethane solution using a Perkin-Elmer Lambda 15 UV/Vis spectrophotometer.

6.19. Polymerizations in supercritical CO_2

Polymerizations of FEMA in supercritical carbon dioxide were done under pressure of 300 bar, at 70°C. The reagent mixture was the same as was used in the case of bulk polymerization. 1 ml of the mixture of reagents was poured into a 2 ml cell, which was filled with supercritical carbon dioxide. Then the temperature was raised and the polymerization was carried out for the desired time. The heat and pressure were removed and the polymer was isolated either by precipitation from methanol or by evaporation of the monomer in *vacuo*. Experiments in supercritical CO_2 were carried out in collaboration with Nagarajan Vedaraman and Axel Schlewing.

7. Abbreviations & remarks

AIBN - 2,2'-Azobis-*iso*-butyronitrile

Ann. – Annalen

ATRP – Atom Transfer Radical Polymerization

Aust. J. Chem. – Australian Journal Of Chemistry

Ber. d. D. Chem. Geselschaft – Berichte der Deutschen Chemischen Geselschaft

Chem. Abstr. – Chemical Abstracts

Chem. Rev. – Chemical Reviews

CRP – Controlled Radical Polymerization

DMF – Dimethylformamide

DMSO – Dimethylsulfoxide

DNA – Deoxyribonucleic acid

DPBT – 1,3-Diphenyl-1,2,4-benzotriazin-4-yl

FD – Field Desorption

GPC – Gel-Permeation Chromatography

J. Appl. Pol. Sci. – Journal of Applied Polymer Science

J. Polym. Sci. – Journal of Polymer Science

J. Russ. Phys. Chem. Soc. – Journal of the Russian Physical Chemical Society

JACS – Journal of the American Chemical Society

JOC – Journal of Organic Chemistry

JPS – Journal of Polymer Science

m/z – Ratio: mass to charge

Macro. – Macromolecules

Macro. Symp. – Macromolecular Symposia

Macromol. Chem. Rapid Comm. – Macromolecular Chemistry Rapid Communications

Makromol. Chem. – Makromolekulare Chemie

NMR – Nuclear Magnetic Resonance

RAFT – Reversible Addition-Fragmentation Chain Transfer

SFRP – Stable Free Radical Polymerization

THF – Tetrahydrofuran

TMS – Trimethylsilyl

-*b*- - block

-*g*- - gradient

In references: the year of the publication is given in bold **1999**; volumes, numbers, editions are given in italic *23, 1 (2e), ...*; book titles are given in bold italic ***Sovremennaya Obshaya Khimiya***; the pages and the Chemical Abstracts numbers are given in simple font: 2345; 23 – 34, 312612q, …
In NMR: s – singlet, d – doublet, m - multiplet

8. Acknowledgements

This work was only possible because very many of you, my relatives, friends, colleagues, teachers, workmates and simply all friendly persons I have communicated with have helped me. The support and advice I have received from you was absolutely invaluable. I acknowledge and thank all of you (in no particular order):

My dear Parents, my Grandmother, Aunt, my Wife, Eva Sebold, Cecile Troccon, Vladimir Atanasov, Nikolay Nenov, Thorsten Brand, Nawel Khelfallah, Emma Caputo, Dmitrii Orsoev, Valentina Orsoeva, Alla Orsoeva, Ivan Ishigenov, Tujana Antonova, Zhenja Vlasov, Andrey Vlasov, Sergey Fokin, Roma Blagodetelev, Valja Lulevich, Bair Chemitsyrenov, Dima Burlov, Leonid Bazarov, Anastasia Menshikova, Tatjana Evseeva, Boris Shabsels, Prof. Alexandr Bilibin, Natasha Tschebotareva, Nicolas Gogibus, Misha Rogal, Alisa Katsalan, Julia Petrova, Darima Baldanova, Lena Alexeeva, Inga Potapova, Petko Petkov, Tanja Nemnich, Piotr Minkin, Mark Watson, Weicheng Wu, Christophe Ego, Raisa Dvorikova, Luke Oldridge, Manfred Wagner, Dondok Bazarov, Sayan Tangasov, Roland Bauer, Doerthe Grebel-Koehler, Vesselin Sinigerski, Karl Wang, Christopher Simpson, Zeljko Tomovic, Kaloian Koynov, Hans-Joachim Raeder, Nicola Ranieri, Sewa Ksenofontov, Lena Jarkova, Eva Diez, Erik Reuther, Stefan Becker, Andreas Herrmann, Martin Baumgarten, Harm-Anton Klok, Juan Rodriguez, Guido Vandermeulen, Germar Schlegel, Frank Petzke, Christian Huebner, Bin Zhang, Lee Yezek, Beate Schiewe, Elizabeth Lupton, Jean-Noel Pedeutour, Gleb Yakubov, Olga Sokolova, Ivan Zorin, Liletta Chergel, Tomas Bleicher, Anton Sorokovikov, Natasha Bezotechestvo, Lena Zaljauskaite, Kostja Zaljauskaite, Sasha Bjakov, Eugeny Goreshnik, Sergey Minko, Maxim Chernyh, Dima Solodukhin, Gosha Dorzhiev, Charlotta Muench, Dagmar Stiep, Axel Schlewing, Stefan Matile, Naomi Sakai, Pinaki Tulukbar, Flarant Perret, Svetlana Litvinchuk, Yoann Boundry, Benoit Lambert.

Special thanks to Dr. Markus Klapper & Prof. Dr. Klaus Müllen for supervising this work; to Dr. Andrew Grimsdale and Dr. Christopher Clark for revising English and Natalia Stoyanova for help.

9. Supplementary information

The supplement chapter is provided in order to assist repetition of the experiments and to simplify further investigation of the subject by other workers.

9.1. Uncompleted syntheses

9.1.1. Synthesis of 1,3–diphenyl-5,5-di-(4{2-[2-(2-methoxy-ethoxy)-ethoxy]-ethoxy}phenyl)-Δ^2-1,2,4-triazolin

An attempt to synthesize 1,3–diphenyl-5,5-di-(4{2-[2-(2-methoxy-ethoxy)-ethoxy]-ethoxy}phenyl)-Δ^2-1,2,4-triazolin has been made. The synthetic route is shown in Scheme 9.1. However, the purification of the product at the last step proved difficult, what did not permit isolation of the target triazolinyl compound.

Step 1.

In the first step triethylene glycol monomethyl ether (Fluka) was tosylated to assist subsequent nucleophilic substitution with phenolate anion. A 1000 ml two-necked round-bottom flask equipped with reflux condenser and magnetic stirrer bar was dried using the standard procedure (Method 6.1). 8.21 g (7.83 ml, 0.05 mol) of triethylene glycol monomethyl ether was dissolved in 400 ml of pyridine and poured into the flask. The second neck of the flask was sealed with a rubber septum and on the top of the reflux condenser a water absorbing cap was set. 19.07 g (0.1 mol) of tosyl chloride (Aldrich) in 100 ml of dioxane were added dropwise to the stirred solution through the septum *via* syringe. The mixture was stirred at room temperature for 24 hours. The mixture was poured into NaCl solution, and the products were extracted with ethyl acetate. The organic layers were collected, washed by brine and dried over magnesium sulfate. Triethylene glycol monomethyl monotosyl ether was isolated by column chromatography with ethyl acetate as eluent. The yield was 71 %.

Analysis:

Mass spectra (FD): m/z: 1012.1 (M^+) (100 %); 2023.6 ($2*M^+$) (60 %); 3039.0 ($3*M^+$) (60 %)

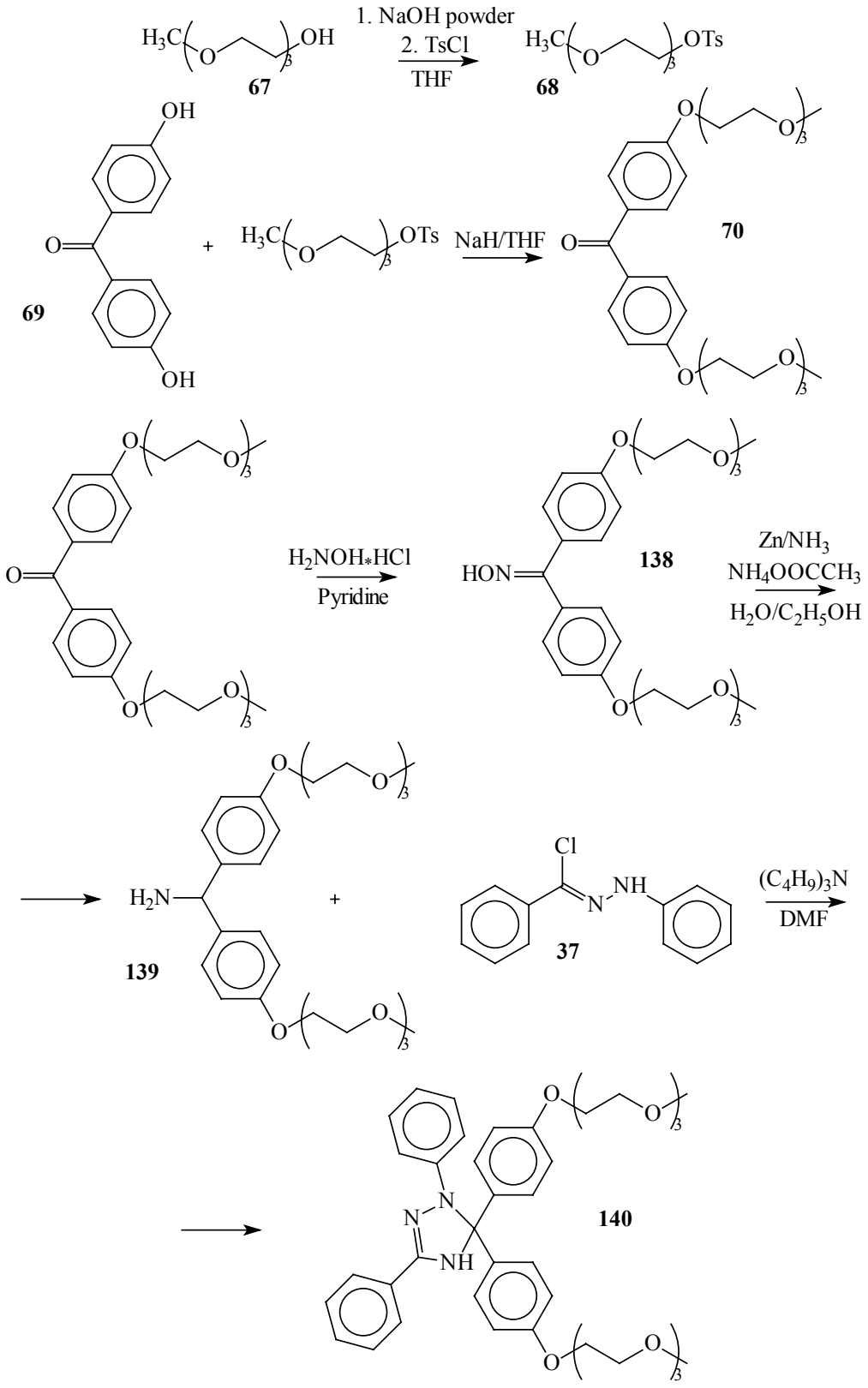

Scheme 9.1. Synthetic route to 1,3–diphenyl-5,5-di-(4{2-[2-(2-methoxy-ethoxy)-ethoxy]-ethoxy}phenyl)-Δ^2-1,2,4-triazolin.

Step 2.

In a previously dried (Method 6.1) 250 ml two-necked round-bottom flask 1 g (0.0047 mol) of 4,4′-dihydroxybenzophenone (Fluka) was dissolved in 100 ml of DMF. 2.6 g (0.0188

mol) of potassium carbonate (Riedel-de Haen) were added to the stirred solution and argon atmosphere was introduced. A reflux condenser was attached and the mixture was heated to 80°C for 20 minutes. Then 3 g (0.0094 mol) of triethylene glycol monomethyl monotosyl ether dissolved in 50 ml of DMF was added dropwise. The mixture was stirred at 80°C for 10 hours after which the reaction was quenched by pouring into water. The products were extracted with chloroform. The organic layers were collected, washed with brine and water and dried over magnesium sulfate. 4,4′-di{2-[2-(2-methoxy-ethoxy)-ethoxy]-ethoxy}benzophenone was isolated by column chromatography on silica gel 60 with chloroform/ethyl acetate mixture as eluent. The yield was 58 %.

Analysis:

Mass spectra (FD): m/z: 506.5 (M^+) (only peak)

Step 3.

2.5 g (0.0049 mol) of 4,4′-di{2-[2-(2-methoxy-ethoxy)-ethoxy]-ethoxy}benzophenone were dissolved in 150 ml of pyridine in a two-necked round-bottom flask. A Dean-Stark trap equipped with a reflux condenser was attached with its outlet filled by previously dried molecular sieves 4 Å. 1.05 g (0.015 mol) of hydroxylamine hydrochloride were added to the stirred solution, the second neck was sealed and argon atmosphere was introduced. The mixture was heated to 125°C for 20 hours after which excess of the pyridine was distilled off and the residue poured to water. The aqueous solution was saturated with NaCl and extracted with chloroform. The combined organic layers were washed with brine and dried over magnesium sulfate. The 4,4′-di{2-[2-(2-Methoxy-ethoxy)-ethoxy]-ethoxy}benzophenone oxime so obtained was used further without purification. The yield was 68 %.

Analysis:

Mass spectra (FD): m/z: 522.3 (M^+) (only peak)

Step 4.

2.3 g (0.0044 mol) of 4,4′-di{2-[2-(2-methoxy-ethoxy)-ethoxy]-ethoxy}benzophenone oxime, 40 ml of ethanol, 20 ml of 25 % ammonia solution, 10 ml of water and 1 g of ammonium acetate were mixed in a 250 ml round-bottom two-necked flask, equipped with magnetic stirrer bar and reflux condenser. The reactor was immersed in an oil bath and the temperature was elevated to 75°C. 3 g (0.046 mol) of Zn dust were added in portions to the stirred solution. After all zinc was added the temperature of the oil bath was raised to 100°C and the mixture was stirred for additional 5 hours. On completion of the reaction unreacted zinc was removed by filtration. The solution was then diluted with water and ammonia solution and the products were extracted with chloroform. The combined organic layers were washed with brine and dried over magnesium sulfate. The 4,4′-di{2-[2-(2-methoxy-ethoxy)-ethoxy]-ethoxy}benzhydrylamine was

isolated by column chromatography on silica gel 60 with chloroform/ethyl acetate as eluent. The yield was 61 %.

Analysis:

Mass spectrum (FD): m/z: 508.5 (M^+) (65 %); 1016.9 ($2*M^+$) (100 %); 1525.3 ($3*M^+$) (15 %) (only peaks)

Step 5.

7.8 g (0.0154 mol) of 4,4′-di{2-[2-(2-methoxy-ethoxy)-ethoxy]-ethoxy}benzhydrylamine, 3.55 g (0.015 mol) of **37** and 3.83 ml (2.98 g, 0.016 mol) of tri-*n*-butylamine were dissolved in 150 ml of DMF in a 250 ml one-necked round-bottom flask, equipped with a magnetic stirrer bar and reflux condenser (dried using Method 6.1) under an argon atmosphere. The flask was immersed in an oil bath heated to 180°C, and the mixture was stirred under reflux for 60 minutes, then the heating was removed and the mixture was stirred for 10 hours at room temperature. On completion of the reaction the mixture was poured into water and the products were extracted with chloroform. The combined organic layers were washed with brine and dried over calcium sulfate (Fluka). The substance was not isolated. In the mass spectra peaks corresponding to 1,3–diphenyl-5,5-di-(4{2-[2-(2-methoxy-ethoxy)-ethoxy]-ethoxy}phenyl)-Δ^2-1,2,4-triazolin and 1,3–diphenyl-5-(4{2-[2-(2-methoxy-ethoxy)-ethoxy]-ethoxy}phenyl)-5-(4-hydroxyphenyl)-Δ^2-1,2,4-triazolin were observed, indicating cleavage of one of the triethylene glycol monomethyl ether chain. Oxidation of the crude product leads to formation of very dark product, which might indicate formation of the corresponding radical.

Analysis:

Mass spectra (FD): m/z: 699.3 (M^+) 1,3–diphenyl-5,5-di-(4{2-[2-(2-methoxy-ethoxy)-ethoxy]-ethoxy}phenyl)-Δ^2-1,2,4-triazolin; 553.65 (M^+) the same compound but with one of the triethylene glycol monomethyl ether chains cleaved

9.1.2. Synthesis of 1′,3′,1′′,3′′-tetraphenyl-dispiro(9,10-dihydroanthracene-[9.5′,10.5′′]di(1,2,4-triazolin-2-yl)

The synthesis of 1′,3′,1′′,3′′-tetraphenyl-dispiro(9,10-dihydroantracene-[9.5′,10.5′′]di(1,2,4-triazolin-2-yl) was attempted. Unfortunately the triazolin ring formation step proceeded in a very low yield and formation of many side products was observed. This did not permit isolation of the target compound. The attempted synthetic route to 1′,3′,1′′,3′′-tetraphenyl-dispiro(9,10-dihydroantracene-[9.5′,10.5′′]di(1,2,4-triazolin-2-yl) is shown in Scheme 9.2.

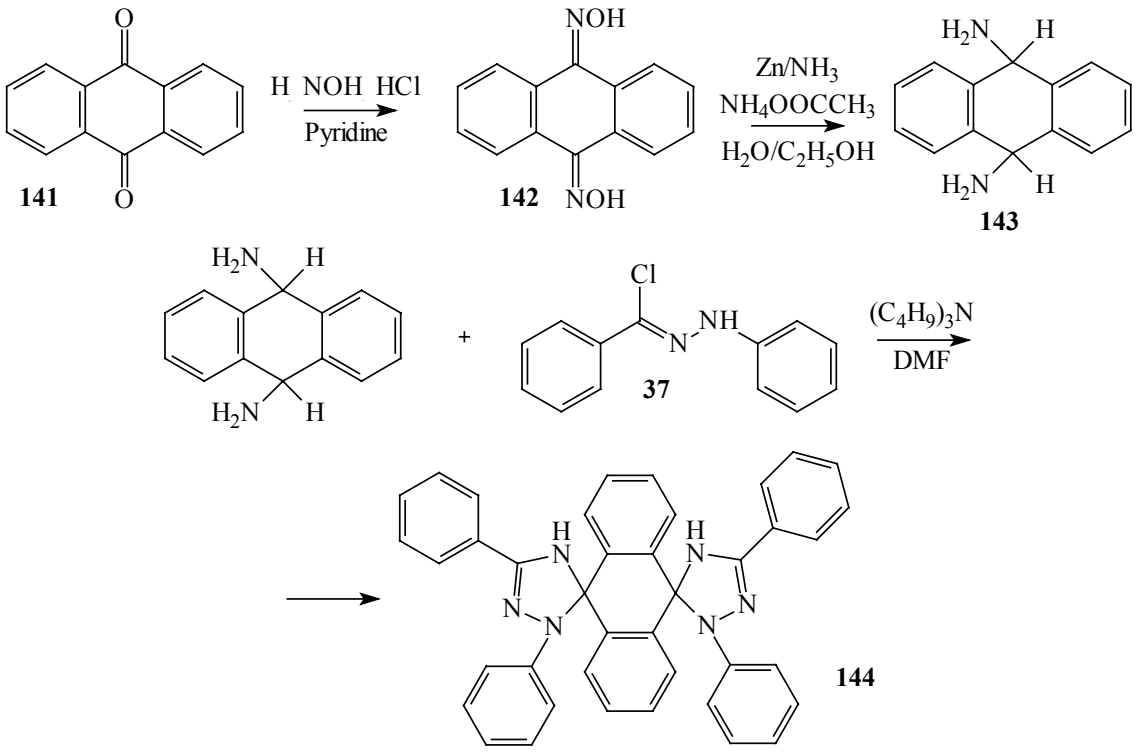

Scheme 9.2. Synthetic route to 1′,3′,1′′,3′′-tetraphenyl-dispiro(9,10-dihydroantracene-[9.5′,10.5′′]di(1,2,4-triazolin-2-yl).

Step 1.

The first step was performed according to the published procedure.[220] 1.07 g (0.0051 mol) of 9,10-anthraquinone, 3.4 g (0.049 mol) of hydroxylamine hydrochloride were dissolved in 100 ml of pyridine in a 250 ml one-necked round-bottom flask, previously dried according to the Method 6.1 equipped with a magnetic stirrer bar and a Dean-Stark trap with reflux condenser. The outlet of the trap was filled with dried molecular sieves 4 Å. An argon atmosphere was introduced and the flask was put into an oil bath heated to 130°C. After stirring for 5 hours at this temperature the solution was poured into diluted sulfuric acid. Formed colorless solid was collected by filtration and washed with water. The 9,10-anthraquinone dioxime so obtained was pure without further purification. The yield was quantitative.

Analyses:

Mass spectra (FD): m/z: 238.2 (M^+) (only peak)

Step 2.

3 g (0.013 mol) of 9,10-anthraquinone dioxime, 250 ml of ethanol, 60 ml of water, 90 ml of 25 % ammonia solution and 4.5 g of ammonium acetate were mixed in a 1000 ml round-bottom three-necked flask equipped with magnetic stirrer bar and reflux condenser and the flask was immersed into oil bath heated to 100°C. Zn powder (11 g, 0.17 mol) was added in portions to the stirred solution. After addition of all the zinc the mixture was refluxed for 5 hours.

Unreacted zinc was removed by filtration and bright orange solution was cooled down. During cooling orange crystals of 9,10-dihydroantracene-9,10-diamine precipitated as a very bright red solid which slowly decomposed during handling. This substance has been previously obtained electrochemically.[221] The yield was 72 %.

Analysis:

Mass spectra (FD): m/z: 206.2 (only peak), the value is smaller than substance's molecular weight to charge by 4 (210.27)

Step 3.

1.05 g (0.005 mol) of 9,10-dihydroantracene-9,10-diamine, 2.75 g (0.012 mol) of **37** and 2.5 ml (1.94 g, 0.011 mol) of tri-*n*-butylamine were dissolved in 50 ml of DMF in a dried (Method 6.1) 250 ml one-necked round-bottom flask equipped with reflux condenser and magnetic stirrer bar under argon atmosphere. The flask was put in an oil bath heated to 180°C and the mixture was stirred at this temperature for 1 hour. The heating was removed, and the mixture was stirred for 10 hours at room temperature, then poured into water and extracted with dichloromethane. The combined organic layers were washed with water and dried over magnesium sulfate. The crude products were subjected to column chromatography on silica gel 60 subsequently with petroleum ether/diethyl ether and dichloromethane/petroleum ether as eluents, but isolation of pure components was not achieved. Mass spectra analysis showed presence of products of bicondensation and monocondensation. Attempts to oxidise the crude product led to formation of products with the color and ESR spectra characteristic for triazolinyls. The intensity of the ESR signal at 90°C did not decrease with time as in the cases of other triazolinyl, allowing to surmise the presence of a cyclic structure, which does not permit decomposition *via* cleavage of substituent at 5-position (similarly to the spiro-triazolinyl **40**).

Analysis:

Mass spectra (FD): m/z: 400.8 (M^+) (product of monocyclization, second amino group is possibly hydrolyzed); 592.0 (M^+) (product of bicyclization)

9.2. Polymerizations in supercritical CO_2

In collaboration with Nagarajan Vedaraman and Axel Schlewing several radical polymerizations in the presence of the triazolinyl radicals in supercritical CO_2 as reaction medium were carried out. The triazolinyls used as counter radicals were **78** and **86**. These radicals have shown enough solubility in CO_2 to be completely dissolved in the amounts

[220] J. Meisenheimer; E. Mahler, Ann., *508*, 185, **1934**.
[221] R. M. Elofson; J. G. Atkins, Canadian Journal of Chemistry, *34*, 4 – 13, **1956**.

necessary for the polymerization. Subsequently it was observed that **33** can also be dissolved in supercritical CO_2, though it has no solubilizing groups. 2,2,2-trifluoroethylmethacrylate (FEMA) was used as monomer. This monomer is soluble in supercritical CO_2, due to the presence of CF_3 group.

For technical reasons the kinetic studies of the polymerizations were difficult to perform and the conclusions about the polymerization process could only be reached on the base of the properties of the polymer obtained. Conditions of the polymerization are described in Section 6.19.

The reaction time was 72 hours after which the heating was removed, the CO_2 allowed to evaporate and the polymer obtained was analysed. In all cases the yield of the polymer obtained did not exceeded 20 %. Molecular weights were around 10000 and polydispersity was below 1.5. The low yield was crucial barrier for obtaining efficient polymerization in the presence of the triazolinyl radicals under these conditions. Similarly the polymerization of the same momomer in bulk in the presence of **86** proceeded only in low yield (Section 3.3). The change of the radical in the bulk polymerization allowed controlled radical polymerization of the monomer. However, further investigations in supercritical CO_2 were stopped due to the difficulties in following the polymerization by kinetics measurments, and shortage of time.

9.3. Datasheets for polymerization experiments

Table 9.1. Kinetic investigation of bulk polymerization of 4-VP in the presence of **82**, 4-VP/AIBN (mol.): 1000, Tr/AIBN (mol.): 1.5, T = 120°C.

Time, min.	Sample, g	Polymer, g	Conversion, %	$\ln([M]_0/[M])$	M_w	M_n	D
0	-	-	-	-	-	-	-
10	0.7548	0.0053	0.7	0.007	-	-	-
41	0.5791	0.0378	6.5	0.07	-	-	-
75	0.2479	0.0216	8.7	0.09	26900	15500	1.73
111	0.6001	0.1108	18.5	0.204	50000	30800	1.62
176	0.6101	0.1615	26.5	0.308	71900	43100	1.67
235	0.3757	0.1008	27	0.312	-	-	-
294	0.5442	0.19	35	0.429	94000	56800	1.66
355	0.4449	0.1397	31	0.377	-	-	-
417	0.4376	0.1807	41	0.533	107900	65000	1.66
472	0.4172	0.1783	42.7	0.558	110400	61500	1.80
1312	0.4131	0.2106	51	0.713	122000	67000	1.82

Table 9.2. Kinetic investigation of bulk polymerization of EMA in the presence of **77**, EMA/BPO (mol.): 1000, Tr/BPO (mol.): 1.5, T = 70°C.

Time, min.	Sample, g	Polymer, g	Conversion, %	$\ln([M]_0/[M])$	M_w	M_n	D
18	0.9288	-	-	-	-	-	-
44	0.8235	-	-	-	-	-	-
87	0.7236	0.1082	15	0.162	91700	62200	1.47

118	0.5855	0.0832	14.2	0.153	68800	47200	1.46
152	0.5772	0.1755	30.4	0.362	121900	77200	1.58
184	0.6108	0.223	36.5	0.454	131500	87900	1.5
219	0.5065	0.2192	43.3	0.567	145800	95900	1.52
316	0.4988	0.3046	61	0.943	179000	111000	1.61
361	0.4818	-	-	-	179500	109000	1.65

Table 9.3. Kinetic investigation of bulk polymerization of FEMA in the presence of **77**, FEMA/BPO (mol.): 1000, Tr/BPO (mol.): 1.5, T = 70°C, conversion are determined by GC.

Time, min.	Sample, g	Polymer, g	Conversion, %	$\ln([M]_0/[M])$	M_w	M_n	D
14	0.1636	0.00594	3.6	0.037	-	-	-
37	0.1884	0.00934	5	0.051	-	-	-
55	0.1885	0.01311	7	0.072	14200	12400	1.15
74	0.211	0.01844	8.7	0.0914	24900	17900	1.39
106	0.3443	0.03792	11	0.117	34200	22800	1.5
134	0.3447	0.05842	17	0.186	-	-	-
166	0.37	0.08957	24.2	0.277	57400	38500	1.49
204	0.3056	0.09365	30.7	0.366	68000	48200	1.41
247	0.401	0.1531	38.2	0.481	71400	40900	1.74
390	0.4972	0.22673	45.6	0.609	98000	51700	1.9
450	0.4477	0.21749	48.6	0.665	105200	59100	1.78
1297	0.4292	0.28113	65.5	1.064	144700	55900	2.59

Table 9.4. Kinetic investigation of bulk polymerization of MMA in the presence of **81**, MMA/BPO (mol.): 1000, Tr/BPO (mol.): 1.5, T = 70°C.

Time, min.	Sample, g	Polymer, g	Conversion, %	$\ln([M]_0/[M])$	M_w	M_n	D
13	1.9072	0.0698	3.6	0.0372	13900	8370	1.66
30	1.8029	0.1098	6.1	0.0628	22700	11800	1.9
50	1.8589	0.1664	8.9	0.0937	26500	12800	2.07
66	1.7504	0.1429	8.1	0.0851	25400	12200	2.06
82	1.5703	0.1267	8	0.0841	25000	12000	2.09
100	1.481	0.1222	8.2	0.0861	24900	11800	2.1
121	1.4822	0.1274	8.5	0.0898	24200	11600	2.1
138	1.5244	0.13	8.5	0.0891	24700	11500	2.15
158	1.8213	0.1672	9.1	0.0962	23500	11400	2.05
177	2.2106	0.2108	9.5	0.1	-	-	-

Table 9.5. Kinetic investigation of bulk polymerization of MMA in the presence of **77**, MMA/BPO (mol.): 1000, Tr/BPO (mol.): 1.5, T = 70°C.

Time, min.	Sample, g	Polymer, g	Conversion, %	$\ln([M]_0/[M])$	M_w	M_n	D
18	0.9714	0.0143	1.5	0.0148	-	-	-
42	1.136	0.0307	2.7	0.0274	-	-	-
57	0.9376	0.0196	2.1	0.0211	-	-	-
73	0.8426	0.0252	3	0.0304	9040	6790	1.33
94	0.8386	0.0431	5.1	0.0528	-	-	1.43
114	0.8041	0.057	7.1	0.0735	21300	14800	1.44
138	0.8032	0.0876	11	0.116	32200	22100	1.46
163	0.6244	0.0961	15.4	0.167	47700	33300	1.43
188	0.5605	0.113	20.2	0.225	62900	43600	1.44
221	0.4168	0.1053	25.3	0.291	81700	53700	1.52

Table 9.6. Kinetic investigation of bulk polymerization of MMA in the presence of **79**, MMA/BPO (mol.): 1000, Tr/BPO (mol.): 1.5, T = 70°C.

Time, min.	Sample, g	Polymer, g	Conversion, %	$\ln([M]_0/[M])$	M_w	M_n	D
22	0.9556	-	-	-	-	-	-
49	0.9341	0.0059	0.6	0.00634	-	-	-
93	0.7872	0.0442	5.6	0.0578	32600	18600	1.75
120	0.6185	0.0731	11.8	0.126	52100	30900	1.69
148	0.8923	0.1098	12.3	0.131	43600	22000	1.98
182	0.8739	0.1709	19.6	0.218	61300	36300	1.69
207	0.8173	0.1871	22.9	0.26	73400	47000	1.56
234	1.0524	0.2462	23.4	0.267	67400	43100	1.57
283	0.7892	0.2632	33.4	0.406	98600	57900	1.7
353	0.6615	0.3532	53.4	0.764	162600	88100	1.85
414	0.9999	0.5889	58.9	0.889	148300	87100	1.7

Table 9.7. Kinetic investigation of bulk polymerization of MMA in the presence of **78**, MMA/BPO (mol.): 1000, Tr/BPO (mol.): 1.5, T = 70°C.

Time, min.	Sample, g	Polymer, g	Conversion, %	$\ln([M]_0/[M])$	M_w	M_n	D
35	0.8269	0.134	16.2	0.177	-	-	-
64	0.7555	0.1298	17.1	0.189	50100	38700	1.3
89	0.5949	0.1261	22.2	0.238	58300	40400	1.44
125	0.5046	0.1382	27.4	0.320	66800	44700	1.49
153	0.4061	0.1246	30.7	0.366	69100	48000	1.44
187	0.4668	0.1566	33.5	0.409	-	-	-
211	0.4088	0.1479	36.2	0.449	77600	50400	1.54
248	0.3974	0.1406	35.4	0.437	79600	49700	1.60
271	0.4679	0.1789	38.2	0.482	81800	45100	1.81
330	0.3977	0.148	37.2	0.465	83600	52200	1.60
388	0.8499	0.3419	40.2	0.514	83100	49900	1.67

Table 9.8. Kinetic investigation of bulk polymerization of *n*-BMA in the presence of **77**, *n*-BMA/BPO (mol.): 1000, Tr/BPO (mol.): 1.5, T = 70°C.

Time, min.	Sample, g	Polymer, g	Conversion, %	$\ln([M]_0/[M])$	M_w	M_n	D
20	0.8286	0.0129	1.6	0.0157	4510	3390	1.33
45	0.9391	0.0204	2.2	0.022	-	7010	-
68	0.7412	0.0203	2.7	0.0278	11500	7400	1.56
91	1.0402	0.0386	3.7	0.0378	14500	9500	1.53
116	0.876	0.0531	6.1	0.0625	26700	15400	1.73
160	0.7375	0.0977	13.2	0.142	59700	37000	1.61
212	0.6252	0.1529	24	0.281	-	-	-
240	0.6924	0.1636	23	0.27	94800	54700	1.73
298	0.7723	0.2665	34.5	0.423	140700	75400	1.87
343	0.847	0.3875	45.7	0.612	180700	95900	1.88
419	0.7834	0.5051	64.5	1.035	202600	-	-
491	0.9752	0.6859	70.3	1.215	285100	131900	2.16

Table 9.9. Kinetic investigation of bulk polymerization of styrene in the presence of **77**, styrene/BPO (mol.): 1000, Tr/BPO (mol.): 2, T = 110°C.

Time, min.	Sample, g	Polymer, g	Conversion, %	$\ln([M]_0/[M])$	M_w	M_n	D
19.5	0.4119	0.04	9.7	0.102	67000	32800	2.04
51.5	0.3062	0.0699	22.8	0.259	76600	36600	2.09
73	0.3307	0.0299	-	-	75900	36800	2.06
88.5	0.34	0.093	27.4	0.32	76200	35500	2.15
105	0.1948	0.0451	23.2	0.263	74100	34600	2.14
123	0.2013	0.0169	-	-	74200	33900	2.19
141	0.3363	0.0776	-	-	73400	35100	2.09
161	0.5057	0.1539	30.4	0.363	73700	34500	2.13
178	0.4954	0.1498	30.2	0.360	73500	34400	2.14
195	0.3144	0.1053	33.5	0.408	73400	33700	2.18
216	0.1625	0.0639	39.3	0.5	72700	30800	-
234	0.1831	0.0689	37.6	0.472	73100	34500	2.12
253	0.176	0.0701	39.8	0.508	73100	34300	2.13
278	0.1782	0.0729	40.9	0.526	73200	34200	2.14

Table 9.10. Kinetic investigation of bulk polymerization of styrene in the presence of **77**, styrene/BPO (mol.): 1000, Tr/BPO (mol.): 2, T = 120°C.

Time, min.	Sample, g	Polymer, g	Conversion, %	$\ln([M]_0/[M])$	M_w	M_n	D
21	0.9463	0.1553	16.4	0.179	59500	29700	2
39	1.0174	0.2006	19.7	0.220	52400	27400	1.9
61	1.0028	0.208	20.7	0.233	50000	24800	2
79	1.033	0.2274	22	0.249	51300	26400	1.9
220	0.9355	0.3837	41	0.528	58200	31700	1.84
244	1.0044	0.4629	46	0.618	61100	33800	1.81
121	0.9186	0.2908	31.7	0.381	49500	25000	1.98
140	0.7688	0.2625	34	0.418	50900	26200	1.94
164	0.8586	0.3141	36.6	0.455	-	-	-
179	0.8546	0.3092	36.2	0.449	55000	28500	1.93
201	0.559	0.2037	36.4	0.453	56000	29800	1.88
101	0.4141	0.1012	24.4	0.282	50600	25600	1.98

Table 9.11. Kinetic investigation of bulk polymerization of styrene in the presence of **77**, styrene/BPO (mol.): 1000, Tr/BPO (mol.): 1.5, T = 120°C.

Time, min.	Sample, g	Polymer, g	Conversion, %	$\ln([M]_0/[M])$	M_w	M_n	D
10.8	0.4211	0.0626	14.9	0.161	49000	25300	1.93
26	0.3321	0.0704	21.2	0.238	55200	26800	2.06
43.3	0.3655	0.0896	24.5	0.281	56100	27800	2.02
61	0.3728	0.1036	27.8	0.326	57100	28000	2.04
80	0.3199	0.103	32.2	0.389	58700	29400	2
103	0.2122	0.0755	35.6	0.44	60800	30900	1.96
122	0.202	0.076	37.6	0.472	62600	31500	1.99
159	0.2189	0.0828	-	-	66200	33900	1.95
180	0.1564	0.0661	42.3	0.549	68300	35100	1.94
198	0.0963	0.0381	-	-	70500	36200	1.95
216.5	0.1589	0.071	44.7	0.592	72300	37800	1.92
231	0.0583	0.0269	46.1	0.619	-	-	-
250	0.0577	0.0179	-	-	76600	39200	1.99

Table 9.12. Kinetic investigation of bulk polymerization of styrene in the presence of **82**, styrene/BPO (mol.): 1000, Tr/BPO (mol.): 1.5, T = 120°C.

Time, min.	Sample, g	Polymer, g	Conversion, %	$\ln([M]_0/[M])$	M_w	M_n	D
30	0.8266	-	-	-	-	-	-
60	0.9534	0.0057	0.6	0.006	-	-	-
93	0.8722	0.0321	3.7	0.0375	-	-	-
132	0.666	0.0562	8.4	0.0882	32100	20100	1.6
160	0.7211	0.0912	12.6	0.135	43700	28600	1.53
182	0.6857	0.1051	15.3	0.166	50000	33500	1.49
223	0.6678	0.137	20.5	0.230	62200	41400	1.50
251	0.6182	0.1409	22.8	0.259	68100	45500	1.5
277	0.6179	0.159	25.7	0.298	73100	49600	1.47
580	0.5688	0.2891	50.8	0.71	130500	80800	1.61

Table 9.13. Kinetic investigation of bulk polymerization of styrene in the presence of **84**, styrene/BPO (mol.): 1000, Tr/BPO (mol.): 1.5, T = 120°C.

Time, min.	Sample, g	Polymer, g	Conversion, %	$\ln([M]_0/[M])$	M_w	M_n	D
19	0.8459	0.1316	15.5	0.17	37000	19700	1.88
42	0.7473	0.1621	21.7	0.245	37500	20200	1.85
62	0.6076	0.1536	25.3	0.291	38900	21700	1.8
88	0.7435	0.2214	29.8	0.354	42100	24100	1.75
117	0.7345	0.2449	33.3	0.406	44800	24700	1.81
142	0.7501	0.2736	36.5	0.454	49200	30200	1.63
175	0.7035	0.2883	41	0.527	51000	28800	1.77
203	0.9196	0.4208	45.8	0.612	53800	31000	1.73
237	0.7348	0.3619	49.3	0.678	57600	34200	1.69
267	0.4675	0.2195	-	-	58500	34900	1.7

Table 9.14. Kinetic investigation of bulk polymerization of styrene in the presence of **79**, styrene/BPO (mol.): 1000, Tr/BPO (mol.): 1.5, T = 120°C.

Time, min.	Sample, g	Polymer, g	Conversion, %	$\ln([M]_0/[M])$	M_w	M_n	D
17	0.8694	0.1371	15.8	0.172	54100	26700	2.02
34	1.0398	0.2052	19.7	0.22	53500	26100	2.05
54	0.6471	0.1507	23.3	0.265	53300	25000	2.12
77	0.5747	0.1501	26.1	0.303	53300	25700	2.07
93	0.6778	0.1958	28.9	0.341	54800	27600	1.98
113	0.4922	0.1507	30.6	0.366	54500	26700	2.04
141	0.567	0.1971	34.7	0.427	60700	30500	1.99
175	0.6426	0.2507	39	0.494	60600	31900	1.9
224	0.4244	0.1763	41.5	0.537	60300	30400	1.98
256	0.4424	0.1975	44.6	0.591	63200	32800	1.93
307	0.5508	0.2768	50.3	0.698	67500	34900	1.93
372	0.3662	0.1745	47.7	0.647	68100	34300	1.99

Table 9.15. Kinetic investigation of bulk polymerization of styrene in the presence of **81**, styrene/BPO (mol.): 1000, Tr/BPO (mol.): 1.5, T = 120°C.

Time, min.	Sample, g	Polymer, g	Conversion, %	$\ln([M]_0/[M])$	M_w	M_n	D
13	0.4512	0.0376	8.3	0.087	31200	16100	1.94
26	0.3162	0.0399	12.6	0.135	-	15100	-
42	0.3047	0.0428	14	0.151	30200	15300	1.97
61	0.1753	0.029	16.5	0.181	-	-	-
81	0.4463	0.0924	20.7	0.232	34000	18600	1.83
104	0.4651	0.1191	25.6	0.296	36700	20700	1.77
122	0.473	0.1295	27.4	0.320	39100	22500	1.74
137	0.4223	0.1131	26.8	0.312	40600	23400	1.74
154	0.4415	0.1347	30.5	0.364	42700	25100	1.70
170	0.4239	0.1512	35.7	0.441	44900	27300	1.64
185	0.3175	0.1137	35.8	0.443	46600	28200	1.65
203	0.3214	0.1216	37.8	0.475	48400	29900	1.62
222	0.4434	0.1748	39.4	0.501	50600	30800	1.64
236	0.308	0.1386	45	0.598	51700	32000	1.61
255	0.2838	0.1435	50.6	0.704	53200	33400	1.6
272	0.4842	0.2082	-	-	53600	34500	1.55

Table 9.16. Kinetic investigation of bulk polymerization of styrene in the presence of **33**, styrene/BPO (mol.): 1000, Tr/BPO (mol.): 1.5, T = 120°C.

Time, min.	Sample, g	Polymer, g	Conversion, %	$\ln([M]_0/[M])$	M_w	M_n	D
12	0.4262	0.0484	11.4	0.121	38300	19800	1.94
26	0.3818	0.0472	12.4	0.132	36900	19000	1.94
40.5	0.2325	-	-	-	-	-	-
59	0.44	0.1051	23.9	0.273	37900	19300	1.97
81	0.4142	0.1138	27.5	0.321	39100	20800	1.88
100	0.3838	0.1129	29.4	0.348	39900	21700	1.84
122	0.6949	0.2298	33	0.402	42200	23000	1.84
138	0.4217	0.1599	37.9	0.477	44000	25300	1.74
154	0.2099	0.0808	38.5	0.486	45400	25800	1.76
171	0.2095	0.0889	42.4	0.552	47200	27000	1.74
188	0.1819	0.0763	42	0.544	49500	29200	1.70
202	0.1628	0.0725	44.5	0.589	50500	30600	1.65
217	0.1408	0.0688	48.9	0.671	52300	30700	1.70
234	0.1061	0.0521	49.1	0.675	53900	31800	1.70
252	0.107	0.0503	-	-	55700	33500	1.66

10. Biography

Maxim V. Peretolchin

Born: 03.12.1976, Ulan-Ude, Buryatia, Russia

E-mail: maximp@rambler.ru

Nationality/Citizenship: Russian

Family status: married

Education

Secondary school:

- 09.1983 - 06.1993, secondary school of general education No. 65, Ulan-Ude, Buryatia, Russia
- *During the study in the school 4th place in chemistry and 3rd place in programming in the city's inter-school competition were taken.*

Higher educational institutions:

- 09.1993 – 12.1996, Buryat Branch of Novosibirsk State University (BB of NSU), Ulan-Ude, Russia, natural sciences faculty, department of chemistry
- 01.1997 – 06.1999, Saint-Petersburg State University (SPbSU), Saint-Petersburg, Russia, chemical department

  Course works: inorganic chemistry, analytical chemistry and organic chemistry

  Practical works: fore diploma practice 4 weeks; pedagogical practice 4 weeks

  Specialization: the chair of macromolecular chemistry, the head of the chair Prof. Dr. Alexander Yu. Bilibin, scientific supervisor Dr. Olga S. Sokolova

  Diploma work: has been performed in Institute of Macromolecular Compounds of Russian Academy of Science and defended in SPbSU, scientific supervisors: Dr. Anastasia Yu. Menshikova, Dr. Tatyana G. Evseeva

  Topic: surfactant-free emulsion polymerization of methylmethacrylate as the method for preparation of monosize microspheres

  Field: investigation of mechanism of surfactant-free emulsion polymerization, obtaining particles with very narrow size distribution for medical diagnostics purposes

  The work has been excellently (mark 5) defended in June of 1999

  - *The work was presented at international conferences in Saint-Petersburg (May and June 1999) and Chernogolovka (May 2000)*

- *During the study in both BB of NSU and SPbSU higher grants for good progress have been awarded several times*

Ph. D. work:

10.1999 - 10.2002, Max-Planck-Institute for Polymer Research (MPI-P), Johannes-Gutenberg-University, Mainz, Germany

Topic: controlled radical polymerization

Field: organic syntheses of stable 1,3,5,5-tetraphenyl-Δ^3-1,2,4-triazolin-2-yl radical derivatives, investigations of their stability depending on the type of structure variations, realization of controlled radical polymerization of various monomers in the presence of such radicals, kinetic investigations of the polymerization processes, syntheses of copolymers.

Scientific supervisors: Prof. Dr. Klaus Müllen, Dr. Markus Klapper

- *A member of the Max-Planck research school; have participated meetings in Heraklion, Greece (September - October 2000); Borkum, Germany (March – April 2001); Berlin, Germany (September 2001); Zurich, Switzerland (May 2002)*
- *The work was presented at conferences in Berlin (September 2000 and October 2002), Lucca (June 2001), Eindhoven (July 2001), Bayreuth (September 2001)*

Publications

on the basis of Diploma work: *Polymer Science*, *Ser. A*, 43, N. 4, **2001**, 366; *Vysokomolekulyarnye Soedinenia*, *Ser. A*, 43, N. 4, **2001**, 607 (in Russian); on the basis of the Ph.D. work: are in preparation for submission

Communication abilities

Russian: native language

English: speaking: fluent; writing: fluent; reading: fluent

German: speaking: good; writing: basic; reading: good